

KINETIC ISOTOPE EFFECTS IN THE $\text{CH}_4 + \text{H} \rightleftharpoons \text{CH}_3 + \text{H}_2$
SYSTEM. PREDICTIONS OF THE LMR SIX-BODY
POTENTIAL-ENERGY REACTION HYPERSURFACE

By

TERRY DON MARRIOTT

Bachelor of Science

Oklahoma State University

Stillwater, Oklahoma

1969

Submitted to the Faculty of the Graduate College
of the Oklahoma State University
in partial fulfillment of the requirements
for the Degree of
DOCTOR OF PHILOSOPHY
December, 1976

Thesis
1976D
M359k
cop. 2



KINETIC ISOTOPE EFFECTS IN THE $\text{CH}_4 + \text{H} \rightleftharpoons \text{CH}_3 + \text{H}_2$
SYSTEM. PREDICTIONS OF THE LMR SIX-BODY
POTENTIAL-ENERGY REACTION HYPERSURFACE

Thesis Approved:

Stewart E. Schuppale

Thesis Adviser

L. M. Raff

J. Paul Newlin

E. J. Limpson

H. Olin Spivey

Norman N. Durham

Dean of the Graduate College

997300

ACKNOWLEDGEMENTS

I wish to extend my appreciation to my major adviser, Dr. Stuart E. Scheppele for his guidance, encouragement, patience, and friendship throughout the course of this study. I would also like to thank my advisory committee: Drs. L. M. Raff, E. J. Eisenbraun, J. Paul Devlin, and H. O. Spivey. I wish to express my appreciation to Dr. L. M. Raff for providing a copy of his potential energy surface computer programs. I am pleased to acknowledge Drs. J. P. Devlin and L. B. Sims for many helpful discussions and suggestions regarding normal mode frequency calculations. Appreciation is also extended to Dr. H. Burchard for his assistance in deriving some of the numerical partial differentiation algorithms. I wish also to extend my appreciation to my fellow graduate students for their friendship and helpful discussions.

I am indebted to the Oklahoma State University Chemistry Department for financial assistance in the form of a Special Summer Research Award from the Graduate College, a Special Summer Appointment, and teaching assistantships.

I am pleased to acknowledge Peggy Peaden for her excellent job in typing and preparation of the final copy of this thesis.

Finally, I wish to extend my special appreciation to my parents, Mr. and Mrs. D. L. Marriott, for their enduring patience, encouragement, and moral and financial support.

TABLE OF CONTENTS

Chapter	Page
I. INTRODUCTION.	1
II. COMPUTATIONAL PROCEDURES.	19
Calculation of Force Constants and Geometries.	19
General	19
Description of the LMR-PES.	20
Reactant and Product Geometries and Coordinates	26
Transition-State Geometry and Coordinates	27
Numerical Methods of Force Constant Determination	30
Force Constant Calculation.	39
III. THEORETICAL KINETIC ISOTOPE EFFECTS FOR THE REACTION $\text{CH}_4 + \text{H} \rightleftharpoons \text{CH}_3 + \text{H}_2$	55
Results and Discussion	55
Comparison of Theoretical Vibrational Frequencies and Force Constants	55
Theoretical and Experimental Temperature Dependences	75
Theoretical Primary Carbon Effects.	91
Theoretical Secondary α -Deuterium Effects	96
The Effect of Transition-State Geometry on the Isotope Effects	104
Contributions of the Bending and Stretching Frequencies to the Primary KIE.	110
Relating Primary Deuterium and Tritium Isotope Effects	119
Relating ^{13}C and ^{14}C Isotope Effects.	122
Rule of the Geometric Mean Relationships.	124
A SELECTED BIBLIOGRAPHY.	127
APPENDIX A - LMR-PES COORDINATE RELATIONSHIPS.	131
APPENDIX B - CALCULATION OF NORMAL MODE FREQUENCIES AND ASSOCIATED PARAMETERS.	139

TABLE OF CONTENTS (Continued)

Chapter	Page
APPENDIX C - TABULATION OF ISOTOPIC NORMAL MODE FREQUENCIES AND PARAMETERS USED IN TRANSITION-STATE THEORY ISOTOPE EFFECT CALCULATIONS	146
APPENDIX D - TABULATION OF THE KIE_s USED TO OBTAIN TEMPERATURE DEPENDENCE PARAMETERS	175
APPENDIX E - LISTING OF COMPUTER PROGRAMS.	189

LIST OF TABLES

Table	Page
I. Experimental KIEs.	7
II. Temperature Dependence of Experimental KIEs.	8
III. LMR-PES and Valence Internal Coordinates Designations and Values for Reactants	22
IV. LMR-PES Parameters	24
V. LMR-PES and Valence Internal Coordinates Designations and Values for the Transition State.	28
VI. Transition-State Scanning Results.	29
VII. Summary of Three-Point Cross-Term Difference Equations .	35
VIII. Transition-State Diagonal Internal Coordinate Force Constant Values.	40
IX. Transition-State Diagonal Cartesian Coordinate Force Constants Calculated by Different Numerical Methods. .	43
X. Transition-State Normal Mode Frequencies	45
XI. Transition-State Cartesian Coordinate Eigenvectors . . .	48
XII. Tetrahedral CH ₄ Normal Mode Frequencies.	50
XIII. Planar CH ₃ and H ₂ Frequencies.	51
XIV. Planar CH ₃ Force Constants and Bondlengths	54
XV. CH ₃ -H-H Transition-State Frequencies from Different Sources.	56
XVI. Comparison of Transition-State Parameters.	57
XVII. Experimental and Theoretical Kinetic Isotope Effects . .	66
XVIII. Experimental and Theoretical Temperature Dependences for k(CH ₄ ,H)/k(CH ₄ ,D).	76

LIST OF TABLES (Continued)

Table	Page
XIX. Experimental and Theoretical Temperature Dependences for $k(\text{CH}_3, \text{H}_2)/k(\text{CH}_3, \text{D}_2)$	78
XX. Experimental and Theoretical Temperature Dependences for $k(\text{CD}_3, \text{H}_2)/k(\text{CD}_3, \text{D}_2)$	80
XXI. Experimental and Theoretical Temperature Dependences for $k(\text{CH}_3, \text{HD})/k(\text{CH}_3, \text{DH})$	82
XXII. Experimental and Theoretical Temperature Dependences for $k(\text{CD}_3, \text{HD})/k(\text{CD}_3, \text{DH})$	84
XXIII. Comparison of $k(\text{CH}_4, \text{H})/k(^{13}\text{CH}_4, \text{H})$ Results	92
XXIV. Comparison of $k(\text{CH}_3, \text{H}_2)/k(^{13}\text{CH}_3, \text{H}_2)$ Results.	93
XXV. Comparison of Secondary α -Deuterium $k(\text{CH}_4, \text{H})/k(\text{CH}_4, \text{D})$ Results.	97
XXVI. Comparison of Secondary α -Deuterium $k(\text{CH}_3, \text{H}_2)/k(\text{CD}_3, \text{H}_2)$ Results.	100
XXVII. The Effect of CH_3 Geometry in the Activated Complex. . .	106
XXVIII. The Effect of CH_3 Geometry on the Temperature Dependences.	108
XXIX. Reactant Isotopic Frequencies.	111
XXX. Transition-State Isotopic Frequencies.	112
XXXI. Bending and Stretching Frequency Contributions to the ZPE.	113
XXXII. Bending and Stretching Frequency Contributions to the EXC.	115
XXXIII. Bending and Stretching Frequency Contributions to the VP	117
XXXIV. Bending and Stretching Frequency Contributions to the KIE.	118
XXXV. Relationships of Tritium and Deuterium Isotope Effects.	120
XXXVI. Relationships of ^{13}C and ^{14}C Isotope Effects	123

LIST OF TABLES (Continued)

Table	Page
XXXVII. Rule of the Geometric Mean Relationships for Secondary Isotope Effects.	125
XXXVIII. LMR-PES Data for Isotopic Hydrogen	147
XXXIX. LMR-PES Data for Isotopic Methyl Radical	148
XL. LMR-PES Data for Isotopic Methane.	149
XLI. LMR-PES Activated Complex Data	151
XLII. LMR-PES Activated Complex Data ϕ_i (i=1,2,3) = 90° and ϕ_i (i=4,5,6) = 120°	155
XLIII. LMR-PES Activated Complex Data for ϕ_i (i=1-6) = 109°28'.	157
XLIV. BEBO Activated Complex Data.	159
XLV. LEPS Activated Complex Data.	161
XLVI. BEBO3 Activated Complex Data for $F_{\beta}^{\ddagger} = 0.0001 \text{ mdyne-}\overset{\circ}{\text{A}}$. . .	163
XLVII. LEPS2 Activated Complex Data for $F_{\beta}^{\ddagger} = 0.0001 \text{ mdyne-}\overset{\circ}{\text{A}}$. . .	165
XLVIII. BEBO3 Activated Complex Data for $F_{\beta}^{\ddagger} = 0.26 \text{ mdyne-}\overset{\circ}{\text{A}}$. . .	167
XLIX. LEPS2 Activated Complex Data for $F_{\beta}^{\ddagger} = 0.26 \text{ mdyne-}\overset{\circ}{\text{A}}$. . .	169
L. BEBO3 Activated Complex Data for $F_{\beta}^{\ddagger} = 0.568 \text{ mdyne-}\overset{\circ}{\text{A}}$. . .	171
LI. LEPS2 Activated Complex Data for $F_{\beta}^{\ddagger} = 0.568 \text{ mdyne-}\overset{\circ}{\text{A}}$. . .	173
LII. Values for $k(\text{CH}_4, \text{H})/k(\text{CH}_4, \text{D})$	176
LIII. Values for $k(\text{CH}_3, \text{H}_2)/k(\text{CH}_3, \text{D}_2)$	177
LIV. Values for $k(\text{CD}_3, \text{H}_2)/k(\text{CD}_3, \text{D}_2)$	178
LV. Values for $k(\text{CH}_3, \text{HD})/k(\text{CH}_3, \text{DH})$	179
LVI. Values for $k(\text{CD}_3, \text{HD})/k(\text{CD}_3, \text{DH})$	180
LVII. Values for $k(\text{CH}_4, \text{H})/k(^{13}\text{CH}_4, \text{H})$	181
LVIII. Values for $k(\text{CH}_3, \text{H}_2)/k(^{13}\text{CH}_3, \text{H}_2)$	182

LIST OF TABLES (Continued)

Table	Page
LIX. Values for $k(\text{CH}_4, \text{H})/k(\text{CD}_3\text{H}, \text{H})$	183
LX. Values for $k(\text{CH}_3, \text{H}_2)/k(\text{CD}_3, \text{H}_2)$	184
LXI. LMR-PES KIES Using Different Transition-State Geometries	185
LXII. LMR-PES KIEs Using Different Transition-State Geometries	186
LXIII. LMR-PES KIEs Using Different Transition-State Geometries	187
LXIV. LMR-PES KIEs Using Different Transition-State Geometries	188

LIST OF FIGURES

Figure	Page
1. Interatomic Distances Used in the LMR-PES	21
2. Grid of Incremented Coordinate Positions for Which Energies Were Calculated	38

CHAPTER I

INTRODUCTION

Within the limits of the Born-Oppenheimer approximation, the equilibrium molecular configuration and the hypersurface expressing the electronic potential energy for nuclear motion as a function of inter-nuclear coordinates are independent of isotopic substitution. However, the kinetics of nuclear motion on the potential-energy surface are affected by isotopic substitution. This phenomenon leads to isotope effects on equilibria and rates of chemical reactions. Since kinetic isotope effects (KIEs) can be treated within the framework of transition-state (absolute rate) theory,¹ experimental kinetic isotope effects can be either predicted from or used to extract information about the potential-energy reaction hypersurface. This research is concerned with experimental and theoretically calculated KIEs in the following reactions.



The purpose of this theoretical investigation is two-fold. First, it serves to test in part the usefulness of the LMR six-body potential-energy surface (LMR-PES) for the thermal reactions (I-1) and (I-2).² In this regard the agreement between experimental and theoretical KIEs,

if the former values are assumed to be accurate, provides information concerning the accuracy of the curvature of the potential-energy surface for motion both parallel and perpendicular to the reaction coordinate. Second, these isotope effects were used to assess the validity of a number of the qualitative interpretations of KIEs developed in physical organic chemistry. It should be pointed out that this research is meant to augment the extensive theoretical studies of KIEs on model systems³ and/or the deduction of transition-state parameters from experimental KIEs.^{3,6,3h,4} Klein has most recently published a literature review of current isotope-effect publications.⁵

The KIEs for various labelled reactants in equations (I-1) and (I-2) were computed within the framework of absolute-reaction-rate theory. The exact equations are expressed in equations (I-3) and (I-4) using the simplified notation of Wolfsberg and Stern,^{3b,6} where

$$\text{KIE} = \frac{k_1}{k_2} \left(\frac{s_2 s_1^\ddagger}{s_1 s_2^\ddagger} \right) = (\text{MMI})(\text{EXC})(\text{ZPE}) \quad (\text{I-3})$$

$$\text{KIE} = \frac{k_1}{k_2} \left(\frac{s_2 s_1^\ddagger}{s_1 s_2^\ddagger} \right) = \frac{v_{1L}^\ddagger}{v_{2L}^\ddagger} (\text{VP})(\text{EXC})(\text{ZPE}) \quad (\text{I-4})$$

k_1/k_2 is the isotopic rate constant ratio and $\left(\frac{s_2 s_1^\ddagger}{s_1 s_2^\ddagger} \right)$ is the ratio of symmetry numbers associated with the isotopic configurations.⁷ MMI is the mass moment of inertia term composed of the molecular weights, M_j , and the moments of inertia, I_{A_j} , I_{B_j} and I_{C_j} , about the three principal axes of the labelled and unlabelled reactants and transition states, see

equation (I-5).⁷ The vibrational excitation term, EXC, and the zero

$$\text{MMI} = \frac{\left(\frac{M_2}{M_1}\right)^{3/2} \left(\frac{I_{A_2} I_{B_2} I_{C_2}}{I_{A_1} I_{B_1} I_{C_1}}\right)^{1/2}}{\left(\frac{M_2^\ddagger}{M_1^\ddagger}\right)^{3/2} \left(\frac{I_{A_2}^\ddagger I_{B_2}^\ddagger I_{C_2}^\ddagger}{I_{A_1}^\ddagger I_{B_1}^\ddagger I_{C_1}^\ddagger}\right)^{1/2}} \quad (\text{I-5})$$

point energy term, ZPE, are given by (I-6) and (I-7), respectively,

$$\text{EXC} = \frac{\prod_{i=1}^{3n-6} \frac{1 - \exp(-u_{1i})}{1 - \exp(-u_{2i})}}{\prod_{i=1}^{3n^\ddagger-7} \frac{1 - \exp(-u_{1i}^\ddagger)}{1 - \exp(-u_{2i}^\ddagger)}} \quad (\text{I-6})$$

$$\text{ZPE} = \frac{\exp \left[\sum_{i=1}^{3n-6} (u_{1i} - u_{2i})/2 \right]}{\exp \left[\sum_{i=1}^{3n^\ddagger-7} (u_{1i}^\ddagger - u_{2i}^\ddagger)/2 \right]} \quad (\text{I-7})$$

where $u_{ji} = hc\nu_{ji}/kT$; h is Planck's constant; c is the velocity of light; k is Boltzmann's constant; T is the temperature in °K; and ν_{ji} is the i^{th} normal mode frequency in cm^{-1} for the j^{th} isotopic species.⁷ By the Teller-Redlich product theorem, MMI can be equated to the vibrational product term, VP, times the ratio $\nu_{1L}^\ddagger/\nu_{2L}^\ddagger$, ν_{1L}^\ddagger and ν_{2L}^\ddagger are the imaginary frequencies representing motion of the light and heavy isotopic species, respectively, along the reaction coordinate

in the transition-state configuration, see (I-8).⁸ Therefore,

$$\text{MMI} = \nu_{1L}^{\ddagger} / \nu_{2L}^{\ddagger} \quad \text{VP} = \nu_{1L}^{\ddagger} / \nu_{2L}^{\ddagger} \frac{\prod_{i=1}^{3n-6} u_{2i}^{\ddagger} / u_{1i}^{\ddagger}}{\prod_{i=1}^{3n-7} u_{2i}^{\ddagger} / u_{1i}^{\ddagger}} \quad (\text{I-8})$$

equations (I-3) and (I-4) are completely equivalent.

The normal mode frequencies and the moments of inertia for the variously labelled species were calculated using force constants and geometries computed from the LMR-PES in the Wolfsberg-Stern modification of the Schachtschneider (WMS) normal mode frequency computer program.⁹ In this way, the theoretically calculated KIEs are expressed as a function of the LMR-PES.

In the reaction represented by (I-1), quasiclassical-trajectory analysis has shown that the LMR-PES reasonably reproduces the isotopic yield ratio $(\text{HT}/\text{CH}_4)/(\text{DT}/\text{CD}_4)$ obtained by Chou and Rowland using translationally hot (2.8 eV) tritium atoms.¹⁰ Chou and Rowland report a value for the yield ratio isotope effect $(\text{HT}/\text{CH}_4)/(\text{DT}/\text{CD}_4)$ of 1.43¹⁰ compared to the computed value of 1.18.² This agreement indicates that the LMR-PES predicted relative isotopic reaction cross sections are reasonably accurate.²

The high temperature limit for KIEs calculated using transition-state theory corresponds to $\nu_{1L}^{\ddagger} / \nu_{2L}^{\ddagger}$.¹¹ The 2.8 eV of translational energy contained by the tritium atoms used in the LMR-PES trajectory analysis computation of the isotopic yield ratio $(\text{HT}/\text{CH}_4)/(\text{DT}/\text{CD}_4)$ corresponds to an ideal gas temperature of approximately 22,000°K. These high-energy tritium atoms collide with room temperature (~300°K

or approximately stationary relative to the tritium atoms) isotopic methane molecules. Even though the tritium atoms translational energies will be moderated to some extent prior to their reactions with methane, their energy distribution will not be Boltzmann. However, as a first approximation translationally hot tritium atoms might exhibit an isotope effect similar to the KIE for the reactions represented by (I-9) and (I-10) at high temperature.



Comparison of the $v_{1L}^\ddagger/v_{2L}^\ddagger$ ratio for (I-9) and (I-10) to the isotopic yield ratio $(\text{HT}/\text{CH}_4)/(\text{DT}/\text{CD}_4)$ is discussed in Chapter III.

Abstraction is the only reaction observed between thermalized hydrogen atoms and thermalized methane molecules, see (I-1). However, translationally hot hydrogen (tritium) atoms also react with methane via substitution as shown in (I-11).



where T^* represents a translationally hot tritium atom.¹⁰ Since transition-state theory assumes a Maxwellian distribution of atom and molecule energies, it is only applicable to computation of KIEs for reactions that occur at thermal energies, for example (I-1) and (I-2).

Kurylo, Hollinden and Timmons have investigated the temperature dependence of the hydrogen (deuterium) atom abstraction from methane.¹²



The isotopic reactions, see (I-1) and (I-12), were run independently and monitored by following the hydrogen or deuterium atom decay with ESR spectroscopy as a function of flow rate and distance down the fast flow reactor tube. Equation (I-13) gives the experimentally observed temperature dependence of k_H/k_D which corresponds to a value of

$$k_H/k_D = 1.38 \exp[(-500 \pm 150)/RT] \quad (\text{I-13})$$

$k_H/k_D = 0.762$ at 424°K .¹² Analysis of the data is complicated by the fact that the deuterium atoms react at a measurable rate with the product CH_3 radicals to give CH_2D and H atoms as well as abstracting H from methane; see equations (I-14) and (I-12).¹²



Due to the error introduced into the experimental determination of the rate constant for (I-12) by (I-14), Kurylo, Hollinden and Timmons found it necessary to approximate the preexponential factor, 1.38, in (I-13) using a simple collision theory calculation.¹²

Kurylo, Hollinden and Timmons compared their experimental results to KIEs calculated using London-Eyring-Polanyi-Sato (LEPS) and bond-energy-bond-order (BEBO) potential-energy surfaces using a computational approach developed by Weston.³ These results are compared to the corresponding transition-state theory computations on the LMR-PES.

The experimental KIEs for the variously isotopically labelled reactants in equation (I-2) are given in Table I. Table II gives the temperature dependences of these results. The different KIEs in Tables I and II are designated according to the isotopic ratio of the

TABLE I
EXPERIMENTAL KIEs

Isotopic Rate Constant Ratio	Temperature °K	k_1/k_2	Source
$k(\text{CH}_3, \text{H}_2)$	296	2.12	a
$k(\text{CH}_3, \text{D}_2)$	399	4.80	b
	403	4.79	c
	403	5.50	d
$k(\text{CD}_3, \text{H}_2)$	296	0.465	a
$k(\text{CD}_3, \text{D}_2)$	402	3.33	b
	403	2.98	c
	403	4.11	d
$k(\text{CH}_3, \underline{\text{H}}\text{D})^{\text{f}}$	296	6.37 ^e	a
$k(\text{CH}_3, \underline{\text{D}}\text{H})$	403	2.33	c
	467	2.08	b
$k(\text{CD}_3, \underline{\text{H}}\text{D})^{\text{f}}$	402	1.81	b
$k(\text{CD}_3, \underline{\text{D}}\text{H})$	402	1.76	c

^aSee Reference 13.

^bSee Reference 14.

^cSee Reference 15.

^dSee Reference 16.

^eTing and Weston state that this value is probably excessively high due to the effect of the high HD pressures required for the hot methyl radical reaction. See Reference 13.

^fThe atom underlined is the one being abstracted by the methyl group.

TABLE II
TEMPERATURE DEPENDENCE OF EXPERIMENTAL KIEs

KIE	A_1/A_2	ΔE cal./mole	Temperature Range °K	Source
$k(\text{CH}_3, \text{H}_2)$	0.911	1327	399-645	b
$k(\text{CH}_3, \text{D}_2)$	0.194	1760	403-564 ^e	c
	0.246	2516	408-571 ^e	d
		1100	409-591	e
$k(\text{CD}_3, \text{H}_2)$	1.592	588	402-611	b
$k(\text{CD}_3, \text{D}_2)$	3.724	-201	410-572 ^e	c
	1.727	701	407-570 ^e	d
$k(\text{CH}_3, \text{HD})$	0.283	1929	467-651	b
$k(\text{CH}_3, \text{DH})$	0.452	1350	408-569	c
$k(\text{CD}_3, \text{HD})$	0.932	546	402-611	b
$k(\text{CD}_3, \text{DH})$	1.73	0	410-572	c

^aKIEs were fit to the Arrhenius equation of the form $\ln(k_1/k_2) = \ln(A_1/A_2) + \Delta E/RT$.

^bSee Reference 14.

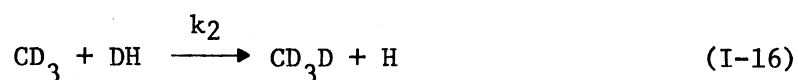
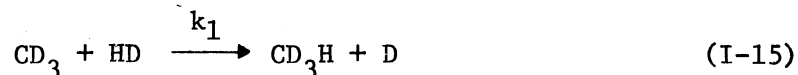
^cSee Reference 15.

^dSee Reference 16.

^eDavison and Burton assumed a steric factor of $S_1/S_2 = 1$ in their calculation of ΔE from their data. See Reference 17.

^fSince Whittle and Steacie and Majury and Steacie did not run simultaneous isotopic reactions the temperatures indicate the smallest range encompassing both isotopic reactions.

corresponding reactants. For example, the KIE designated $k(\text{CD}_3, \text{HD})/k(\text{CD}_3, \text{DH})$ refers to the k_1/k_2 rate constant ratio for the reactions represented by equation (I-15) and (I-16).



Theoretical KIEs were computed for a comparison to the experimental values in Tables I and II and are discussed relative to each other in Chapter III.

Except in the studies done by Ting and Weston,¹³ methyl radicals were generated by photolysis of acetone or acetone-d₆ using a mercury-vapor lamp.^{14,15,16,17} The intensity of the 253.7 nm radiation was minimized in order to reduce the mercury sensitized decomposition and scrambling of isotopic reactants.^{14,15,16,17} Only a small percentage of the initial acetone was photolyzed (Shapiro and Weston,¹⁴ 1-2%; Whittle and Steacie,¹⁵ $\leq 5\%$; Majury and Steacie,¹⁶ $< 10\%$) in order to reduce the occurrence of secondary reactions of methyl radicals with the product methanes. The experimental KIE rate constant ratios in Table I were calculated in terms of the initial concentrations of the isotopic reactants, molecular hydrogen and acetone,^{13b} and the final concentrations of the products, methane¹³⁻¹⁷ and ethane.^{15,16} Shapiro and Weston used competitive techniques to determine the KIEs for CH₃ and CD₃ abstraction from H₂/D₂ mixtures.¹⁴ Majury and Steacie¹⁶ and Whittle and Steacie¹⁵ determined these KIEs by measuring the individual rate constants. As seen in Table I, the Shapiro values appear to agree reasonably well with those of Whittle and Steacie.

However, the temperature dependence data in Table II show that the agreement is somewhat fortuitous. Due to the effect of identical isotopic reaction conditions the KIEs determined by competitive techniques should be the more accurate over the temperature range reported, other factors being equal. Indeed the ensemble of experimental data is contradictory in nature and indicates the necessity for precise evaluation of the status of experimental procedures.

Shapiro and Weston used LEPS and BEBO methods together with their experimental results in an attempt to deduce the transition-state geometry and force constants for reaction (I-2).¹⁴ One deficiency in the LEPS and BEBO functions is that they do not include valence bending force constants between the nonreacting methyl hydrogens and between the nonreacting methyl hydrogens and the hydrogen being abstracted. Therefore, Shapiro and Weston used bending force constants from spectroscopic methane data for the HCH bending coordinates not directly associated with the reaction coordinate motion.¹⁴ These authors investigated the dependence of the KIEs on the assumed magnitudes of the HCH valence bending force constants, F_{β} , associated with the partially formed C-H bond in the transition state.¹⁴ The results from these calculations are discussed in detail in Chapter III. However, it is worth noting that a self-consistent set of transition-state parameters cannot be deduced from the various isotope effects measured for reaction (I-2). It can be seen in Tables I and II that there is considerable difference between the corresponding CH_3 and CD_3 KIE results. This difference must be associated with the transition state force constants. By adjusting the HCH bending force constant in the transition state, Shapiro and Weston could approximately fit either the CH_3 or the CD_3 KIE results, but not both.

Ting and Weston generated hot methyl radicals by photolyzing CH_3Br and CD_3Br with 185 nm light.¹³ The KIE determined for reaction of hot CH_3 with H_2 or D_2 was normal ($k_{\text{H}}/k_{\text{D}} = 2.12$) while the corresponding KIE for CD_3 was inverse ($k_{\text{H}}/k_{\text{D}} = 0.465$); see Table I. Ting and Weston attempted to explain these unusual results using activated-complex theory to calculate the average cross sections for reaction as a function of total energy. The resultant KIEs, $k(\text{CH}_3, \text{H}_2)/k(\text{CH}_3, \text{D}_2) = 1.30$ and $k(\text{CD}_3, \text{H}_2)/k(\text{CD}_3, \text{D}_2) = 1.79$, are not close to the experimental values.¹³ Chapman and Bunker¹⁸ calculated relative cross sections for reaction of both CH_3 and CD_3 with H_2 and D_2 , that is, $\sigma(\text{CH}_3, \text{H}_2)/\sigma(\text{CH}_3, \text{D}_2) = 1.84$ and $\sigma(\text{CD}_3, \text{H}_2)/\sigma(\text{CD}_3, \text{D}_2) = 0.70$, which correlate with Ting and Weston's experimental isotope effects.¹³ The significance of this result is not clear since a cross section ratio is not the same measured or calculated quantity as a KIE. These isotope effects were indicated to occur only for ground state vibrational energy in the methyl radical.¹⁸ However, the Chapman and Bunker results show that vibrational excitation of $\text{H}_2(\text{D}_2)$ tended to preserve this unusual isotope effect and enhance the reaction rates. This enhancement of reaction rates is in agreement with the experimental data of Sims and others for reactions of halogen atoms with H_2 .¹⁹

The transition-state configuration for reactions (I-1) and (I-2) is treated as being linear along the two bonds directly involved in the hydrogen transfer reactions, see (I-17), where r_1^\ddagger is the C-H₁ bondlength,



r_2^\ddagger is the H₁-H₂ bond length and r_1^\ddagger and r_2^\ddagger are collinear. If the CH_3

moiety is treated as a point group, then there are four normal mode frequencies associated with the linear configuration (I-17); ν_S^\ddagger is the symmetric stretching frequency, ν_L^\ddagger is the imaginary asymmetric stretching frequency representing translational motion along the reaction coordinate and ν_B^\ddagger corresponds to the doubly degenerate linear bending frequency. Theoretical treatments of the linear three-center transition-state configuration have often neglected the linear-bending frequencies on the assumption that the sum of the two frequencies compensates for the loss in reactant-state bending frequencies. (That is, in passing from the reactant state to the activated complex no net change in vibrational energy due to the normal vibrational bending modes is associated with the H(D) being transferred.) This allowed the isotope effect to be rationalized as a result of the normal mode stretching vibrations ν_S^\ddagger and ν_L^\ddagger . The transition state harmonic potential energy expression for this simplified configuration is given in (I-18),

$$2V = f_1^\ddagger \Delta r_1^\ddagger + f_2^\ddagger \Delta r_2^\ddagger + 2f_{12}^\ddagger \Delta r_1^\ddagger \Delta r_2^\ddagger \quad (\text{I-18})$$

where f_1^\ddagger and f_2^\ddagger are the stretching force constants associated with r_1^\ddagger and r_2^\ddagger , respectively, f_{12}^\ddagger is the stretching interaction force constant, and Δr_1^\ddagger and Δr_2^\ddagger are deviations from the equilibrium values for r_1^\ddagger and r_2^\ddagger , respectively.²⁰ Bigeleisen²⁰ and Willi and Wolfsberg²¹ have shown that the primary hydrogen (deuterium) KIE is a maximum for a symmetric transition-state configuration where $r_1^\ddagger \approx r_2^\ddagger$ and $f_1^\ddagger \approx f_2^\ddagger$ when $\nu_L^\ddagger = 0$. (That is, the PES is flat at the top of the barrier along the reaction coordinate.) However, Willi and Wolfsberg have demonstrated that if ν_L^\ddagger has an imaginary value then the transition-state bond orders can be

very unequal and still yield a KIE value that is almost identical to the KIE calculated for the symmetric transition-state configuration.²¹

This shows that knowledge of the temperature independent factor, $\nu_{1L}^\ddagger/\nu_{2L}^\ddagger$, is really essential in determining the transition-state configuration. Thus, insight into the transition-state bonding and geometry requires comparison of $\nu_{1L}^\ddagger/\nu_{2L}^\ddagger$ ratios and KIEs calculated from a complete and reasonably accurate potential-energy surface with experimental KIEs and their temperature dependency data.

The approximation of neglecting all bending frequencies associated with the isotopic atom being transferred in a reaction proceeding via a linear three-center activated complex may have some validity at least in certain instances. Kresge and Chiang determined a KIE for a proton transfer reaction involving the hydrolysis of ethyl vinyl ether by HF (or DF). These reactions assumably proceed through a linear transition-state configuration.²² The magnitude of this KIE was considerably less than the value expected. Kresge and Chiang attributed the low KIE to the existence of a doubly degenerate linear-bending frequency in the transition-state configuration which tends to compensate for the loss in the HF (DF) stretching vibration. The magnitude of the bending vibration necessary to cause the observed lowering of the KIE was about 1100 cm^{-1} .²² Kresge and Chiang noted that since 1100 cm^{-1} is not very different from HCX bending frequencies in many molecules this could account for the reasonable success in predicting maximum KIEs with neglect of the bending frequencies associated with the atom being transferred in the activated complex.²² A semi-quantitative estimate of the effect on the KIEs of the C-H-H linear bend in the six-body transition-state configuration, $\text{CH}_3\text{-H-H}$, was

made on the basis of a normal mode frequency analysis using force constants obtained from the LMR-PES. This normal mode frequency analysis allowed an estimate of the inaccuracy that would be incurred by neglecting bending frequencies in the calculation of KIEs for (I-1) and (I-2).

The Swain-Schaad relationship, see (I-19), provides a simple method of relating primary deuterium and tritium KIEs.²³ The

$$k_H/k_T = (k_H/k_D)^{1.442} \quad (\text{I-19})$$

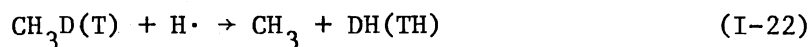
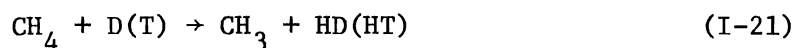
Swain-Schaad relationship takes advantage of the fact that at low temperatures primary hydrogen isotope effects principally reflect changes in the zero-point energy associated with the hydrogen (deuterium or tritium) being transferred in passing from the reactant state to the transition state. The assumptions basic to the Swain-Schaad relationship are as follows. First, in a reaction like (I-1) the isotopic H being transferred is bonded to a polyatomic and relatively heavy molecular entity. Thus, as a reasonable first approximation isotopic substitution affects only the harmonic frequencies associated with the bond to the isotopically substituted atom. Second, no tunneling is assumed to occur.²³ Consequently, the KIE is effectively equated to the ZPE term, see (I-7), involving only the vibrations associated with the H being transferred. For high temperatures Swain and others included a vibrational excitation correction factor, α , based on the temperature dependency of EXC, see (I-6), such that $k_H/k_T = \alpha(k_H/k_D)^{1.442}$.²³

Bigeleisen, using a more complete transition-state theory approach, predicted a range of $1.33 \leq r \leq 1.58$ for the relative deuterium to tritium KIEs where r is defined by (I-20) and $r = 1.442$ is

$$r = \frac{\ln(k_H/k_T)}{\ln(k_H/k_D)} \quad (\text{I-20})$$

equivalent to the Swain-Schaad equation (I-19).²⁴ Stern and Vogel calculated the temperature dependences for r in a large number of model calculations and agreed with Bigeleisen's observation that an experimental value for r lower than 1.33 would be evidence for the existence of tunneling provided that the isotope effects are large primary (or mixed secondary-primary) normal individual isotope effects exhibiting a monotonic temperature dependence.²⁵ However, in a more recent paper Stern and Weston found that there was no direct general correlation between the magnitude of r and the extent of tunneling.²⁶

In this research values of r as a function of temperature were obtained from the calculated KIEs for reaction (I-1) relative to (I-21) and (I-22). Correspondingly similar calculations of r were also



made for the isotopic reactions of equation (I-2). These values are discussed in Chapter III.

A relationship similar to the Swain-Schaad equation has been developed for relating carbon-13 and carbon-14 KIEs. This relationship was tested relative to the transition-state theory

calculated KIEs in a manner similar to that used for the tritium-deuterium relationship.

Bigeleisen has developed equations for relating, $S_2/S_1 f(\frac{2}{1})$, the vibrational partition function ratios of isotopically substituted molecules which are commonly referred to as the rule of the geometric mean (RGM).²⁷ These equations were developed from the relationship between the vibrational frequency sum rules of Decius and Wilson^{27c} and the approximation of the Bigeleisen $S_2/S_1 f(\frac{2}{1})$ factor by the truncated expansion in powers of u_i , see (I-23), where u_i is as

$$\ln[S_2/S_1 f(\frac{2}{1})] \approx 1/24 \sum_i u_{1i}^2 - u_{2i}^2 \quad (\text{I-23})$$

previously defined, see (I-7), and S_2/S_1 is the symmetry number ratio.^{7b} Equation (I-23) is the first-order approximation to the exact equation for $S_2/S_1 f(\frac{2}{1})$, see (I-24), and is valid at sufficiently high tempera-

$$S_2/S_1 f(\frac{2}{1}) = \prod_i \frac{u_{2i}}{u_{1i}} \left(\frac{e^{-u_{2i}/2}}{1 - e^{-u_{2i}}} \right) \left(\frac{e^{-u_{1i}/2}}{1 - e^{-u_{1i}}} \right) \quad (\text{I-24})$$

ture that $u_{1i} \ll 2\pi$. The sum-rule relationships between isotopically different $S_2/S_1 f(\frac{2}{1})$ values approximated by (I-23) require the involvement of three or more different isotopic molecular species.^{27c} Bigeleisen has given a general expression for higher order approximations to $S_2/S_1 f(\frac{2}{1})$, see (I-25), where the B's are Bernoulli numbers

$$\ln(S_2/S_1 f(\frac{2}{1})) = \sum_i^{3n-6} \sum_{j=1}^m (-1)^{j+1} \frac{B_{2j-1} \delta u_i^{2j}}{2j(2j!)} \quad (\text{I-25})$$

($B_1 = \frac{1}{6}$, $B_3 = \frac{1}{30}$, $B_5 = \frac{1}{42}$, et cetera), and $\delta u_i = u_{1i} - u_{2i}$ for $u_{1i} < 2\pi$.^{27b}

Bigeleisen has stated that systems that obey sum rules through the order m will obey the RGM through the order of δu_i^{2m} .^{27b} Some examples of RGM relationships given by Bigeleisen are exhibited in (I-26) through (I-28).^{27b}

$$\left[S_2/S_1 f\left(\frac{\text{CH}_2\text{D}_2}{\text{CH}_3\text{D}}\right) \right]^3 = S_2/S_1 f\left(\frac{\text{CHD}_3}{\text{CH}_4}\right) \quad (\text{I-26})$$

$$\left[S_2/S_1 f\left(\frac{\text{CHD}_3}{\text{CH}_2\text{D}_2}\right) \right]^3 = S_2/S_1 f\left(\frac{\text{CD}_4}{\text{CH}_3\text{D}}\right) \quad (\text{I-27})$$

$$\left[S_2/S_1 f\left(\frac{\text{CHD}_3}{\text{CH}_3\text{D}}\right) \right]^2 = S_2/S_1 f\left(\frac{\text{CD}_4}{\text{CH}_4}\right) \quad (\text{I-28})$$

The Bigeleisen $S_2/S_1 f$ factors are also defined in terms of equation (I-29), where VP·EXC·ZPE are as previously defined, see (I-4).⁷ Using

$$\frac{S_2/S_1 f\left(\frac{2}{1}\right)}{S_2^\ddagger/S_1^\ddagger f\left(\frac{2}{1}\right)} = \text{VP} \cdot \text{EXC} \cdot \text{ZPE} \quad (\text{I-29})$$

(I-29), calculations similar to (I-26) through (I-28) were done using the normal mode frequencies obtained from the LMR-PES, see (I-30) through (I-33). The results of these relationships are discussed in Chapter III.

$$\left[\frac{s_2/s_1 f\left(\frac{\text{CH}_3\text{D}}{\text{CH}_4}\right)}{s_2^\dagger/s_1^\dagger f^\dagger\left(\frac{\text{CH}_2\text{D-H-H}}{\text{CH}_3\text{-H-H}}\right)} \right]^3 = \frac{s_2/s_1 f\left(\frac{\text{CHD}_3}{\text{CH}_4}\right)}{s_2^\dagger/s_1^\dagger f^\dagger\left(\frac{\text{CD}_3\text{-H-H}}{\text{CH}_3\text{-H-H}}\right)} \quad (\text{I-30})$$

$$\left[\frac{s_2/s_1 f\left(\frac{\text{CH}_3\text{D}}{\text{CH}_4}\right)}{s_2^\dagger/s_1^\dagger f^\dagger\left(\frac{\text{CH}_2\text{D-H-H}}{\text{CH}_3\text{-H-H}}\right)} \right]^2 = \frac{s_2/s_1 f\left(\frac{\text{CH}_2\text{D}_2}{\text{CH}_4}\right)}{s_2^\dagger/s_1^\dagger f^\dagger\left(\frac{\text{CHD}_2\text{-H-H}}{\text{CH}_3\text{-H-H}}\right)} \quad (\text{I-31})$$

$$\left[\frac{s_2/s_1 f\left(\frac{\text{CH}_2\text{D}}{\text{CH}_3}\right)}{s_2^\dagger/s_1^\dagger f^\dagger\left(\frac{\text{CH}_2\text{D-H-H}}{\text{CH}_3\text{-H-H}}\right)} \right]^3 = \frac{s_2/s_1 f\left(\frac{\text{CD}_3}{\text{CH}_3}\right)}{s_2^\dagger/s_1^\dagger f^\dagger\left(\frac{\text{CD}_3\text{-H-H}}{\text{CH}_3\text{-H-H}}\right)}$$

$$\left[\frac{s_2/s_1 f\left(\frac{\text{CH}_2\text{D}}{\text{CH}_3}\right)}{s_2^\dagger/s_1^\dagger f^\dagger\left(\frac{\text{CH}_2\text{D-H-H}}{\text{CH}_3\text{-H-H}}\right)} \right]^2 = \frac{s_2/s_1 f\left(\frac{\text{CHD}_2}{\text{CH}_3}\right)}{s_2^\dagger/s_1^\dagger f^\dagger\left(\frac{\text{CHD}_2\text{-H-H}}{\text{CH}_3\text{-H-H}}\right)} \quad (\text{I-33})$$

CHAPTER II

COMPUTATIONAL PROCEDURES

Calculation of Force Constants and Geometries

General

The application of transition-state theory to the calculation of kinetic isotope effects for reactions (I-1) and (I-2) by equations (I-3) and (I-4) requires the normal-mode vibrational frequencies associated with the isotopic reactant and transition-state molecular species. Calculation of these normal mode frequencies requires the force constant description of the bonding in the various molecular species and the associated geometry and atomic masses. The harmonic force-constant description is calculated as the second derivative of the internal energy of a molecular species with respect to an internal coordinate motion.²⁸ For example, molecular hydrogen, H₂, has the bond stretching internal coordinate defined by r_H.

If V is the internal potential function for H₂, then the force constant F_H is given by $\frac{\partial^2 V}{\partial r_H^2} \Big|_{r_H = (r_H)_{eq}}$. The normal-mode frequency for this simple

molecule is calculated by $\nu_H = 2\pi \left(\frac{F_H}{\mu_H} \right)^{1/2}$, where μ_H is the reduced mass of the H₂ molecule. Normal-mode frequencies for large molecular species are calculated using the WMS program method described in Appendix B.⁹

Description of the LMR-PES

The LMR-PES is defined as a sum of three-body interactions plus harmonic bond-bond interactions, where the three-body terms,

$$\begin{aligned}
 V(R_i, \theta_j) = & T(r_1, r_5, r_6) + T(r_2, r_5, r_7) + T(r_3, r_5, r_8) \\
 & + T(r_4, r_5, r_9) + \frac{1}{2} \sum_{j=1}^6 k_j (\theta_j - \theta_j^0)^2
 \end{aligned}
 \tag{II-1}$$

$T(r_{AB}, r_{AC}, r_{BC})$, and the harmonic bond-bond terms $k_j (\theta_j - \theta_j^0)^2$ are defined in terms of the LMR-PES internal coordinates shown in Figure 1 and/or designated in Table III. Values of the internal coordinates for the $\text{CH}_4 + \text{H}$ and $\text{CH}_3 + \text{H}_2$ reactant states are also presented in Table III. Each of the three-body terms in equation (II-1) are defined in terms of the interaction energies between the two atoms in the diatomic pairs represented by the interatomic distances r_i , r_j , and r_k ,

$$T(r_i, r_j, r_k) = Q_{AB} + Q_{AC} + Q_{BC}
 \tag{II-2a}$$

$$1/2[(J_{AB} - J_{BC})^2 + (J_{AC} - J_{AB})^2 + (J_{BC} - J_{AC})^2]^{1/2}$$

$$Q_{\alpha\beta} = [{}^1E_{\alpha\beta} + {}^3E_{\alpha\beta}] / 2
 \tag{II-2b}$$

$$J_{\alpha\beta} = [{}^1E_{\alpha\beta} - {}^3E_{\alpha\beta}] / 2
 \tag{II-2c}$$

where ${}^1E_{\alpha\beta}$ and ${}^3E_{\alpha\beta}$ are the singlet and triplet state energies, respectively, for each $\alpha\beta$ diatomic system. The singlet state energy is represented by a Morse function, see(II-3), where r_n is the interatomic

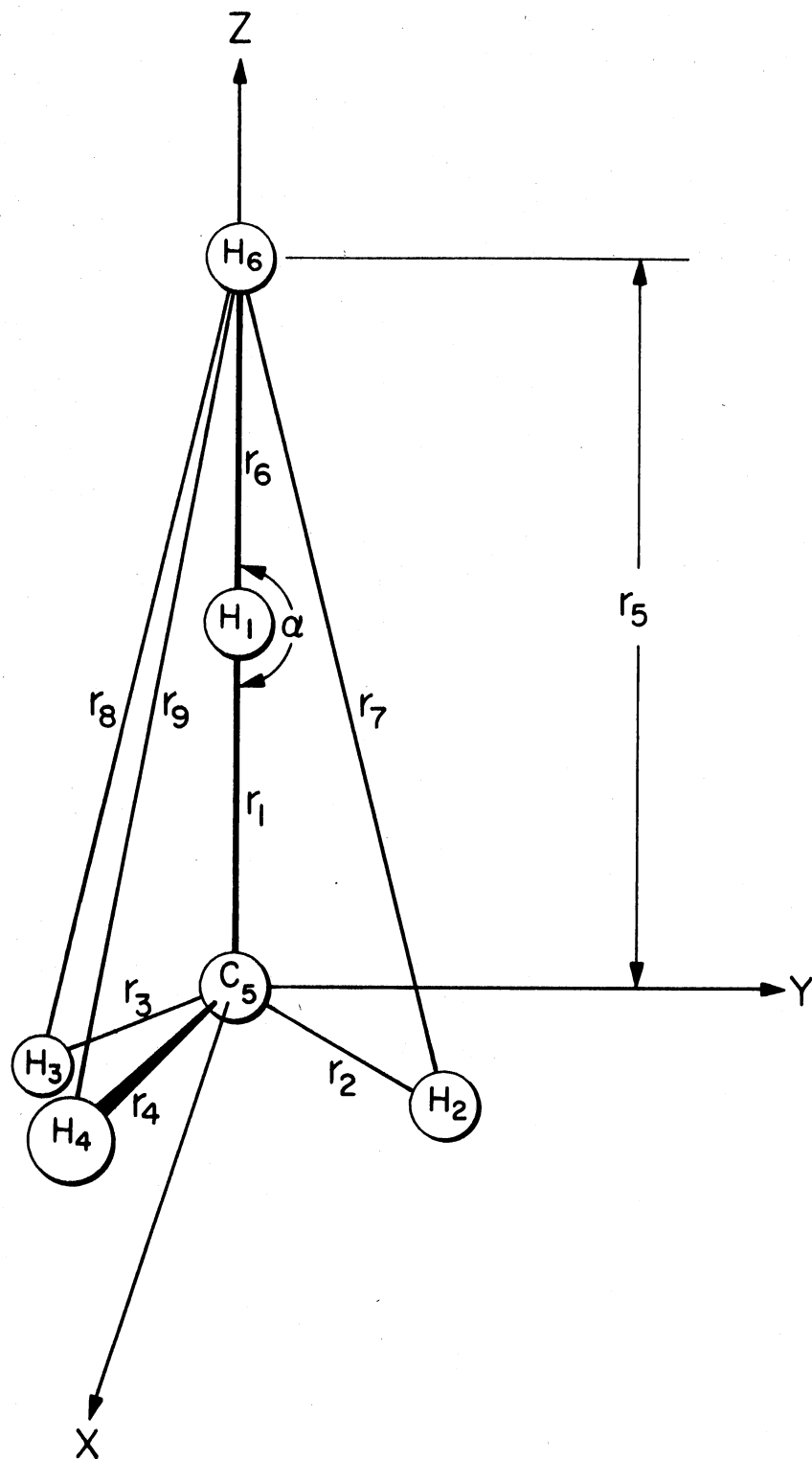


Figure 1. Interatomic Distances Used in the LMR-PES

TABLE III
 LMR-PES AND VALENCE INTERNAL COORDINATES
 DESIGNATIONS AND VALUES FOR REACTANTS

Atoms in Coordinate	LMR-PES Designation	Equilibrium Values and Valence Coordinates Designations for			
		CH ₄ + H		CH ₃ + H ₂	
		Value ^a	Coordinate ^b	Value ^a	Coordinate ^b
CH ₁	r ₁	2.0673	R ₁	20.0000	
CH ₂	r ₂	2.0673	R ₂	2.0673	R ₁
CH ₃	r ₃	2.0673	R ₃	2.0673	R ₂
CH ₄	r ₄	2.0673	R ₄	2.0673	R ₃
CH ₆	r ₅	1002.0673		21.4020	
H ₁ H ₆	r ₆	1000.0000		1.4020	R ₁ ^c
H ₂ H ₆	r ₇	1002.7583		21.5016	
H ₃ H ₆	r ₈	1002.7583		21.5016	
H ₄ H ₆	r ₉	1002.7583		21.5016	
H ₁ CH ₂	θ ₁	109.4712	φ ₁	90	
H ₁ CH ₃	θ ₂	109.4712	φ ₂	90	
H ₁ CH ₄	θ ₃	109.4712	φ ₃	90	
H ₂ CH ₃	θ ₄	109.4712	φ ₄	120	φ ₁
H ₂ CH ₄	θ ₅	109.4712	φ ₅	120	φ ₂
H ₃ CH ₄	θ ₆	109.4712	φ ₆	120	φ ₃

^aBond lengths and interatomic distances in atomic units and bond angles are in degrees.

^bOut-of-plane bending valence coordinate for CH₃ is not defined by the LMR-PES.

^cSpecifies the vibrational motion of H₂.

$${}^1E_{\alpha\beta} = D[\exp\{-2\alpha(r_n - r_e)\} - 2\exp\{-\alpha(r_n - r_e)\}] \quad (\text{II-3})$$

distance between one of the nine $\alpha\beta$ diatomic pairs in Table III, r_e is the equilibrium $\alpha\beta$ bond distance, D is the bond dissociation energy plus the zero-point energy, and α is the exponential Morse parameter.² As shown in equation (II-4), the triplet state energy is given by a

$${}^3E_{\alpha\beta} = {}^3D[\exp\{-2\beta(r_n - r_e)\} + 2\exp\{-\beta(r_n - r_e)\}] \quad (\text{II-4})$$

similar functional representation for the condition that all $r_n \leq r^*$. If $r_n > r^*$ then ${}^3E_{\alpha\beta}$ is represented by (II-5). Thus, r^* is the

$${}^3E_{\alpha\beta} = C[r_n + A]\exp(\sigma r_n) \quad (\text{II-5})$$

changeover point between the functional forms (II-4) and (II-5). Values for the triplet state parameters in (II-4) and (II-5) are given in Table IV. These parameters were empirically determined by a procedure previously described by Raff and coworkers.^{2,29} The harmonic bond-bond interaction terms, $1/2 \sum_{j=1}^6 k_j (\theta_j - \theta_j^0)^2$, are a function of the six HCH angles described in Table III, where the θ_j^0 are the angles characteristic of the equilibrium molecular configuration and the θ_j and k_j are the angles and bending force constants, respectively, for a specified molecular configuration. The force constant values are determined by (II-6),

$$k_j = k_j^0 f(r_{C-H_i}, r_{H_i-H_6}) f(r_{C-H_\ell}, r_{H_\ell-H_6}) \quad (\text{II-6})$$

with $i = 1, 2, 3, 4$, $\ell = 1, 2, 3, 4$ and $\ell \neq i$. The equilibrium bending force

TABLE IV
LMR-PES PARAMETERS

Parameter	Diatomic Pair		
	C-H	C-H' ^a	H-H
D ^b	4.5808	1.1452	4.7466
α ^c	0.98058	0.98058	1.04435
r _e ^d	2.0673	2.0673	1.402
D _e ^b	1.63	0.4075	1.9668
β ^c	0.60	0.60	1.000122
C ^b	3675.92	918.98	25.55301785
A ^d	-2.360263	-2.360263	1.0
σ ^c	2.296479	2.296479	1.6756385
r* ^d	3.0	3.0	1.6
a ₁ ^e	0.8999975		
a ₂ ^e	0.448035		
a ₃ ^e	0.606528		
a ₄ ^e	3.239921		
a ₅ ^e	0.080768		

^aCorresponds to the two atoms describing r₅ in Table III.

^bIn units of electron volts (eV).

^cIn (atomic units (a.u.))⁻¹.

^dIn a.u.

^eIn (a.u.)⁻².

constant k_j^0 equals 3.4436 eV/rad.² Each $f(r_{C-H}, r_{H-H_6})$ term is a function of one of the C-H bonds defining the angle θ_j and the corresponding interatomic distance between the hydrogen bonded to the carbon and the abstracting hydrogen, H_6 . The form of the $f(r_{C-H}, r_{H-H_6})$ function was determined by a nonlinear least squares fit to INDO calculated results as given by (II-7),

$$f(r_{C-H}, r_{H-H_6}) = k_j/k_j^0 = A_1 \exp\{-A_2 [r_{C-H} - r_e(C-H)]^2\} \quad (\text{II-7a})$$

$$A_1 = 1.0 - \exp(-a_1 r_{H-H_6}^2) \quad (\text{II-7b})$$

$$A_2 = a_2 + a_3 \exp\{-a_4 [r_{H-H_6} - r_e(H-H)]^2\} \quad (\text{II-7c})$$

where the coefficients A_1 , A_2 , a_1 , a_2 , a_3 , and a_4 were all determined by nonlinear least squares procedures and $r_e(C-H)$ in (II-7a) and $r_e(H-H)$ in (II-7c) refer to the equilibrium C-H and H-H bond lengths, respectively.² The equilibrium frontside angles, θ_f ($f=1,2,3$), are determined by the functional relationship given by (II-8),

$$\theta_f^0 = \tau - a_5 [r^+ - r_e(C-H)], \quad (r^+ \leq 6.274 \text{ a.u.}) \quad (\text{II-8a})$$

$$\theta_f^0 = 90^\circ, \quad (r^+ > 6.274 \text{ a.u.}) \quad (\text{II-8b})$$

where τ is the tetrahedral angle in radians, and a_5 and the value 6.274 were determined from INDO computational results. The longest C-H bond length in the five atom CH_4 methane configuration is designated as r^+ (in the transition state $r^+ = r_1$), and r_e is the equilibrium C-H bond

length. The equilibrium backside angles, θ_b ($b=4,5,6$), are functions of the frontside angles, see (II-9). The values of the constants used in

$$\theta_b^\circ = \arccos(1.0 - 1.5 \sin^2 \theta_f^\circ) \quad (\text{II-9})$$

the LMR-PES function calculations are given in Table IV. It should be noted that the energy parameters, D , D_3 , and C , for the C-H' values are 25 percent of the C-H values because the C-H' interaction is counted once in each of the four three-body terms in (II-1).

Reactant and Product Geometries and Coordinates

The general six-atom configuration is given by Figure 1. Table III compares the LMR-PES internal coordinate designations and geometry values for the reactants and products in equations (I-1) and (I-2) to the corresponding internal valence coordinate designations for which force constants are calculated. The two-atom internal valence coordinate designations describe bond stretching vibrational motion and the three-atom designations describe bond bending vibrational motion. It should be noted that in Table III the internal valence coordinates for the reactants and products are direct functions of the corresponding LMR-PES internal coordinates except for the out-of-plane bending valence coordinate which is not defined by the functional form of the LMR-PES. By equation (II-8), the LMR-PES predicts a planar CH_3 geometry. However, by (II-6) and (II-7) when CH_3 is planar then the k_j ($j=1,2,3$) force constant terms in the LMR-PES which describe the out-of-plane bending motion in CH_3 are effectively zero. For this reason the calculation of the out-of-plane bending force constant value is handled separately from the LMR-PES force constant calculations which follow.

Transition-State Geometry and Coordinates

The transition-state geometry values are given in Table V for the LMR-PES coordinates. Unlike the reactants and products coordinates, all of the transition-state LMR-PES coordinates contribute significantly to the calculated energy. Therefore, since not all the LMR-PES coordinates correspond to a valence coordinate, the valence coordinates were expressed as a function of the appropriate LMR-PES coordinates involved in each internal valence coordinate designation. Force constants were calculated with respect to these designated internal valence coordinates.

The transition-state geometry values in Table V were obtained by scanning the LMR-PES for the top of the barrier along the reaction coordinate. The coordinates r_1 and r_6 were initialized at values greater and less than their corresponding equilibrium values from Table IV, respectively. The r_1 coordinate is then decremented 100 times (or until a minimum energy is found) at each r_6 incremented coordinate value. These minimum energy configurations describe the reaction coordinate for reactions (I-1) and (I-2). The maximum energy along the reaction coordinate corresponds to the top of the barrier. The barrier height energy is obtained by subtracting the reactant $\text{CH}_4 + \text{H}$ internal energy from the configuration energy at the top of the barrier. Table VI shows the results of a consecutive series of concurrent scans of the LMR-PES to find the top of the barrier.

TABLE V
 LMR-PES AND VALENCE INTERNAL COORDINATES DESIGNATIONS
 AND VALUES FOR THE TRANSITION STATE

LMR-PES Coordinates			Valence Coordinates	
Atoms in Coordinate	Designation	Equilibrium ^a Value	Atoms in Coordinate	Designation
CH ₁	r ₁	3.0178	CH ₁	R ₁ = f(r ₁ , r ₅ , r ₇ , r ₈ , r ₉)
CH ₂	r ₂	2.0673	CH ₂	R ₂ = f(r ₂ , r ₇)
CH ₃	r ₃	2.0673	CH ₃	R ₃ = f(r ₃ , r ₈)
CH ₄	r ₄	2.0673	CH ₄	R ₄ = f(r ₄ , r ₉)
CH ₆	r ₅	4.4982	H ₁ H ₆	R ₅ = f(r ₅ , r ₆ , r ₇ , r ₈ , r ₉)
H ₁ H ₆	r ₆	1.4804	H ₁ CH ₂	φ ₁ = f(θ ₁ , r ₇)
H ₂ H ₆	r ₇	5.4170	H ₁ CH ₃	φ ₂ = f(θ ₂ , r ₈)
H ₃ H ₆	r ₈	5.4170	H ₁ CH ₄	φ ₃ = f(θ ₃ , r ₉)
H ₄ H ₆	r ₉	5.4170	H ₂ CH ₃	φ ₄ = f(θ ₄ , r ₇ , r ₈)
H ₁ CH ₂	θ ₁	105.0726	H ₂ CH ₄	φ ₅ = f(θ ₅ , r ₇ , r ₉)
H ₁ CH ₃	θ ₂	105.0726	H ₃ CH ₄	φ ₆ = f(θ ₆ , r ₈ , r ₉)
H ₁ CH ₄	θ ₃	105.0726	(CH ₁ H ₆) _{xz} ^b	α _x = f(r ₅ , r ₇ , r ₈ , r ₉)
H ₂ CH ₃	θ ₄	113.4886	(CH ₁ H ₆) _{yz} ^c	α _y = f(r ₅ , r ₇ , r ₈ , r ₉)
H ₂ CH ₄	θ ₅	113.4886		
H ₃ CH ₄	θ ₆	113.4886		

^aBond lengths and interatomic distances in atomic units and bond angles in degrees.

^bSpecifies linear bending in the xz plane.

^cSpecifies linear bending in the yz plane.

TABLE VI
TRANSITION-STATE SCANNING RESULTS

Scan Number	r_1^a	r_6^a	Increment Size ^a	Barrier Height Energy ^b
Start 1 ^c	3.5	1.25	7.5×10^{-3}	5.60624735710553
End 1 ^d	3.02	1.49		
Start 2 ^c	3.0275	1.475	1.5×10^{-4}	5.59759021152999
End 2 ^d	3.0179	1.48055		
Start 3 ^c	3.0182	1.48025	6.0×10^{-6}	5.59758731815947
End 3 ^d	3.017804	1.480382		
Start 4 ^c	3.017816	1.48037	2.4×10^{-7}	5.59758731610498
End 4 ^d	3.0177992	1.4803774		
Start 5 ^c	3.01779968	1.48037696	9.6×10^{-9}	5.59758731609884
End 5 ^d	3.0177991232	1.4803772096		
Start 6 ^c	3.0177991424	1.4803771904	3.84×10^{-10}	5.59758731609884
End 6 ^d	3.017799132032	1.480377204608		

^aValues in atomic units (a.u.).

^bValues in kilocalories per mole for reaction (I-1).

^cValues at the start of the scan.

^dValues at the end of the scan.

Numerical Methods of Force Constant

Determination

Force constants were calculated numerically for each of the internal valence coordinates described in Tables III and V. Additionally, off-diagonal cross term force constants were calculated. These force constants determine the amount of interaction between any two of the valence coordinates in a particular molecular species. These force constants are defined by the value of $(\frac{\partial}{\partial q_i} \frac{\partial}{\partial q_j})_{q_k \neq q_i, q_j}$, where q_i and q_j are valence coordinates of a molecular species defined in Table III or Table V. If $q_i = q_j$, then the second derivative is a diagonal force constant, but if $q_j \neq q_i$, it is an interaction force constant.

The simplest numerical partial differentiation technique used is the two function-point definition of a derivative,

$$\lim_{h \rightarrow 0} \frac{f(x+h, y) - f(x, y)}{h} = f_{1,1}(x, y) = \frac{\partial f(x, y)}{\partial x} \quad (\text{II-10})$$

where $f(x, y)$ is a function of variables x and y , and h is the increment size.³⁰ Equation (II-10) was used to generate the three-point second derivative method given by (II-11).³⁰

$$\lim_{h \rightarrow 0} \left[\frac{\left(\frac{f(x+h, y) - f(x, y)}{h} \right) - \left(\frac{f(x, y) - f(x-h, y)}{h} \right)}{h} \right] =$$

$$\lim_{h \rightarrow 0} \frac{f(x+h, y) + f(x-h, y) - 2f(x, y)}{h^2} = f_{1,1}(x, y) = \frac{\partial^2 f(x, y)}{\partial x^2}$$

$$f_{1,1}(x, y) \approx \frac{f(x+h, y) + f(x-h, y) - 2f(x, y)}{h^2} \quad (\text{II-11})$$

The error in (II-11) is equal to

$$E_d = -\frac{h^2}{12} f^{IV}(\xi) \quad (\text{II-12})$$

where h is the increment size and $f^{IV}(\xi)$ is the fourth derivative of the function being differentiated with $|\xi-x| < |h|$.³⁰ This error is referred to as the discretization error due to the method of finite differences and is in addition to any round-off error.³⁰ For double precision accuracy on the IBM 360/65 used for these calculations, the relative round-off error is approximately 1×10^{-16} . An estimate of the error involved in the calculation of (II-11) with $f(x,y) = [g(x) + k(y)]$, where $g(x) = C^2 e^{-2x} - 2Ce^{-x}$, $C = e^2$, $x = 2$, $h = 1 \times 10^{-4}$ and $k(y) = 0$ is given by

$$E = (E_d + \frac{4E_r}{h^2}) = [\frac{-(1 \times 10^{-4})^2}{12} (16C^2 e^{-2x} - 2Ce^{-x}) + \frac{4E_r}{(1 \times 10^{-4})^2}] \quad (\text{II-13})$$

where E_r is the approximate round-off error in each of the four function values in (II-11). If $E_r \cong 1 \times 10^{-16}$ then the relative error in the evaluation of (II-11) for $f(x,y)$ is given by $E_{\text{Rel}} = E/f(x,y) \cong -1.4 \times 10^{-8}$. Although the exact error involved in numerical differentiation of (II-1) is not calculated, the functional form is composed primarily of negative exponential terms with relatively small exponents. Therefore, the relative error involved in applying (II-11) to (II-1) should be close to that for (II-13) within two or three orders of magnitude. The following difference method for cross-terms should have comparably small error.

A computational method was derived for calculation of the off-diagonal (cross term) second derivatives of the form $\frac{\partial}{\partial x} (\frac{\partial f(x,y)}{\partial y})_x = f_{1,2}(x,y)$. For purposes of derivation, a function of the incremented coordinates was defined by

$$Q_{h,k}(\delta) = f(x + \delta h, y + \delta k) \quad (\text{II-14})$$

where δ/x and $\delta/y \ll 1$ and h and k are unit directional coefficients of δ having possible values of 1, 0, or -1. By deriving a functional form for the second derivative of $Q_{h,k}(\delta)$ it was possible to obtain a numerical approximation to $f_{1,2}(x,y)$. The first derivative of $Q_{h,k}(\delta)$ is defined by (II-15),

$$\begin{aligned} Q'_{h,k}(\delta) &= \frac{\partial f(x + \delta h, y + \delta k)}{\partial \delta} \\ Q'_{h,k}(\delta) &= \frac{\partial f(x + \delta h, y + \delta k)}{\partial (x + \delta h)} \cdot \frac{\partial (x + \delta h)}{\partial \delta} + \frac{\partial f(x + \delta h, y + \delta k)}{\partial (y + \delta k)} \cdot \frac{\partial (y + \delta k)}{\partial \delta} \\ Q'_{h,k}(\delta) &= hf_1(x + \delta h, y + \delta k) + kf_2(x + \delta h, y + \delta k) \end{aligned} \quad (\text{II-15})$$

where $f_2(x + \delta h, y + \delta k) = \frac{\partial f(x + \delta h, y + \delta k)}{\partial (y + \delta k)}$, f_1 is defined by (II-10), $h = \frac{\partial (x + \delta h)}{\partial \delta}$ and $k = \frac{\partial (y + \delta k)}{\partial \delta}$. Therefore, the second derivative of $Q_{h,k}(\delta)$ is given by (II-16),

$$\begin{aligned} Q''_{h,k}(\delta) &= h \left[\frac{\partial f_1(x + \delta h, y + \delta k)}{\partial (x + \delta h)} \cdot \frac{\partial (x + \delta h)}{\partial \delta} + \frac{\partial f_1(x + \delta h, y + \delta k)}{\partial (y + \delta k)} \cdot \frac{\partial (y + \delta k)}{\partial \delta} \right] \\ &+ k \left[\frac{\partial f_2(x + \delta h, y + \delta k)}{\partial (x + \delta h)} \cdot \frac{\partial (x + \delta h)}{\partial \delta} + \frac{\partial f_2(x + \delta h, y + \delta k)}{\partial (y + \delta k)} \cdot \frac{\partial (y + \delta k)}{\partial \delta} \right] \end{aligned}$$

$$Q''_{h,k}(\delta) = h^2 f_{1,1}(x + \delta h, y + \delta k) + 2hkf_{1,2}(x + \delta h, y + \delta k) + k^2 f_{2,2}(x + \delta h, y + \delta k) \quad (\text{II-16})$$

where $f_{2,2}(x + \delta h, y + \delta k) = \frac{\partial^2 f(x + \delta h, y + \delta k)}{[\partial (y + \delta k)]^2}$ and $f_{1,2}(x + \delta h, y + \delta k) =$

$f_{2,1}(x + \delta h, y + \delta k)$. Therefore, the second derivative, $Q''_{h,k}(\delta)$, for $\delta = 0$ is given by (II-17).

$$Q''_{h,k}(0) = h^2 f_{1,1}(x,y) + 2hkf_{1,2}(x,y) + k^2 f_{2,2}(x,y) \quad (\text{II-17})$$

Using the definition of $Q_{h,k}(\delta)$ in equation (II-14), $Q''_{h,k}(0)$ is also defined by (II-18).

$$Q''_{h,k}(0) = \lim_{\delta \rightarrow 0} \frac{Q_{h,k}(\delta) - 2Q_{h,k}(0) + Q_{h,k}(-\delta)}{\delta^2} \quad (\text{II-18})$$

The difference equations used to calculate the second derivatives of the form of $f_{1,2}(x,y)$ were obtained by combining (II-14), (II-17) and (II-18) for various pairs of (h,k) values. For example, one difference equation is given by substituting $h=1, k=0$ into (II-17), see (II-19a); then equating (II-19a) to (II-18) in (II-19b). The specific form of (II-19b) used to obtain the numerical second derivative is given by substitution of (II-14) with $(h,k) = (1,0)$ into (II-19b), see (II-19c).

$$Q''_{h,k}(0) = Q''_{1,0}(0) = (1)^2 f_{1,1}(x,y) + 2(1)(0)f_{1,2}(x,y) + (0)^2 f_{2,2}(x,y) \quad (\text{II-19a})$$

$$Q''_{1,0}(0) = f_{1,1}(x,y) = \lim_{\delta \rightarrow 0} \frac{Q_{1,0}(\delta) - 2Q_{1,0}(0) + Q_{1,0}(-\delta)}{\delta^2} \quad (\text{II-19b})$$

$$Q''_{1,0}(0) = f_{1,1}(x,y) = \lim_{\delta \rightarrow 0} \frac{f(x+\delta,y) - 2f(x,y) + f(x-\delta,y)}{\delta^2} \quad (\text{II-19c})$$

Similarly for $(h,k) = (0,1)$, equations (II-14) and (II-18) lead to equation (II-20) which defines $f_{2,2}(x,y)$.

$$Q''_{0,1}(0) = \lim_{\delta \rightarrow 0} \frac{f(x, y + \delta) - 2f(x, y) + f(x, y - \delta)}{\delta^2} \quad (\text{II-20})$$

Finally, substitution of $(h, k) = (1, 1)$ into (II-17), (II-18) and (II-14) produces an expression which includes the desired cross term $f_{1,2}(x, y)$, see (II-21).

$$Q''_{1,1}(0) = (1)^2 f_{1,1}(x, y) + 2(1)(1) f_{1,2}(x, y) + (1)^2 f_{2,2}(x, y)$$

$$Q''_{1,1}(0) = f_{1,1}(x, y) + 2f_{1,2}(x, y) + f_{2,2}(x, y) \quad (\text{II-21a})$$

$$Q''_{1,1}(0) = \lim_{\delta \rightarrow 0} \frac{Q_{1,1}(\delta) - 2Q_{1,1}(0) + Q_{1,1}(-\delta)}{\delta^2}$$

$$Q''_{1,1}(0) = \lim_{\delta \rightarrow 0} \frac{f(x + \delta, y + \delta) - 2f(x, y) + f(x - \delta, y - \delta)}{\delta^2} \quad (\text{II-21b})$$

By rearrangement of (II-21a), $f_{1,2}(x, y) = [Q''_{1,1}(0) - f_{1,1}(x, y) - f_{2,2}(x, y)]/2$. This result and the definition of $f_{1,1}(x, y)$ and $f_{2,2}(x, y)$ in (II-19) and (II-20), respectively, led to equation (II-22) which defines the cross term second derivative.

$$f_{1,2}(x, y) = \frac{Q''_{1,1}(0) - Q''_{1,0}(0) - Q''_{0,1}(0)}{2} \quad (\text{II-22})$$

The general difference method equations are summarized in Table VII.

The symbols A, B, C, D and E in Table VII represent second derivatives in the limit as the increment size δ approaches zero. Thus for a given δ , A and B constitute numerical approximations to the diagonal force constants (second derivatives), $(\delta^2 f(x, y) / \delta x^2)_y$ and

TABLE VII
SUMMARY OF THREE-POINT CROSS-TERM DIFFERENCE EQUATIONS^a

Unit ^b Increment Pair	Definition of ^c Second Derivative	Difference Method Approximation ^d to the Second Derivative
(h,k) = (1,0)	$f_{1,1}(x,y) = \lim_{\delta \rightarrow 0} A$	$A = \frac{f(x+\delta,y) - 2f(x,y) + f(x-\delta,y)}{\delta^2}$
(h,k) = (0,1)	$f_{2,2}(x,y) = \lim_{\delta \rightarrow 0} B$	$B = \frac{f(x,y+\delta) - 2f(x,y) + f(x,y-\delta)}{\delta^2}$
(h,k) = (1,1)	$Q''_{1,1}(0) = \lim_{\delta \rightarrow 0} D$	$D = \frac{f(x+\delta,y+\delta) - 2f(x,y) + f(x-\delta,y-\delta)}{\delta^2}$
(h,k) = (1,-1)	$Q''_{1,-1}(0) = \lim_{\delta \rightarrow 0} E$	$E = \frac{f(x+\delta,y-\delta) - 2f(x,y) + f(x-\delta,y+\delta)}{\delta^2}$
	$f_{1,2}(x,y) = \lim_{\delta \rightarrow 0} C$	$C = \frac{D-A-B}{2} = \frac{A+B-E}{2} = \frac{D-E}{4}$

^aSee Reference 31.

^bSee Equations (II-19), (II-20), and (II-21).

^cDefinitions based on combination of Equations (II-14), (II-17), and (II-18).

^dDifference methods based on Equations (II-14) and (II-18). Note Equation C is only definable as a combination of other difference methods. Also, the increment size δ should be identical in all equations used for each calculation of C.

$(\partial^2 f(x,y)/\partial y^2)_x$, respectively. For a given δ , D is the numerical estimate of $\partial^2 Q_{1,1}(0)/\partial \delta^2$. Therefore, given a specific δ the numerical approximation to the off-diagonal force constant, $\partial^2 f(x,y)/\partial x \partial y$, is obtained by substituting A, B, and D into (II-22). The symbol E in Table VII is defined in the same manner as D, except for $(h,k) = (1,-1)$. Thus for a given δ , E is the numerical estimate of $\partial^2 Q_{1,-1}(0)/\partial \delta^2$. By substituting the numerical approximations A, B, and C for the appropriate analytical second derivatives in (II-17) with $(h,k) = (1,-1)$, E is defined as the quantity $(A - 2C + B)$. This definition of E leads to the last two quantities equated to C in Table VII which constitute two additional numerical approximations to the off-diagonal force constant (or cross-term second derivative).

The energy values obtained from six equal increments and decrements about a particular cartesian coordinate were least squares fitted to a quadratic equation, see (II-23).³² A numerical estimate of the

$$V = Kx^2 + Lx + M \quad (\text{II-23})$$

cartesian coordinate force constant is then provided by the analytic second derivative of this quadratic equation, $\partial^2 V/\partial x^2 = 2K$.

A seven point difference method based on the differentiation of a Lagrangian interpolation function was also used to calculate force constants for comparison to the three-point and polynomial least-squares methods.³³ As shown in Equation (II-24) the derivative is

$$V'_0 = \frac{\partial V_0}{\partial q_1} = \frac{1}{60h} [45(V_1 - V_{-1}) - 9(V_2 - V_{-2}) + (V_3 - V_{-3})] \quad (\text{II-24})$$

calculated at the center (equilibrium) point, $V_0 = f(q_1)$, using

energies $V_\ell = f(q_i + \ell h)$ for three equally incremented and decremented (that is $\ell = \pm 3, \pm 2, \pm 1$) points, where h is the increment size and q_i is the coordinate being incremented. Thus a particular force constant V_j'' was evaluated as follows. For a given h , potential energies V_j were computed for $j = 0$ and ± 1 to ± 6 . Equation (II-24) and these V_j were used to obtain first derivatives V_j' at $j = \pm 3, \pm 2, \pm 1$. Equation (II-24) and these V_j' values were then used to calculate V_j'' at $j = 0$. The error in the seven-point difference method, E , is given by (II-25),

$$E = -\frac{h^6}{140} f^{VII}(\xi) \quad (II-25)$$

where h is the increment size and $f^{VII}(\xi)$ is the seventh derivative of the function being differentiated for $(q_i - 3h) \leq \xi \leq (q_i + 3h)$. An accurate estimate of this error cannot be made but it can be seen that a sufficiently small increment size, h , will tend to overshadow the $f^{VII}(\xi)$ function. Since $h \leq 1 \times 10^{-4}$ was used then $f^{VII}(\xi)$ must exceed 1×10^{22} to significantly affect the calculated force constant. In view of the functional form of (II-1) this is unlikely.

Values for the cross-term second derivative force constants were calculated using the seven point difference method. This method requires a seven by seven point grid of energy values. These were obtained by concomitantly incrementing two different coordinates q_i and q_j . Figure 2 displays the grid of coordinate positions for which energy values were calculated. The calculated energy values falling on a line perpendicular to the q_i axis in Figure 2 were substituted into Equation (II-24) to calculate the first derivatives at $V(q_i + \ell h, q_j)$ for $\ell = \pm 1$ to ± 3 on the q_i axis. These $V'(q_i + \ell h, q_j)$ for

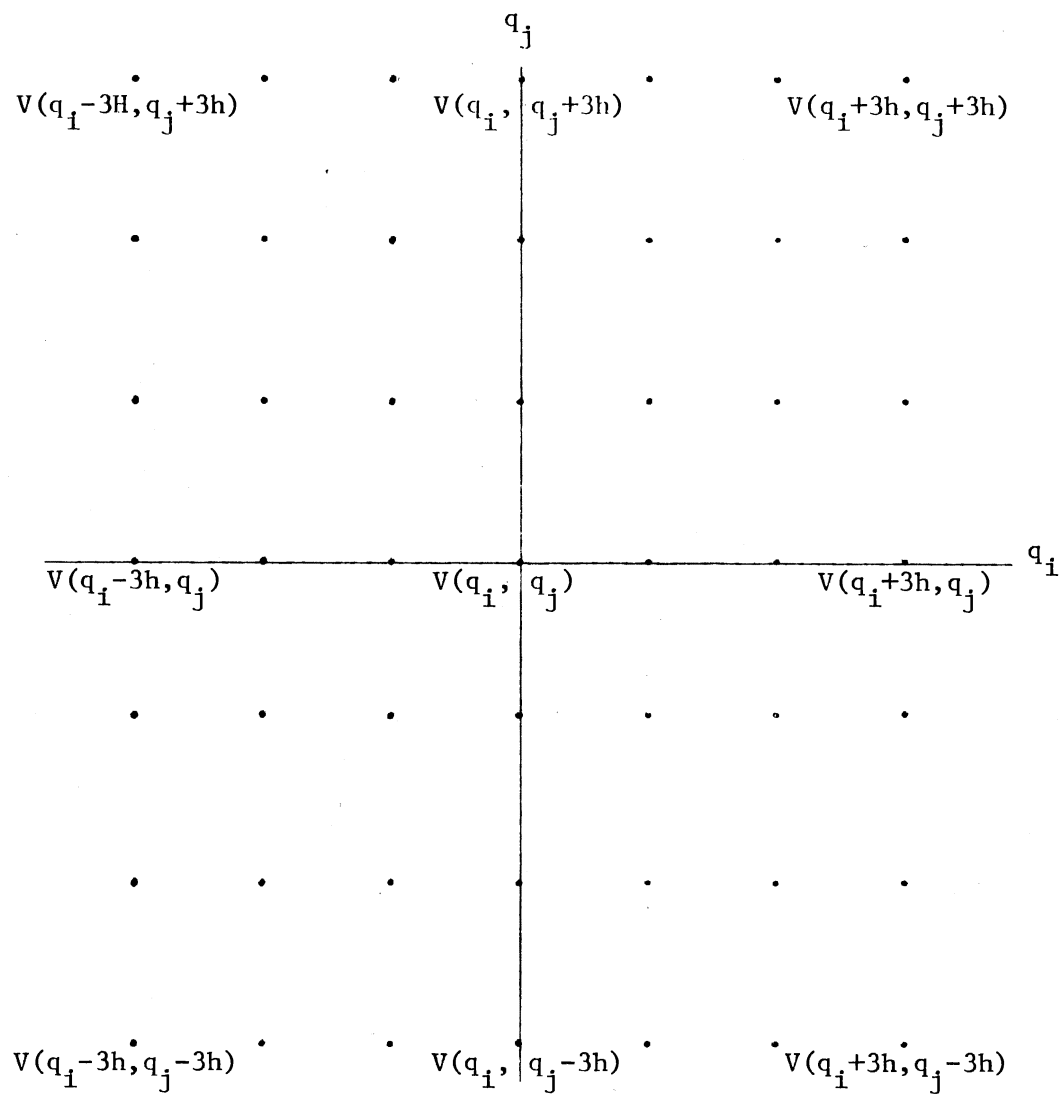


Figure 2. Grid of Incremented Coordinate Positions for Which Energies were Calculated

$\ell = \pm 1$ to ± 3 were then substituted into Equation (II-24) to obtain $\partial^2 V / \partial q_i \partial q_j$ or $V''(q_i + \ell h, q_j)$ for $\ell = 0$. These interaction force constant values obtained by the seven-point difference method are not based on as sound a theoretical background as those determined by the three-point method summarized in Table VI. For this reason, the three-point method interaction force constants were used to evaluate the isotopic normal mode frequencies for the isotope effect calculations. However, the seven-point method values were very close if not identical to the three-point method values.

Force Constant Calculation

The previously described difference methods were applied to energies obtained from the LMR-PES and its coordinate relationships, see Appendix A, to calculate force constants for the internal valence coordinates described in Tables III and V. The transition-state internal valence coordinate force constants (TS-VFC) were calculated for several increment sizes using both the three-point and seven-point difference methods, see Table VIII. The increment sizes, 1×10^{-4} and 5×10^{-5} , were found to give the best agreement between degenerate force constants. Overall, the best agreement between the force constants calculated by the two difference method techniques is given by an increment size of 1×10^{-4} . The force constants in Table VIII show a lack of consistency between degenerate force constants calculated using increment sizes of 5×10^{-6} and 5×10^{-7} . The validity of both numerical difference methods and the LMR-PES coordinate relationships was established as follows. First, force constants were calculated with respect to the cartesian coordinates of

TABLE VIII (Continued)

Valence Coordinate q_i	Three Point Method ^b		Seven Point Method ^c			
	$\frac{\partial^2 V^d}{\partial q_i^2}$	$\frac{\partial^2 V^e}{\partial q_i^2}$	$\frac{\partial^2 V^e}{\partial q_i^2}$	$\frac{\partial^2 V^d}{\partial q_i^2}$	$\frac{\partial^2 V^f}{\partial q_i^2}$	$\frac{\partial^2 V^g}{\partial q_i^2}$
ϕ_5^i	0.5517	0.5517	0.5517	0.5517	0.5517	0.5530
ϕ_6^i	0.5517	0.5517	0.5517	0.5517	0.5517	0.5530
α_x^i	0.0270	0.0270	0.0270	0.0270	0.0269	0.0257
α_y^i	0.0270	0.0270	0.0270	0.0270	0.0270	0.0256

^aForce constants calculated for the internal valence coordinates described in Table V.

^bValues calculated by the three point difference method, see (II-11).

^cValues calculated by the seven point difference method, see (II-27).

^dIncrement size $h = 5 \times 10^{-5}$.

^eIncrement size $h = 1 \times 10^{-4}$.

^fIncrement size $h = 5 \times 10^{-6}$.

^gIncrement size $h = 5 \times 10^{-7}$.

^hStretching force constants in mdyne/Å.

ⁱBending force constants in mdyne-Å.

each atom in the transition-state configuration. These cartesian coordinate force constants (CCFC) were compared to the CCFC obtained from conversion of the TS-VFC matrix using the B matrix method described in Appendix B. It can be seen in Table IX that the agreement is reasonably good but not quantitative. Second, transition-state normal mode frequencies were calculated using the VFC, converted CCFC, and directly calculated CCFC. These values are compared in Table X. When the CCFC are used to calculate normal-mode frequencies there are six degrees of freedom in the eigenvalues in addition to those corresponding to the normal-mode frequencies. These six extra degrees of freedom correspond to the translation and rotation of the transition-state molecular configuration. It can be seen that the directly calculated CCFC generate some small residual values that correspond to rotational and translational degrees of freedom. Theoretically these rotational and translational values should be zero but the directly calculated CCFC were not normalized with respect to the internal coordinates. Due to the form of the ICFC normal mode frequency calculation, the six extra degrees of freedom are not allowed. Also, the method of converting the ICFC to CCFC normalizes the converted CCFC to the internal coordinates. Therefore, only zero or negligibly small values for the translational and rotational degrees of freedom are obtained. Neglecting the rotational and translational degrees of freedom, it can be observed that the various sets of normal-mode frequencies in Table X agree very well; the largest deviation being about 2.5 cm^{-1} . This indicates the validity of the LMR-PES coordinate relationships and the numerical difference methods.

TABLE IX

TRANSITION-STATE DIAGONAL CARTESIAN COORDINATE FORCE CONSTANTS
CALCULATED BY DIFFERENT NUMERICAL METHODS^a

Cartesian Coordinate ^b	Seven Point ^c	Three Point ^d	Quadratic ^e	Converted ^f
x_1	0.2112	0.2112	0.2112	0.2095
y_1	0.2112	0.2112	0.2112	0.2095
z_1	1.2552	1.2552	1.2552	1.2552
x_2	0.7680	0.7680	0.7680	0.7665
y_2	4.7208	4.7208	4.7208	4.7190
z_2	0.6271	0.6271	0.6271	0.6265
x_3	3.7326	3.7326	3.7326	3.7309
y_3	1.7562	1.7562	1.7562	1.7546
z_3	0.6271	0.6271	0.6271	0.6265
x_4	3.7326	3.7326	3.7326	3.7309
y_4	1.7562	1.7562	1.7562	1.7546
z_4	0.6271	0.6271	0.6271	0.6265

TABLE IX (Continued)

Cartesian Coordinate ^b	Seven Point ^c	Three Point ^d	Quadratic ^e	Converted ^f
x_5	8.7621	8.7621	8.7621	8.7640
y_5	8.7621	8.7621	8.7621	8.7640
z_5	0.3412	0.3412	0.3412	0.3394
x_6	0.0439	0.0439	0.0439	0.0439
y_6	0.0439	0.0439	0.0439	0.0439
z_6	4.4043	4.4043	4.4043	4.4043

^aForce constant values in mdyne/Å. All values calculated using an increment size of 5×10^{-5} .

^bCoordinate subscript is the atom number, see Figure 1.

^cValues calculated by the seven point difference method, see (II-27).

^dValues calculated by the three point difference method, see (II-11).

^eValues calculated by the quadratic least squares fit method, see (II-23).

^fValues converted from internal coordinate force constant values by the B-matrix conversion method described in Appendix B.

TABLE X
TRANSITION-STATE NORMAL MODE FREQUENCIES^a

Normal Mode	Internal ^b	Cartesian ^c	Cartesian ^d	Assignment of the Normal Mode
ν_1^e	3388.5	3388.5	3388.5	Symmetric C-H-H stretching
ν_2^e	2937.7	2937.7	2937.6	Symmetric CH ₃ stretching
ν_3^e	964.7	964.7	967.2	CH ₃ bending deformation
ν_4^e	1479.3i	1479.3i	1479.3i	Antisymmetric C-H-H stretching
ν_5^f	3085.7	3085.7	3085.7	Antisymmetric CH ₃ stretching
ν_6^f	1502.9	1502.9	1503.7	Degenerate CH ₃ bending deformation
ν_7^f	752.3	752.3	754.5	Linear bending + CH ₃ bending
ν_8^f	367.3	367.3	369.8	Linear bending - CH ₃ bending
R ₁ ^g		0	50.8	Rotation about Z-axis
R ₂ ^g		0	39.4	Rotation about Y-axis

TABLE X (Continued)

Normal Mode	Internal ^b	Cartesian ^c	Cartesian ^d	Assignment of the Normal Mode
R ₃ ^g		0	39.4	Rotation about X-axis
T ₁ ^h		0	1.5	
T ₂ ^h		0	.5	
T ₃ ^h		0	-.2	

^aFrequencies in cm⁻¹. Force constants calculated using an increment size of 5×10^{-5} .

^bFrequencies calculated using the internal coordinate force constants in Table VIII plus all off-diagonal interaction force constants.

^cFrequencies calculated using cartesian coordinate force constants converted from the internal coordinate force constants described in footnote b.

^dFrequencies calculated using the three point method cartesian coordinate force constants from Table IX plus all off-diagonal interaction force constants.

^eNon-degenerate normal mode frequencies.

^fDoubly degenerate normal mode frequencies.

^gRotational degree of freedom.

^hTranslational degree of freedom.

The assignments of the normal modes in Table X are based on the eigenvectors given in Table XI. The cartesian coordinate eigenvectors make assigning a normal mode of motion relatively easy, since each eigenvector value represents relative motion along or parallel to the cartesian coordinates for each atom in Figure 1. The rotational assignments are particularly easy. For example, the R_1 eigenvector shows that atom two has motion in the positive x direction, atom three has motion in the negative x and positive y directions, and atom four has motion in the negative x and negative y directions. Thus, R_1 is an eigenvector representing rotation about the Z axis in Figure 1.

Force constants were calculated for the reactant molecular species in reactions (I-1) and (I-2) with respect to the internal valence coordinates described in Table III. Normal-mode frequencies calculated using these force constants are compared with spectroscopic values in Tables XII and XIII. The CH_4 frequency values from the LMR-PES VFC agree well with those calculated from the diagonal Herzberg VFC matrix in Table XII.³⁴ However, the numerically determined VFC matrix from the LMR-PES is not a diagonal matrix due to strong internal coupling between the CH stretching and HCH bending VFC. The diagonal Herzberg force constants,³⁴ 5.04 mdyne/Å and 0.5517 mdyne-Å for CH stretching and HCH bending, respectively, appear implicitly and explicitly, respectively, in the LMR-PES.² However, the numerically determined CH stretching VFC from the LMR-PES is 5.08 mdyne/Å. The agreement between frequencies predicted by the LMR-PES and Herzberg VFC reflects the fact that the C-H stretching modes are coupled, 1) between themselves by a small -0.01 mdyne/Å value and 2) to the HCH bending VFC by a larger ±0.042 mdyne value (+0.042 coupled to adjacent C-H bonds and

TABLE XI

TRANSITION-STATE CARTESIAN COORDINATE EIGENVECTORS^a

Cartesian Coordinate	Transition-State Normal Modes ^b								Rotation ^c			Translation ^d
	v_1	v_2	v_3	v_4	v_5	v_6	v_7	v_8	R_1	R_2	R_3	T_1
x_1	0	0	0	0	-.003	.010	-.758	.087	0	-.450	.007	.241
y_1	0	0	0	0	0	.015	.087	-.374	0	-.007	-.450	.022
z_1	.547	-.018	.117	.787	0	0	0	0	0	0	0	.004
x_2	0	0	0	0	-.023	-.405	-.080	-.023	.575	.149	-.002	.241
y_2	.018	.550	-.116	.025	.016	.126	.006	.092	0	.002	.150	.002
z_2	-.013	-.150	-.499	.005	-.004	.152	.052	.507	0	.005	.333	.004
x_3	-.015	-.476	.144	-.021	-.553	.287	-.060	-.026	-.288	.149	-.002	.241
y_3	-.009	-.275	.083	-.012	-.306	-.232	.020	.099	.498	.003	.149	.022
z_3	-.013	-.150	-.499	.005	-.173	-.160	.365	-.152	0	-.290	-.162	.004
x_4	.015	.476	-.144	.021	-.567	-.369	-.058	-.018	-.288	.149	-.003	.241
y_4	-.009	-.275	.083	-.012	.314	-.653	-.004	.098	-.498	.001	.149	.022
z_4	-.013	-.150	-.499	.005	.177	.008	-.417	-.355	0	.285	-.171	.004

TABLE XI (Continued)

Cartesian Coordinate	Transition-State Normal Modes ^b								Rotation ^c			Translation ^d
	v_1	v_2	v_3	v_4	v_5	v_6	v_7	v_8	R_1	R_2	R_3	T_1
x_5	0	0	0	0	.096	.040	.065	.010	0	.060	-.001	.241
y_5	0	0	0	0	-.002	.062	-.007	-.004	0	.001	.060	.022
z_5	.027	.036	.105	-.108	0	0	0	0	0	0	0	.004
x_6	0	0	0	0	.001	.001	.186	-.140	.001	-.716	.011	.241
y_6	0	0	0	0	0	.001	-.021	.605	0	-.011	-.716	.022
z_6	-.826	.045	.132	.481	0	0	0	0	0	0	0	.004

^aThe values are relative potential motion vectors along or parallel to the cartesian coordinates for each numbered atom in Figure 1.

^bNormal modes correspond to those in Table X.

^cRepresent nonzero rotational contributions from cartesian force constant frequency calculation, see Table X.

^dTypical eigenvector for the negligibly small translational energy contribution from cartesian force constant frequency calculation, see Table X.

TABLE XII
TETRAHEDRAL CH₄ NORMAL MODE FREQUENCIES^a

Normal Mode	Calculated		Herzberg		Shimanouchi ^c
	LMR-PES	Force Constants	Calculated	Spectroscopic	Spectroscopic
ν_1		2917	2914	2914	2917
ν_2^d		1527	1527	1526	1534
ν_3^e		3080	3080	3020	3019
ν_4^e		1366	1363	1306	1306

^aAll values in cm⁻¹.

^bSee Reference 34.

^cSee Reference 35.

^dDoubly degenerate.

^eTriply degenerate.

TABLE XIII
 PLANAR CH₃ AND H₂ FREQUENCIES^a

Normal Mode	Snelson ^b	MJ ^c	TWP ^d	LMR-PES ^e	Gaussian 70 ^f	Herzberg ^g
ν_1	3044			2914	3251	
ν_2	617	611	607	847	847	
ν_3^h	3162			3100	3455	
ν_4^h	<u>1396</u>			<u>1606</u>	<u>1538</u>	
sum ⁱ $\nu(\text{CH}_3)$	12777			13173	14084	
sum ^j $\nu(\text{CH}_3)$	12160			12326	13237	
$\nu(\text{H}_2)$				4468		4395

^aAll values in cm⁻¹.

^bSee Reference 36. Since ν_1 is infrared inactive, the value corresponds to Snelson's calculated value.

^cSee Reference 37.

^dSee Reference 38.

^eCalculated using LMR-PES valence force constants except for the $\nu_2(\text{CH}_3)$ obtained from Gaussian 70, see Reference 39.

^fCalculated from Gaussian 70, 6-31G basis set force constants.

^gSee Reference 40.

^hDoubly degenerate frequencies.

ⁱSum includes the ν_2 value.

^jSum excludes the ν_2 value.

-0.042 coupled to non-adjacent C-H bonds). These interaction VFC values effectively decrease the calculated normal mode frequency values. The diagonal HCH bending VFC from the LMR-PES are identical to the Herzberg values.³⁴ It can be seen in Table XII that the Shimanouchi spectroscopic values³⁵ differ somewhat from the Herzberg³⁴ spectroscopic values and agree somewhat better with the calculated values.

The spectroscopic CH_3 frequencies in Table XIII reported by Snelson for ν_1 , ν_3 and ν_4 compare reasonably well with the corresponding LMR-PES values. In terms of KIE calculations it should be noted that differences in the ν_4 values would tend to be offset by opposing differences in the ν_1 and ν_3 values.³⁶ Thus, the LMR-PES curvatures governing the symmetric and asymmetric CH stretching are realistic. However, the ν_4 in-plane bending VFC may be somewhat large compared to the spectroscopic value. The frequencies calculated from Gaussian 70 VFC are all greater than the corresponding spectroscopic values by about nine percent on the average. The ν_2 out-of-plane bending frequency is about 235 cm^{-1} greater than the corresponding spectroscopic frequencies.^{36,37,38} The effect of using either the Gaussian 70 or the spectroscopic isotopic ν_2 frequencies in conjunction with the corresponding LMR-PES calculated frequencies to obtain KIEs from (I-3) and (I-4) is discussed in Chapter III. The H_2 frequency (4468 cm^{-1}) obtained from the LMR-PES VFC (5.924 mdyne/\AA) is less than two percent greater than the Herzberg spectroscopic frequency (4395 cm^{-1}) having a VFC of 5.732 mdyne/\AA .

The force constants used to calculate the LMR-PES and Gaussian 70 frequencies for CH_3 are compared to the spectroscopically determined

force constants in Table XIV. It can be seen in Table XIV, that the Gaussian 70 in-plane bending VFC agrees well with the LMR-PES value, but the spectroscopic value is somewhat lower. This corresponds to the agreement between ν_4 frequencies in Table XIII. However, the two C-H stretching VFC differ considerably. This difference is reflected in disagreement between the ν_1 and ν_3 values in Table XIII. As discussed earlier in the coordinates section, the LMR-PES predicts no out-of-plane bending force constant. Therefore, the Gaussian 70 ab initio program was used with its 6-31G internal basis set to calculate the value for F_γ in Table XIV.³⁹ The out-of-plane bending internal coordinate corresponds to bending all three CH bonds out-of-plane simultaneously by the angle γ in radians. The numerical methods discussed earlier were applied to the incremented Gaussian 70 energies to obtain the CH_3 VFC in Table XIV. The Gaussian 70 out-of-plane bending VFC is almost twice as large as the spectroscopically determined value. This difference is clearly reflected in the calculated and spectroscopic ν_2 values.

TABLE XIV
 PLANAR CH₃ FORCE CONSTANTS AND BONDLENGTHS^a

Label	LMR-PES ^b	Gaussian 70 ^c	Snelson ^d	MJ ^e	TWP ^f
$F_{r_i}^g$ (i=2,3,4)	5.040	6.273	5.2		
$F_{\phi_i}^h$ (i=4,5,6)	0.461	0.422	0.315		
F_{γ}^i		0.340	0.179	0.177	0.174
r_i (i=2,3,4)	1.094	1.072	1.079	1.079	1.079

^aAll force constants are in mdyne/Å and the bondlengths, r_i (i=2,3,4) are in Å.

^bValues calculated from the LMR-PES.

^cValues calculated using (II-11) and (II-23) methods applied to 6-31G basis set energies from Gaussian 70, see Reference 39.

^dSee Reference 36. In-plane force constants are calculated Urey-Bradley force constants.

^eSee Reference 37.

^fSee Reference 38.

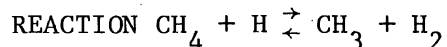
^gC-H stretching force constant.

^hHCH in-plane bending force constant.

ⁱOut-of-plane bending force constant.

CHAPTER III

THEORETICAL KINETIC ISOTOPE EFFECTS FOR THE



Results and Discussion

Comparison of Theoretical Vibrational

Frequencies and Force Constants

The activated complex normal mode frequencies calculated for the LMR-PES and the various BEBO and LEPS models reported by Kurylo, Hollinden, and Timmons¹² and Shapiro and Weston¹⁴ are compared in Table XV. It should be noted that most of these normal mode frequencies are of comparable magnitude except for the symmetric stretching frequency for motion along the reaction coordinate, ν_1 , and the linear bending modes, ν_7 and ν_8 . Also, the imaginary frequency, ν_4 , for the LMR-PES is considerably smaller in value, than the corresponding BEBO and LEPS values indicating that the former potential-energy barrier along the reaction coordinate has less curvature than either of the latter two. This lower degree of curvature in the barrier may be at least partially the result of the LMR-PES having a somewhat lower barrier height as can be seen in Table XVI. Table XVI also shows that the imaginary frequency for the BEBO and LEPS models results from a large interaction force constant between the C-H₁ and H₁-H₆ stretching force constants. In contrast the imaginary frequency for the LMR-PES

TABLE XV

CH₃-H-H TRANSITION-STATE FREQUENCIES FROM DIFFERENT SOURCES^a

Normal Mode	Frequencies From								
	LMR-PES ^b	KHT ^c		SW ^d					
		BEBO	LEPS	BEBO3 ^e	LEPS2 ^e	BEBO3 ^f	LEPS2 ^f	BEBO3 ^g	LEPS2 ^g
v ₁	3388	1610	1397	1568	1392	1577	1412	1603	1482
v ₂	2938	2980	2980	3149	3149	3149	3149	3149	3149
v ₃	965	1179	1147	958	954	1156	1142	1337	1279
v ₄	1479i	1689i	2024i	1691i	1839i	1691i	1838i	1690i	1838i
v ₅	3086	3047	3047	3165	3165	3166	3167	3168	3168
v ₆	1503	1459	1458	1473	1472	1480	1480	1527	1535
v ₇	752	1046	1077	623	779	1008	1078	1355	1384
v ₈	367	446	502	14	14	430	500	458	555

^aAll frequencies in cm⁻¹.^bCalculated using LMR-PES parameters.^cCalculated using the BEBO and LEPS parameters in Reference 12.^dCalculated using the BEBO3 and LEPS2 parameters in Reference 14 with the HCH₁ bending force constant value specified in the footnotes.^eCalculated with $F_{\phi_i}^{\ddagger}$ (i=1,2,3) = 0.0001 mdyne-Å.^fCalculated with $F_{\phi_i}^{\ddagger}$ (i=1,2,3) = 0.26 mdyne-Å.^gCalculated with $F_{\phi_i}^{\ddagger}$ (i=1,2,3) = 0.568 mdyne-Å.

TABLE XVI
COMPARISON OF TRANSITION-STATE PARAMETERS^a

Value Label	Values from					Units
	LMR-PES ^b	KHT ^c		SW ^d		
		BEBO	LEPS	BEBO3	LEPS2	
$F_{R_1}^\ddagger$	-1.534	1.157	0.775	1.096	0.930	mdyne/Å
$F_{R_5}^\ddagger$	4.404	1.157	0.565	1.096	0.653	mdyne/Å
F_{int}^\ddagger	0.807	1.879	1.653	1.818	1.597	mdyne/Å
F_{α}^\ddagger	0.0270	0.0526	0.0821	0.0486	0.0799	mdyne-Å
$F_{\phi_i}^\ddagger$ (i=1,2,3)	0.180	0.280	0.260	--- ⁱ	--- ⁱ	mdyne-Å
$F_{\phi_i}^\ddagger$ (i=4,5,6)	0.552	0.568	0.568	0.568	0.568	mdyne/Å
$F_{R_i}^\ddagger$ (i=2,3,4)	5.039	5.040	5.040	5.50	5.50	mdyne/Å
$F_{R_i R_j}^\ddagger$ (i≠j=2,3,4)	0.0	0.050	0.050	0.124	0.124	mdyne/Å

TABLE XVI (Continued)

Value Label	Values from					Units
	LMR-PES ^b	KHT ^c		SW ^d		
		BEBO	LEPS	BEBO3	LEPS2	
$F_{R_i \phi_{i-2}}^\ddagger$ (i=2,3,4)	0.0	0.165	0.165	0.165	0.165	mdyne
$F_{R_i \phi_{i-2}}^\ddagger$ (i=2,3,4)	0.0	-0.165	-0.165	0.0	0.0	mdyne
$F_{R_1 R_i}^\ddagger$ (i=2,3,4)	-0.0015	0	0	0	0	mdyne/Å
$F_{R_1 \phi_i}^\ddagger$ (i=1,2,3)	0.0268	0	0	0	0	mdyne
$F_{\phi_i R_{i+1}}^\ddagger$ (i=1,2,3)	0.0007	0	0	0	0	mdyne
$F_{R_5 \phi_i}^\ddagger$ (i=1,2,3)	-0.0014	0	0	0	0	mdyne
r_1	1.597	1.27	1.29	1.27	1.28	Å
r_6	0.783	0.92	0.96	0.92	0.95	Å
r_i (i=2,3,4)	1.094	1.091	1.091	1.09	1.09	Å
$V_a(\text{CH}_4 + \text{H})^f$	5.60	12.24	12.22			kilocalories/mole

TABLE XVI (Continued)

Value Label	Values from					Units
	LMR-PES ^b	KHT ^c		SW ^d		
		BEBO	LEPS	BEBO3	LEPS2	
$V_a(\text{CH}_3 + \text{H}_2)^f$	9.42			13.46	10.63	kilocalories/mole
$E_a(\text{CH}_3 + \text{H}_2)^g$	11.11			13.1 ^j	10.9	kilocalories/mole
$E_a(\text{CH}_4 + \text{H})^h$	6.44	11.73	11.53			kilocalories/mole

^aAll force constants have subscript designations from Table V. The bondlength designations are also from Table V; see Reference 7.

^bValues determined from the LMR-PES.

^cBEBO and LEPS parameters described in Reference 12.

^dBEBO3 and LEPS2 parameters described in Reference 14.

^eInteraction force constant between the C-H₁ and H₁-H₆ stretching force constants.

^fBarrier height in kilocalories/mole.

^gActivation energy calculated at 500°K.

^hActivation energy calculated at 625°K.

ⁱThree different values 0.0001, 0.26, and 0.568 mdyne-Å were used; see Reference 14.

^jIncludes a tunneling correction.

activated complex results from a negative C-H₁ stretching force constant. This difference in force constants is not unreasonable since the LMR-PES predicts C-H₁ and H₁-H₆ bond lengths in the transition state approximately 0.3 Å longer and 0.15 Å shorter, respectively, than the BEBO and LEPS models. For this reason, the LMR-PES activated complex more closely resembles a methyl radical and hydrogen molecule than the BEBO and LEPS models. This geometry and the large H₁-H₆ force constant, $F_{R_5}^\ddagger$, give rise to the exceptionally large ν_1 value for the LMR-PES in Table XV. Although the differences in the ν_7 and ν_8 frequencies reflect the differences in the linear-bending force constant, F_α^\ddagger , differences in these frequencies result primarily from differences in the HCH₁ bending force constants, $F_{\phi_{1-3}}^\ddagger = F_{\phi_i}^\ddagger$ (i=1,2,3), between the surfaces. The frequency changes associated with the changes in the $F_{\phi_{1-3}}^\ddagger$ values can be observed in Table XV. The force constants in Table XVI and the frequencies in Table XV considered together show that a BEBO3 and LEPS2 value of $F_{\phi_{1-3}}^\ddagger = 0.26 \text{ mdyne-Å}^{0.14}$ gives the best agreement with the LMR-PES and Kurylo, Hollinden, and Timmons (KHT)¹² ν_7 and ν_8 frequencies. For the KHT BEBO and LEPS surfaces the F_α^\ddagger values in columns three and four of Table XVI vary by a factor of 1.56 but produce a negligible change in ν_7 and ν_8 , see columns three and four of Table XV. Thus the magnitude of the linear bending frequencies is not strongly dependent on the magnitude of the bending force constant, F_α^\ddagger .

For purposes of comparison, the values for the LMR-PES activation energies were calculated using the method of Kibby and Weston.⁴¹ The values predicted by the LMR-PES are compared to the BEBO and LEPS E_a reported by KHT¹² and Shapiro and Weston (SW),¹⁴ which were also

reportedly calculated by this method. The method, as given by Kibby and Weston,⁴¹ follows the approach of Johnston.⁴² The experimental activation energy, E_a , is treated as a linear function of the rate constant and temperature.⁴²

$$E_a = \frac{-Rd \ln k}{d(T^{-1})} \quad (\text{III-1})$$

Integration of (III-1) gives the natural log form of the Arrhenius equation.

$$\ln k = \ln A - \frac{E_a}{RT} \quad (\text{III-2})$$

Johnston then gives an equation similar to (III-2) derived from transition-state theory,

$$\ln k = \ln(B(T)) - \frac{V_a}{RT} \quad (\text{III-3})$$

where V_a is the barrier height along the reaction coordinate in kilocalories per mole, $B(T)$ is a temperature dependent form of the Arrhenius preexponential factor, and R and T are the gas constant and temperature in $^{\circ}\text{K}$, respectively. The relation between the theoretical $B(T)$ and V_a on the one hand and the A and E_a on the other hand is given by:

$$\Omega = \frac{d \ln B(T)}{d \ln T} \quad (\text{III-4a})$$

$$A = B(T) \exp(\Omega) \quad (\text{III-4b})$$

$$E_a = V_a + \Omega RT \quad (\text{III-4c})$$

The expressions in (III-4) assume that the $(\partial \ln k / \partial T)_p$ for (III-2) and (III-3) are identical and that (III-2) and (III-3) may be equated. Kibby and Weston (KW) then define w_i for each vibrational degree of freedom by

$$w_i = (u_i/2) \coth(u_i/2) - 1 \quad (\text{III-5})$$

where u_i is the same as u_{1i} in (I-6) and (I-7).⁴¹ The temperature dependent factor, Ω , is defined by KW as

$$\Omega = w^* + 1/2(d^\ddagger - d_r) + \frac{d^\ddagger - 1}{\sum_{i=1}^{\ddagger} w_i} - \frac{d_r}{\sum_{i=1}^r w_i} \quad (\text{III-6})$$

where w^* is a tunneling correction factor (if used, zero otherwise); d^\ddagger is the number of vibrational degrees of freedom in the activated complex including the imaginary frequency; d_r is the number of vibrational degrees of freedom in the reactants, and w_i^\ddagger and w_i^r have a value for each transition-state and reactant vibrational degree of freedom calculated by (III-5), respectively. As a result of the 3.82 kcalorie/mole (0.1658 eV) difference between the C-H₁ (4.5808 eV) and H₁-H₆ (4.7466 eV) bond energies used in the LMR-PES,² the V_a (9.42 kilocalories/mole) and E_a (11.11 kilocalories/mole) for reaction of CH₃ + H₂ calculated at 500°K are reasonably comparable to the corresponding V_a (13.46 and 10.63 kilocalories/mole for the BEBO3 and LEPS2 models, respectively) and E_a (13.1 and 10.9 kilocalories/mole for the BEBO3 and LEPS2 models, using $F_{\phi_i}^\ddagger$ (i=1,2,3) = 0.26 mdyne-Å, respectively) calculated by SW.¹⁴ However, the LMR-PES V_a (5.60 kilocalories/mole) and E_a (6.44 kilocalories/mole) for reaction of

$\text{CH}_4 + \text{H}$ calculated at 625°K are about five kilocalories per mole smaller than the corresponding V_a (12.24 and 12.22 kilocalories/mole for the BEBO and LEPS models, respectively) and E_a (11.73 and 11.53 kilocalories/mole for the BEBO and LEPS models, respectively) values calculated by KHT.¹² The difference in the relationships between E_a and V_a for the various models is primarily the result of the diversity in the magnitude of the $\sum_{i=1}^{d^\ddagger-1} w_i^\ddagger - \sum_{i=1}^{d_r} w_i^r$ differences in equation (III-6). The $\sum_{i=1}^{d^\ddagger-1} w_i^\ddagger$ values were easily determined by (III-5) using the frequencies in Table XV with no tunneling correction. However, calculation of the $\sum_{i=1}^{d_r} w_i^r$ values requires a full set of reactant frequencies. For the reaction of CH_4 and H it was determined that KHT¹² used the spectroscopic frequency values for methane that are reported by Herzberg,³⁴ since their reported E_a could be reproduced using these frequency values. For the reaction of CH_3 and H_2 it is not known what set of reactant frequencies that SW used to calculate their reported E_a since they do not specify which of the various spectroscopic of calculated sets of CH_3 frequency values they used.¹⁴ The LMR-PES E_a values were calculated using the harmonic methane and CH_3 and H_2 calculated normal mode frequencies given in Appendix C. Since the $\sum_{i=1}^{d_r} w_i^r$ values at 625°K are 13.89 for the LMR-PES harmonic CH_4 frequencies and 13.52 for the Herzberg spectroscopic CH_4 frequencies, it can be seen that the positive deviation between the LMR-PES V_a and E_a values and the negative deviation between the KHT-BEBO (or LEPS) V_a and E_a values is the result of the $\sum_{i=1}^{d^\ddagger-1} w_i^\ddagger$ values. The $\sum_{i=1}^{d^\ddagger-1} w_i^\ddagger$ values calculated at 625°K are 13.07 for the LMR-PES activated complex, 11.61 for the KHT-BEBO activated complex, and 11.47 for the KHT-LEPS activated complex. By application of equation (III-6), the Ω values 0.68, -0.41, and -0.55 were calculated for the LMR-PES, KHT-BEBO, and

KHT-LEPS $\text{CH}_4 + \text{H}$ models, respectively. Therefore, the LMR-PES data generate a larger Ω value than any of the BEBO or LEPS models leading to a greater difference in the corresponding V_a and E_a values. The reason for the larger Ω value can be traced to the very large LMR-PES transition-state ν_1^\ddagger (3388 cm^{-1}) value which is more than twice as large as any of the BEBO and LEPS ν_1^\ddagger values.

Assuming that the curvature parameter for motion perpendicular to the reaction coordinate are essentially independent of the barrier height, then the inadequacies of the LMR-PES in this regard have a negligible effect on the quantum mechanical contribution to the predicted KIEs. However, the curvature of the barrier for motion parallel to the reaction coordinate is not necessarily independent of the barrier height and clearly effects the magnitude of ν_L^\ddagger . Consequently, an inaccurate barrier height would affect the classical mechanical contribution to the calculated KIE. The magnitude of the effect should be largest for a primary KIE where isotopic motion is directly considered in the reaction coordinate and much smaller for a secondary KIE.

Since SW report their calculated KIEs only in the form of temperature dependence plots, accurate comparison to the LMR-PES KIEs required recalculation of the SW KIE values. Using the activated complex parameters in Table XVI and tetrahedral geometry for the CH_3 group relative to the linear C-H-H entity, isotopic normal-mode frequencies consistent with the monoisotopic frequencies in Table XV were calculated for the BEBO and LEPS models and are tabulated in Appendix C along with the mass moment of inertia parameters. These frequencies and parameters were combined with the H_2 and D_2 harmonic

frequencies reported by Persky and Klein, that is, 4395.2 and 3109.1 cm^{-1} , respectively, to calculate the SW KIEs.⁴³ Table XVII presents isotope effects determined experimentally and calculated from the various theoretical models. It should be noted that the H_2 and D_2 frequencies are the only reactant-state frequencies which contribute to the calculated KIEs in Table XVII, since all other reactant contributions to the KIEs cancel out. However, SW¹⁴ report that they used the rotationally corrected H_2 and D_2 quantities reported by Persky and Klein (PK)⁴³ to calculate the $k(\text{CH}_3, \text{H}_2)/k(\text{CH}_3, \text{D}_2)$ and $k(\text{CD}_3, \text{H}_2)/k(\text{CD}_3, \text{D}_2)$ values in their data. The transition-state theory equation used by SW¹⁴ is equivalent to (I-4) plus a rotational correction factor added to the reactant ZPE term. The SW reactant and transition state vibrational partition function ratios, $f(\text{H}_2, \text{D}_2)$ and f^\ddagger , respectively, are defined in (III-7),

$$k_{\text{H}}/k_{\text{D}} = \frac{v_{1\text{L}}^\ddagger/v_{2\text{L}}^\ddagger}{f^\ddagger} \frac{f(\text{H}_2/\text{D}_2)}{f^\ddagger} = \frac{(m_{\text{H}}/m_{\text{D}})^{\frac{1}{2}} \exp\left(\frac{Z_{\text{H}_2} - Z_{\text{D}_2}}{T}\right)}{\prod_{i=1}^{\infty} \frac{u_{2i}^\ddagger \sinh(u_{1i}^\ddagger/2)}{u_{1i}^\ddagger \sinh(u_{2i}^\ddagger/2)}} \quad (\text{III-7})$$

where m_{H} and m_{D} are the isotopic masses of hydrogen, 1.007825 and 2.0141 amu, respectively, T is in $^\circ\text{K}$, the u_{ji} terms are the same as in (I-6) and (I-7), and Z_{x_2} equals $(u_{x_2}/2) - (\sigma_{x_2}/3)$. The $\sigma_{x_2}/3$ value is the rotational correction to the $(u_{x_2}/2) = (h\nu_{x_2})/(2kT)$. The combined ZPE exponent, $(Z_{\text{H}_2} - Z_{\text{D}_2})/T$, can be expanded to $[(u_{\text{H}_2} - u_{\text{D}_2}) (\frac{1}{2}) - (\sigma_{\text{H}_2} - \sigma_{\text{D}_2}) (1/3)]/T$. Since σ_{H_2} and σ_{D_2} have the values 87.5 and 43.8, respectively, then obviously, the application of the rotational

TABLE XVII

EXPERIMENTAL AND THEORETICAL KINETIC ISOTOPE EFFECTS

Rate Constant Ratio	Temp. K	LMR-PES ^a					Experimental					Theoretical ^b							
		HF ^c	BT ^d	OF ^e	RC ^f	KHT ^g	SW ^h	WS ⁱ	MS ^j	DB ^k	TW ^l	BEBO3 P _B =0.0001	BEBO3 F _B =0.26	BEBO3 F _B =0.568	LEPS2 F _B =0.0001	LEPS2 F _B =0.26	LEPS2 F _B =0.568	BEBO	LEPS
k(CH ₄ ,H)	500	0.509	0.611			0.834						0.739	0.738	0.738	0.786	0.786	0.786	0.724	0.785
k(CH ₄ ,D)	546	0.554	0.639			0.870						0.773	0.773	0.773	0.818	0.818	0.818	0.763	0.821
k(CH ₃ ,H ₂)	296	1.99	---	1.85	1.67					2.12	7.14	5.40	4.25	6.82	5.26	4.19	5.07	5.32	
k(CH ₃ ,D ₂)	399	1.90	5.04	1.80	1.67		4.80				4.85	4.06	3.44	4.77	4.04	3.44	3.91	4.07	
	403	1.90	4.87	1.80	1.67			4.79	5.50		4.79	4.03	3.42	4.72	4.00	3.42	3.87	4.04	
	409	1.89	4.61	1.79	1.67						4.71	3.98	3.39	4.65	3.96	3.39	3.82	3.99	
	426	1.88	3.98	1.78	1.67						5.75								
	428	1.88	3.93	1.78	1.67						5.32								
	428	1.88	3.93	1.78	1.67		4.45				4.47	3.82	3.29	4.42	3.81	3.30	3.67	3.83	
	482	1.83	3.26	1.75	1.65			2.80	3.33		3.92	3.45	3.04	3.90	3.45	3.05	3.33	3.47	
k(CD ₃ ,H ₂)	296	1.98	---	1.83	1.67					0.465	7.13	5.32	4.08	6.82	5.19	4.04	4.99	5.26	
k(CD ₃ ,D ₂)	402	1.90	4.89	1.79	1.67		3.33				4.81	4.01	3.36	4.73	3.99	3.37	3.89	4.03	
	403	1.90	4.85	1.79	1.67			2.98	4.11		4.79	4.01	3.36	4.72	3.98	3.36	3.85	4.02	
	468	1.84	3.18	1.76	1.65		3.07				4.06	3.53	3.07	4.03	3.53	3.08	3.40	3.55	
	483	1.83	3.01	1.75	1.65			2.98	3.48		3.92	3.44	3.01	3.90	3.44	3.02	3.32	3.47	
k(CH ₃ ,HD)	296	2.02	---							6.37	2.06	1.56	1.23	1.57	1.22	0.972	1.55	1.20	
k(CH ₃ ,DH)	403	1.73	2.57					2.33			1.77	1.49	1.26	1.47	1.25	1.07	1.48	1.24	
	467	1.63	2.07				2.08				1.67	1.46	1.27	1.43	1.26	1.11	1.46	1.25	
	483	1.61	2.00					1.79			1.65	1.45	1.28	1.42	1.26	1.12	1.45	1.25	
	532	1.55	1.83				1.92				1.60	1.43	1.30	1.40	1.27	1.14	1.43	1.25	
k(CD ₃ ,HD)	402	1.73	2.56				1.81				1.77	1.48	1.24	1.47	1.24	1.05	1.48	1.23	
k(CD ₃ ,DH)	403	1.73	2.55					1.76			1.77	1.48	1.24	1.47	1.24	1.05	1.47	1.23	
	468	1.63	2.06				1.71				1.67	1.45	1.26	1.43	1.25	1.10	1.45	1.24	
	483	1.61	2.00					1.73			1.65	1.45	1.26	1.42	1.26	1.10	1.44	1.25	

^aTransition-state theory calculated KIEs using the LMR-PES geometries and force constants (plus Gaussian 70 out-of-plane bending force constant) except as noted.

^bTransition-state theory calculated KIE values using the LEPS2 and BEBO3 model parameters from Reference 14 [$F_B = P_{\phi_1}^{\ddagger}$ ($i=1,2,3$)] and using the BEBO and LEPS model parameters from Reference 12.

^cTransition-state theory calculated using the harmonic calculated LMR-PES normal mode frequencies.

^dLMR-PES-HF values including Bell tunneling.

^eLMR-PES KIEs calculated using the H₂ and D₂ observed frequencies from Reference 40.

^fLMR-PES-HF values corrected to the rotationally corrected H₂ and D₂ values in Reference 43; see text.

^gResults from Reference 12.

^hResults from Reference 14.

ⁱResults from Reference 15.

^jResults from Reference 16.

^kResults from Reference 17.

^lResults from Reference 13.

correction in (III-7), reduces the KIE value below that produced by the same set of frequencies used in (I-4).⁴³ At about 400°K the amount of this reduction is approximately three percent. The interatomic H₂ distance, $r_{H_2} = 0.742 \text{ \AA}$, was used in both the PK⁴³ and the LMR-PES² calculations. Therefore, use of the PK σ_{H_2} and σ_{D_2} values to apply a rotational correction to the LMR-PES KIEs in Table XVII is valid [since, $\sigma_{x_2} = h^2 / (8\pi^2 k T u_{x_2}^2)$, where h, k, T, u, and r_{x_2} are the Planck's constant, Boltzmann's constant, temperature in °K, reduced mass of the diatomic molecule, and the interatomic distance, respectively]. The application of a rotational correction to the LMR-PES $k(CH_3, H_2)/k(CH_3, D_2)$ values in the column labeled HF at 296 and 483°K reduces the values 1.99 and 1.83 to 1.89 and 1.78, respectively. Similarly for $k(CD_3, H_2)/k(CD_3, D_2)$ in the column labeled HF the values at 296 and 483°K are reduced by rotational correction from 1.98 and 1.83 to 1.88 and 1.78, respectively.

Since our transition-state-theory computer routine was not designed to handle a rotational correction in the manner of (III-7) directly, the rotationally corrected frequency values reported by PK were used to obtain a temperature dependent correction factor which could be multiplied times the KIEs obtained by (I-3) or (I-4). One factor value was used to correct the SW values and another factor value was used to obtain LMR-PES values which are directly comparable to the rotationally corrected SW values.¹⁴ The SW correction factor is obtained as follows. The reactant exponent in the ZPE term for (I-3) and (I-4) is given by (III-8),

$$\frac{u_{H_2} - u_{D_2}}{2} = \frac{1.4388(4395.2 - 3109.1)}{2T} = \frac{925.2}{T} \quad (\text{III-8})$$

where $u_1 = \frac{h\nu_1}{kT} = \frac{1.4388\nu_1}{T}$ is the conversion factor used in the computer code. The rotationally corrected exponent reported by Persky and Klein is $\frac{889.4}{T}$.⁴³ Therefore, the reactant ZPE term using (III-8) is converted to the PK rotationally corrected ZPE term by multiplying by (III-9).

$$\frac{\exp\left(\frac{889.4}{T}\right)}{\exp\left(\frac{925.2}{T}\right)} = \exp\left(\frac{889.4 - 925.2}{T}\right) = \exp\left(\frac{-35.8}{T}\right) \quad (\text{III-9})$$

The rotationally corrected KIE is given by (III-10) since the reactant EXC value is to at least five significant digits unity.

$$k_H/k_D(\text{corrected}) = k_H/k_D \cdot \exp\left(\frac{-35.8}{T}\right) \quad (\text{III-10})$$

All of the BEBO3, LEPS2, BEBO, and LEPS $k(\text{CH}_3, \text{H}_2)/k(\text{CH}_3, \text{D}_2)$ and $k(\text{CD}_3, \text{H}_2)/k(\text{CD}_3, \text{D}_2)$ values in Table XVII were calculated by application of (III-10) to those KIEs calculated using (I-3) and the H_2 and D_2 frequencies in (III-8). The same type correction was applied to the LMR-PES KIEs; these rotationally corrected LMR-PES KIEs are given in the column labeled RC in Table XVII. The LMR-PES H_2 and D_2 harmonic frequencies, 4468.1 and 3160.6 cm^{-1} , respectively, were used to calculate this correction factor, and the corrected LMR-PES KIE is given by (III-11c).

$$\frac{u_{H_2} - u_{D_2}}{2} (\text{LMR-PES}) = \frac{1.4388(4468.1-3160.6)}{2T} = \exp\left(\frac{940.6}{T}\right) \quad (\text{III-11a})$$

$$\frac{\exp\left(\frac{889.4}{T}\right)}{\exp\left(\frac{940.6}{T}\right)} = \exp\left(\frac{889.4-940.6}{T}\right) = \exp\left(\frac{-51.2}{T}\right) \quad (\text{III-11b})$$

$$k_H/k_D (\text{corrected LMR-PES}) = k_H/k_D (\text{LMR-PES}) \exp\left(\frac{-51.2}{T}\right) \quad (\text{III-11c})$$

Therefore, the values in the column labeled RC in Table XVII are obtained by multiplying the values in the column labeled HF by (III-11b). Obviously, adjusting the LMR-PES reactant ZPE values to the rotationally corrected PK reactant ZPE values does lead to lower calculated KIES and does further increase the disagreement between experiment and theory. However, some of the LEPS2, BEBO3, LEPS, and BEBO KIEs were larger than their corresponding experimental values. Therefore, lowering these theoretical KIEs by application of the rotational correction improved their agreement with experiment. This improvement occurs for the BEBO3 and LEPS2 $k(\text{CH}_3, \text{H}_2)/k(\text{CH}_3, \text{D}_2)$ values in columns 13 and 16 only in Table XVII (that is, for the KIEs calculated using $F_{\phi_i}^\ddagger (i=1,2,3) = 0.0001 \text{ mdyne-}\overset{\circ}{\text{A}}$). However, for the $k(\text{CD}_3, \text{H}_2)/k(\text{CD}_3, \text{D}_2)$ values the rotational correction improves the agreement with most of the experimental values (that is, most all of the values in columns 13 through 19 in Table XVII exceed or are approximately equal to the corresponding experimental value). One exception to the latter statement for the $k(\text{CD}_3, \text{H}_2)/k(\text{CD}_3, \text{D}_2)$ values is that the Majury and Steacie experimental values, 4.11 and 3.48,¹⁶

exceed the calculated LEPS2 and BEBO3 KIEs using $F_{\phi_1}^\ddagger (i=1,2,3) = 0.26$ and $0.568 \text{ mdyne-}\text{\AA}^{0.14}$ and the LEPS and BEBO¹² KIEs.

Columns five and six of Table XVII show that use of the observed H_2 and D_2 frequencies, 4395.2_4 and 3118.4_6 cm^{-1} , respectively, in place of the LMR-PES harmonic frequencies leads to KIEs which are about five percent lower than those calculated using harmonic frequencies.⁴⁰ Clearly, the agreement between theory and experiment is not as strongly dependent upon the magnitude of the fundamental frequencies for H_2 and D_2 used in the calculation as upon other factors.

Application of Bell tunneling to the LMR-PES KIEs in the column labeled HF produces the values in the column labeled BT.⁴⁴ Bell tunneling treats the potential-energy barrier along the reaction coordinate as being parabolic in shape and is assumably valid for all $u_L^\ddagger = \frac{hcv_L^\ddagger}{kT} < 2\pi$, where h is Planck's constant, c is the velocity of light, k is Boltzmann's constant, T is in $^\circ\text{K}$ and v_L^\ddagger is the imaginary frequency representing translational motion along the reaction coordinate for the activated complex.⁴⁴ The Bell tunneling correction factor B_t is calculated for the isotopic $u_L^\ddagger < 2\pi$ using equation (III-12).

$$B_t(T) = \frac{u_{1L}^\ddagger \sin(u_{2L}^\ddagger/2)}{u_{2L}^\ddagger \sin(u_{1L}^\ddagger/2)} \quad (\text{III-12})$$

The condition $u_L^\ddagger < 2\pi$ is valid for the LMR-PES above 340°K ; for the BEBO model above $\sim 390^\circ\text{K}$; and for the LEPS model above $\sim 465^\circ\text{K}$. The Bell tunneling correction factor is a function of the absolute temperature and is simply multiplied by the transition-state theory LMR-PES-HF KIE

at the corresponding temperature to obtain the Bell tunneling corrected KIEs in the column labeled BT. It can be seen that the application of Bell tunneling to the LMR-PES KIEs improves the agreement with the corresponding experimental KIEs with the possible exceptions of the $k(\text{CD}_3, \text{HD})/k(\text{CD}_3, \text{DH})$ and the $k(\text{CD}_3, \text{H}_2)/k(\text{CD}_3, \text{D}_2)$ values. This improvement in the agreement between theoretically calculated KIEs and experimental KIEs upon applying a correction for tunneling does not necessarily indicate the presence of tunneling in that reaction. It could also indicate deficiencies in the LMR-PES and/or inaccuracies in the experimentally determined KIE.

The only experimental KIE for reaction of $\text{CH}_4 + \text{H}$ involves the effect of D atoms versus H atoms on the abstraction rate.¹² The activated complexes principally determine this KIE since the reactants contribution only reflects the momentum of H relative to D along the reaction coordinate. Similarly the intramolecular isotope effects for the reaction of CH_3 and CD_3 with HD are entirely determined by the isotopic properties of the activated complexes. Obviously, the $k(\text{CH}_3, \text{HD})/k(\text{CH}_3, \text{DH})$ and $k(\text{CD}_3, \text{HD})/k(\text{CD}_3, \text{DH})$ values predicted by the LMR-PES KIEs with and without tunneling agree reasonably well, although not quantitatively with the experimental KIEs. This amount of agreement between the LMR-PES and experimental KIEs indicates that the force constants governing vibrational motion both parallel and perpendicular to the reaction coordinate at the top of the barrier (or saddle point) are reasonable.

The various BEBO and LEPS models produce values for $k(\text{CH}_4, \text{H})/k(\text{CH}_4, \text{D})$ in better agreement with experiment than does the LMR-PES. Also, variation of the HCH_1 bending force constant,

$F_{\phi_1}^\ddagger$ ($i=1,2,3$), from 0.0001 to 0.568 mdyne-Å in the SW BEBO3 and LEPS2 models has no effect on the $k(\text{CH}_4, \text{H})/k(\text{CH}_4, \text{D})$ KIE values. However, the LMR-PES $k(\text{CH}_3, \text{HD})/k(\text{CH}_3, \text{DH})$ and $k(\text{CD}_3, \text{HD})/k(\text{CD}_3, \text{DH})$ KIEs agree with experiment much better than the corresponding BEBO and LEPS KIEs except for the BEBO3 model with the unrealistically small HCH_1 bending force constant $F_{\phi_1}^\ddagger$ ($i=1,2,3$) = 0.0001 mdyne-Å. Comparison of the BEBO3 and LEPS2 $k(\text{CH}_3, \text{HD})/k(\text{CD}_3, \text{DH})$ and $k(\text{CD}_3, \text{HD})/k(\text{CD}_3, \text{DH})$ values as a function of the $F_{\phi_1}^\ddagger$ ($i=1,2,3$) values shows that as the HCH_1 force constant becomes larger, these intramolecular isotope effects become smaller and hence the agreement between theory and experiment worsens. The LMR-PES predicts a value for the $F_{\phi_1}^\ddagger$ ($i=1,2,3$) of 0.18 mdyne-Å which is comparable to but slightly smaller than both the median value used by SW and the value assumed by KHT, see Table XVI.

In view of the results in Table XVII, the KIEs for the reactions $\text{CH}_4 + \text{H}(\text{D})$, $\text{CH}_3 + \text{H}_2(\text{D}_2)$ and $\text{CD}_3 + \text{H}_2(\text{D}_2)$ could be construed as indicating inadequacies in the LMR-PES compared to the BEBO and LEPS models relative to experiment. However, the results for the reactions $\text{CH}_3 + \text{HD}$ and $\text{CD}_3 + \text{HD}$ in Table XVII could be taken to suggest that the BEBO and LEPS models are inadequate relative to the LMR-PES when compared to experiment. These contradictory results are indicative of one or more of the following. First, both the LMR-PES and the BEBO3, LEPS2, BEBO, and LEPS models contain inadequacies specific to a certain type of calculated KIE. Absolute reaction rate theory requires that the correct potential energy hypersurface reproduce all experimental KIEs assuming that the latter are accurate and precise. Therefore, it seems illogical that a model could reasonably predict results for only one of two related experiments. Second, the

experimental determination of one type of KIE is subject to errors and the correction of these errors would lead to agreement between only one theoretical model and experiment. Although this is not inconceivable, it is impossible to tell which model (BEB03, LEPS2, BEBO, LEPS, or the LMR-PES) if any would best fit a set of revised experimental results, provided the present results were found to be in error. Empirical variation of various LMR-PES transition-state force constants was attempted, but no completely self-consistent set of isotopic frequencies could be found to reproduce the experimental differences between the CH_3 and CD_3 reactions with $\text{H}_2(\text{D}_2)$ and HD. A similar conclusion was reached by Shapiro and Weston.¹⁴

As seen in Table XVII, Ting and Weston observed normal intermolecular and intramolecular isotope effects on the abstraction of hydrogen from H_2 by hot CH_3^* ; that is, $k(\text{CH}_3, \text{H}_2)/k(\text{CH}_3, \text{D}_2) = 2.12$ and $k(\text{CH}_3, \text{HD})/k(\text{CH}_3, \text{DH}) = 6.37$ at 296°K .¹³ However, reaction of hot CD_3 with $\text{H}_2(\text{D}_2)$ produced an inverse isotope effect, $k(\text{CD}_3, \text{H}_2)/k(\text{CD}_3, \text{D}_2)$ of 0.465.¹³ As discussed in Chapter I, these results are difficult to interpret either qualitatively or quantitatively. Since a thermal distribution of reactant energies is a prerequisite to the use of absolute-reaction-rate theory, kinetic isotope effects can not be calculated for these reactions by this approach.

For the hot-atom reactions $\text{T}^* + \text{CH}_4 \rightarrow \text{CH}_3 + \text{TD}$ and $\text{T}^* + \text{CD}_4 \rightarrow \text{CD}_3 + \text{TD}$ the hot atom yield ratios, $[(\text{HT}/\text{CH}_4)/(\text{DT}/\text{CD}_4)]$, found experimentally by Chou and Rowland¹⁰ and calculated by Raff² are 1.43 and 1.18, respectively. The calculated yield ratio was obtained using the LMR-PES, an integrated reaction probability equation, and reactant and Br_2 moderator concentrations equivalent to those used by Chou and

Rowland.^{2,10} Both the calculated and experimental yield ratios assumably reflect the reaction of thermalized (or relatively stationary with respect to H and T atoms) CH_4 and CD_4 with tritium atoms possessing translational energies ≤ 65 kilocalories/mole. The temperature equivalent of these translational energies is $\leq 22,000$ °K. In terms of equation (I-4) it is important to note that as T in °K approaches infinity VPxEXC approaches ZPE^{-1} .^{3a,b,11} Thus, in the limit of high temperature the isotope effect for a given reaction equals $v_{1L}^\ddagger/v_{2L}^\ddagger$; that is, the observed KIE is classical mechanical in origin. It is thus interesting to note, that for the abstraction reactions of thermalized tritium atoms with CH_4 and CD_4 , the LMR-PES predicts an "infinite"-temperature isotope effect, $v_{1L}^\ddagger/v_{2L}^\ddagger$, of 1.19. This value is in good agreement with both the experimental and hot atom yield ratios. Thus, this agreement maybe tentatively taken to suggest that in a reactive collision between T^* and CH_4 and T^* and CD_4 , the T^* atom translational energies are on the average sufficiently large to obscure the differences in quantum mechanical effects for the two reactions.

However, for the reactions $\text{CH}_3^* + \text{H}_2(\text{D}_2)$ and $\text{CD}_3^* + \text{H}_2(\text{D}_2)$ using hot methyl radicals, the isotope effects reported by Ting and Weston, $k_{\text{H}}/k_{\text{D}} = 2.12$ and 0.465 , respectively, are not approximated by the $v_{1L}^\ddagger/v_{2L}^\ddagger$ ratios calculated for the corresponding thermal reactions, $v_{1L}^\ddagger/v_{2L}^\ddagger = 1.327$ and 1.328 , respectively. The following comments are thus pertinent. First, the agreement between the hot atom yield ratios and the $v_{1L}^\ddagger/v_{2L}^\ddagger$ ratio is merely fortuitous. Second, the CH_3 and CD_3 excitation energy involves principally internal rather than translational modes of the radicals. It is to be noted that Chapman

and Bunker¹⁸ claim isotope effects of 1.84 and 0.70 on the ratios of reactive cross sections, $\sigma(\text{CH}_3, \text{H}_2)/\sigma(\text{CH}_3, \text{D}_2)$ and $\sigma(\text{CD}_3, \text{H}_2)/\sigma(\text{CD}_3, \text{D}_2)$, respectively. These results supposedly reproduce the corresponding normal and inverse isotope effects reported by Ting and Weston¹² for $\text{CH}_3^* + \text{H}_2(\text{D}_2)$ and $\text{CD}_3^* + \text{H}_2(\text{D}_2)$. Chapman and Bunker (CB) also claim that these isotope effects do not reflect vibrational excitation in CH_3 and CD_3 .¹⁸ However, their data does appear to show that vibrational excitation of H_2 (or D_2) does enhance the reaction rate and preserve the unusual isotope effect, as previously mentioned in Chapter I.¹⁸ However, these conclusions could be fortuitous, since each normal mode frequency is assigned an apparently arbitrary dynamic energy which is used to obtain and then adjust the internal coordinates of the molecule to obtain some specified total energy for the molecule. It is not clear whether this adjustment procedure or the method of choosing the initial energies allows for the proper representation of the CB potential energy surface in these calculations. Also, the validity of comparing isotopic reactive cross sections with the experimental isotope effects of Ting and Weston is unclear.

Theoretical and Experimental

Temperature Dependences

The temperature dependences for the experimental KIEs in Table XVII are compared to the temperature dependences of the corresponding LMR-PES, BEBO, BEBO3, LEPS, and LEPS2 theoretically calculated KIEs summarized in Tables XVIII through XXII. The ratio of the preexponential factors, $A_{\text{H}}/A_{\text{D}}$, and the difference in activation energies for labeled and unlabeled reactions, ΔE , was determined for each isotope

TABLE XVIII

EXPERIMENTAL AND THEORETICAL TEMPERATURE DEPENDENCES FOR $k(\text{CH}_4, \text{H})/k(\text{CH}_4, \text{D})^a$

$A_{\text{H}}/A_{\text{D}}$	ΔE (calories/mole)	Temperature Range ($^{\circ}\text{K}$)	Reference ^b Source	Source ^c Label
1.391 ± 0.003	-1000 ± 2	396-969	2	LMR-PES
0.903 ± 0.053	-355 ± 59	396-696	2,44	LMR-PES + Bell Tunneling
1.38	-500 ± 300	500-732	12	KHT experimental result
1.268 ± 0.008	-541 ± 6	396-696	14	BEBO3 $F_{\phi}^{\ddagger} = 0.0001 \text{ mdyne-}\overset{\text{od}}{\text{A}}$
1.269 ± 0.008	-541 ± 6	396-696	14	BEBO3 $F_{\phi}^{\ddagger} = 0.26 \text{ mdyne-}\overset{\text{od}}{\text{A}}$
1.269 ± 0.008	-541 ± 6	396-696	14	BEBO3 $F_{\phi}^{\ddagger} = 0.658 \text{ mdyne-}\overset{\text{od}}{\text{A}}$
1.263 ± 0.008	-475 ± 6	396-696	14	LEPS2 $F_{\phi}^{\ddagger} = 0.0001 \text{ mdyne-}\overset{\text{od}}{\text{A}}$
1.264 ± 0.008	-476 ± 6	396-696	14	LEPS2 $F_{\phi}^{\ddagger} = 0.26 \text{ mdyne-}\overset{\text{od}}{\text{A}}$
1.265 ± 0.008	-477 ± 6	396-696	14	LEPS2 $F_{\phi}^{\ddagger} = 0.568 \text{ mdyne-}\overset{\text{od}}{\text{A}}$

TABLE XVIII (Continued)

A_H/A_D	ΔE (calories/mole)	Temperature Range ($^{\circ}K$)	Reference ^b Source	Source ^c Label
1.224 ± 0.007	-561 ± 6	396-696	12	BEBO
1.261 ± 0.008	-469 ± 6	396-696	12	LEPS

^aAll results except experimental results are from the least squares fits to equation (III-13) for 12 temperatures over the specified range. All deviations are standard deviations.

^bReferences from which the experimental values and/or the force constants and geometries used for the theoretical calculations were obtained.

^cDescribes information obtained from the references.

^d $F_{\phi}^{\ddagger} = F_{\phi_i}^{\ddagger}$ ($i=1,2,3$), see Table XVI.

TABLE XIX

EXPERIMENTAL AND THEORETICAL TEMPERATURE DEPENDENCES FOR $k(\text{CH}_3, \text{H}_2)/k(\text{CH}_3, \text{D}_2)^a$

A_H/A_D	ΔE (calories/mole)	Temperature Range ($^{\circ}\text{K}$)	Reference ^b Source	Source ^c Label
1.483 ± 0.009	201 ± 6	396-696	2	LMR-PES
0.612 ± 0.064	1584 ± 102	396-696	2,44	LMR-PES + Bell Tunneling
0.911 ± 0.020	1327 ± 24	399-645	14	SW experimental
$0.194 (0.659)^d$	$1760 (707)^d$	403-564	15	WS experimental
0.246 ± 0.134 $(0.809 \pm 0.673)^d$	2516 ± 613 $(1560 \pm 1693)^d$	408-571	16	MS experimental
	1100	409-591	17	DB experimental
1.337 ± 0.013	1028 ± 10	396-696	14	BEBO3 $F_{\phi}^{\ddagger} = 0.0001 \text{ mdyne-}\overset{\circ}{\text{A}}^e$
1.455 ± 0.018	822 ± 12	396-696	14	BEBO3 $F_{\phi}^{\ddagger} = 0.26 \text{ mdyne-}\overset{\circ}{\text{A}}^e$
1.540 ± 0.019	646 ± 13	396-696	14	BEBO3 $F_{\phi}^{\ddagger} = 0.568 \text{ mdyne-}\overset{\circ}{\text{A}}^e$

TABLE XIX (Continued)

A_H/A_D	ΔE (calories/mole)	Temperature Range ($^{\circ}K$)	Reference ^b Source	Source ^c Label
1.379 ± 0.016	993 ± 12	396-696	14	LEPS2 $F_{\phi}^{\ddagger} = 0.0001 \text{ mdyne-}\overset{0}{\text{A}}^e$
1.488 ± 0.020	801 ± 14	396-696	14	LEPS2 $F_{\phi}^{\ddagger} = 0.26 \text{ mdyne-}\overset{0}{\text{A}}^e$
1.566 ± 0.021	635 ± 14	396-696	14	LEPS2 $F_{\phi}^{\ddagger} = 0.568 \text{ mdyne-}\overset{0}{\text{A}}^e$
1.533 ± 0.019	777 ± 13	396-696	12	BEBO
1.484 ± 0.020	809 ± 14	396-696	12	LEPS

^aAll results except experimental results are from the least squares fits to equation (III-13) for 12 temperatures over the specified range. All deviations are standard deviations.

^bReferences from which the experimental values and/or the force constants and geometries used for the theoretical calculations were obtained.

^cDescribes information obtained from the references.

^dValues in parentheses are calculated by a different method, see text.

^e $F_{\phi}^{\ddagger} = F_{\phi_i}^{\ddagger}$ ($i=1,2,3$), see Table XVI.

TABLE XX
 EXPERIMENTAL AND THEORETICAL TEMPERATURE DEPENDENCES FOR $k(\text{CD}_3, \text{H}_2)/k(\text{CD}_3, \text{D}_2)$

$A_{\text{H}}/A_{\text{D}}$	ΔE (calories/mole)	Temperature Range ($^{\circ}\text{K}$)	Reference ^b Source	Source ^c Label
1.488 ± 0.010	197 ± 7	396-696	2	LMR-PES
0.616 ± 0.064	1576 ± 101	396-696	2,44	LMR-PES + Bell Tunneling
1.592 ± 0.124	588 ± 70	402-611	14	SW experimental
$3.724 (1.702)^{\text{d}}$	$-201 (714)^{\text{d}}$	410-572	15	WS experimental
1.727 ± 0.279 $(1.062 \pm 0.699)^{\text{d}}$	701 ± 462 $(1100 \pm 480)^{\text{d}}$	407-570	16	MS experimental
1.339 ± 0.013	1027 ± 10	396-696	14	BEBO3 $F_{\phi}^{\ddagger} = 0.0001 \text{ mdyne-}\overset{\circ}{\text{A}}^{\text{e}}$
1.466 ± 0.018	813 ± 13	396-696	14	BEBO3 $F_{\phi}^{\ddagger} = 0.26 \text{ mdyne-}\overset{\circ}{\text{A}}^{\text{e}}$
1.572 ± 0.021	616 ± 14	396-696	14	BEBO3 $F_{\phi}^{\ddagger} = 0.568 \text{ mdyne-}\overset{\circ}{\text{A}}^{\text{e}}$

TABLE XX (Continued)

A_H/A_D	ΔE (calories/mole)	Temperature Range ($^{\circ}K$)	Reference ^b Source	Source ^c Label
1.380 ± 0.016	992 ± 12	396-696	14	LEPS2 $F_{\phi}^{\ddagger} = 0.001 \text{ mdyne-}\overset{\circ}{\text{A}}^e$
1.497 ± 0.021	792 ± 14	396-696	14	LEPS2 $F_{\phi}^{\ddagger} = 0.26 \text{ mdyne-}\overset{\circ}{\text{A}}^e$
1.595 ± 0.023	607 ± 15	396-696	14	LEPS2 $F_{\phi}^{\ddagger} = 0.568 \text{ mdyne-}\overset{\circ}{\text{A}}^e$
1.490 ± 0.019	777 ± 13	396-696	12	BEBO
1.493 ± 0.021	800 ± 14	396-696	12	LEPS

^aAll results except experimental results are from the least squares fits to equation (III-13) for 12 temperatures over the specified range. All deviations are standard deviations.

^bReferences from which the experimental values and/or the force constants and geometries used for the theoretical calculations were obtained.

^cDescribes information obtained from the references.

^dValues in parentheses are calculated by a different method, see text.

^e $F_{\phi}^{\ddagger} = F_{\phi_i}^{\ddagger}$ ($i=1,2,3$), see Table XVI.

TABLE XXI

EXPERIMENTAL AND THEORETICAL TEMPERATURE DEPENDENCES FOR $k(\text{CH}_3, \text{HD})/k(\text{CH}_3, \text{DH})^a$

A_H/A_D	ΔE (calories/mole)	Temperature Range ($^{\circ}\text{K}$)	Reference ^b Source	Source ^c Label
1.083 ± 0.003	379 ± 3	396-969	2	LMR-PES
0.761 ± 0.027	945 ± 36	396-696	2,44	LMR-PES + Bell Tunneling
0.283 ± 0.258	1929 ± 690	367-651	14	SW experimental
0.452^d	1350^d	408-569	15	WS experimental
1.170 ± 0.002	330 ± 2	396-696	14	BEBO3 $F_{\phi}^{\ddagger} = 0.0001 \text{ mdyne-}\overset{\circ}{\text{A}}^e$
1.273 ± 0.001	125 ± 1	396-696	14	BEBO3 $F_{\phi}^{\ddagger} = 0.26 \text{ mdyne-}\overset{\circ}{\text{A}}^e$
1.346 ± 0.001	-51 ± 1	396-696	14	BEBO3 $F_{\phi}^{\ddagger} = 0.568 \text{ mdyne-}\overset{\circ}{\text{A}}^e$
1.213 ± 0.001	154 ± 1	396-696	14	LEPS2 $F_{\phi}^{\ddagger} = 0.0001 \text{ mdyne-}\overset{\circ}{\text{A}}^e$

TABLE XXI (Continued)

A_H/A_D	ΔE (calories/mole)	Temperature Range ($^{\circ}K$)	Reference ^b Source	Source ^c Label
1.308 ± 0.002	-362 ± 1	396-696	14	LEPS2 $F_{\phi}^{\ddagger} = 0.26 \text{ mdyne-}\overset{\circ}{\text{A}}^e$
1.375 ± 0.002	-201 ± 1	396-696	14	LEPS2 $F_{\phi}^{\ddagger} = 0.568 \text{ mdyne } \overset{\circ}{\text{A}}^e$
1.278 ± 0.001	120 ± 1	396-696	12	BEBO
1.309 ± 0.002	-44 ± 1	396-696	12	LEPS

^aAll results except experimental results are from the least squares fits to equation (III-13) for 12 temperatures over the specified range. All deviations are standard deviations.

^bReferences from which the experimental values and/or the force constants and geometries used for the theoretical calculations were obtained.

^cDescribes information obtained from the references.

^dAverage of the results at two different reactant pressures.

^e $F_{\phi}^{\ddagger} = F_{\phi_i}^{\ddagger}$ ($i=1,2,3$), see Table XVI.

TABLE XXII

EXPERIMENTAL AND THEORETICAL TEMPERATURE DEPENDENCES FOR $k(\text{CD}_3, \text{HD})/k(\text{CD}_3, \text{DH})^a$

A_H/A_D	ΔE (calories/mole)	Temperature Range ($^{\circ}\text{K}$)	Reference ^b Source	Source ^c Label
1.085 ± 0.003	375 ± 3	396-696	2	LMR-PES
0.764 ± 0.027	939 ± 35	396-696	2,44	LMR-PES + Bell Tunneling
0.932 ± 0.133	546 ± 131	402-611	14	SW experimental
1.698	0	410-572	15	WS experimental
1.171 ± 0.002	329 ± 2	396-696	14	BEBO3 $F_{\phi}^{\ddagger} = 0.0001 \text{ mdyne-}\overset{\circ}{\text{A}}^d$
1.282 ± 0.001	115 ± 1	396-696	14	BEBO3 $F_{\phi}^{\ddagger} = 0.26 \text{ mdyne-}\overset{\circ}{\text{A}}^d$
1.374 ± 0.002	-82 ± 2	296-696	14	BEBO3 $F_{\phi}^{\ddagger} = 0.568 \text{ mdyne-}\overset{\circ}{\text{A}}^d$
1.214 ± 0.001	153 ± 1	396-696	14	LEPS2 $F_{\phi}^{\ddagger} = 0.0001 \text{ mdyne-}\overset{\circ}{\text{A}}^d$
1.316 ± 0.002	-46 ± 1	396-696	14	LEPS2 $F_{\phi}^{\ddagger} = 0.26 \text{ mdyne-}\overset{\circ}{\text{A}}^d$

TABLE XXII (Continued)

A_H/A_D	ΔE (calories/mole)	Temperature Range ($^{\circ}K$)	Reference ^b Source	Source ^c Label
1.401 ± 0.003	-230 ± 2	396-696	14	LEPS $F_{\phi}^{\ddagger} = 0.568 \text{ mdyne-}\overset{\circ}{A}^d$
1.289 ± 0.001	109 ± 1	396-696	12	BEBO
1.317 ± 0.002	-54 ± 2	396-696	12	LEPS

^aAll results except experimental results are from the least squares fits to equation (III-13) for 12 temperatures over the specified range. All deviations are standard deviations. The atom underlined is being abstracted.

^bReferences from which the experimental values and/or the force constants and geometries used for the theoretical calculations were obtained.

^cDescribes information obtained from the references.

^d $F_{\phi}^{\ddagger} = F_{\phi_i}^{\ddagger}$ ($i=1,2,3$), see Table XVI.

effect by applying equation (III-13) to the KIE data using the method of least squares.

$$\ln(k_1/k_2) = \ln(A_1/A_2) + \Delta E/RT \quad (\text{III-13})$$

In (III-13) the subscripts 1 and 2 refer to the light and heavy isotopes, respectively, and k_1/k_2 is the KIE at a specific temperature T in °K.

For the isotope effect $k(\text{CH}_4, \text{H})/k(\text{CH}_4, \text{D})$, the data in Table XVIII shows that the error in the KHT experimental ΔE value encompasses all but the LMR-PES ΔE value. The application of Bell tunneling to the LMR-PES KIEs apparently over-corrects the LMR-PES ΔE value, but it does cause the value to fall within the error bounds of the experimental value. However, inclusion of the Bell tunneling correction produces a calculated $A_{\text{H}}/A_{\text{D}}$ value of 0.903 which is lower than either the experimental value, 1.38, or the values obtained from the various BEBO and LEPS models. As previously mentioned the improvement in the agreement with experiment by application of tunneling may be more indicative of inadequacies in either one or more of the theoretical models or in the experimental results or both than the existence of tunneling. The maximum error in the experimental $A_{\text{H}}/A_{\text{D}}$ value, 1.38, is estimated by KHT to probably be within ± 0.14 .¹² However, due to the experimental problems discussed in Chapter I, this $A_{\text{H}}/A_{\text{D}}$ value, 1.38, and the associated error were estimated using simple collision theory.¹² It should be noted that changes in the value of $F_{\phi_i}^\ddagger$ ($i=1,2,3$) has no more

effect on the calculated Arrhenius equation parameters than it does on the $k(\text{CH}_4, \text{H})/k(\text{CH}_4, \text{D})$ values in Table XVII.

As seen in Table XIX, the ΔE for the reaction $\text{CH}_3 + \text{H}_2(\text{D}_2)$ calculated from the experimental KIEs is greater than the values obtained from the isotope effects calculated without inclusion of tunneling; the lowest value being that from the LMR-PES data. For the LMR-PES, inclusion of Bell tunneling into the isotope effects significantly improves the agreement between predicted and experimental ΔE values. However, this result does not necessarily indicate that tunneling is present. Precise comparison between theory and experiment is necessarily precluded by the considerable discrepancies between the experimental ΔE values. The individual experimental ΔE values differ by more than the uncertainties measured for any one reported value. The experimental $A_{\text{H}}/A_{\text{D}}$ values in Table XIX seem too low except for the value reported by SW.¹⁴ The differences in these experimental $A_{\text{H}}/A_{\text{D}}$ values may be at least partially due to the experimental technique. Davison and Burton¹⁷ and SW¹⁴ determined their KIE values for the reaction of methyl radicals with a mixture of H_2 and D_2 , whereas Whittle and Steacie¹⁵ and Majury and Steacie¹⁶ reacted methyl radicals with H_2 or D_2 separately. Davison and Burton (DB) determined their ΔE value by fitting a line to their KIE values assuming a steric factor ratio of unity. The collision theory equation used by DB is equivalent to the Arrhenius equation used by SW except that the steric factor ratio (S_1/S_2) must be multiplied by a collision number ratio (C_1/C_2) to obtain a value equivalent to the $A_{\text{H}}/A_{\text{D}}$ values given by fitting data to (III-13). The collision number ratio, C_1/C_2 , is given by

$$C_1/C_2 = \left[\frac{\sigma(\text{CH}_3, \text{H}_2)}{\sigma(\text{CH}_3, \text{D}_2)} \right]^2 \frac{1/M_{\text{CH}_3} + 1/M_{\text{H}_2}}{1/M_{\text{CH}_3} + 1/M_{\text{D}_2}} \quad (\text{III-14})$$

where the M values are molecular weights of the species specified in the subscript and the σ values are the collision diameters of the reactant species.¹⁷ Assuming the same collision diameter for H₂ and D₂, a C₁/C₂ value of 1.337 is obtained from (III-14) using the masses (in amu): C= 12; H = 1.007825; D = 2.0141. Therefore, the S₁C₁/S₂C₂ value 1.337 could be taken as the A_H/A_D associated with the DB ΔE value of 1100 calories/mole and could be compared to the other A_H/A_D values in Table XIX. The Arrhenius parameters reported by Whittle and Steacie (WS)¹⁵ and by Majury and Steacie (MS)¹⁶ were calculated from rate constants obtained by two methods. These two different methods are only applicable to the determination of the individual rate constants for the reactions CH₃ + D₂ and CD₃ + H₂ which are used to calculate the Arrhenius parameters in Table XIX and Table XX, respectively. The values obtained by using method I rate constants are given in parentheses in Tables XIX and XX. For method I the rate constants were calculated by subtracting the concentration of methane obtained from photolysis of acetone alone from the total concentration of isotopic methanes obtained from photolysis of acetone or acetone-d₆ in the presence of D₂ or H₂ to obtain the concentration of CH₃D or CD₃H, respectively. These concentrations are needed to determine the individual rate constants for formation of CH₃D or CD₃H, respectively.^{15,16} For method II, rate constants were obtained from mass spectrometric determination of the ratios [CH₃D]/[CH₄] or

$[\text{CD}_3\text{H}]/[\text{CD}_4]$ in the product gases from photolysis of acetone or acetone- d_6 in the presence of either D_2 or H_2 , respectively.^{15,16} The individual $k(\text{CH}_3, \text{H}_2)/k(\text{CH}_3, \text{D}_2)$ and $k(\text{CD}_3, \text{H}_2)/k(\text{CD}_3, \text{D}_2)$ values that were reported in Table XVII and attributed to MS were calculated by us using the rate constants reported by MS in a summary table and are averages of the method I and method II rate constant values.¹⁶

However, WS considered the method II rate constants to be the more accurate. Therefore, the $k(\text{CH}_3, \text{H}_2)/k(\text{CH}_3, \text{D}_2)$ and $k(\text{CD}_3, \text{H}_2)/k(\text{CD}_3, \text{D}_2)$ values reported in Table XVII in the column labeled WS were calculated using the method II rate constants $k(\text{CH}_3, \text{D}_2)$ and $k(\text{CD}_3, \text{H}_2)$.¹⁵ WS did not report individual method I rate constant values in their summary table from which the other WS values in Table XVII were calculated.¹⁵ It should be noted that the rate constants for reaction of $\text{CH}_3 + \text{H}_2$ and $\text{CD}_3 + \text{D}_2$ could only be determined by method I. Therefore, the generally better agreement between the method I Arrhenius equation parameters given in parentheses in Tables XIX and XX for MS¹⁶ and WS¹⁵, and the parameter values reported by Shapiro and Weston¹⁴ and by Davison and Burton¹⁷ reflects the probable cancellation of consistent errors in the method I values yielding reasonably accurate KIEs. Although, the method II rate constants determined by MS¹⁶ and WS¹⁵ may be more accurate, by themselves, the KIEs determined by a ratio of one method I and one method II rate constant may actually compound the error of each rate constant into a greater error in the resultant KIE value.

The data in Tables XIX and XX clearly show that transition state theory predicts only negligible differences between the $k(\text{CH}_3, \text{H}_2)/k(\text{CH}_3, \text{D}_2)$ and $k(\text{CD}_3, \text{H}_2)/k(\text{CD}_3, \text{D}_2)$ Arrhenius parameters

are in serious disagreement with this prediction. Furthermore, for the reactions of CH_3 and CD_3 with H_2 and D_2 the LMR-PES and SW transition-state force constants could not be arbitrarily adjusted to produce a single set that would produce a variation in the KIEs and Arrhenius parameters comparable to the variation in the experimental values. It can be seen that decreasing the $F_{\phi_i}^\ddagger$ ($i=1,2,3$) force constants from 0.568 to 0.0001 mdyne-Å increases the calculated ΔE values and decreases the $A_{\text{H}}/A_{\text{D}}$ values. Therefore, the BEBO3 and LEPS2 Arrhenius parameters calculated using $F_{\phi_i}^\ddagger$ ($i=1,2,3$) = 0.0001 mdyne-Å are in much better agreement with the Table XIX experimental results than those using larger $F_{\phi_i}^\ddagger$ ($i=1,2,3$) values. However, a force constant value of $F_{\phi_i}^\ddagger$ ($i=1,2,3$) = 0.568 mdyne-Å produces BEBO3 and LEPS2 theoretically calculated Arrhenius parameters in best agreement with the experimental values in Table XX. Similarly for the LMR-PES, other transition-state force constants including off-diagonal cross-term force constants can be adjusted to produce KIEs and Arrhenius parameters which are in agreement with one but not both of the $\text{CH}_3 + \text{H}_2(\text{D}_2)$ or $\text{CD}_3 + \text{H}_2(\text{D}_2)$ experimental values.

The $k(\text{CH}_3, \text{HD})/k(\text{CH}_3, \text{DH})$ and $k(\text{CD}_3, \text{HD})/k(\text{CD}_3, \text{DH})$ Arrhenius parameters are given in Tables XXI and XXII, respectively. The LMR-PES gives $k_{\text{H}}/k_{\text{D}}$ values which lead to $A_{\text{H}}/A_{\text{D}}$ and ΔE values in much better agreement with experiment than are the values predicted by the BEBO3, LEPS2, BEBO and LEPS models. This result is opposite to that observed for the reaction of CH_3 and CD_3 with H_2 and D_2 . As can be seen, the reproducibility in the $A_{\text{H}}/A_{\text{D}}$ and ΔE values derived from experiment leaves much to be desired. Also, as in Tables XVIII through XX the addition of Bell tunneling to the LMR-PES values

improves the agreement with experiment for reactions involving CH_4 or CH_3 radicals but tends to over-correct those values obtained for reactions involving CD_3 radicals. The differences in the values reported by both SW^{14} and WS^{15} between the experimental ΔE values in Table XXI and the corresponding values in Table XXII are about 1.4 kilocalories/mole. However, for each isotope effect the ΔE value reported by SW^{14} is about 500 calories/mole greater than the ΔE values reported by WS^{15} . This latter difference is most pronounced in Table XXII where WS report the isotope effect is temperature independent. Since the rate determining step involves transfer of either H or D, the result is clearly incorrect and casts doubt upon the experimental results obtained by Whittle and Steacie¹⁵. For the theoretically calculated Arrhenius parameters, it can be seen that the LEPS2 and BEBO3 models predict increasingly large $A_{\text{H}}/A_{\text{D}}$ values and decreasing ΔE values which actually become negative as $F_{\phi_i}^\ddagger$ ($i=1,2,3$) increases. It should also be noted that the error bounds on the SW ΔE values do not encompass any of the theoretically calculated ΔE values, although the LMR-PES ΔE and $A_{\text{H}}/A_{\text{D}}$ values are closer to the SW experimental result than any other theoretical result.

Theoretical Primary Carbon Effects

Tables XXIII and XXIV tabulate ^{13}C -carbon isotope effects and their temperature dependences based upon the LMR-PES. These tables also present ^{13}C -carbon KIEs based upon BEBO¹² and BEBO3¹⁴ models. These latter values are based upon force constants and geometry that were also used to calculate secondary α -deuterium isotope effects (see below).

Although k_{12}/k_{13} for both reactions are nowhere maximal, the $k(\text{CH}_4, \text{H})/k(^{13}\text{CH}_4, \text{H})$ are much larger than $k(\text{CH}_3, \text{H}_2)/k(^{13}\text{CH}_3, \text{H}_2)$. This result is

TABLE XXIII
COMPARISON OF $k(\text{CH}_4, \text{H})/k(^{13}\text{CH}_4, \text{H})$ RESULTS^a

Activated Complex Used	Transition State Theory Results					Arrhenius Results ^b		
	Temperature °K	MMI	EXC	ZPE	KIE	A_1/A_2	ΔE	Temperature Range °K
LMR-PES ^c	296	1.002	0.999	1.034	1.035			
	546	1.002	0.998	1.018	1.018	$0.999 \pm 3 \times 10^{-5}$	21.1 ± 0.02	273-546
BEBO ^d	296	1.003	0.999	1.020	1.022			
	546	1.003	0.998	1.010	1.011	$0.999 \pm 7 \times 10^{-5}$	13.0 ± 0.06	273-546
BEBO3 ^e	296	1.003	0.993	1.032	1.028			
	546	1.003	0.993	1.017	1.013	$0.995 \pm 4 \times 10^{-5}$	19.0 ± 0.03	273-546
BEBO3 ^f	296	1.003	0.999	1.006	1.008			
	546	1.003	0.999	1.003	1.005	$1.001 \pm 3 \times 10^{-5}$	3.9 ± 0.03	273-546

^aFor purposes of comparison all results were calculated using the LMR-PES reactant data with the activated complex parameters from the specified source.

^bResults obtained by linear least squares fit of $\ln(k_{12}/k_{13})$ versus T^{-1} for 12 values over the specified temperature range. See Appendix D. ΔE is in calories per mole.

^cCalculated using the LMR-PES data.

^dCalculated using the BEBO activated complex data from Reference 12.

^eCalculated using the BEBO3 activated complex data with $F_{\phi_i}^\ddagger (i=1,2,3) = 0.0001 \text{ mdyne-}\text{\AA}$ from Reference 14.

^fCalculated using the BEBO3 activated complex data with $F_{\phi_i}^\ddagger (i=1,2,3) = 0.568 \text{ mdyne-}\text{\AA}$ from Reference 14.

TABLE XXIV
 COMPARISON OF $k(\text{CH}_3, \text{H}_2)/k(^{13}\text{CH}_3, \text{H}_2)$ RESULTS^a

Activated Complex Used	Transition State Theory Results				Arrhenius Results ^b		Temperature Range °K	
	Temperature °K	MMI	EXC	ZPE	KIE	A_1/A_2		ΔE
LMR-PES ^c	296	1.008	0.999	0.999	1.006	$1.006 \pm 4 \times 10^{-5}$	0.4 ± 0.03	273-546
	546	1.008	0.998	1.000	1.006			
BEBO ^d	296	1.009	0.999	0.985	0.993	$1.007 \pm 1 \times 10^{-4}$	-7.7 ± 0.09	273-546
	546	1.009	0.998	0.992	0.999			
BEBO3 ^e	296	1.009	0.993	0.997	0.999	$1.002 \pm 1 \times 10^{-5}$	-1.8 ± 0.01	273-546
	546	1.009	0.993	0.999	1.001			
BEBO3 ^f	296	1.009	1.000	0.972	0.979	$1.008 \pm 9 \times 10^{-5}$	-16.8 ± 0.07	273-546
	546	1.009	1.000	0.984	0.993			

TABLE XXIV (Continued)

Activated Complex Used	Transition State Theory Results				Arrhenius Results ^b			
	Temperature °K	MMI	EXC	ZPE	KIE	A_1/A_2	ΔE	Temperature Range °K
Pimentel ^g	296	1.008	1.000	0.995	1.003	$1.007 \pm 7 \times 10^{-5}$	-2.7 ± 0.05	273-546
	546	1.008	1.000	0.997	1.005			

^aFor purposes of comparison all results were calculated using the LMR-PES reactant data with the activated complex parameters from the specified source.

^bResults obtained by linear least squares fit $\ln(k_{12}/k_{13})$ vs. T^{-1} for 12 values over the specified temperature range. See Appendix D. ΔE is in calories per mole.

^cCalculated using the LMR-PES data with Gaussian 70 out-of-plane bending frequency values.

^dCalculated using the BEBO activated complex data from Reference 12.

^eCalculated using the BEBO3 activated complex data with $F_{\phi_i}^{\ddagger}(i=1,2,3) = 0.0001$ mdyne-Å from Reference 14.

^fCalculated using the BEBO3 activated complex data with $F_{\phi_i}^{\ddagger}(i=1,2,3) = 0.568$ mdyne-Å from Reference 14.

^gCalculated using the LMR-PES data with out-of-plane bending frequency values corresponding to the harmonic values from Reference 38.

not unreasonable qualitatively since reaction (I-1) involves almost total breaking of the C-H₁ bond in passing from reactant-state to the transition state (that is, the transition-state configuration for (I-1) is very product-like). However, the small primary carbon effect for H atom abstraction on CH₄ reflects the fact that the loss in the frequencies associated with the C-H₁ bond being broken is compensated to a large extent by the frequencies associated with the H₁-H₆ bond being formed. Conversely, for reaction (I-2) passing from the reactant state to the transition state involves very little of both H₁-H₆ bond breaking and C-H₁ bond making (that is the transition state for reaction (I-2) is very reactant-like). Since the 13-carbon KIE is largely dependent on frequency changes associated with the C-H₁ bond and reaction (I-2) involves less of a change in the C-H₁ bonding in passing from reactant state to transition state than reaction (I-1), then the Table XXIV KIEs for reaction (I-2) tend to be less than the corresponding KIEs for reaction (I-1). Also, the BEBO3 13-carbon effect using $F_{\phi_i}^\ddagger (i=1,2,3) = 0.568$ mdyne-Å gives an inverse KIE for reaction (I-2) and a very small KIE for reaction (I-1). Comparison of the BEBO and BEBO3 13-carbon KIEs shows that all the KIEs values become lower or more inverse as the value of $F_{\phi_i} (i=1,2,3)$ is increased. This is the result of the effect of the $F_{\phi_i} (i=1,2,3)$ values on the frequencies most strongly associated with the C-H₁ bond in the transition state. Specifically, the carbon effect is the result of differences in the CH₃ asymmetric stretching, ν_5 , and degenerate bending, ν_6 , frequencies in the activated complex and their corresponding reactant state values. The ν_1 and ν_4 activated complex frequencies for the symmetric and asymmetric motion along the reaction coordinate, respectively, also contribute to the carbon effect.

However, the ν_7 and ν_8 linear bending frequencies are virtually unaffected by isotopic carbon substitution. It should be noted that the values labeled "Pimentel" in Table XXIV are calculated with all LMR-PES harmonic frequencies except the isotopic out-of-plane bending frequencies which are calculated using a harmonic force constant adjusted to produce a CH_3 out-of-plane bending frequency of 607 cm^{-1} which corresponds to the spectroscopic frequency reported by Tan, Winer and Pimentel (also, see discussion of this force constant in the secondary α -deuterium KIE section).³⁸ The 13-carbon KIE calculated using this frequency is normal but exhibits an inverse temperature dependence. The LMR-PES 13-carbon KIE using the Gaussian 70 out-of-plane bending frequency is normal with a very small normal temperature dependence. This difference is the result of the smaller isotopic change in the "Pimentel" calculated, 607 cm^{-1} , than the Gaussian 70 calculated, 847 cm^{-1} , CH_3 out-of-plane bending frequencies.³⁸

Precise experimental determinations of carbon isotope effects for reaction (I-1) and/or (I-2) would allow some additional insight into which one if any of the LMR-PES, BEBO and BEBO3 theoretical models have any validity. Also, carbon effects could be interpreted and contrasted with the primary effects already discussed to give a more quantitative description of the bonding that occurs in the transition state for the abstraction reaction. This information could possibly be used to construct a better theoretical model of the reaction hypersurface.

Theoretical Secondary α -Deuterium Effects

"Exact" calculations for model reactions within the framework of absolute rate theory show that secondary α -deuterium isotope effects are

TABLE XXV

COMPARISON OF SECONDARY α -DEUTERIUM $k(\text{CH}_4, \text{H})/k(\text{CD}_3\text{H}, \text{H})$ RESULTS^a

Activated Complex Used	Transition State Theory Results				Arrhenius Results ^b			
	Temperature °K	MMI	EXC	ZPE	KIE	A_1/A_2	ΔE	Temperature Range °K
LMR-PES ^c	296	1.319	0.858	1.395	1.579			
	546	1.319	0.771	1.198	1.218	0.889 ± 0.002	332 ± 2	273-546
BEBO ^d	296	1.274	0.903	1.123	1.293			
	546	1.274	0.830	1.065	1.127	0.962 ± 0.003	175 ± 2	273-546
BEBO3 ^e	296	1.275	0.645	1.832	1.507			
	546	1.275	0.642	1.389	1.136	0.807 ± 0.003	367 ± 2	273-546
BEBO3 ^f	296	1.275	0.930	0.601	0.712			
	546	1.275	0.879	0.759	0.850	1.052 ± 0.002	-229 ± 1	273-546

^aFor purposes of comparison all results were calculated using the LMR-PES reactant data with the activated complex parameters from the specified source.

^bResults obtained by linear least squares fit of $\ln(k_{\text{H}}/k_{\text{D}})$ vs. T^{-1} for 12 values over the specified temperature range. ΔE is in calories per mole. Deviations are standard deviations.

^cCalculated using the LMR-PES data.

^dCalculated using the BEBO activated complex data from Reference 12.

^eCalculated using the BEBO3 activated complex data with $F_{\phi_i}^\ddagger (i=1,2,3) = 0.0001 \text{ mdyne-}\overset{\circ}{\text{A}}$ from Reference 14.

^fCalculated using the BEBO3 activated complex data with $F_{\phi_i}^\ddagger (i=1,2,3) = 0.568 \text{ mdyne-}\overset{\circ}{\text{A}}$ from Reference 14.

principally determined by the change in the α -hydrogen to carbon to leaving (entering) group bending force constants $[F_{\phi_i}^\ddagger (i=1,2,3)]$ in passing from the reactant state to the transition state.^{3b-d} Since SW varied $F_{\phi_i}^\ddagger (i=1,2,3)$ in their BEBO3 activated-complex models, the smallest and largest values of these force constants were used with the other reported BEBO3 parameters in Table XVI to calculate secondary α -deuterium KIEs.¹⁴ The BEBO parameters reported by KHT¹² were also used to calculate secondary α -deuterium KIEs since their reported $F_{\phi_i}^\ddagger (i=1,2,3)$ value is almost the same as the median value used by SW¹⁴, see Table XVI. For purposes of comparison, the LMR-PES reactant-state frequencies and parameters were used in all the secondary α -deuterium KIE calculations. The secondary α -deuterium KIEs for reaction (I-1) are presented in Table XXV. Obviously, using the very large $F_{\phi_i}^\ddagger (i=1,2,3)$ value of 0.568 mdyne- \AA in the BEBO3 model¹⁴ has a dramatic effect on the secondary α -deuterium KIEs; it produces inverse KIEs while the LMR-PES², BEBO¹² and the BEBO3 with $F_{\phi_i}^\ddagger (i=1,2,3) = 0.0001$ mdyne- \AA all predict normal KIEs. This change to an inverse KIE for large values of $F_{\phi_i}^\ddagger (i=1,2,3)$ occurs because the differences in the isotopic activated-complex frequencies exceeds the differences in the isotopic reactant frequencies as is evidenced by the ZPE values in Table XXV. The differences in the MMI terms are the result of the differences in the activated complex geometries which produce different moments of inertia about the cartesian coordinate axes. The method of calculating these moments of inertia about the cartesian coordinate axes is given in Appendix B. The Arrhenius activation-energy differences, ΔE , and preexponential factors (A_1/A_2) for the LMR-PES and BEBO3 $[F_{\phi_i}^\ddagger (i=1,2,3) = 0.0001$ mdyne- \AA] appear to show the best agreement in both Table XXV and Table

XXVI. However, this agreement is apparently due to a fortuitous set of compensating factors. As seen in Table XXVI all secondary α -deuterium isotope effects for reaction (I-2) are inverse. The large $F_{\phi_i}^\ddagger$ ($i=1,2,3$) = 0.568 mdyne-Å for BEBO3 merely causes the secondary KIE to become more inverse. The more inverse KIEs for larger $F_{\phi_i}^\ddagger$ ($i=1,2,3$), as expected, show a larger negative ΔE compared to the other ΔE values in Table XXVI. It should be noted that the LMR-PES isotopic CH_3 normal-mode frequencies are used in all the secondary KIEs in Table XXVI and include the isotopic out-of-plane bending frequencies calculated using the Gaussian 70 out-of-plane bending force constant given in Chapter II, except for the KIEs labeled Pimentel. The α effects labeled as Pimentel are based on the use of the out-of-plane bending normal mode frequency calculated using the out-of-plane bending force constant of Tan, Winer and Pimentel (TWP).³⁸ These authors obtained this force constant from their spectroscopic frequencies.³⁸ It should be noted that their reported force constant could not be weighted or adjusted in such a way as to exactly reproduce the harmonic frequencies that TWP report having calculated.³⁸ However, the difference is negligible, both our calculation and TWP give 607.0 cm^{-1} for CH_3 , but TWP gives 470.2 cm^{-1} for CD_3 compared to our 470.5 cm^{-1} for CD_3 . The various isotopic CH_3 harmonic normal-mode frequencies that were calculated using this force constant are tabulated in Appendix C. Harmonic normal-mode frequencies were used instead of spectroscopic methyl radical frequencies for three reasons: First, TWP did not report spectroscopic frequencies for all the isotopic methyl radicals needed. Second, for the purpose of consistency, all other frequencies used to calculate the KIEs are harmonic normal-mode frequencies. Third, the use of spectroscopic frequencies for the

TABLE XXVI

COMPARISON OF SECONDARY α -DEUTERIUM $k(\text{CH}_3, \text{H}_2)/k(\text{CD}_3, \text{H}_2)$ RESULTS^a

Activated Complex Used	Transition State Theory Results				Arrhenius Results ^b			
	Temperature °K	MMI	EXC	ZPE	KIE	A_1/A_2	ΔE	Temperature Range °K
LMR-PES ^c	296	1.669	0.871	0.577	0.838	1.138 ± 0.008	-179 ± 5	273-546
	546	1.669	0.773	0.742	0.958			
Pimentel ^d	296	1.669	0.895	0.506	0.756	1.190 ± 0.010	-266 ± 3	273-546
	546	1.669	0.800	0.691	0.923			
BEBO3 ^f	296	1.613	0.917	0.464	0.686	1.217 ± 0.001	-336 ± 6	273-546
	546	1.613	0.833	0.660	0.886			
BEBO3 ^f	296	1.613	0.655	0.757	0.800	1.021 ± 0.002	-144 ± 1	273-546
	546	1.613	0.644	0.860	0.894			

TABLE XXVI (Continued)

Activated Complex Used	Transition State Theory Results				Arrhenius Results ^b			
	Temperature °K	MMI	EXC	ZPE	KIE	A_1/A_2	ΔE	Temperature Range °K
BEBO3 ^g	296	1.613	0.943	0.248	0.377	1.331 ± 0.009	-739 ± 5	273-546
	546	1.613	0.882	0.470	0.668			

^aFor purposes of comparison all results were calculated using the LMR-PES reactant data with Gaussian-70 out-of-plane bending frequencies (unless specified otherwise) with the activated complex parameters from the specified source.

^bResults obtained by linear least squares fit of $\ln(k_H/k_D)$ vs. T^{-1} for 12 values over the specified temperature range. See Appendix D. ΔE is calories per mole.

^cCalculated using the LMR-PES data with Gaussian-70 out-of-plane bending frequencies.

^dCalculated using the LMR-PES data with the methyl radical out-of-plane bending frequencies corresponding to the calculated harmonic values in Reference 38.

^eCalculated using the BEBO activated complex data from Reference 12.

^fCalculated using the BEBO3 activated complex data with $F_{\phi_i}^\ddagger (i=1,2,3) = 0.0001 \text{ mdyne-}\text{\AA}$ from Reference 14.

^gCalculated using the BEBO3 activated complex data with $F_{\phi_i}^\ddagger (i=1,2,3) = 0.568 \text{ mdyne-}\text{\AA}$ from Reference 14.

out-of-plane bending mode in the transition-state-theory calculation would only raise the KIE by about 2-5 percent over the KIE calculated using harmonic frequencies. The Pimentel KIEs in Table XXVI have a slightly greater more inverse temperature dependence than the corresponding KIE calculated using the Gaussian 70 force constant. However, this difference is smaller than the differences in the transition-state theory KIEs obtained using the BEBO and BEBO3 models.

Careful experimental determination of the KIEs in Tables XXV and XXVI might help distinguish which model if any adequately describes the real reaction hypersurface. The experimental rate constants reported by Majury and Steacie (MS)¹⁶ and Whittle and Steacie (WS)¹⁵ can be used to calculate secondary α -deuterium isotope effects. The values for $k(\text{CH}_3, \text{H}_2)/k(\text{CD}_3, \text{H}_2)$ are 0.91, 0.80, and 0.72 for MS¹⁶, and 0.85, 0.69, and 0.60 for WS¹⁵ at the temperatures 403, 483 and 563 °K, respectively, using the method I rate constants for $k(\text{CD}_3, \text{H}_2)$. For the method II $k(\text{CD}_3, \text{H}_2)$ values, the experimental $k(\text{CH}_3, \text{H}_2)/k(\text{CD}_3, \text{H}_2)$ isotope effects are 0.89, 0.71, and 0.62 for MS,¹⁶ and 1.23, 0.83, and 0.64 for WS¹⁵ at 403, 483, and 563 °K, respectively. Obviously, these experimental secondary α -deuterium KIEs become more inverse with increasing temperature. This experimental result defies both logical and theoretical predictions, since isotopic substitution should become less important at higher temperatures, especially at temperatures well above room temperature, and the KIEs should approach unity (or $v_{1L}^\ddagger/v_{2L}^\ddagger$) as the temperature increases. Nevertheless, the individual experimental KIEs are all inverse, except for one WS value at 403 °K, as are all of the theoretical KIEs, and the magnitudes of the experimental and theoretical KIEs are not greatly different. Therefore, one can conclude that the

true secondary α -deuterium KIE for the reaction $\text{CH}_3(\text{CD}_3) + \text{H}_2$ is most likely inverse. However, the experimental temperature dependence for this reaction is questionable. The transition-state theory calculated KIEs in Table XXVI have more reasonable temperature dependences than experiment. Therefore, a more accurate determination of the experimental secondary α -deuterium KIE for this reaction would be very helpful in quantifying the theoretical results. Quantitative comparison of the present theoretical and experimental KIEs is virtually impossible or at best meaningless due to the opposing trends of their temperature dependences.

The fact that the transition-state theory secondary α -deuterium KIEs for reaction (I-1) of $\text{CH}_4(\text{CD}_3\text{H}) + \text{H}$ in Table XXV produces normal KIEs and for reaction (I-2) of $\text{CH}_3(\text{CD}_3) + \text{H}_2$ in Table XXVI produces inverse KIEs is explained by the change in bonding between reactants and activated complex. For reaction (I-1) the HCH_1 bending force constant, F_{ϕ_i} ($i=1,2,3$), is usually reduced to a smaller $F_{\phi_i}^\ddagger$ ($i=1,2,3$) in the activated complex. This means that α -deuterium substitution produces less change in the normal-mode frequencies in the activated complex than in reactants. This produces a normal KIE. However, if F_{ϕ_i} ($i=1,2,3$) \leq $F_{\phi_i}^\ddagger$ ($i=1,2,3$), as is the case with one BEBO3 value in Table XXV and all the KIEs in Table XXVI, then inverse KIEs are produced. The inverse BEBO3 KIE in Table XXV is the result of the unrealistic assumption that F_{ϕ_i} ($i=1,2,3$) = $F_{\phi_i}^\ddagger$ ($i=1,2,3$). However, the inverse KIEs in Table XXVI for reaction (I-2) are the result of more bonds being associated with the α -deuteriums in the activated complex than in the reactants (that is, there is no F_{ϕ_i} ($i=1,2,3$) value in the

reactants, since there is no C-H₁ bond). Therefore, the α -deuterium substitution in reaction (I-2) causes a greater change in the normal mode frequencies in the activated complex than in the reactants. Observing the form of the equations (I-3) and (I-4), it is then reasonable that the secondary α -deuterium KIEs in Table XXVI should be inverse and the corresponding KIEs for reaction (I-1) in Table XXV should be normal.

A comparison of the magnitude of the MMI terms in Tables XXIII and XXIV show that the BEBO and BEBO3 models have somewhat larger MMI values than the LMR-PES. However, in Tables XXV and XXVI for the secondary α -deuterium KIEs the MMI terms using the BEBO and BEBO3 models are smaller than the corresponding MMI values for the LMR-PES. The difference in these MMI relationships is directly related to the differences in the activated complex geometries. The LMR-PES has longer non-reacting C-H bond lengths than does either the BEBO or BEBO3 models. Therefore, the α -deuterium atom substitution causes a greater change in the moments of inertia for the LMR-PES isotopic configurations than in the BEBO and BEBO3 models. Similarly, differences in the C-H, reacting bondlength create slightly greater differences in the 13-carbon MMI terms for BEBO and BEBO3 models than for the LMR-PES.

The Effect of Transition-State Geometry on the Isotope Effects

Shapiro and Weston (SW) report that a change in the geometry of the CH₃ group relative to the C-H-H entity in the activated complex from tetrahedral to planar produced significant changes in the activated-complex normal-mode frequencies.¹⁴ However, these authors found for the reaction CH₃ + H₂ that this geometry change altered the primary

KIEs by less than one percent.¹⁴ The effect of CH_3 geometry in the activated complex was extensively tested by calculating various KIEs based upon the LMR-PES. The results are presented in Tables XXVII and XXVIII. The frequencies used to calculate these KIEs are tabulated in Appendix C. It can be seen in Table XXVII that the primary deuterium and ^{14}C KIEs all show a maximum percentage deviation between the highest and lowest values for the three KIEs in each row of less than one percent. This is in agreement with the findings of SW for primary effects.¹⁴ However, the secondary deuterium KIEs for reactions (I-1) and (I-2) at 296 $^\circ\text{K}$ differ by a maximum of 10 percent. This somewhat larger effect on the secondary deuterium KIEs is expected, since changing the CH_3 geometry affects the positions of the isotopic atoms in the activated complex. Wolfsberg and Stern have shown for a similar reaction involving elimination of χ from $\text{CH}_3\chi$ or $\text{CD}_3\chi$ that at 300 $^\circ\text{K}$ a change from tetrahedral CH_3 or CD_3 to planar CH_3 or CD_3 geometry produces a 5.3% change in the secondary α -deuterium isotope effect.^{3c} They also state that this change is directly related to the MMI factor, but that information about the MMI factor and the corresponding geometry of the activated complex seem impossible to obtain directly from an experimental set of KIEs.^{3c} However, Wolfsberg and Stern also state that the secondary α -deuterium isotope effects are primarily the result of force constant changes between reactants and activated complex.^{3c} In summary, since secondary deuterium KIEs are more strongly affected by such geometry changes than primary KIEs, then more uncertainty can be expected in the force constants deduced from experimental secondary deuterium KIEs. The values in Table XXVIII are the Arrhenius parameters obtained by fitting the KIEs in Table XXVII over the specified

TABLE XXVII
THE EFFECT OF CH₃ GEOMETRY IN THE ACTIVATED COMPLEX

Rate Constant Ratios	Temperature °K	Calculated Isotope Effects ^a			Standard Deviation ^e	Maximum ^f Percent Deviation
		Tetrahedral ^b	LMR-PES ^c	Planar ^d		
$k(\text{CH}_4 + \text{H})$	296	1.549	1.579	1.704	± 0.082	10.0
$k(\text{CD}_3\text{H} + \text{H})$	546	1.213	1.218	1.236	± 0.012	1.9
$k(\text{CH}_4 + \text{H})$	296	1.067	1.066	1.068	± 0.0009	0.2
$k(^{14}\text{CH}_4 + \text{H})$	546	1.035	1.034	1.034	± 0.0004	0.1
$k(\text{CH}_4 + \text{H})$	296	0.251	0.251	0.252	± 0.0007	0.4
$k(\text{CH}_4 + \text{D})$	546	0.554	0.554	0.555	± 0.0006	0.2
$k(\text{CH}_4 + \text{H})$	296	5.593	5.590	5.618	± 0.015	0.5
$k(\text{CH}_3\text{D} + \text{H})$	546	2.422	2.421	2.426	± 0.003	0.2
$k(\text{CH}_3 + \text{H}_2)$	296	0.822	0.838	0.904	± 0.044	10.0
$k(\text{CD}_3 + \text{H}_2)$	546	0.954	0.958	0.972	± 0.010	1.9
$k(\text{CH}_3 + \text{H}_2)$	296	1.013	1.012	1.014	± 0.0009	0.2
$k(^{14}\text{CH}_3 + \text{H}_2)$	546	1.012	1.011	1.011	± 0.0004	0.1

TABLE XXVII (Continued)

Rate Constant Ratios	Temperature °K	Calculated Isotope Effects ^a			Standard Deviation ^e	Maximum ^f Percent Deviation
		Tetrahedral ^b	LMR-PES ^c	Planar ^d		
$k(\text{CH}_3 + \text{H}_2)$	296	0.929	0.930	0.934	± 0.003	0.5
$k(\text{CH}_3 + \text{HD})$	546	1.055	1.055	1.057	± 0.001	0.2
$k(\text{CH}_3 + \text{H}_2)$	296	1.875	1.874	1.883	± 0.005	0.5
$k(\text{CH}_3 + \text{DH})$	546	1.622	1.621	1.625	± 0.002	0.2

^aKinetic isotope effects calculated using the harmonic LMR-PES reactant frequencies.

^bCalculated using tetrahedral CH_3 geometry in the activated complex.

^cCalculated using the LMR-PES CH_3 geometry in the activated complex.

^dCalculated using the planar CH_3 geometry in the activated complex.

^eStandard deviation in the three KIEs in the row.

^fLargest difference relative to the smallest KIE in the row.

TABLE XXVIII

THE EFFECT OF CH₃ GEOMETRY ON THE TEMPERATURE DEPENDENCES^a

Rate Constant Ratios	A ₁ /A ₂ ^b			Std. ^g Dev.
	Tetrahedral ^d	LMR-PES ^e	Planar ^f	
$\frac{k(\text{CH}_4 + \text{H})}{k(\text{CD}_3\text{H} + \text{H})}$	0.901 ± 6 × 10 ⁻⁴	0.889 ± 3 × 10 ⁻⁴	0.846 ± 0.002	±.029
$\frac{k(\text{CH}_4 + \text{H})}{k(^{14}\text{CH}_4 + \text{H})}$	0.997 ± 8 × 10 ⁻⁵	0.998 ± 9 × 10 ⁻⁵	0.995 ± 2 × 10 ⁻⁴	±.002
$\frac{k(\text{CH}_4 + \text{H})}{k(\text{CH}_4 + \text{D})}$	1.407 ± 0.002	1.406 ± 0.002	1.404 ± 0.002	±.002
$\frac{k(\text{CH}_4 + \text{H})}{k(\text{CH}_3\text{D} + \text{H})}$	0.896 ± 0.001	0.895 ± 0.001	0.894 ± 0.001	±.001
$\frac{k(\text{CH}_3 + \text{H}_2)}{k(\text{CD}_3 + \text{H}_2)}$	1.115 ± 0.005	1.101 ± 0.005	1.047 ± 0.002	±.036
$\frac{k(\text{CH}_3 + \text{H}_2)}{k(^{14}\text{CH}_3 + \text{H}_2)}$	1.010 ± 5 × 10 ⁻⁵	1.010 ± 4 × 10 ⁻⁵	1.008 ± 7 × 10 ⁻⁵	±.001
$\frac{k(\text{CH}_3 + \text{H}_2)}{k(\text{CH}_3 + \text{HD})}$	1.219 ± 0.002	1.218 ± 0.002	1.216 ± 0.002	±.002
$\frac{k(\text{CH}_3 + \text{H}_2)}{k(\text{CH}_3 + \text{DH})}$	1.341 ± 0.006	1.340 ± 0.006	1.338 ± 0.006	±.002

Rate Constant Ratios	ΔE ^c (calories/mole)			Std. ^g Dev.
	Tetrahedral ^d	LMR-PES ^e	Planar ^f	
$\frac{k(\text{CH}_4 + \text{H})}{k(\text{CD}_3\text{H} + \text{H})}$	323 ± 0.6	341 ± 0.3	410 ± 1.9	±46
$\frac{k(\text{CH}_4 + \text{H})}{k(^{14}\text{CH}_4 + \text{H})}$	40 ± 0.1	39 ± 0.1	41 ± 0.2	±1

TABLE XXVIII (Continued)

Rate Constant Ratios	ΔE^c (calories/mole)			Std. ^g Dev.
	Tetrahedral ^d	LMR-PES ^e	Planar ^f	
$\frac{k(\text{CH}_4 + \text{H})}{k(\text{CH}_4 + \text{D})}$	-1011 ± 1	-1010 ± 1	-1006 ± 1	± 2
$\frac{k(\text{CH}_4 + \text{H})}{k(\text{CH}_3\text{D} + \text{H})}$	1079 ± 1	1079 ± 1	1083 ± 1	± 2
$\frac{k(\text{CH}_3 + \text{H}_2)}{k(\text{CD}_3 + \text{H}_2)}$	-166 ± 4	-149 ± 4	-79 ± 2	± 46
$\frac{k(\text{CH}_3 + \text{H}_2)}{k(^{14}\text{CH}_3 + \text{H}_2)}$	1.7 ± 0.05	1.0 ± 0.04	3.2 ± 0.05	± 1.1
$\frac{k(\text{CH}_3 + \text{H}_2)}{k(\text{CH}_3 + \text{HD})}$	-156 ± 1	-155 ± 1	-151 ± 1	± 2
$\frac{k(\text{CH}_3 + \text{H}_2)}{k(\text{CH}_3 + \text{DH})}$	209 ± 4	209 ± 4	213 ± 4	± 2

^aAll deviations are standard deviations in the Arrhenius equation parameters from a least squares fit to $\ln(k_1/k_2) = \ln(A_1/A_2) + (\Delta E/R)(1/T)$ using LMR-PES reactant frequencies over the temperature range 371-546°K.

^bIsotopic ratio of Arrhenius preexponential factors.

^cIsotopic difference in Arrhenius activation energies in kcal/mole.

^dCalculated using tetrahedral CH_3 geometry in the activated complex.

^eCalculated using the LMR-PES CH_3 geometry in the activated complex.

^fCalculated using the planar CH_3 geometry in the activated complex.

^gStandard deviation in the preceding three values in the row.

range of temperatures to equation (III-13). As expected from Table XXVII the largest deviations in Table XXVIII are for the secondary deuterium KIEs. The geometry caused deviations in the primary carbon and deuterium effects are negligible.

Contributions of the Bending and Stretching

Frequencies to the Primary KIE

At reasonably low temperatures ($\leq 100^{\circ}\text{C}$), primary deuterium isotope effects primarily reflect the magnitude of ZPE. Therefore, an estimate of the degree to which the KIE is influenced by normal mode bending frequencies can be made by calculating the ZPE contributions to the KIE using stretching and bending normal-mode frequency values in separate calculations. The isotopic reactant and transition-state frequencies used for these calculations are given in Tables XXIX and XXX respectively, along with the summations over the separate sets of stretching and bending normal modes. The isotopic differences between these summations are used in equation (I-7) to obtain the contributions to the ZPE term tabulated in Table XXXI. For the $\text{CH}_4 + \text{H}$ reaction, ZPE values calculated using only the stretching normal-mode frequencies are in better agreement with the "total ZPE" values than those ZPE contributions calculated with either the bending normal mode frequencies alone or the stretching plus linear bending frequencies. However, for the reaction of CH_3 with H_2 and D_2 or HD, the addition of the isotopic linear bending frequency values to the corresponding isotopic stretching frequency values produced two ZPE contributions within three percent of the corresponding "Total ZPE" values in Table XXXI. The ZPE contributions involving abstraction of D from HD differ considerably

TABLE XXIX
 REACTANT ISOTOPIC FREQUENCIES^a

Normal Modes	Methane		Methyl and Molecular Hydrogen			
	CH ₄	CH ₃ D	CH ₃	H ₂	D ₂	HD
v ₁	2917.0	2224.1	2914.2	4468.1	3160.6	3870.0
v _{2a}	1526.6	1476.3	847.1			
v _{2b}	1526.6	1476.3				
v _{3a}	3080.1	3080.1	3099.6			
v _{3b}	3080.1	3080.1	3099.6			
v _{3c}	3080.1	2966.4				
v _{4a}	1366.1	1356.7	1605.9			
v _{4b}	1366.1	1197.9	1605.9			
v _{4c}	1366.1	1197.9				
	<u>CH₄</u>	<u>CH₃D</u>	<u>CH₃ + H₂</u>	<u>CH₃ + D₂</u>	<u>CH₃ + HD</u>	
3n-6 $\sum_{i=1}^b v_i$	19308.8	18055.8	17640.4	16332.9	17042.3	
Sum(v ₂ +v ₄) ^c	7151.5	6705.1	4058.9	4058.9	4058.9	
Sum(v ₁ +v ₃) ^d	12157.3	11350.7	13581.5	12274.0	12983.4	

^aAll values in cm⁻¹. All values calculated using LMR-PES force constants and geometry except v₂ under CH₃ determined from Gaussian-70 force constant and geometry.

^bSum of all isotopic frequencies for a particular reactant or reactants.

^cSum of all isotopic bending frequencies for a particular reactant or reactants.

^dSum of all isotopic stretching frequencies for a particular reactant or reactants.

TABLE XXX
 TRANSITION-STATE ISOTOPIC FREQUENCIES^a

Normal Modes	CH ₃ -H-H	CH ₃ -D-D	CH ₃ -D-H	CH ₃ -H-D
ν_1	3388.4	2405.0	3106.0	2720.9
ν_2	2937.7	2939.3	2937.0	2941.2
ν_3	964.7	953.6	959.3	956.9
ν_4	1479.3i	1115.0i	1181.7i	1350.4i
ν_5^b	3085.6	3085.7	3085.7	3085.7
ν_6^b	1502.9	1502.9	1502.9	1502.9
ν_7^b	752.3	632.6	636.6	746.1
ν_8^b	367.3	296.0	345.7	327.5
$\sum_{i=1}^{3n-7} \nu_i^c$	18707.0	17332.3	18144.1	17943.4
Sum($\nu_3 + \nu_6$)	3970.5	3959.4	3965.1	3962.7
Sum($\nu_7 + \nu_8$) ^d	2239.2	1857.2	1964.6	2147.2
Bending sum ν^e	6209.7	5816.6	5929.7	6109.9
Stretching sum ν^f	12497.3	11515.7	12214.4	11833.5

^aAll values in cm⁻¹. Based upon the LMR-PES.

^bDoubly degenerate normal mode frequencies.

^cSum of all real frequencies omitting ν_4 the imaginary frequency.

^dSum of the associated linear bending frequencies ν_7 and ν_8 .

^eSum of all the bending frequencies ν_3 , ν_6 , ν_7 and ν_8 .

^fSum of all the real stretching frequency values ν_1 , ν_2 and ν_5 .

TABLE XXXI
 BENDING AND STRETCHING FREQUENCY CONTRIBUTIONS TO THE ZPE^a

Isotopic Ratio of Reactants	Bending ^b		Stretching ^c		Linear Bending ^d + Stretching		Total ^e ZPE
	ZPE	% Dev. ^f	ZPE	% Dev. ^f	ZPE	% Dev. ^f	
$\frac{\text{CH}_4 + \text{H}}{\text{CH}_3\text{D} + \text{D}}$	1.138	53.0	0.654	-12.1	0.258	-65.3	0.744
$\frac{\text{CH}_4 + \text{H}}{\text{CH}_3\text{D} + \text{H}}$	1.499	-72.0	3.571	-33.2	1.832	-65.8	5.349
$\frac{\text{CH}_4 + \text{H}}{\text{CH}_4 + \text{D}}$	0.785	403.2	0.199	27.6	0.249	59.6	0.156
$\frac{\text{CH}_3 + \text{H}_2}{\text{CH}_3 + \text{D}_2}$	0.385	-54.6	2.206	160.1	0.872	2.7	0.849
$\frac{\text{CH}_3 + \text{H}_2}{\text{CH}_3 + \text{DH}}$	0.506	-53.5	2.151	97.5	1.558	43.1	1.089
$\frac{\text{CH}_3 + \text{H}_2}{\text{CH}_3 + \text{HD}}$	0.785	17.3	0.852	27.4	0.681	1.8	0.669

^aFrequency contributions to the vibrational zero point energy term (ZPE) calculated at 296°K, see (I-7).

^bCalculated using only the bending frequencies from the LMR-PES reactant and transition-state species.

^cCalculated using only the stretching frequencies from the LMR-PES reactant and transition-state species.

^dCalculated using only the linear bending and stretching frequencies from the isotopic LMR-PES reactant and transition-state species.

^eCalculated using all the isotopic LMR-PES frequencies.

^fPercent deviation from the total ZPE.

from the "Total ZPE" value, but the linear bending plus stretching frequencies still produce a ZPE contribution in better agreement with the "Total ZPE" value than either the bending or stretching ZPE contribution alone. Clearly, the addition of linear bending frequency values to the stretching frequencies improves the agreement of the calculated ZPE contributions with the "Total ZPE" values for reaction (I-2) [that is, $\text{CH}_3 + \text{isotopic H}_2$]. However, combination of linear bending and stretching frequencies produces ZPE contributions in worse agreement with the "Total ZPE" values for reaction (I-1) [that is, isotopic $\text{CH}_4 + \text{H(D)}$] than obtained from use of stretching frequencies alone. The origin of this difference between the ZPE contributions for reactions (I-1) and (I-2) is the relative magnitude of the differences between the reactant and transition-state bending frequencies. For reaction (I-2), the transition-state linear bending frequencies have a dominate effect on the ZPE contributions. However, for reaction (I-1) the reactant bending frequencies contribute approximately as much as the transition-state linear-bending frequencies to the ZPE value. Therefore, the addition of only the transition-state linear-bending frequencies to the stretching frequencies in reaction (I-1) without the compensating effect of the reactant bending frequencies actually decreases the agreement of the calculated ZPE contributions with the "Total ZPE" values in Table XXXI.

The separate bending, stretching and linear-bending plus stretching frequency contributions to the EXC values are given in Table XXXII. Due to the function form of the equation for calculating the EXC values, (that is, $1 - e^{-u_i}$), see (I-6), the largest frequency values have the least effect on the calculated

TABLE XXXII

BENDING AND STRETCHING FREQUENCY CONTRIBUTIONS TO THE EXC^a

Isotopic Ratio of Reactants	Bending ^b		Stretching ^c		Linear Bending ^d + Stretching		Total ^e EXC
	EXC	% Dev. ^f	EXC	% Dev. ^f	EXC	% Dev. ^f	
$\frac{\text{CH}_4 + \text{H}}{\text{CH}_3\text{D} + \text{D}}$	0.808	0	1.000	23.8	0.805	-0.4	0.808
$\frac{\text{CH}_4 + \text{H}}{\text{CH}_3\text{D} + \text{H}}$	0.921	0	1.000	8.6	0.918	-0.3	0.921
$\frac{\text{CH}_4 + \text{H}}{\text{CH}_4 + \text{D}}$	0.914	0	1.000	9.4	0.914	0	0.914
$\frac{\text{CH}_3 + \text{H}_2}{\text{CH}_3 + \text{D}_2}$	0.805	0	1.000	24.2	0.805	0	0.805
$\frac{\text{CH}_3 + \text{H}_2}{\text{CH}_3 + \text{DH}}$	0.918	0	1.000	8.9	0.918	0	0.918
$\frac{\text{CH}_3 + \text{H}_2}{\text{CH}_3 + \text{HD}}$	0.914	0	1.000	9.4	0.914	0	0.914

^aFrequency contributions to the vibrational excitation factor (EXC), see (I-6). All values calculated at 296°K.

^bCalculated using only the bending frequencies from the isotopic LMR-PES reactant and transition-state species.

^cCalculated using only the stretching frequencies from the isotopic LMR-PES reactant and transition-state species.

^dCalculated using only the linear bending and stretching frequencies from the isotopic LMR-PES reactant and transition-state species.

^eCalculated using all the isotopic LMR-PES frequencies.

^fPercent deviation from the total EXC.

EXC values. For this reason, the relatively large stretching frequencies produce negligibly small EXC contributions. Since the transition-state linear-bending frequencies are the smallest in magnitude, then the combinations of the stretching and linear-bending frequencies produce EXC contributions almost identical to the "Total EXC" values in Table XXXII. The bending frequencies alone produce EXC contributions identical to the "Total EXC" values to the accuracy expressed in Table XXXII.

The separate frequency contributions to the VP values are given in Table XXXIII. The stretching frequencies alone do not produce VP contributions in good agreement with the "Total VP" values. Use of the linear-bending frequencies plus the stretching frequencies produces VP contributions in excellent agreement with the "Total VP" values except for the first two cases in Table XXXIII. For these two cases the reactant H_1CH_1 ($i=2,3,4$) bending frequencies exert a considerable influence on the magnitude of VP. The bending frequencies alone produce VP values that are very close to the total VP values in the first and fourth rows in Table XXXIII. This excellent agreement can be interpreted as the complimentary effect of the isotopic reactant HCH bending and activated complex linear bending frequencies on the former VP, and the dominate influence of the isotopic activated complex linear bending frequencies over the latter VP in row four. The VP values involving the CH_3-H-D and CH_3-D-H frequencies require more compensating effects between the bending and stretching isotopic frequencies to obtain the total VP value.

The contributions of the bending, stretching and linear-bending plus stretching frequencies to the ZPE, EXC and VP values tabulated in Tables XXXI through XXXIII are combined in Table XXXIV with the $v_{1L}^\ddagger/v_{2L}^\ddagger$

TABLE XXXIII
BENDING AND STRETCHING FREQUENCY CONTRIBUTIONS TO THE VP^a

Isotopic Ratio of Reactants	Bending ^b		Stretching ^c		Linear Bending ^d + Stretching		Total ^e VP
	VP	% Dev. ^f	VP	% Dev. ^f	VP	% Dev. ^f	
$\frac{\text{CH}_4 + \text{H}}{\text{CH}_3\text{D} + \text{D}}$	1.573	-3.3	1.034	-36.4	2.252	38.4	1.627
$\frac{\text{CH}_4 + \text{H}}{\text{CH}_3\text{D} + \text{H}}$	1.132	24.8	0.801	-11.7	1.263	39.3	0.907
$\frac{\text{CH}_4 + \text{H}}{\text{CH}_4 + \text{D}}$	1.289	-19.6	1.244	-22.4	1.591	-0.8	1.604
$\frac{\text{CH}_3 + \text{H}_2}{\text{CH}_3 + \text{D}_2}$	2.203	-0.4	0.996	-54.6	2.169	-1.1	2.194
$\frac{\text{CH}_3 + \text{H}_2}{\text{CH}_3 + \text{DH}}$	1.585	-5.7	0.945	-37.0	1.490	-0.6	1.499
$\frac{\text{CH}_3 + \text{H}_2}{\text{CH}_3 + \text{HD}}$	1.289	-7.2	1.077	-22.5	1.378	-0.8	1.389

^aFrequency contributions to the vibrational product (VP) factor, see (I-8). All values calculated at 296°K.

^bCalculated using only the bending frequencies from the isotopic LMR-PES reactant and transition-state species.

^cCalculated using only the stretching frequencies from the isotopic LMR-PES reactant and transition-state species.

^dCalculated using only the stretching and linear bending frequencies from the LMR-PES reactant and transition-state species.

^eCalculated using all the isotopic LMR-PES frequencies.

^fPercent deviation from the total VP.

TABLE XXXIV

BENDING AND STRETCHING FREQUENCY CONTRIBUTIONS TO THE KIE^a

Isotopic Ratio of Reactants	Bending ^b		Stretching ^c		Linear Bending ^d + Stretching		$\frac{\nu_{1L}^\ddagger}{\nu_{2L}^\ddagger}$	Total ^e KIE
	KIE	% Dev. ^f	KIE	% Dev. ^f	KIE	% Dev. ^f		
$\frac{\text{CH}_4 + \text{H}}{\text{CH}_3\text{D} + \text{D}}$	1.919	48.1	0.897	-30.8	0.621	-52.1	1.3267	1.296
$\frac{\text{CH}_4 + \text{H}}{\text{CH}_3\text{D} + \text{H}}$	1.956	-65.0	3.581	-35.9	2.659	-52.4	1.2518	5.590
$\frac{\text{CH}_4 + \text{H}}{\text{CH}_4 + \text{D}}$	1.013	304.6	0.271	8.0	0.397	58.2	1.0955	0.251
$\frac{\text{CH}_3 + \text{H}_2}{\text{CH}_3 + \text{D}_2}$	0.906	-54.4	2.915	46.6	2.020	1.6	1.3267	1.988
$\frac{\text{CH}_3 + \text{H}_2}{\text{CH}_3 + \text{DH}}$	0.922	-50.8	2.545	35.8	2.668	42.4	1.2518	1.874
$\frac{\text{CH}_3 + \text{H}_2}{\text{CH}_3 + \text{HD}}$	1.013	-8.9	1.005	8.1	0.940	1.1	1.0955	0.930

^aBending and stretching KIE values calculated using the VP, EXC, and ZPE quantities in the accompanying tables, see (I-4). All values calculated at 296°K.

^bCalculated using only the bending frequencies from the isotopic LMR-PES reactant and transition-state species times $\frac{\nu_{1L}^\ddagger}{\nu_{2L}^\ddagger}$.

^cCalculated using only the stretching frequencies from the isotopic LMR-PES reactant and transition-state species times $\frac{\nu_{1L}^\ddagger}{\nu_{2L}^\ddagger}$.

^dCalculated using only the linear bending plus the stretching frequencies from the isotopic LMR-PES reactant and transition-state species times $\frac{\nu_{1L}^\ddagger}{\nu_{2L}^\ddagger}$.

^eCalculated using all the isotopic LMR-PES frequencies.

^fPercent deviation from the total KIE.

values to give the corresponding comparisons for the calculated KIE values. It can be seen that few of the individual contributions to the total KIE come close to agreeing with the total KIE values. Two notable exceptions are the contributions due to the linear bending plus stretching frequencies in rows four and six of Table XXXIV. These differ from the total KIE value by 1.6% and 1.1%, respectively. The other values differ by about 8 percent to as much as 304.6 percent. The data in Table XXXIV show that the stretching frequencies alone tend to reproduce the KIE values as well or better than all the other bending or linear-bending plus stretching frequency sets, except for the two cases previously mentioned. However, except for these two exceptions, the error due to using an incomplete vibrational frequency data set, as discussed in Chapter I, can lead to very large errors in the calculated KIEs.

Relating Primary Deuterium and Tritium Isotope

Effects

The relationship between tritium and deuterium primary KIEs is commonly referred to as the Swain-Schaad relation.²³ This relationship was tested for its applicability to the CH_4+H and CH_3+H_2 reactions by using the LMR-PES isotopic frequencies to obtain transition-state theory calculated KIEs which are compared using Bigeleisen's definition of r (see footnote a in Table XXXV).²⁴ The results are given in Table XXXV. The isotopic reactions compared in Table XXXV were chosen based upon the feasibility of their experimental determination rather than their being pure primary isotope effects. As discussed in Chapter I, the Swain-Schaad relation is only supposed to be applicable to reac-

TABLE XXXV

RELATIONSHIPS OF TRITIUM AND DEUTERIUM ISOTOPE EFFECTS

Ratio of Rate Constants	k_H/k_D	k_H/k_T	r^a	Δr_{ss}^b	Temperature °K
$k(\text{CH}_4, \text{H})^c$	2.311×10^4	1.640×10^6	1.424	-.018	50
$k(\text{CH}_3\text{X}, \text{H})$	1.614×10^2	1.407×10^3	1.426	-.016	100
	5.4573	11.230	1.425	-.017	300
	2.4207	3.5396	1.430	-.012	546
	1.2518	1.4324	1.600	0.158	∞
$k(\text{CH}_4, \text{H})^c$	2.970×10^{-5}	4.103×10^{-7}	1.411	-.031	50
$k(\text{CH}_4, \text{X})$	7.165×10^{-3}	9.610×10^{-4}	1.407	-.035	100
	0.2569	0.1517	1.388	-.054	300
	0.5539	0.4501	1.351	-0.091	546
	1.0955	1.1641	1.666	0.224	∞
$k(\text{CH}_3, \text{HX})^c$	22.085	96.327	1.476	0.034	50
$k(\text{CH}_3, \text{XH})$	5.2396	11.607	1.480	0.038	100
	2.0011	2.7751	1.471	0.029	300
	1.5370	1.8741	1.461	0.019	546
	1.1428	1.2306	1.554	0.112	∞
$k(\text{CH}_3, \text{H}_2)^c$	1.0995	1.4199	3.696	2.254	50
$k(\text{CH}_3, \text{X}_2)$	1.7567	2.6103	1.703	0.261	100
	1.9847	2.8476	1.527	0.085	300
	1.7908	2.3950	1.499	0.057	546
	1.3267	1.5394	1.526	0.084	∞

^a $r = \ln(k_H/k_T)/\ln(k_H/k_D)$, see Reference 24.

$$^b \Delta r_{ss} = r - r_{ss}, \text{ where } r_{ss} = \frac{(1/m_H)^{.5} - (1/m_T)^{.5}}{(1/m_H)^{.5} - (1/m_D)^{.5}} = 1.442.$$

^cX = D or T. The underlined element represents the atom being abstracted if there is more than one possibility.

tions involving transfer of the isotopic hydrogen at rather low temperatures ($< 100^{\circ}\text{C}$). It can be seen that the only pure primary isotope effect in Table XXXV is $k(\text{CH}_4, \text{H})/k(\text{CH}_3\text{X}, \text{H})$. Over the temperature range considered, the calculated value of $k(\text{CH}_4, \text{H})/k(\text{CH}_3\text{X}, \text{H})$ agrees quite well with the theoretical $r_{\text{ss}} = 1.442$ determined only from the H, D, and T atomic weights (as shown in footnote b of Table XXXV). The KIEs and r values reported for infinite temperature are obtained from the high temperature limits to the KIEs (that is, $v_{1\text{L}}^{\ddagger}/v_{2\text{L}}^{\ddagger}$). The other extreme is represented by the $k(\text{CH}_4, \text{H})/k(\text{CH}_4, \text{X})$ values which are pure end atom effects. It can be seen that these KIE values are inverse (that is, the heavier isotopic reactants react faster) and that the KIE values go past (or crossover) unity at some temperature above 546°K (approximately 1500 to 2000°K). It has been noted by Stern and Vogel that when the KIEs are very near unity, the r values become anomalous and useless as a method of approximately tritium KIEs from deuterium KIEs or vice versa.²⁵ The other two KIEs for which r values were determined in Table XXXV are combined end atom plus normal primary KIEs. Their calculated r values decrease toward $r_{\text{ss}} = 1.442$ until between 600 and 1000°K , and then increase until the infinite temperature value is reached. The $k(\text{CH}_3, \text{HX})/k(\text{CH}_3, \text{XH})$ values show better overall agreement with the $r_{\text{ss}} = 1.442$ since each individual D or T KIE increases monotonically with lowering temperature. The $k(\text{CH}_3, \text{H}_2)/k(\text{CH}_3, \text{X}_2)$ values have an inflection point at approximately 200°K and decrease in value at lower temperature. Since the D and T inflection points do not occur at exactly the same temperature the calculated r values decrease in their agreement with r_{ss} at lower temperatures. These results in Table XXXV seem to indicate that this simple Swain-Schaad relationship can

be used to give a reasonable estimate of the expected k_H/k_T value given an accurate value for k_H/k_D and raising it to the $r_{ss} = 1.442$ power. The values for the first three KIEs in Table XXXV indicate that such a relationship would be reasonably correct over a very broad range of temperature. However, the $k(\text{CH}_3, \text{H}_2)/k(\text{CH}_3, \text{X}_2)$ values show that the Swain-Schaad relationship will yield only fair results at the supposedly most optimum temperature and worse results at lower temperatures.

Relating ^{13}C and ^{14}C Isotope Effects

Since the Swain-Schaad relationship in its most abbreviated form appears to work for the $\text{CH}_4 + \text{H} \rightleftharpoons \text{CH}_3 + \text{H}_2$ reaction system even at higher temperatures ($> 100^\circ\text{C}$) than it is supposed to be valid, and since reasonable values were obtained for isotopic configurations other than the strictly primary D(or T) effects, it was reasoned that possibly a similar relation might be applicable to 13-carbon and 14-carbon KIEs. The results obtained from the extension to carbon isotope effects using the LMR-PES predicted 13-carbon and 14-carbon effects are shown in Table XXXVI. To estimate the magnitude of a 14-carbon KIE at a particular temperature, the 13-carbon KIE at that temperature is raised to the $r = 1.888$ power (see footnote b in Table XXXVI). The estimated accuracy of this relation is given by calculating the r_c values (see footnote (a) in Table XXXVI) and determining the differences between these r_c values and the theoretical $r = 1.888$. It can be seen in Table XXXVI that the $\text{CH}_4 + \text{H}$ carbon effects fit the theoretical $r = 1.888$ very well over the entire temperature range. However, the $\text{CH}_3 + \text{H}_2$ carbon effects tend to fall off rather rapidly at low temperature and the relationship is not very accurate below room temperature ($\sim 300^\circ\text{K}$). This

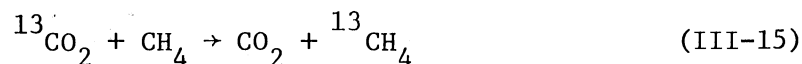
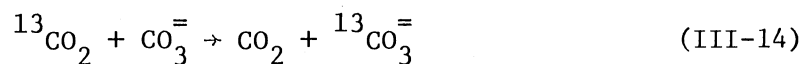
TABLE XXXVI
 RELATIONSHIPS OF ^{13}C and ^{14}C ISOTOPE EFFECTS

Ratio of Rate Constants	k_{12}/k_{13}	k_{12}/k_{14}	r_c^a	Δr_c^b	Temperature °K
$k(\text{CH}_4, \text{H})$	1.2241	1.4566	1.860	-.028	50
$k(^*\text{CH}_4, \text{H})$	1.1074	1.2089	1.860	-.028	100
	1.03513	1.06633	1.860	-.028	296
	1.01825	1.03422	1.860	-.028	546
	1.00544	1.01024	1.878	-0.10	∞
$k(\text{CH}_3, \text{H}_2)$	1.00396	1.00639	1.614	-.274	50
$k(^*\text{CH}_3, \text{H}_2)$	1.00584	1.01048	1.792	-.096	100
	1.00637	1.01186	1.857	-.031	296
	1.00601	1.01123	1.864	-.024	546
	1.00544	1.01024	1.878	-.010	∞

$$^a r_c = \ln(k_{12}/k_{14}) / \ln(k_{12}/k_{13}).$$

$$^b \Delta r_c = r_c - r, \text{ where } r = \frac{(1/m_{12})^{.5} - (1/m_{14})^{.5}}{(1/m_{12})^{.5} - (1/m_{13})^{.5}} = 1.888.$$

relationship was also tested with some fractionation factor equilibria values reported by Hartshorn and Shiner that were calculated at 298^oK.⁴⁵ The reactions used are given by equations (III-14) and (III-15).



Hartshorn and Shiner (HS) report a value of 1.0066 for the 13-carbon effect in (III-14). By raising this value to the 1.888 power, a value of 1.0125 was obtained which compares favorably with 14-carbon effect value of 1.0122 reported by HS.⁴⁵ Similarly, the relation for the 14-carbon effect in (III-15) is given by

$$(0.9429)^{1.888} = 0.8949 \quad (\text{III-16})$$

The 14-carbon effect value reported by HS is 0.8948.⁴⁵ The fact that these calculated values agree within 0.03% of the absolute rate theory calculated values reported by HS supports the validity of the relationship expressed in Table XXXVI.

Rule of the Geometric Mean Relationships

As discussed in Chapter I, the rule of the geometric mean is based on the applicability of vibrational frequency sum rules to the calculation of transition-state theory isotope effects. Table XXXVII shows the relationship between the various secondary α -deuterium KIEs for both the $\text{CH}_4 + \text{H}$ and the $\text{CH}_3 + \text{H}_2$ reactions. It can be seen that the $k(\text{H}/\text{D})$ and $F(\text{H}/\text{D})$ (see footnote a in Table XXXVII) values for one

TABLE XXXVII

RULE OF THE GEOMETRIC MEAN RELATIONSHIPS FOR SECONDARY ISOTOPE EFFECTS

Isotope Effect Relationship ^{a,b}	Temperature of Isotope Effect					
	50°K	273°K	546°K	746°K	1046°K	2246°K
$k(\text{CH}_4, \text{H}/\text{CD}_3\text{H}, \text{H})$	9.4826	1.6502	1.2182	1.1251	1.06675	1.01563
$F(\text{CH}_4, \text{H}/\text{CD}_3\text{H}, \text{H})$	9.4755	1.6490	1.2173	1.1243	1.06595	1.01487
$[k(\text{CH}_4, \text{H}/\text{CH}_2\text{DH}, \text{H})]^3$	8.6101	1.6430	1.2176	1.1249	1.06668	1.01559
$[F(\text{CH}_4, \text{H}/\text{CH}_2\text{DH}, \text{H})]^3$	8.6038	1.6418	1.2167	1.1241	1.06590	1.01486
$k(\text{CH}_4, \text{H}/\text{CHD}_2\text{H}, \text{H})$	4.3250	1.3942	1.1404	1.08171	1.04399	1.01038
$F(\text{CH}_4, \text{H}/\text{CHD}_2\text{H}, \text{H})$	4.3229	1.3935	1.1399	1.08117	1.04348	1.00989
$[k(\text{CH}_4, \text{H}/\text{CH}_2\text{DH}, \text{H})]^2$	4.2009	1.3924	1.1403	1.08164	1.04397	1.01037
$[F(\text{CH}_4, \text{H}/\text{CH}_2\text{DH}, \text{H})]^2$	4.1988	1.3917	1.1397	1.08112	1.04346	1.00988
$k(\text{CH}_4, \text{H}/\text{CH}_2\text{DH}, \text{H})$	2.0496	1.1800	1.06783	1.04002	1.02175	1.00517
$F(\text{CH}_4, \text{H}/\text{CH}_2\text{DH}, \text{H})$	2.0491	1.1797	1.06757	1.03977	1.02150	1.00493
$k(\text{CH}_3, \text{H}_2/\text{CD}_3, \text{H}_2)$.06413	.8115	.9579	.9804	.9915	.99902
$F(\text{CH}_3, \text{H}_2/\text{CD}_3, \text{H}_2)$.06408	.8109	.9572	.9796	.9908	.99827
$[k(\text{CH}_3, \text{H}_2/\text{CH}_2\text{D}, \text{H}_2)]^3$.05756	.8093	.9574	.9800	.9913	.99898
$[F(\text{CH}_3, \text{H}_2/\text{CH}_2\text{D}, \text{H}_2)]^3$.05751	.8088	.9568	.9794	.9907	.99826
$k(\text{CH}_3, \text{H}_2/\text{CHD}_2, \text{H}_2)$.1548	.8697	.9717	.9868	.9943	.99934
$F(\text{CH}_3, \text{H}_2/\text{CHD}_2, \text{H}_2)$.1547	.8692	.9712	.9863	.9938	.99884
$[k(\text{CH}_3, \text{H}_2/\text{CH}_2\text{D}, \text{H}_2)]^2$.1491	.8684	.9714	.9866	.9942	.99932
$[F(\text{CH}_3, \text{H}_2/\text{CH}_2\text{D}, \text{H}_2)]^2$.1490	.8681	.9710	.9862	.9938	.99884
$k(\text{CH}_3, \text{H}_2/\text{CH}_2\text{D}, \text{H}_2)$.3861	.9319	.9856	.9933	.9971	.99966
$F(\text{CH}_3, \text{H}_2/\text{CH}_2\text{D}, \text{H}_2)$.3860	.9317	.9854	.9931	.9969	.99942

^a $k(1/2) = (v_{1L}^\ddagger / v_{2L}^\ddagger) F(1/2)$, where 1 and 2 represent the light and heavy isotope species respectively and $F(1/2) = \frac{s_2/s_1 f(2/1)}{s_2^\ddagger/s_1^\ddagger f^\ddagger(2/1)} = \text{VP} \cdot \text{EXC} \cdot \text{ZPE}$, see (I-29).

^bWhere applicable the atom being abstracted is underlined.

α -deuterium when squared and cubed give reasonable approximations to the transition-state theory calculated $k(H/D)$ and $F(H/D)$ values having two and three α -deuteriums, respectively. This relationship produces better results at higher temperature, since the sum rules upon which this relationship is based apply to the high temperature approximation to the transition-state theory calculated KIEs which is only valid at elevated temperatures, see (I-23) and (III-17).⁴⁶

$$\ln(k_H/k_D) = \ln(v_{1L}^\ddagger/v_{2L}^\ddagger) + \frac{1}{24} \left[\sum_{i=1}^{3n-6} (u_{i1}^2 - u_{i2}^2) - \sum_{i=1}^{3n-7} (u_{i1}^{\ddagger 2} - u_{i2}^{\ddagger 2}) \right] \quad (\text{III-17})$$

An indepth study of the deviations from the rule of the mean as it is related to the method of finite orthogonal polynomial expansions has been recently given by Ishida and Bigeleisen, see (I-25).^{27,47} However, the simple relationships expressed in Chapter I satisfy the comparisons made in Table XXXVII.

A SELECTED BIBLIOGRAPHY

1. S. Glasstone, K. J. Laidler, and H. Eyring, "Theory of Rate Processes", McGraw-Hill Book Co., Inc., New York, N.Y., 1941.
2. L. M. Raff, J. Chem. Phys., 60, 2220 (1974). We are indebted to Dr. Raff for making available to us his potential energy surface computer programs.
3. a) J. Bigeleisen and M. Wolfsberg, Advan. Chem. Phys., 1, 15 (1958); b) M. Wolfsberg and M. J. Stern, Pure Appl. Chem., 8, 225 (1964); c) M. Wolfsberg and M. J. Stern, Pure Appl. Chem., 8, 325 (1964); d) M. J. Stern and M. Wolfsberg, J. Pharm. Sci., 54, 849 (1965); e) M. J. Stern and M. Wolfsberg, J. Chem. Phys., 45, 2618 (1966); f) A. V. Willi, Can. J. Chem., 44, 1889 (1966); g) S. Seltzer and E. J. Hamilton, Jr., J. Am. Chem. Soc., 88, 3775 (1966); h) S. Seltzer and S. G. Mylonakis, J. Am. Chem. Soc., 89, 6584 (1967); i) R. E. Weston, Jr., Science, 158, 332 (1967); j) M. E. Schneider and M. J. Stern, J. Am. Chem. Soc., 95, 1355 (1973).
4. a) S. Seltzer, J. Am. Chem. Soc., 83, 1861 (1961); b) A. A. Zavitsas and S. Seltzer, ibid., 86, 3836 (1964); c) C. Y. Wu and P. E. Robertson, Chem. Ind. (London), 195 (1966); d) C. M. Won and A. V. Willi, J. Phys. Chem., 76, 427 (1972).
5. F. S. Klein, Am. Rev. Phys. Chem., 26, 191 (1975).
6. For an excellent review of the theory of kinetic isotope effects see, W. A. VanHook, "Isotope Effects in Chemical Reactions", ACS Monograph 167, Ed. by C. J. Collins and N. S. Bowman, Van Nostrand-Reinhold Company, New York, N. Y., 1970, Chapter 1.
7. a) All notations having the superscript † refers to the transition-state configuration (no superscript refers to the reactants); b) The subscripts 1 and 2 refer to the light and heavy isotopic species respectively.
8. a) O. Redlich, Z. Physik. Chem., B28, 371 (1935); b) E. Teller, quoted in W. R. Angus and others, J. Chem. Soc., 1936, 971.
9. J. H. Schachtschneider and R. G. Snyder, Spectrochim. Acta, 19, 117 (1973). We gratefully acknowledge Dr. Max Wolfsberg for making available to us his modification of this program.

10. a) C. C. Chou and F. S. Rowland, J. Phys. Chem., 75, 1283 (1971).
Chou and Rowland added small amounts of Br₂ to their reaction mixtures to scavenge moderated product free radicals;
b) C. C. Chou and F. S. Rowland, J. Chem. Phys., 50, 5133 (1969) and references cited therein.
11. See Reference 6, page 36.
12. M. J. Kurylo, G. A. Hollinden, and R. B. Timmons, J. Chem. Phys., 52, 1773 (1970).
13. a) C. Ting and R. E. Weston, Jr., J. Phys. Chem., 77, 2257 (1973);
b) Ting and Weston photolyzed CH₃Br with 185 nm radiation to generate hot methyl radicals with 86-88 kcal/mole distributed between CH₃ and Br.
14. J. S. Shapiro and R. E. Weston, Jr., J. Phys. Chem., 76, 1669 (1972).
15. E. Whittle and E. W. R. Steacie, J. Chem. Phys., 21, 993 (1953).
16. a) T. G. Majury and E. W. R. Steacie, Can. J. Chem., 30, 800 (1952); b) T. G. Majury and E. W. R. Steacie, Disc. Faraday Soc., 14, 45 (1952).
17. S. Davison and M. Burton, J. Am. Chem. Soc., 74, 2307 (1952).
18. S. Chapman and D. L. Bunker, J. Chem. Phys., 62, 2890 (1975).
19. L. B. Sims, L. R. Dosser, and P. S. Wilson, Chem. Phys. Lett., 32, 150 (1975).
20. J. Bigeleisen, Pure Appl. Chem., 8, 217 (1964).
21. A. V. Willi and M. Wolfsberg, Chem. Ind. (London), 2097 (1964).
22. A. J. Kresge and Y. Chiang, J. Am. Chem. Soc., 91, 1026 (1969).
23. C. G. Swain, E. C. Stivers, J. F. Reuwer, Jr., and L. J. Schaad, J. Am. Chem. Soc., 80, 5885 (1958).
24. J. Bigeleisen, "Tritium in the Physical and Biological Sciences", I.A.E.A., Vienna, 1, 161 (1962).
25. M. J. Stern and P. C. Vogel, J. Am. Chem. Soc., 93, 4664 (1971).
26. M. J. Stern and R. E. Weston, Jr., J. Chem. Phys., 60, 2815 (1974).
27. a) J. Bigeleisen, J. Chem. Phys., 23, 2264 (1955); b) J. Bigeleisen, J. Chem. Phys., 28, 694 (1958); c) J. C. Decius and E. Bright Wilson, Jr., J. Chem. Phys., 19, 1409 (1951).

28. E. B. Wilson, Jr., J. C. Decius, and P. C. Cross, "Molecular Vibrations", McGraw-Hill Book Co., New York, N. Y., 1955, pages 29-30.
29. L. M. Raff, L. Stivers, R. N. Porter, D. L. Thompson, and L. B. Sims, J. Chem. Phys., 52, 3449 (1970).
30. S. D. Conte and Carl de Boor, "Elementary Numerical Analysis", McGraw-Hill Cook Co., Inc., New York, N. Y., 1972, pages 278-280.
31. We gratefully acknowledge Dr. H. Burchard of the Oklahoma State University Mathematics Department for his help in deriving this numerical method.
32. The polynomial least squares program used is a double precision version of the one given in D. D. McCracken and W. S. Dorn, "Numerical Methods and Fortran Programming", John Wiley and Sons, Inc., New York, N. Y., 1964, pages 262-275.
33. F. B. Hildebrand, "Introduction to Numerical Analysis", McGraw-Hill, Inc., New York, N. Y., 1974, page 112.
34. G. Herzberg, "Infrared and Raman Spectra of Polyatomic Molecules", D. Van Nostrand, New York, N. Y., 1945, page 40.
35. T. Shimanouchi, "Tables of Molecular Vibrational Frequencies, Consolidated Volume I," Nat. Stand. Ref. Data Ser., Nat. Bur. Stand. No. 39, 45 (1972).
36. A. Snelson, J. Chem. Phys., 74, 537 (1970).
37. D. E. Milligan and M. E. Jacox, J. Chem. Phys., 47, 5146 (1967).
38. L. Y. Tan, A. M. Winer, and G. C. Pimentel, J. Chem. Phys., 57, 4028 (1972).
39. a) See: Indiana University, Quantum Chemistry Program Exchange, Catalog and Procedures, Vol. X (1974), program No. 236;
b) W. A. Lathan, W. J. Hehre, L. A. Curtiss, and J. A. Pople, J. Amer. Chem. Soc., 93, 6377 (1971).
40. G. Herzberg, "Molecular Spectra and Molecular Structure, Vol. I," D. Van Nostrand Co., Inc., New York, N. Y., 1950, page 532.
41. C. L. Kibby and R. E. Weston, Jr., J. Chem. Phys., 49, 4825 (1968).
42. H. S. Johnston, "Gas Phase Reaction Rate Theory", Ronald Press Co., New York, N. Y., 1966, page 169.
43. A. Persky and F. S. Klein, J. Chem. Phys., 44, 3617 (1966).

44. R. P. Bell, Trans. Faraday. Soc., 55, 1 (1959).
45. S. R. Hartshorn and V. J. Shiner, Jr., J. Amer. Chem. Soc., 94, 9002 (1972).
46. See Reference 6, page 17.
47. T. Ishida and J. Bigeleisen, J. Chem. Phys., 64, 4775 (1976).
48. See Reference 28, page 55.
49. a) E. B. Wilson, Jr., J. Chem. Phys., 9, 76 (1941); b) See Reference 28, page 61.
50. See Reference 28, page 309.
51. a) W. D. Gwinn, J. Chem. Phys., 55, 477 (1971); b) M. A. Pariseau, I. Suzuki, and J. Overend, J. Chem. Phys., 42, 2335 (1965); c) L. B. Sims, private communication.
52. Computer program FXGEN in Appendix E, page 223, was used to perform this calculation on the activated complex internal coordinate force constants.
53. See Reference 28, page 284.

APPENDIX A

LMR-PES COORDINATE RELATIONSHIPS

The relationship between cartesian coordinates and the LMR-PES internal coordinates is controlled by three sets of equations in the computer code. The first set, shown in Equation (A-1) initializes the cartesian coordinates for each numbered atom in Figure 1 given values for Z_1 and Z_6 equal to r_1 and $(r_1 + r_6)$, respectively, in Table III or Table V,

$$\begin{aligned}
 y_2 &= r_e \sin\theta \\
 z_2 &= r_e \cos\theta \\
 x_3 &= r_e \sin\theta \cos(11\pi/6) \\
 y_3 &= r_e \sin\theta \sin(11\pi/6) \\
 z_3 &= r_e \cos\theta \\
 x_4 &= r_e \sin\theta \cos(7\pi/6) \\
 y_4 &= r_e \sin\theta \sin(7\pi/6) \\
 z_4 &= r_e \cos\theta
 \end{aligned}
 \tag{A-1}$$

with θ defined by

$$\begin{aligned}
 \theta &= 90^\circ, \quad (r_1 > 6.274) \\
 \theta &= \tau, \quad (r_1 \leq r_e) \\
 \theta &= \tau - a_5(r_1 - r_e), \quad (r_e < r_1 \leq 6.274)
 \end{aligned}
 \tag{A-2}$$

where r_e has the value 2.0673 atomic units, a_5 is defined in Table IV,

τ is the tetrahedral angle and $x_1, y_1, x_2, x_5, y_5, z_5, x_6,$ and y_6 are set equal to zero. These cartesian coordinates are converted to the 15 possible interatomic distances by the DIST routine defined by (A-3),

$$D_{ij} = [(x_i - x_j)^2 + (y_i - y_j)^2 + (z_i - z_j)^2]^{1/2} \quad (\text{A-3})$$

where i and j are the atom numbers 1 through 6 with $i \neq j$. The corresponding interatomic distances defined in Tables III and V are given by (A-4).

$$\begin{aligned} r_1 &= D_{1,5} \\ r_2 &= D_{2,5} \\ r_3 &= D_{3,5} \\ r_4 &= D_{4,5} \\ r_5 &= D_{6,5} \\ r_6 &= D_{1,6} \\ r_7 &= D_{2,6} \\ r_8 &= D_{3,6} \\ r_9 &= D_{4,6} \\ r_{10} &= D_{1,2} \\ r_{11} &= D_{1,3} \\ r_{12} &= D_{1,4} \\ r_{13} &= D_{2,3} \\ r_{14} &= D_{2,4} \\ r_{15} &= D_{3,4} \end{aligned} \quad (\text{A-4})$$

The last six interatomic distances (r_{10} through r_{15}) are used to calculate the six angles θ_1 through θ_6 . The ANGLE routine uses the

law of cosines and the interatomic distances in (A-4) to calculate θ_i ($i=1,2,3,4,5,6$), see (A-5).

$$\begin{aligned}\theta_i &= \arccos[(r_1^2 + r_{i+1}^2 - r_{i+9}^2)/(2r_1 r_{i+1})], \quad (i=1,2,3) \\ \theta_{j+3} &= \arccos [(r_2^2 + r_{j+2}^2 - r_{j+12}^2)/(2r_2 r_{j+2})], \quad (i=1,2) \\ \theta_6 &= \arccos [(r_3^2 + r_4^2 - r_{15}^2)/(2r_3 r_4)]\end{aligned}\tag{A-5}$$

Therefore, when a cartesian coordinate is incremented the DIST and ANGLE routines convert that change to LMR-PES coordinates before the energy is calculated.

The relationships between the internal valence coordinates designations (given in Table V) and the corresponding LMR-PES coordinates was established by equations relating the valence coordinates designations to the proper cartesian coordinate representations. The cartesian coordinate values calculated using these equations were then used in subroutine DIST to obtain the proper values for the LMR-PES coordinates designations. Each valence coordinate in the last column of Table V has a discrete functional cartesian coordinate representation programmed into the routine QRESET or ALBEND. For example, when R_1 is incremented by h the QRESET function is given by (A-6),

$$\begin{aligned}r_1 &= r_{C1} + h \\ Z_6 &= (r_1 - Z_{C1}) + Z_{C6} \\ Z_1 &= r_1\end{aligned}\tag{A-6}$$

where r_{C1} and Z_{C1} and Z_{C6} are the equilibrium LMR-PES and cartesian coordinate values, respectively, for the molecular configuration for

which force constants are being determined. The Z_1 and Z_6 values are then used in the DIST routine to obtain the corresponding LMR-PES coordinates changes relative to $R_1 = f(r_1, r_5, r_7, r_8, r_9)$. The same notation is used for each of the following valence coordinate relationships. The non-reacting C-H bond stretching relationships from incrementation of R_i ($i=2,3,4$) by h is given by (A-7),

$$\begin{aligned}
 r_i &= r_{Ci} + h \\
 A &= \phi_{i-1} - \left(\frac{\pi}{2}\right) \\
 r_{pi} &= r_i \cos(A) \\
 T &= \arctan(x_{Ci}/y_{Ci}) \\
 x_i &= r_{pi} \sin(T) \\
 y_i &= r_{pi} \cos(T) \\
 z_i &= -r_i \sin(A)
 \end{aligned} \tag{A-7}$$

where $i=2,3,4$, r_{pi} is r_i projected into the xy plane, see Figure 1, and A is the angle of r_i out of the xy plane. DIST then converts x_i , y_i and z_i , ($i=2,3,4$) to the corresponding LMR-PES coordinates.

The H-H bond stretching relationship for incrementation of R_5 by h is geometrically related to the linear-bending valence coordinates α_x and α_y . Therefore, R_5 , α_x and α_y relationships are all handled by the same set of equations programmed in the ALBEND routine. These equations relating the incremented coordinates $r_6 = r_{C6} + h$, $\alpha_x = \alpha_x + h$, or $\alpha_y = \alpha_y + h$ to the LMR-PES coordinates are given in (A-8),

$$\begin{aligned}
 \Delta\alpha_x &= \pi - \alpha_x \\
 \Delta\alpha_y &= \pi - \alpha_y \\
 S &= 1 - \sin^2(\Delta\alpha_x) \sin^2(\Delta\alpha_y)
 \end{aligned}$$

$$\begin{aligned}
R_{x_6} &= r_6 \cos^2(\Delta\alpha_y) / S \\
R_{y_6} &= r_6 \cos^2(\Delta\alpha_x) / S \\
x_6 &= R_{x_6} \sin(\Delta\alpha_x) \\
y_6 &= R_{x_6} \sin(\Delta\alpha_y) \\
z_6 &= [R_{x_6} \cos(\Delta\alpha_x)] + r_1
\end{aligned}
\tag{A-8}$$

where R_5 and r_6 correspond to the same interatomic distance, but R_5 is also a function of the LMR-PES coordinates r_5 , r_7 , r_8 and r_9 as are the α_x and α_y valence coordinates from Table V. Application of the DIST equations complete the transformation of the incremented R_5 , α_x or α_y coordinates to the corresponding set of LMR-PES coordinates.

The incremented ϕ_i ($i=1,2,3$) valence angle coordinates are transformed into LMR-PES coordinates by (A-9),

$$\begin{aligned}
\theta_i &= \phi_i + h \\
A &= \theta_i - (\pi/2) \\
r_{pi+1} &= r_{i+1} \cos A \\
T &= \arctan(x_{i+1}/y_{i+1}) \\
x_{i+1} &= r_{pi+1} \sin(T) \\
y_{i+1} &= r_{pi+1} \cos(T) \\
z_{i+1} &= r_{i+1} \sin(A)
\end{aligned}
\tag{A-9}$$

where x_{i+1} , y_{i+1} and z_{i+1} ($i=1,2,3$) correspond to the cartesian coordinates of the non-reacting hydrogens in Figure 1. The corresponding change in the r_{i+6} ($i=1,2,3$) values during incrementation of

$\phi_i = f(\theta_i, r_{i+6})$, ($i=1,2,3$) is calculated by application of the DIST equations.

Equation (A-10) interrelates valence angle coordinates ϕ_i ($i=4,5,6$) and the LMR-PES coordinates for the HCH angles associated with the non-reacting C-H bonds.

$$\theta_i = \phi_i + h$$

$$A_1 = \phi_1 - (\pi/2)$$

$$A_2 = \phi_{i-2} - (\pi/2)$$

$$r_{p1} = r_2 \cos(A_1)$$

$$r_{p2} = r_{i-1} \cos(A_2)$$

$$r_{\theta_i} = [r_2^2 + r_{i-1}^2 - 2r_2 r_{i-1} \cos\theta_i]^{1/2}$$

$$pr_{\theta_i} = r_{\theta_i} \cos[\arcsin(\frac{|z_2 - z_{i-1}|}{r_{\theta_i}})]$$

$$p_{\theta_i} = \arccos[(r_{p1}^2 + r_{p2}^2 - pr_{\theta_i}^2)/(2r_{p1}r_{p2})]$$

$$D_{\theta_i} = 1/2[(2\pi/3) - p_{\theta_i}]$$

$$\theta_{x_2} = D_{\theta_i} + \arcsin(x_2/r_{p1})$$

$$x_2 = r_{p1} \sin(\theta_{x_2})$$

$$y_2 = r_{p1} \cos(\theta_{x_2})$$

$$z_2 = -r_2 \sin(A_1)$$

$$\theta_{y_i} = D_{\theta_i} - (\pi/6) + \arcsin(x_2/r_{p1})$$

$$\begin{aligned}
 x_{i-1} &= r_{p2} \cos(\theta_{y_i}) \\
 y_{i-1} &= r_{p2} \sin(\theta_{y_i}) \\
 z_{i-1} &= -r_{i-1} \sin(A_2)
 \end{aligned}
 \tag{A-10}$$

For $i=4$ or 5 in equation (II-35) r_{p1} and r_{p2} are the r_2 and r_{i-1} bond-lengths projected into the xy plane, respectively, and the cartesian coordinates $x_2, y_2, z_2, x_{i-1}, y_{i-1}$, and z_{i-1} convert the incremented ϕ_4 and ϕ_5 coordinates into the properly changed LMR-PES coordinate values through application of (A-3) and (A-4). The valence coordinate transformation for incrementation of ϕ_6 by h is given by (A-11),

$$\begin{aligned}
 \theta_6 &= \phi_6 + h \\
 A_3 &= \phi_2 - (\pi/2) \\
 A_4 &= \phi_3 - (\pi/2) \\
 r_{p3} &= r_3 \cos(A_3) \\
 r_{p4} &= r_4 \cos(A_4) \\
 r_{\theta_6} &= [r_3^2 + r_4^2 - 2r_3r_4 \cos\theta]^{1/2} \\
 pr_{\theta_6} &= r_{\theta_6} \cos[\arcsin(\frac{z_2 - z_3}{r_{\theta_6}})] \\
 p_{\theta_6} &= \arccos[(r_{p3}^2 + r_{p4}^2 - pr_{\theta_6}^2)/(2r_{p3}r_{p4})] \\
 D_{\theta_6} &= 1/2[(2\pi/3) - P_{\theta_6}] \\
 \theta_{y_3} &= -\frac{\pi}{6} - D_{\theta_6}
 \end{aligned}$$

$$\begin{aligned}
 \theta_{y_4} &= \theta_{y_3} \\
 x_3 &= r_{p3} \cos(\theta_{y_3}) \\
 y_3 &= r_{p3} \sin(\theta_{y_3}) \\
 z_3 &= -r_3 \sin(A_3) \\
 x_4 &= -r_{p4} \cos(\theta_{y_4}) \\
 y_4 &= r_{p4} \sin(\theta_{y_4}) \\
 z_4 &= -r_4 \sin(A_4)
 \end{aligned}
 \tag{A-11}$$

where r_{p3} and r_{p4} are the r_3 and r_4 bondlengths projected into the xy plane, respectively, and the cartesian coordinates x_3 , y_3 , z_3 , x_4 , y_4 and z_4 transform the incremented ϕ_6 coordinate into the proportionally changed LMR-PES coordinates through application of (A-3) and (A-4). It should be noted that the ANGLE transformation routine was not used in incrementing a valence angle coordinate(s) since the internal valence coordinates not being used to obtain a particular derivative must be held constant while the energy values are computed as a function of a particular coordinate's values. Use of the ANGLE routine equations would not allow this to be done.

APPENDIX B

CALCULATION OF NORMAL MODE FREQUENCIES AND ASSOCIATED PARAMETERS

Calculation of Normal Mode Frequencies

The normal mode frequencies for the various isotopic configurations were calculated using the Wilson FG matrix method which has been programmed in the Wolfsberg modification of the Schachtschneider program (WMS).⁹ The purpose of this appendix is to describe the relationship between the cartesian coordinate force constant matrices and the internal coordinate force constant matrices used in the FXGEN ROUTINE in addition to describing the calculational methods generally associated with the Wilson FG matrix calculations used in the Schachtschneider program.⁹

The usual input procedures requires the masses and cartesian coordinates associated with each atom and an internal coordinate code for each internal coordinate in the molecule.^{9,48} The LMR-PES cartesian coordinates are easily obtained from Tables III and V and the equations (A-1) and (A-2) in Appendix A. The internal coordinate specifications are also obtained from Tables III and V. These specifications are combined with the cartesian coordinates of each atom to generate the transformation matrix, B, having I rows and 3N columns where I is the number of internal coordinates and N is the

number of atoms.⁴⁹ The B matrix transforms the cartesian coordinate column vector X, where $X^t = [x_1, y_1, z_1, x_2, \dots, z_N]$, into the column vector of internal coordinates R, where $R^t = [R_1, R_2, \dots, R_I]$, by (B-1),

$$R = Bx \quad (B-1)$$

where the superscript t indicates transposition of the column vector to the corresponding row vector.^{9,48} The inverse kinetic energy matrix, G, is calculated by (B-2),

$$G = BM^{-1}B^t \quad (B-2)$$

where M^{-1} is the diagonal inverse mass matrix in which m_{ix} , m_{iy} , and m_{iz} are the masses associated with each atom i from one to N for each cartesian coordinate in (B-3).⁴⁹

$$M = \begin{bmatrix} 1/m_{1x} & 0 & 0 & \dots & \dots & \dots & 0 \\ 0 & 1/m_{1y} & & & & & \vdots \\ 0 & & 1/m_{1z} & & & & \vdots \\ \vdots & & & \ddots & & & \vdots \\ \vdots & & & & \ddots & & \vdots \\ \vdots & & & & & \ddots & \vdots \\ \vdots & & & & & & \vdots \\ 0 & \dots & \dots & \dots & \dots & \dots & 1/m_{NZ} \end{bmatrix} \quad (B-3)$$

The resultant G matrix is an I by I square matrix. Frequencies are obtained by solution of the corresponding GF product matrix secular equation, (B-4),

$$GFL = LA \quad (B-4)$$

where F is the I by I internal coordinate force constant matrix, L is the transformation matrix which must be normalized to properly remove any redundant internal coordinates from the diagonal eigenvalue matrix Λ .⁵⁰ The Λ matrix values are related to the vibrational frequency values ν_i (cm^{-1}) by (B-5),

$$\Lambda_{ii} = \frac{4\pi^2 c^2 \nu_i^2}{N} = (5.88852 \times 10^{-7}) \nu_i^2 \quad (\text{B-5})$$

The numerical constant in (B-5) is that used in the Schachtschneider program.⁹

The vibrational potential energy, V , is defined by (B-6).^{9,50}

$$2V = R^t F R \quad (\text{B-6})$$

Substitution of (B-1) into (B-6) gives (B-7).

$$2V = (Bx)^t F (Bx) = x^t B^t F B x \quad (\text{B-7})$$

Since the vibrational potential energy is defined as the scalar product of a force constant matrix and its associated coordinate vectors as in (B-6) then the $3N$ by $3N$ cartesian coordinate force constant matrix F_x in equation (B-8) is equivalent to $B^t F B$ in equation (B-7).⁵¹

$$2V = x^t F_x x \quad (\text{B-8})$$

Combining (B-7) and (B-8) produces a method of transforming internal coordinate force constant matrices into their corresponding cartesian coordinate force constant matrices.^{51,52}

$$F_x = B^t F B \quad (B-9)$$

If a cartesian coordinate force constant matrix is used in the frequency calculation then the G matrix equals M^{-1} and the secular equation reduces from (B-4) to (B-10).⁵¹

$$M_x^{-1} F_x L = L \Lambda \quad (B-10)$$

The functional form of the secular equation (B-10) with the symmetric $M_x^{-1} F_x$ product matrix allows it to be solved more easily than the unsymmetric GF product matrix. Also, if F_x is obtained from (B-9) it is properly normalized and all eigenvalues except the normal mode frequencies will be zero upon solution of (B-10).^{9,51} If F_x is calculated directly from a potential energy surface the eigenvalue solution to (B-10) may exhibit some small residual rotational-translational character unless special care is taken in the calculation of F_x .

The more involved solution of the internal coordinate GF secular equation used in the WMS program as described by Schachtschneider follows.⁹ The solution of an unsymmetric GF matrix is avoided by solving two symmetric secular equations. The G matrix is factored into conjugate W matrices by an eigenvalue-eigenvector diagonalization procedure to solve (B-11),

$$G D = D \Gamma \quad (B-11)$$

where D is the eigenvector matrix of G and Γ is the diagonal eigenvalue matrix of G. Since G is a symmetric matrix of real values, D must be orthogonal and the Γ_i roots must be real. Therefore, (B-12) is

correct and the W matrix is defined by (B-13),

$$G = D\Gamma D^t = (D\Gamma^{\frac{1}{2}})(\Gamma^{\frac{1}{2}}D^t) \quad (\text{B-12})$$

$$W = D\Gamma^{\frac{1}{2}} \quad (\text{B-13})$$

where $\Gamma^{\frac{1}{2}}$ is the diagonal matrix of square roots of the Γ_i eigenvalues.⁹

The G matrix is then defined by (B-14).

$$G = WW^t \quad (\text{B-14})$$

A real symmetric H matrix which is equivalent to the corresponding GF product matrix is defined by (B-15).

$$H = W^tFW \quad (\text{B-15})$$

The solution of the secular equation (B-16) by diagonalization of H

$$HC = CA \quad (\text{B-16})$$

produces the eigenvector matrix C and the diagonal eigenvalue matrix Λ which is the same as the Λ in (B-4) and (B-5). The major difference between (B-4) and (B-16) is that in (B-4) L must be properly normalized to remove the redundant normal coordinate representations in the GF matrix (that is those over the 3N-6 limit). However, the symmetric form of H causes these redundancies to be automatically removed during the solution of (B-16).⁹

Calculation of Moments of Inertia

The first step in the calculation of the mass moments of inertia, I_x , I_y , and I_z for a particular molecular species is the calculation

of the cartesian coordinates of the center of mass, C_x , C_y , and C_z , for that molecular species using equation (B-17),

$$C_x = -\frac{1}{M} \sum_{i=1}^N m_i x_i$$

$$C_y = -\frac{1}{M} \sum_{i=1}^N m_i y_i$$

$$C_z = -\frac{1}{M} \sum_{i=1}^N m_i z_i \quad (\text{B-17})$$

where M is the molecular weight, N is the number of atoms, m_i is the atomic weight of atom i ($H = 1.007825$ amu, $D = 2.0141$ amu, $T = 3.01605$ amu, $^{12}\text{C} = 12.000$ amu, $^{13}\text{C} = 13.00335$ amu, and $^{14}\text{C} = 14.0032$ amu), and x_i , y_i , and z_i are the cartesian coordinates of atom i . The next step involves the calculation of the elements of the moment of inertia tensor matrix. The diagonal elements of the moment of inertia tensor matrix require the distance, r_i , of each atom i from the center of mass.

$$r_i = [(x_i + C_x)^2 + (y_i + C_y)^2 + (z_i + C_z)^2]^{1/2} \quad (\text{B-18})$$

The individual elements of the moment of inertia tensor matrix are given by (B-19)

$$I_{xx} = \sum_{i=1}^N m_i [r_i^2 - (x_i + C_x)^2]$$

$$I_{yy} = \sum_{i=1}^N m_i [r_i^2 - (y_i + C_y)^2]$$

$$\begin{aligned}
 I_{zz} &= \sum_{i=1}^N m_i [r_i^2 - (z_i + C_z)^2] \\
 I_{xy} &= I_{yx} = \sum_{i=1}^N m_i (x_i + C_x)(y_i + C_y) \\
 I_{xz} &= I_{zx} = \sum_{i=1}^N m_i (x_i + C_x)(z_i + C_z) \\
 I_{yz} &= I_{zy} = \sum_{i=1}^N m_i (y_i + C_y)(z_i + C_z)
 \end{aligned} \tag{B-19}$$

The moment of inertia tensor T in (B-20) is

$$T = \begin{bmatrix} I_{xx} & I_{xy} & I_{xz} \\ I_{yx} & I_{yy} & I_{yz} \\ I_{zx} & I_{zy} & I_{zz} \end{bmatrix} \tag{B-20}$$

then diagonalized to obtain the eigenvalues I_x , I_y , and I_z which are the principal moments of inertia for a particular molecular species about each of the center of mass cartesian coordinate axes.⁵³

APPENDIX C

TABULATION OF ISOTOPIC NORMAL MODE FREQUENCIES

AND PARAMETERS USED IN TRANSITION-STATE

THEORY ISOTOPE EFFECT CALCULATIONS

All normal mode frequencies, that are tabulated in this Appendix and are specified as being calculated using data from the LMR-PES, were calculated using internal coordinate force constants determined from the LMR-PES by the three-point difference method with an increment size of 1×10^{-4} . The other tabulated frequencies and parameters were calculated using the internal coordinate force constants and geometry from the specified source. The symbol F_{β}^{\ddagger} used in the latter tables refers to the HCH valence angle bending force constant $F_{\phi_{1-3}}^{\ddagger}$, see Table V.

TABLE XXXVIII
LMR-PES DATA FOR ISOTOPIC HYDROGEN

Molecular Hydrogen Isotopic Configurations Data						
	H ₂	HD	D ₂	T ₂	HT	DT
v ₁ ^a	4468.1	3870.0	3160.6	2582.8	3649.3	2886.2
I _x ^b	0.0	0.0	0.0	0.0	0.0	0.0
I _y ^b	0.27736	0.36972	0.54429	0.83004	0.41578	0.66470
I _z ^b	0.27736	0.36972	0.55429	0.83004	0.41578	0.66470
Molecular Weight ^c	2.01565	3.02193	4.02820	6.03210	4.02388	5.03015

^aFrequencies are in cm⁻¹. Data from LMR-PES.

^bThe principal moment of inertia about the respective cartesian coordinate axis in units of amu Å².

^cMolecular weight in amu.

TABLE XXXIX
LMR-PES DATA FOR ISOTOPIC METHYL RADICAL

	Methyl Radical Isotopic Configurations ^a					
	CH ₃	CD ₃	CHD ₂	CH ₂ D	¹³ CH ₃	¹⁴ CH ₃
ν_1^b	2914.2	2061.5	2138.9	2229.4	2914.2	2914.2
$\nu_2^{b,c}$	847.1	656.7	725.7	788.8	840.5	834.8
$\nu_2^{b,d}$	607.0	470.5	520.0	565.2	602.3	598.2
ν_3^e	3099.6	2323.6	2327.7	2989.4	3085.2	3073.0
	3099.6	2323.6	3048.2	3098.9	3085.2	3073.0
ν_4^e	1605.9	1174.7	1461.9	1344.4	1600.8	1596.4
	1605.9	1174.7	1185.6	1590.4	1600.8	1596.4
I_x^f	1.8092	3.6155	3.6155	2.9378	1.8092	1.8092
I_y^f	1.8092	3.6155	2.3402	1.8092	1.8092	1.8092
I_z^f	3.6183	7.2311	5.9557	4.7470	3.6183	3.6183
Molecular ^g Weight	15.0235	18.0423	17.0360	16.0298	16.0268	17.0267

^aFrequencies are in cm⁻¹. Data calculated from the LMR-PES except as stated.

^bNon-degenerate normal mode frequencies.

^cOut-of-plane bending frequency calculated using Gaussian 70 force constant weighted by LMR-PES bond length.

^dOut-of-plane bending frequencies calculated using the adjusted Tan, Winer and Pimental force constant weighted by the LMR-PES bond length. See Reference 38.

^eDoubly degenerate frequencies for symmetric species.

^fThe principal moments of inertia about the respective cartesian coordinate axis in amu-Å².

^gMolecular weight in amu.

TABLE XL
LMR-PES DATA FOR ISOTOPIIC METHANE

	Methane Isotopic Configurations ^a								
	CH ₄	CH ₃ D	CH ₂ D ₂	CHD ₃	CD ₄	¹³ CH ₄	¹⁴ CH ₄	CH ₃ T	CD ₃ T
v ₁ ^b	2917.0	2224.1	2166.4	2113.2	2063.4	2917.0	2917.0	1890.2	1850.5
v ₂ ^c	1526.6	1476.3	1449.3	1303.5	1079.9	1526.6	1526.6	1470.5	1061.4
	1526.6	1476.3	1322.2	1303.5	1079.9	1526.6	1526.6	1470.5	1061.4
v ₃ ^d	3080.1	2966.4	3080.1	3046.2	2287.8	3068.3	3058.3	2964.3	2160.7
	3080.1	3080.1	3008.7	2287.9	2287.8	3068.3	3058.3	3080.1	2287.7
	3080.1	3080.1	2288.1	2287.9	2287.8	3068.3	3058.3	3080.1	2287.7
v ₄ ^d	1366.1	1356.7	1280.7	1040.0	1029.4	1358.0	1350.9	1343.3	1017.7
	1366.1	1197.9	1133.2	1052.6	1029.4	1358.0	1350.9	1121.8	951.7
	1366.1	1197.9	1052.9	1052.6	1029.4	1358.0	1350.9	1121.8	951.7

TABLE XL (Continued)

	Methane Isotopic Configurations ^a								
	CH ₄	CH ₃ D	CH ₂ D ₂	CHD ₃	CD ₄	¹³ CH ₄	¹⁴ CH ₄	CH ₃ T	CD ₃ T
I _x ^e	3.2163	4.3494	5.5352	6.4276	6.4276	3.2163	3.2163	5.3520	7.5696
I _y ^e	3.2163	4.3494	4.8219	5.1597	6.4276	3.2163	3.2163	5.3520	7.5696
I _z ^e	3.2163	3.2163	3.9296	5.1597	6.4276	3.2163	3.2163	3.2163	6.4276
Molecular ^f Weight	16.0313	17.0376	18.0438	19.0501	20.0564	17.0346	18.0345	18.0395	21.0584

^aFrequencies are in cm⁻¹. Data calculated from the LMR-PES.

^bNon-degenerate normal mode frequencies.

^cDoubly degenerate normal mode frequencies for symmetric species.

^dTriply degenerate normal mode frequencies for symmetric species.

^eThe principal moment of inertia about the respective cartesian coordinate axis in amu-Å².

^fMolecular weight in amu.

TABLE XLI

LMR-PES ACTIVATED COMPLEX DATA

Activated Complex Isotopic Configurations ^a						
	CH ₃ -H-H	CH ₂ D-H-H	CHD ₂ -H-H	CD ₃ -H-H	CD ₃ -H-D	CD ₃ -D-H
v ₁ ^b	3388.4	3388.3	3388.1	3387.8	2724.7	3104.8
v ₂ ^b	2937.7	2228.7	2158.0	2095.3	2093.7	2095.2
v ₃ ^b	964.7	906.6	836.4	735.0	726.4	728.0
v ₄ ^b	1479.3i	1478.9i	1478.6i	1478.2i	1349.1i	1180.5i
v ₅ ^c	3085.6	3085.3	3043.1	2303.2	2303.2	2303.2
	3085.6	2995.4	2305.3	2303.2	2303.2	2303.2
v ₆ ^c	1502.9	1478.9	1353.4	1093.8	1093.8	1093.8
	1502.9	1272.6	1130.2	1093.8	1093.8	1093.8
v ₇ ^c	752.3	750.5	703.9	691.9	681.8	552.8
	752.3	696.4	692.0	691.9	681.8	552.8
v ₈ ^c	367.3	365.9	344.2	313.6	274.3	308.7
	367.3	328.5	314.0	313.6	274.3	308.7
I _x ^d	9.6301	10.8995	11.7429	11.8790	16.7999	13.9858
I _y ^d	9.6301	9.8801	10.5286	11.8790	16.7999	13.9858
I _z ^d	3.3736	4.3931	5.5278	6.7427	6.7421	6.7421
Molecular Weight ^e	17.0391	18.0454	19.0517	20.0580	21.0642	21.0642

Activated Complex Isotopic Configurations ^a						
	CH ₃ -H-D	CH ₃ -D-H	CH ₃ -D-D	CD ₃ -D-D	¹³ CH ₃ -H-H	¹⁴ CH ₃ -H-H
v ₁ ^b	2720.9	3106.0	2405.0	2407.6	3387.3	3386.4
v ₂ ^b	2941.2	2937.0	2939.3	2093.2	2936.0	2934.5
v ₃ ^b	956.9	959.3	953.6	721.4	959.7	955.3
v ₄ ^b	1350.4i	1181.7i	1115.0i	1113.5i	1471.3i	1464.3i

TABLE XLI (Continued)

	Activated Complex Isotopic Configurations ^a					
	CH ₃ -H-D	CH ₃ -D-H	CH ₃ -D-D	CD ₃ -D-D	¹³ CH ₃ -H-H	¹⁴ CH ₃ -H-H
v ₅ ^c	3085.7	3085.7	3085.7	2303.2	3072.4	3061.1
v ₆ ^c	1502.9	1502.9	1502.9	1093.8	1499.0	1495.7
v ₇ ^c	746.1	636.6	632.6	543.2	750.8	749.5
v ₈ ^c	327.5	345.7	296.0	262.4	367.0	366.6
I _x ^d	14.2103	11.5250	15.7957	18.6144	9.6625	9.6913
I _y ^d	14.2103	11.5250	15.7957	18.6144	9.6625	9.6913
I _z ^d	3.3736	3.3736	3.3736	6.7421	3.3736	3.3736
Molecular Weight ^e	18.0454	18.0454	19.0517	22.0705	18.0425	19.0423

	Activated Complex Isotopic Configurations ^a					
	CH ₃ -H-T	CD ₃ -H-T	CH ₃ -T-H	CD ₃ -T-H	CH ₃ -T-T	CD ₃ -T-T
v ₁ ^b	2445.6	2449.9	2997.5	2994.2	1973.3	1967.1
v ₂ ^b	2939.9	2091.2	2934.9	2095.2	2938.9	2101.2
v ₃ ^b	950.2	719.0	955.6	722.8	946.8	712.5
v ₄ ^b	1270.8i	1269.3i	1032.7i	1031.1i	961.0i	958.7i
v ₅ ^c	3085.7	2303.2	3085.7	2303.2	3085.7	2303.2
v ₆ ^c	1502.9	1093.8	1502.8	1093.8	1502.9	1093.8
v ₇ ^c	744.1	678.7	596.9	499.5	593.5	489.1
v ₈ ^c	312.8	259.3	331.4	304.6	254.3	232.1
I _x ^d	18.2899	21.2536	13.2127	15.8926	20.8221	25.2528
I _y ^d	18.2899	21.2536	13.2127	15.8926	20.8221	25.2528

TABLE XLI (Continued)

Activated Complex Isotopic Configurations ^a						
	CH ₃ -H-T	CD ₃ -H-T	CH ₃ -T-H	CD ₃ -T-H	CH ₃ -T-T	CD ₃ -T-T
I _z ^d	3.3736	6.7421	3.3736	6.7421	3.3736	6.7421
Molecular Weight ^e	19.0474	22.0662	19.0474	22.0662	21.0556	24.0744
Activated Complex Isotopic Configurations ^a						
	CH ₃ -D-T	CH ₃ -T-D	CD ₃ -D-T	CD ₃ -T-D		
v ₁ ^b	2112.7	2275.3	2135.7	2278.5		
v ₂ ^b	2939.1	2939.0	2071.9	2092.4		
v ₃ ^b	948.3	951.1	715.4	717.5		
v ₄ ^b	1070.21	990.81	1068.41	988.81		
v ₅ ^c	3085.7	3085.7	2303.2	2303.2		
v ₆ ^c	1502.9	1502.8	1093.8	1093.8		
v ₇ ^c	631.4	594.2	540.5	491.3		
v ₈ ^c	277.1	275.8	244.0	253.0		
I _x ^d	19.6223	17.2163	22.8219	20.2638		

TABLE XLI (Continued)

Activated Complex Isotopic Configurations ^a				
	CH ₃ -D-T	CH ₃ -T-D	CD ₃ -D-T	CD ₃ -T-D
I _y ^d	19.6223	17.2163	22.8219	20.2638
I _z ^d	3.3736	3.3736	6.7421	6.7421
Molecular Weight ^e	20.0536	20.0536	23.0724	23.0724

^aFrequencies in cm⁻¹. Data calculated using the LMR-PES force constants and geometry.

^bNon-degenerate normal mode frequencies.

^cDoubly degenerate normal mode frequencies.

^dThe principal moment of inertia about the respective cartesian coordinate axis in amu-Å².

^eMolecular weight in amu.

TABLE XLII

LMR-PES ACTIVATED COMPLEX DATA $\phi_i (i=1,2,3) = 90^\circ$ AND $\phi_i (i=4,5,6) = 120^\circ$

	Planar CH ₃ Activated Complex Isotopic Configurations ^a						
	CH ₃ -H-H	CH ₃ -D-D	CD ₃ -H-H	CH ₃ -D-H	CH ₃ -H-D	¹³ CH ₃ -H-H	¹⁴ CH ₃ -H-H
ν_1^b	3386.3	2403.8	3386.3	3103.8	2720.6	3385.4	3384.6
ν_2^b	2914.0	2914.0	2061.3	2914.0	2914.0	2914.0	2914.0
ν_3^b	555.2	548.9	426.1	551.9	551.5	552.0	549.2
ν_4^b	1469.5i	1108.1i	1469.5i	1174.1i	1340.7i	1461.6i	1454.7i
ν_5^c	3099.8	3099.8	2324.4	3099.7	3099.8	3085.3	3073.0
ν_6^c	1606.7	1606.6	1176.2	1606.6	1606.7	1601.5	1597.0
ν_7^c	746.8	625.9	683.7	629.9	740.5	746.3	745.9
ν_8^c	368.3	297.7	310.0	347.1	328.7	368.2	368.2

TABLE XLII (Continued)

	Planar CH ₃ Activated Complex Isotopic Configurations ^a						
	CH ₃ -H-H	CH ₃ -D-D	CD ₃ -H-H	CH ₃ -D-H	CH ₃ -H-D	¹³ CH ₃ -H-H	¹⁴ CH ₃ -H-H
I _x ^d	9.1465	14.9889	11.0948	10.9083	13.5185	9.1990	9.2457
I _y ^d	9.1465	14.9889	11.0948	10.9083	13.5185	9.1990	9.2457
I _z ^d	3.6183	3.6183	7.2311	3.6183	3.6183	3.6183	3.6183
Molecular ^e Weight	17.0391	19.0517	20.0580	18.0454	18.0454	18.0425	19.0423

^aFrequencies in cm⁻¹. Data calculated using the LMR-PES force constants with the isotopic CH₃ group planar and perpendicular to r₁.

^bNon-degenerate normal mode frequencies.

^cDoubly degenerate normal mode frequencies.

^dThe principal moment of inertia about the respective cartesian coordinate axis in amu-Å².

^eMolecular weight in amu.

TABLE XLIII

LMR-PES ACTIVATED COMPLEX DATA FOR $\phi_i (i=1-6) = 109^\circ 28'$

	Tetrahedral CH ₃ Activated Complex Isotopic Configurations ^a						
	CH ₃ -H-H	CH ₃ -D-D	CD ₃ -H-H	CH ₃ -D-H	CH ₃ -H-D	¹³ CH ₃ -H-H	¹⁴ CH ₃ -H-H
ν_1^b	3389.3	2405.2	3388.3	3107.4	2720.1	3388.1	3387.1
ν_2^b	2952.9	2955.5	2117.4	2951.6	2958.6	2950.1	2947.6
ν_3^b	1104.6	1093.2	837.5	1099.4	1096.0	1099.2	1094.5
ν_4^b	1478.9i	1113.2i	1477.3i	1180.4i	1349.4i	1471.1i	1464.3i
ν_5^c	3077.1	3077.1	2290.6	3077.1	3077.1	3064.5	3053.8
ν_6^c	1451.9	1451.8	1053.1	1451.7	1451.9	1448.7	1440.9
ν_7^c	751.1	631.1	693.2	635.2	744.8	749.3	747.6
ν_8^c	365.8	295.0	313.8	344.6	326.0	365.3	364.9

TABLE XLIII (Continued)

	Tetrahedral CH ₃ Activated Complex Isotopic Configurations ^a						
	CH ₃ -H-H	CH ₃ -D-D	CD ₃ -H-H	CH ₃ -D-H	CH ₃ -H-D	¹³ CH ₃ -H-H	¹⁴ CH ₃ -H-H
I _x ^d	9.7949	16.0533	12.1351	11.7281	14.4346	9.8225	9.8471
I _y ^d	9.7949	16.0533	12.1351	11.7281	14.4346	9.8225	9.8471
I _z ^d	3.2163	3.2163	6.4276	3.2163	3.2163	3.2163	3.2163
Molecular ^e Weight	17.0391	19.0517	20.0580	18.0454	18.0454	18.0425	19.0423

^aFrequencies in cm⁻¹. Data calculated using the LMR-PES force constants with the isotopic CH₃ group tetrahedral relative to r₁.

^bNon-degenerate normal mode frequencies.

^cDoubly degenerate normal mode frequencies.

^dThe principal moment of inertia about the respective cartesian coordinate axis in amu-Å².

^eMolecular weight in amu.

TABLE XLIV
BEBO ACTIVATED COMPLEX DATA^a

	BEBO Activated Complex Isotopic Configurations									
	CH ₃ -H-H	CH ₃ -D-D	CD ₃ -H-H	CD ₃ -D-D	CH ₃ -H-D	CH ₃ -D-H	CD ₃ -H-D	CD ₃ -D-H	¹³ CH ₃ -H-H	¹⁴ CH ₃ -H-H
v ₁ ^b	1610.3	1297.8	1596.6	1218.5	1300.2	1591.5	1226.4	1576.1	1601.7	1594.3
v ₂ ^b	2980.3	2980.0	2139.6	2136.8	2980.0	2980.3	2136.8	2139.6	2977.4	2974.9
v ₃ ^b	1178.9	1077.7	899.5	863.1	1089.0	1173.1	870.7	893.3	1174.3	1170.2
v ₄ ^b	1688.9i	1213.1i	1688.3i	1211.8i	1648.7i	1250.2i	1648.2i	1248.4i	1686.8i	1685.0i
v ₅ ^c	3046.9	3046.8	2249.1	2248.8	3046.9	3046.8	2249.1	2248.8	3036.7	3028.1
v ₆ ^c	1459.0	1457.7	1065.9	1065.4	1459.0	1457.7	1065.9	1065.4	1455.1	1451.8
v ₇ ^c	1046.1	858.3	980.2	761.8	1040.2	862.6	971.6	770.2	1043.1	1040.4
v ₈ ^c	446.4	365.9	383.3	320.5	399.1	422.9	333.7	376.8	445.7	445.1

TABLE XLIV (Continued)

	BEBO Activated Complex Isotopic Configurations									
	CH ₃ -H-H	CH ₃ -D-D	CD ₃ -H-H	CD ₃ -D-D	CH ₃ -H-D	CH ₃ -D-H	CD ₃ -H-D	CD ₃ -D-H	¹³ CH ₃ -H-H	¹⁴ CH ₃ -H-H
I _x ^d	8.1239	13.0996	10.3718	15.8724	12.1165	9.3369	14.7016	11.7648	8.1425	8.1591
I _y ^d	8.1239	13.0996	10.3718	15.8724	12.1165	9.3369	14.7016	11.7648	8.1425	8.1591
I _z ^d	3.1989	3.1989	6.3929	6.3929	3.1989	3.1989	6.3929	6.3929	3.1989	3.1989
Molecular ^e Weight	17.0391	19.0517	20.0580	22.0705	18.0454	18.0454	21.0642	21.0642	18.0425	19.0423

^aFrequencies in cm⁻¹. Data calculated using the BEBO force constants and geometry from Reference 12.

^bNon-degenerate normal mode frequencies.

^cDoubly degenerate normal mode frequencies.

^dThe principal moment of inertia about the respective cartesian coordinate axis in amu-Å².

^eMolecular weight in amu.

TABLE XLV
LEPS ACTIVATED COMPLEX DATA^a

	LEPS Activated Complex Isotopic Configurations							
	CH ₃ -H-H	CH ₃ -D-D	CD ₃ -H-H	CD ₃ -D-D	CH ₃ -H-D	CH ₃ -D-H	CD ₃ -H-D	CD ₃ -D-H
ν_1^b	1396.6	1234.3	1372.8	1080.7	1235.1	1368.6	1090.4	1336.2
ν_2^b	2979.9	2979.7	2136.8	2135.6	2979.7	2979.9	2135.6	2136.8
ν_3^b	1146.6	959.7	883.3	824.2	980.9	1130.1	838.2	873.2
ν_4^b	2024.4i	1448.1i	2024.0i	1447.2i	1948.1i	1525.8i	1947.8i	1524.8i
ν_5^c	3046.8	3046.7	2248.9	2248.6	3046.8	3046.7	2248.9	2248.6
ν_6^c	1458.1	1457.1	1065.6	1065.4	1458.1	1457.2	1065.6	1065.4
ν_7^c	1076.7	856.1	1029.9	779.7	1063.5	867.4	1012.7	799.2
ν_8^c	501.8	425.3	420.6	362.0	453.0	486.2	370.5	418.6

TABLE XLV (Continued)

	LEPS Activated Complex Isotopic Configurations							
	CH ₃ -H-H	CH ₃ -D-D	CD ₃ -H-H	CD ₃ -D-D	CH ₃ -H-D	CH ₃ -D-H	CD ₃ -H-D	CD ₃ -D-H
I _x ^d	8.4210	13.6386	10.6812	16.4413	12.6318	9.6671	15.2420	12.1113
I _y ^d	8.4210	13.6386	10.6812	16.4413	12.6318	9.6671	15.2420	12.1113
I _z ^d	3.1989	3.1989	6.3929	6.3929	3.1989	3.1989	6.3929	6.3929
Molecular ^e Weight	17.0391	19.0517	20.0580	22.0705	18.0454	18.0454	21.0642	21.0642

^aFrequencies in cm⁻¹. Data calculated using the LEPS force constants from Reference 12.

^bNon-degenerate normal mode frequencies.

^cDoubly degenerate normal mode frequencies.

^dThe principal moment of inertia about the respective cartesian coordinate axis in amu-Å².

^eMolecular weight in amu.

TABLE XLVI

BEBO3 ACTIVATED COMPLEX DATA FOR $F_{\beta}^{\ddagger} = 0.0001 \text{ mdyne-Å}^{\text{oa}}$

	BEBO3 Activated Complex Isotopic Configurations									
	CH ₃ -H-H	CH ₃ -D-D	CD ₃ -H-H	CD ₃ -D-D	CH ₃ -H-D	CH ₃ -D-H	CD ₃ -H-D	CD ₃ -D-H	¹³ CH ₃ -H-H	¹⁴ CH ₃ -H-H
v_1^b	1567.6	1195.9	1561.1	1175.7	1203.6	1546.7	1185.4	1539.5	1560.2	1553.9
v_2^b	3148.7	3148.5	2253.2	2251.7	3148.5	3148.7	2251.7	2253.2	3146.1	3144.0
v_3^b	938.4	925.3	730.3	709.4	931.5	954.1	715.1	724.9	953.8	949.8
v_4^b	1691.0i	1214.8i	1690.6i	1213.8i	1649.7i	1253.2i	1649.3i	1252.0i	1688.8i	1687.0i
v_5^c	3165.2	3165.2	2345.4	2345.4	3165.2	3165.2	2345.4	2345.4	3153.5	3143.5
v_6^c	1472.8	1472.7	1074.9	1074.8	1472.8	1472.7	1074.9	1074.8	1468.6	1465.0
v_7^c	622.9	442.7	622.4	442.0	582.9	494.2	582.3	493.6	622.8	622.6
v_8^c	13.7	13.0	11.0	10.1	13.0	13.5	10.2	10.7	13.7	13.6

TABLE XLVI (Continued)

	BEB03 Activated Complex Isotopic Configurations									
	CH ₃ -H-H	CH ₃ -D-D	CD ₃ -H-H	CD ₃ -D-D	CH ₃ -H-D	CH ₃ -D-H	CD ₃ -H-D	CD ₃ -D-H	¹³ CH ₃ -H-H	¹⁴ CH ₃ -H-H
I _x ^d	8.1200	13.0953	10.3642	15.8642	12.1123	9.3329	14.6936	11.7659	8.1386	8.1552
I _y ^d	8.1200	13.0953	10.3642	15.8642	12.1123	9.3329	14.6936	11.7569	8.1386	8.1552
I _z ^d	3.1931	3.1931	6.3812	6.3812	3.1931	3.1931	6.3812	6.3812	3.1931	3.1931
Molecular ^e Weight	17.0391	19.0517	20.0580	22.0705	18.0454	18.0454	21.0642	21.0642	18.0425	19.0423

^aFrequencies in cm⁻¹. Data calculated using the BEB03 force constants from Reference 14 with $F_{\phi 1-3}^{\ddagger}$ equal to 0.0001 mdyne-Å.

^bNone-degenerate normal mode frequencies.

^cDoubly degenerate normal mode frequencies.

^dThe principal moment of inertia about the respective cartesian coordinate axis in amu-Å².

^eMolecular weight in amu.

TABLE XLVII

LEPS2 ACTIVATED COMPLEX DATA FOR $F_{\beta}^{\ddagger} = 0.0001 \text{ mdyne-}\overset{\circ}{\text{A}}^{\text{a}}$

	LEPS2 Activated Complex Isotopic Configurations							
	$\text{CH}_3\text{-H-H}$	$\text{CH}_3\text{-D-D}$	$\text{CD}_3\text{-H-H}$	$\text{CD}_3\text{-D-D}$	$\text{CH}_3\text{-H-D}$	$\text{CH}_3\text{-D-H}$	$\text{CD}_3\text{-H-D}$	$\text{CD}_3\text{-D-H}$
ν_1^b	1391.6	1096.9	1384.1	1055.7	1106.1	1356.2	1071.3	1346.8
ν_2^b	3148.5	3148.4	2252.0	2251.2	3148.4	3148.5	2251.2	2252.0
ν_3^b	954.2	895.2	728.3	701.0	908.2	947.3	709.1	721.4
ν_4^b	1838.7i	1315.7i	1838.4i	1315.0i	1769.5i	1383.5i	1769.2i	1382.7i
ν_5^c	3165.2	3165.2	2345.5	2345.5	3165.2	3165.2	2345.5	2345.5
ν_6^c	1472.9	1472.8	1075.3	1075.0	1472.9	1472.8	1075.2	1075.1
ν_7^c	779.5	554.0	778.5	553.1	730.2	617.6	729.2	616.7
ν_8^c	13.6	12.9	10.9	10.0	13.0	13.4	10.1	10.7

TABLE XLVII (Continued)

	LEPS2 Activated Complex Isotopic Configurations							
	CH ₃ -H-H	CH ₃ -D-D	CD ₃ -H-H	CD ₃ -D-D	CH ₃ -H-D	CH ₃ -D-H	CD ₃ -H-D	CD ₃ -D-H
I _x ^d	8.3096	13.4401	10.5615	16.2277	12.4475	9.5376	15.0449	11.9716
I _y ^d	8.3096	13.4401	10.5615	16.2277	12.4475	9.5376	15.0449	11.9716
I _z ^d	3.1931	3.1931	6.3812	6.3812	3.1931	3.1931	6.3812	6.3812
Molecular Weight ^e	17.0391	19.0517	20.0580	22.0705	18.0454	18.0454	21.0642	21.0642

^aFrequencies in cm⁻¹. Data calculated using the LEPS2 force constants and geometry from Reference 14 with F₁₋₃[†] equal to 0.0001 mdyne-Å.

^bNon-degenerate normal mode frequencies.

^cDoubly degenerate normal mode frequencies.

^dThe principal moment of inertia about the respective cartesian coordinate axis in amu-Å².

^eMolecular weight in amu.

TABLE XLVIII

BEBO3 ACTIVATED COMPLEX DATA FOR $F_{\beta}^{\ddagger} = 0.26 \text{ mdyne-}\overset{\circ}{\text{A}}^{\text{a}}$

	BEBO3 Activated Complex Isotopic Configurations							
	CH ₃ -H-H	CH ₃ -D-D	CD ₃ -H-H	CD ₃ -D-D	CH ₃ -H-D	CH ₃ -D-H	CD ₃ -H-D	CD ₃ -D-H
ν_1^b	1577.5	1273.8	1566.0	1196.3	1276.2	1558.3	1204.1	1545.2
ν_2^b	3148.7	3148.5	2253.6	2252.1	3148.5	3148.7	2252.1	2253.6
ν_3^b	1156.3	1055.0	883.8	846.8	1066.6	1150.3	854.6	877.4
ν_4^b	1690.5i	1214.1i	1690.0i	1212.8i	1649.3i	1252.3i	1648.8i	1250.7i
ν_5^c	3166.5	3166.4	2348.4	2348.2	3166.5	3166.4	2348.4	2348.2
ν_6^c	1479.9	1478.9	1076.6	1076.0	1479.9	1478.9	1076.5	1076.0
ν_7^c	1008.1	827.4	944.0	733.9	1002.5	831.4	935.8	741.9
ν_8^c	429.6	351.9	368.9	308.3	384.1	406.8	321.2	362.6

TABLE XLVIII (Continued)

	BEBO3 Activated Complex Isotopic Configurations							
	CH ₃ -H-H	CH ₃ -D-D	CD ₃ -H-H	CD ₃ -D-D	CH ₃ -H-D	CH ₃ -D-H	CD ₃ -H-D	CD ₃ -D-H
I _x ^d	8.1200	13.0953	10.3642	15.8642	12.1123	9.3329	14.6936	11.7569
I _y ^d	8.1200	13.0953	10.3642	15.8642	12.1123	9.3329	14.6936	11.7569
I _z ^d	3.1931	3.1931	6.3812	6.3812	3.1931	3.1931	6.3812	6.3812
Molecular ^e Weight	17.0391	19.0517	20.0580	22.0705	18.0454	18.0454	21.0642	21.0642

^aFrequencies in cm⁻¹. Data calculated using the BEBO3 force constants and geometry from Reference 14 with $F_{\phi 1-3}^{\dagger}$ equal to 0.26 mdyne-Å.

^bNon-degenerate normal mode frequencies.

^cDoubly degenerate normal mode frequencies.

^dThe principal moment of inertia about the respective cartesian coordinate axis in amu-Å².

^eMolecular weight in amu.

TABLE XLIX

LEPS2 ACTIVATED COMPLEX DATA FOR $F_{\beta}^{\ddagger} = 0.26 \text{ mdyne } \text{\AA}^a$

	LEPS2 Activated Complex Isotopic Configurations							
	CH ₃ -H-H	CH ₃ -D-D	CD ₃ -H-H	CD ₃ -D-D	CH ₃ -H-D	CH ₃ -D-H	CD ₃ -H-D	CD ₃ -D-H
ν_1^b	1411.8	1231.6	1391.6	1091.4	1232.9	1383.4	1102.1	1356.5
ν_2^b	3148.5	3148.5	2252.4	2251.6	3148.4	3148.5	2251.6	2252.4
ν_3^b	1141.9	968.1	879.3	823.3	989.1	1127.7	836.6	869.8
ν_4^b	1838.4i	1315.1i	1838.0i	1314.2i	1769.2i	1382.8i	1768.9i	1381.7i
ν_5^c	3166.5	3166.5	2348.6	2348.3	3166.5	3166.5	2348.6	2348.3
ν_6^c	1480.0	1479.0	1076.8	1076.1	1380.0	1479.0	1076.7	1076.1
ν_7^c	1078.4	858.0	1030.8	781.2	1065.5	869.1	1014.0	800.2
ν_8^c	500.4	423.5	420.0	360.9	451.3	484.7	369.5	417.9

TABLE XLIX (Continued)

	LEPS2 Activated Complex Isotopic Configurations							
	CH ₃ -H-H	CH ₃ -D-D	CD ₃ -H-H	CD ₃ -D-D	CD ₃ -H-D	CH ₃ -D-H	CD ₃ -H-D	CD ₃ -D-H
I _x ^d	8.3096	13.4401	10.5615	16.2277	12.4475	9.5376	15.0449	11.9716
I _y ^d	8.3096	13.4401	10.5615	16.2277	12.4475	9.5376	15.0449	11.9716
I _z ^d	3.1931	3.1931	6.3812	6.3812	3.1931	3.1931	6.3812	6.3812
Molecular ^e Weight	17.0391	10.0517	20.0580	22.0705	18.0454	18.0454	21.0642	21.0642

^aFrequencies in cm⁻¹. Data calculated using the LEPS2 force constants and geometry from Reference 14 with $F_{\ddagger}^{\phi 1-3}$ equal to 0.26 mdyne-Å.

^bNon-degenerate normal mode frequencies.

^cDoubly degenerate normal mode frequencies.

^dThe principal moment of inertia about the respective cartesian coordinate axis in amu-Å².

^eMolecular weight in amu.

TABLE L
 BEBO3 ACTIVATED COMPLEX DATA FOR $F_{\beta}^{\ddagger} = 0.568 \text{ mdyne-}\overset{\circ}{\text{A}}^{\text{a}}$

	BEBO3 Activated Complex Isotopic Configurations									
	$\text{CH}_3\text{-H-H}$	$\text{CH}_3\text{-D-D}$	$\text{CD}_3\text{-H-H}$	$\text{CD}_3\text{-D-D}$	$\text{CH}_3\text{-H-D}$	$\text{CH}_3\text{-D-H}$	$\text{CD}_3\text{-H-D}$	$\text{CD}_3\text{-D-H}$	$^{13}\text{CH}_3\text{-H-H}$	$^{14}\text{CH}_3\text{-H-H}$
ν_1^{b}	1603.4	1432.8	1574.0	1239.7	1432.9	1589.1	1244.2	1554.4	1591.7	1581.8
ν_2^{b}	3148.7	3148.6	2254.3	2252.7	3148.6	3148.7	2252.7	2254.3	3146.2	3144.0
ν_3^{b}	1337.1	1102.7	1033.3	960.6	1116.4	1326.2	971.8	1025.5	1334.1	1331.3
ν_4^{b}	1690.1i	1213.5i	1689.4i	1211.9i	1469.0i	1251.5i	1648.4i	1249.5i	1688.1i	1686.3i
ν_5^{c}	3168.3	3168.1	2353.3	2352.4	3168.3	3168.1	2353.3	2352.4	3156.3	3146.0
ν_6^{c}	1526.9	1497.7	1276.1	1086.8	1526.6	1497.7	1273.4	1087.0	1526.4	1526.0
ν_7^{c}	1355.1	1168.9	1072.8	1011.1	1353.6	1170.0	1072.7	1013.3	1348.0	1341.8
ν_8^{c}	457.5	363.4	403.9	326.9	407.3	421.7	349.4	387.8	457.1	456.7

TABLE L (Continued)

	BEBO3 Activated Complex Isotopic Configurations									
	CH ₃ -H-H	CH ₃ -D-D	CD ₃ -H-H	CD ₃ -D-D	CH ₃ -H-D	CH ₃ -D-H	CD ₃ -H-D	CD ₃ -D-H	¹³ CH ₃ -H-H	¹⁴ CH ₃ -H-H
I _x ^d	8.1200	13.0953	10.3642	15.8642	12.1123	9.3329	14.6936	11.7569	8.1386	8.1552
I _y ^d	8.1200	13.0953	10.3642	15.8642	12.1123	9.3329	14.6936	11.7569	8.1386	8.1552
I _z ^d	3.1931	3.1931	6.3812	6.3812	3.1931	3.1931	6.3812	6.3812	3.1931	3.1931
Molecular Weight ^e	17.0391	19.0517	20.0580	22.0705	18.0454	18.0454	21.0642	21.0642	18.0425	19.0423

^aFrequencies in cm⁻¹. Data calculated using the BEBO3 force constants and geometry from Reference 14 with $F_{\phi 1-3}^{\ddagger}$ equal to 0.568 mdyne-Å.

^bNon-degenerate normal mode frequencies.

^cDoubly degenerate normal mode frequencies.

^dThe principal moment of inertia about the respective cartesian coordinate axis in amu-Å².

^eMolecular weight in amu.

TABLE LI
LEPS2 ACTIVATED COMPLEX DATA FOR $F_{\beta}^{\ddagger} = 0.568 \text{ mdyne-}\text{\AA}^{\text{oa}}$

	LEPS2 Activated Complex Isotopic Configurations							
	$\text{CH}_3\text{-H-H}$	$\text{CH}_3\text{-D-D}$	$\text{CD}_3\text{-H-H}$	$\text{CD}_3\text{-D-D}$	$\text{CH}_3\text{-H-D}$	$\text{CH}_3\text{-D-H}$	$\text{CD}_3\text{-H-D}$	$\text{CD}_3\text{-D-H}$
ν_1^b	1481.7	1417.8	1405.6	1167.0	1417.9	1471.1	1171.1	1374.7
ν_2^b	3148.6	3148.4	2253.0	2252.1	3148.4	3148.6	2252.1	2253.0
ν_3^b	1278.6	988.5	1022.9	905.0	1010.7	1246.7	925.0	1009.0
ν_4^b	1838.1i	1314.6i	1837.6i	1313.5i	1768.9i	1382.2i	1768.6i	1380.7i
ν_5^c	3168.4	3168.2	2353.6	2352.5	3168.4	3168.2	2353.6	2352.5
ν_6^c	1535.4	1497.9	1325.9	1089.5	1534.3	1497.9	1319.4	1090.4
ν_7^c	1384.1	1183.1	1074.8	1033.3	1380.7	1186.0	1074.5	1038.4
ν_8^c	555.2	448.0	482.6	397.6	496.2	518.0	419.7	468.9

TABLE LI (Continued)

	LEPS2 Activated Isotopic Configurations							
	CH ₃ -H-H	CH ₃ -D-D	CD ₃ -H-H	CD ₃ -D-D	CH ₃ -H-D	CH ₃ -D-H	CD ₃ -H-D	CD ₃ -D-H
I _x ^d	8.3096	13.4401	10.5615	16.2277	12.4475	9.5376	15.0449	11.9716
I _y ^d	8.3096	13.4401	10.5615	16.2277	12.4475	9.5376	15.0449	11.9716
I _z ^d	3.1931	3.1931	6.3812	6.3812	3.1931	3.1931	6.3812	6.3812
Molecular ^e Weight	17.0391	19.0517	20.0580	22.0705	18.0454	18.0454	21.0642	21.0642

^aFrequencies in cm⁻¹. Data calculated using the LEPS2 force constants and geometry from Reference 14 with $F_{\phi 1-3}^{\ddagger}$ equal to 0.568 mdyne-Å.

^bNon-degenerate normal mode frequencies.

^cDoubly degenerate normal mode frequencies.

^dThe principal moment of inertia about the respective cartesian coordinate axis in amu-Å².

^eMolecular weight in amu.

APPENDIX D

TABULATION OF THE KIEs USED TO OBTAIN TEMPERATURE DEPENDENCE PARAMETERS

This Appendix presents tables of kinetic isotope effects calculated as a function of temperature. These data were used to calculate the temperature dependence for each kinetic isotope effect.

TABLE LII

VALUES FOR $k(\text{CH}_4, \text{H})/k(\text{CH}_4, \text{D})$

Temperature °K	LMR-PES	LMR-PES ^a + Bell Tunneling	KHT ^b		SW ^c					
			BEBO	LEPS	BEBO3 F _β = 0.0001	BEBO3 F _β = 0.26	BEBO3 F _β = 0.568	LEPS2 F _β = 0.0001	LEPS2 F _β = 0.26	LEPS2 F _β = 0.568
396	0.390	0.618	0.597	0.691	0.634	0.634	0.634	0.687	0.686	0.685
421	0.421	0.592	0.625	0.719	0.663	0.663	0.663	0.715	0.714	0.714
446	0.450	0.590	0.650	0.744	0.690	0.690	0.689	0.740	0.739	0.739
471	0.478	0.598	0.674	0.766	0.713	0.713	0.713	0.762	0.762	0.762
496	0.505	0.610	0.695	0.786	0.735	0.735	0.735	0.783	0.782	0.782
521	0.530	0.624	0.714	0.805	0.755	0.755	0.744	0.801	0.801	0.800
546	0.554	0.639	0.732	0.821	0.773	0.773	0.773	0.818	0.818	0.818
571	0.576	0.654	0.748	0.836	0.789	0.789	0.789	0.838	0.833	0.833
596	0.598	0.669	0.763	0.850	0.804	0.804	0.804	0.846	0.846	0.846
621	0.618	0.684	0.776	0.862	0.818	0.818	0.818	0.859	0.859	0.859
646	0.638	0.699	0.789	0.873	0.830	0.830	0.830	0.870	0.870	0.870
696	0.674	0.727	0.811	0.893	0.853	0.853	0.853	0.890	0.890	0.890

^aValues include a Bell tunneling correction, see (III-12).^bValues calculated using force constants and geometry from Reference 12.^cValues calculated using force constants and geometry from Reference 14. $F_{\beta} = F_{\phi_i}^{\ddagger}$ (i=1,2,3) in mdyne-Å.

TABLE LIII
VALUES FOR $k(\text{CH}_3, \text{H}_2)/k(\text{CH}_3, \text{D}_2)$

Temperature °K	LMR-PES ^a	LMR-PES ^b + Bell Tunneling	KHT ^{c, d}		SW ^{d, e}					
			BEBO	LEPS	BEBO3 F _β = 0.0001	BEBO3 F _β = 0.26	BEBO3 F _β = 0.568	LEPS2 F _β = 0.0001	LEPS2 F _β = 0.26	LEPS2 F _β = 0.568
396	1.904	5.171	4.068	4.098	4.894	4.092	3.460	4.814	4.065	3.463
421	1.883	4.097	3.868	3.890	4.558	3.877	3.321	4.502	3.861	3.331
446	1.863	3.512	3.692	3.707	4.273	3.689	3.198	4.234	3.681	3.211
471	1.844	3.140	3.536	3.544	4.028	3.523	3.087	4.002	3.522	3.102
496	1.825	2.882	3.396	3.399	3.815	3.375	2.986	3.799	3.379	3.003
521	1.808	2.691	3.271	3.268	3.630	3.243	2.895	3.620	3.250	2.913
546	1.791	2.543	3.157	3.150	3.466	3.125	2.811	3.461	3.134	2.829
571	1.775	2.426	3.054	3.043	3.320	3.017	2.734	3.320	3.038	2.752
596	1.759	2.329	2.960	2.945	3.190	2.920	2.662	3.193	2.932	2.681
621	1.745	2.248	2.874	2.856	3.073	2.831	2.597	3.078	2.844	2.615
646	1.731	2.179	2.796	2.774	2.968	2.750	2.536	2.975	2.763	2.554
696	1.704	2.068	2.656	2.629	2.786	2.606	2.426	2.795	2.620	2.444

^aValues calculated using the LMR-PES H₂ and D₂ frequencies.

^bLMR-PES values corrected for Bell tunneling, see (III-12).

^cValues calculated using the force constants and geometry in Reference 12.

^dValues adjusted to the rotationally corrected reactant H₂ and D₂ frequencies of Persky and Klein, see Chapter III and Reference 43.

^eValues calculated using the force constants and geometry in Reference 14. $F_{\beta} = F_{\phi_i}^{\ddagger}$ (i=1,2,3) in mdyne Å.

TABLE LIV
VALUES FOR $k(\text{CD}_3, \text{H}_2)/k(\text{CD}_3, \text{D}_2)$

Temperature °K	LMR-PES ^a	LMR-PES ^b + Bell Tunneling	KHT ^{c,d}		SW ^{d,e}					
			BEB0	LEPS	BEB03 F _β = 0.0001	BEB03 F _β = 0.26	BEB03 F _β = 0.568	LEPS2 F _β = 0.0001	LEPS2 F _β = 0.26	LEPS2 F _β = 0.568
396	1.900	5.149	3.900	4.076	4.893	4.068	3.394	3.813	4.043	3.401
421	1.880	4.085	3.713	3.873	4.558	3.859	3.268	4.501	3.844	3.280
446	1.861	3.505	3.547	3.693	4.273	3.675	3.155	4.234	3.668	3.169
471	1.842	3.136	3.400	3.533	4.028	3.512	3.052	4.002	3.511	3.068
496	1.824	2.879	3.268	3.390	3.816	3.367	2.958	3.799	3.370	2.975
521	1.807	2.689	3.148	3.261	3.630	3.237	2.871	3.620	3.243	2.889
546	1.790	2.542	3.041	3.144	3.467	3.120	2.791	3.462	3.128	2.810
571	1.775	2.425	2.942	3.038	3.321	3.014	2.717	3.320	3.024	2.736
596	1.759	2.329	2.853	2.944	3.191	2.917	2.649	3.193	2.928	2.668
621	1.745	2.248	2.771	2.853	3.074	2.829	2.585	3.079	2.841	2.604
646	1.731	2.179	2.695	2.772	2.969	2.748	2.526	2.975	2.761	2.545
696	1.705	2.068	2.561	2.628	2.787	2.605	2.420	2.795	2.619	2.437

^aValues calculated using the LMR-PES H₂ and D₂ frequencies.

^bLMR-PES values corrected for Bell tunneling, see (III-12).

^cValues calculated using the force constants and geometry in Reference 12.

^dValues adjusted to the rotationally corrected H₂ and D₂ frequencies of Persky and Klein, see Chapter III and Reference 43.

^eValues calculated using the force constants and geometry in Reference 14. $F_{\beta} = F_{\phi_i}^{\dagger}$ (i=1,2,3) in mdyne Å.

TABLE LV
VALUES FOR $k(\text{CH}_3, \text{HD})/k(\text{CH}_3, \text{DH})$

Temperature °K	LMR-PES	LMR-PES ^a + Bell Tunneling	KHT ^b		SW ^c					
			BEBO	LEPS	BEBO3 F _β = 0.0001	BEBO3 F _β = 0.26	BEBO3 F _β = 0.568	LEPS2 F _β = 0.0001	LEPS2 F _β = 0.26	LEPS2 F _β = 0.568
396	1.748	2.637	1.488	1.235	1.782	1.491	1.261	1.476	1.247	1.063
421	1.702	2.366	1.476	1.240	1.737	1.477	1.266	1.459	1.252	1.080
446	1.661	2.183	1.464	1.245	1.697	1.466	1.271	1.443	1.256	1.095
471	1.625	2.049	1.454	1.249	1.663	1.455	1.275	1.430	1.259	1.109
496	1.593	1.946	1.445	1.252	1.633	1.445	1.278	1.418	1.261	1.121
521	1.563	1.863	1.436	1.255	1.607	1.436	1.282	1.407	1.264	1.133
546	1.537	1.795	1.428	1.257	1.584	1.428	1.285	1.398	1.265	1.143
571	1.573	1.738	1.421	1.259	1.563	1.421	1.287	1.389	1.267	1.152
596	1.491	1.689	1.415	1.261	1.545	1.414	1.289	1.381	1.268	1.160
621	1.471	1.647	1.409	1.262	1.528	1.408	1.292	1.374	1.270	1.168
646	1.453	1.610	1.403	1.263	1.514	1.402	1.293	1.368	1.271	1.175
696	1.421	1.549	1.394	1.266	1.488	1.393	1.297	1.357	1.272	1.187

^aValues corrected for Bell tunneling, see (III-12).

^bValues calculated using force constants and geometries in Reference 12.

^cValues calculated using force constants and geometry in Reference 14. $F_{\beta} = F_{\phi_i}^{\ddagger}$ (i=1,2,3) in mdyne-Å.

TABLE LVI
VALUES FOR $k(\text{CD}_3, \text{HD})/k(\text{CD}_3, \text{DH})$

Temperature °K	LMR-PES	LMR-PES ^a + Bell Tunneling	KHT ^b		SW ^c					
			BEBO	LEPS	BEBO3 F _β = 0.0001	BEBO3 F _β = 0.26	BEBO3 F _β = 0.568	LEPS2 F _β = 0.0001	LEPS2 F _β = 0.26	LEPS2 F _β = 0.568
396	1.744	2.628	1.478	1.228	1.782	1.482	1.237	1.475	1.240	1.044
421	1.699	2.360	1.468	1.234	1.736	1.470	1.246	1.458	1.246	1.063
446	1.659	2.179	1.458	1.240	1.697	1.460	1.254	1.443	1.251	1.081
471	1.623	2.046	1.449	1.245	1.663	1.450	1.260	1.430	1.255	1.097
496	1.591	1.943	1.440	1.248	1.633	1.441	1.266	1.418	1.258	1.111
521	1.562	1.861	1.433	1.252	1.607	1.433	1.271	1.407	1.261	1.123
546	1.536	1.794	1.426	1.254	1.584	1.426	1.276	1.398	1.263	1.135
571	1.512	1.737	1.419	1.257	1.564	1.419	1.28	1.389	1.265	1.145
596	1.491	1.688	1.413	1.259	1.545	1.413	1.283	1.381	1.267	1.154
621	1.471	1.646	1.407	1.261	1.529	1.407	1.286	1.374	1.268	1.163
646	1.453	1.610	1.402	1.262	1.514	1.402	1.289	1.368	1.270	1.170
696	1.420	1.549	1.393	1.265	1.489	1.392	1.293	1.357	1.272	1.183

^aValues corrected for Bell tunneling, see (III-12).

^bValues calculated using force constants and geometry in Reference 12.

^cValues calculated using force constants and geometry in Reference 14. $F_{\beta} = F_{\phi_i}^{\ddagger}$ (i=1,2,3) in mdyne-Å.

TABLE LVII
 VALUES FOR $k(\text{CH}_4, \text{H})/k(^{13}\text{CH}_4, \text{H})$

Temperature °K	LMR-PES	BEBO ^a	BEBO3 ^b $F_\beta = 0.0001$	BEBO3 ^b $F_\beta = 0.568$
273	1.038	1.024	1.031	1.0086
296	1.035	1.022	1.028	1.0080
321	1.032	1.020	1.025	1.0075
346	1.030	1.019	1.023	1.0071
371	1.028	1.017	1.021	1.0067
396	1.026	1.016	1.020	1.0064
421	1.024	1.015	1.018	1.0061
446	1.023	1.014	1.017	1.0058
471	1.021	1.013	1.016	1.0056
496	1.020	1.013	1.015	1.0053
521	1.019	1.012	1.014	1.0051
546	1.018	1.011	1.013	1.0049

^aValues calculated using the force constants and geometry in Reference 12.

^bValues calculated using the force constants and geometry in Reference 14.

TABLE LVIII
 VALUE FOR $k(\text{CH}_3, \text{H}_2)/k(^{13}\text{CH}_3, \text{H}_2)$

Temperature °K	LMR-PES ^a	LMR-PES ^b + Pimentel	BEBO ^c	BEBO3 ^d $F_\beta = 0.0001$	BEBO3 ^d $F_\beta = 0.586$
273	1.0064	1.0021	0.9923	0.9993	0.978
296	1.0064	1.0026	0.9935	0.9995	0.980
321	1.0063	1.0030	0.9945	0.9997	0.982
346	1.0063	1.0033	0.9954	0.9999	0.984
371	1.0063	1.0036	0.9962	1.0001	0.986
396	1.0062	1.0038	0.9969	1.0003	0.987
421	1.0062	1.0040	0.9974	1.0004	0.988
446	1.0061	1.0041	0.9979	1.0005	0.990
471	1.0061	1.0043	0.9984	1.0006	0.991
496	1.0061	1.0044	0.9987	1.0007	0.991
521	1.0060	1.0045	0.9990	1.0008	0.992
546	1.0060	1.0046	0.9993	1.0009	0.993

^aValues calculated using the LMR-PES force constants and geometry plus the Gaussian 70 CH₃ out-of-plane bending force constant, see Chapter II.

^bValues calculated using the LMR-PES force constants and geometry plus the Tan, Winer, and Pimentel harmonic CH₃ out-of-plane bending frequency, see Appendix C.

^cValues calculated using the BEBO data in Reference 12.

^dValues calculated using the BEBO3 data in Reference 14. $F_\beta = F_\beta^\dagger / \phi_i$ ($i=1,2,3$) in mdyne-Å.

TABLE LIX
 VALUES FOR $k(\text{CH}_4, \text{H})/k(\text{CD}_3\text{H}, \text{H})$

Temperature °K	LMR-PES	BEBO ^a	BEBO3 ^b $F_\beta = 0.0001$	BEBO3 ^b $F_\beta = 0.568$
273	1.650	1.321	1.591	0.687
296	1.579	1.293	1.507	0.712
321	1.514	1.266	1.434	0.735
346	1.460	1.242	1.374	0.755
371	1.413	1.222	1.324	0.772
396	1.372	1.203	1.283	0.787
421	1.338	1.186	1.248	0.800
446	1.307	1.172	1.219	0.812
471	1.281	1.159	1.193	0.823
496	1.257	1.147	1.172	0.833
521	1.237	1.136	1.153	0.842
546	1.218	1.127	1.136	0.850

^aValues calculated using the BEBO data in Reference 12.

^bValues calculated using the BEBO3 data in Reference 14. $F_\beta =$
 $\frac{F_\beta^\dagger}{\phi_i}$ ($i=1,2,3$) in mdyne-Å.

TABLE LX
 VALUES FOR $k(\text{CH}_3, \text{H}_2)/k(\text{CD}_3, \text{H}_2)$

Temperature °K	LMR-PES ^a	LMR-PES ^b + Pimentel	BEBO ^c	BEBO3 ^d $F_\beta = 0.0001$	BEBO3 ^d $F_\beta = 0.568$
273	0.811	0.722	0.650	0.782	0.338
296	0.838	0.756	0.686	0.800	0.378
321	0.862	0.787	0.721	0.816	0.418
346	0.882	0.813	0.751	0.830	0.456
371	0.898	0.835	0.776	0.842	0.491
396	0.911	0.854	0.799	0.852	0.523
421	0.923	0.871	0.819	0.861	0.552
446	0.932	0.884	0.836	0.869	0.579
471	0.940	0.896	0.851	0.876	0.604
496	0.947	0.907	0.864	0.883	0.627
521	0.953	0.916	0.876	0.888	0.649
546	0.958	0.923	0.886	0.894	0.668

^aValues calculated using the LMR-PES force constants and geometry plus the Gaussian 70 CH₃ out-of-plane bending force constant, see Chapter II, and Appendix C.

^bValues calculated using the LMR-PES force constants and geometry plus the Tan, Winer, and Pimentel harmonic CH₃ out-of-plane bending frequency, see Appendix C.

^cValues calculated using the BEBO data in Reference 12.

^dValues calculated using the BEBO3 data in Reference 14. $F_\beta =$
 F_\dagger in mdyne-Å.
 ϕ_i (i=1,2,3)

TABLE LXI

LMR-PES KIEs USING DIFFERENT TRANSITION-STATE GEOMETRIES

Temperature °K	$k(\text{CH}_4, \text{H})/k(^{14}\text{CH}_4, \text{H})$			$k(\text{CH}_3, \text{H}_2)/k(^{14}\text{CH}_3, \text{H}_2)$		
	Tetrahedral ^a CH ₃	LMR-PES	Planar ^b CH ₃	Tetrahedral ^a CH ₃	LMR-PES	Planar ^b CH ₃
371	1.0527	1.0520	1.0526	1.0124	1.0117	1.0123
396	1.0491	1.0484	1.0488	1.0123	1.0116	1.0120
421	1.0459	1.0453	1.0455	1.0122	1.0115	1.0117
446	1.0431	1.0425	1.0426	1.0121	1.0115	1.0115
471	1.0407	1.0401	1.0400	1.0119	1.0114	1.0113
496	1.0384	0.0379	0.0377	1.0118	1.0113	1.0112
521	1.0365	1.0360	1.0357	1.0117	1.0113	1.0110
546	1.0347	1.0342	1.0339	1.0117	1.0112	1.0109

^a $\phi_i (i=1-6) = 109^\circ 28' 16''$.

^b $\phi_i (i=1, 2, 3) = 90^\circ$, $\phi_i (i=4, 5, 6) = 120^\circ$.

TABLE LXII

LMR-PES KIEs USING DIFFERENT TRANSITION-STATE GEOMETRIES

Temperature °K	$k(\text{CH}_4, \text{H})/k(\text{CH}_4, \text{D})$			$k(\text{CH}_3, \text{H}_2)/k(\text{CH}_3, \text{HD})$		
	Tetrahedral ^a CH ₃	LMR-PES	Planar ^b CH ₃	Tetrahedral ^a CH ₃	LMR-PES	Planar ^b CH ₃
371	0.357	0.357	0.358	0.986	0.986	0.989
396	0.389	0.390	0.391	1.000	1.000	1.003
421	0.420	0.421	0.422	1.012	1.012	1.014
446	0.450	0.450	0.451	1.023	1.023	1.025
471	0.478	0.478	0.479	1.032	1.032	1.035
496	0.505	0.505	0.506	1.041	1.041	1.043
521	0.530	0.530	0.531	1.048	1.048	1.050
546	0.554	0.554	0.555	1.055	1.055	1.057

^a $\phi_i (i=1-6) = 109^\circ 28' 16''$.

^b $\phi_i (i=1, 2, 3) = 90^\circ$, $\phi_i (i=4, 5, 6) = 120^\circ$.

TABLE LXIII

LMR-PES KIEs USING DIFFERENT TRANSITION-STATE GEOMETRIES

Temperature °K	$k(\text{CH}_4, \text{H})/k(\text{CH}_3\text{D}, \text{H})$			$k(\text{CH}_3, \text{H}_2)/k(\text{CH}_3, \text{DH})$		
	Tetrahedral ^a	LMR-PES	Planar ^b	Tetrahedral ^a	LMR-PES	Planar ^b
	CH ₃		CH ₃	CH ₃		CH ₃
371	3.871	3.869	3.883	1.777	1.776	1.782
396	3.529	3.527	3.539	1.749	1.748	1.754
421	3.252	3.250	3.260	1.724	1.723	1.728
446	3.024	3.023	3.031	1.700	1.699	1.704
471	2.835	2.834	2.841	1.679	1.678	1.682
496	2.676	2.674	2.680	1.658	1.658	1.661
521	2.540	2.538	2.544	1.640	1.639	1.642
546	2.423	2.421	2.426	1.622	1.621	1.625

^a $\phi_i (i=1-6) = 109^\circ 28' 16''$.

^b $\phi_i (i=1, 2, 3) = 90^\circ$, $\phi_i (i=4, 5, 6) = 120^\circ$.

TABLE LXIV

LMR-PES KIEs USING DIFFERENT TRANSITION-STATE GEOMETRIES

Temperature °K	$k(\text{CH}_4, \text{H})/k(\text{CD}_3\text{H}, \text{H})$			$k(\text{CH}_3, \text{H}_2)/k(\text{CD}_3, \text{H}_2)$		
	Tetrahedral ^a CH ₃	LMR-PES	Planar ^b CH ₃	Tetrahedral ^a CH ₃	LMR-PES	Planar ^b CH ₃
371	1.396	1.413	1.478	0.887	0.898	0.939
396	1.359	1.372	1.426	0.902	0.911	0.947
421	1.326	1.338	1.381	0.915	0.923	0.953
446	1.298	1.307	1.344	0.925	0.932	0.958
471	1.273	1.281	1.311	0.934	0.940	0.963
496	1.250	1.257	1.283	0.942	0.947	0.966
521	1.231	1.237	1.258	0.948	0.953	0.970
546	1.213	1.218	1.237	0.954	0.958	0.972

^a ϕ_i (i=1-6) = 109°28'16".

^b ϕ_i (i=1,2,3) = 90°, ϕ_i (i=4,5,6) = 120°.

APPENDIX E

LISTING OF COMPUTER PROGRAMS

The following computer programs are arranged in the relative order of usage to calculate transition-state theory kinetic isotope effects. The first program is the SCANNING ROUTINE used to search out and define the LMR-PES activated complex geometric configuration, $\text{CH}_3\text{-H-H}$, for the axial hydrogen abstraction reaction. This is followed by the subroutines describing the LMR-PES, that is, POT6, TRI, PLACE, DIST, ANGLE and READ.² Subroutine TETRAH contains equations describing a geometric derivation of the tetrahedral angle and is called no more than once in any one program. The next program is the INTERNAL COORDINATE FORCE CONSTANT ROUTINE which uses the subroutines describing the LMR-PES² in addition to CPUNCH for punching the force constants in the proper form for use with the Schachtschneider normal mode frequency program,⁹ and ALBEND and QRESET whose functional forms are described in Appendix A. The third program, FXGEN ROUTINE, was used to convert internal coordinate force constants to cartesian coordinate force constants by the matrix methods described in Appendix B. The fourth program is the CARTESIAN COORDINATE FORCE CONSTANT ROUTINE which uses the subroutine describing the LMR-PES² in addition to the polynomial least squares subroutine LESQ.³² The fifth program is the ABSOLUTE RATE THEORY ROUTINE which controls the input to the subroutine THERMO. Then THERMO calculates

the transition-state theory kinetic isotope effect ratios and their temperature dependence using subroutine LESQ.³² THERMO has also been modified to use a temperature dependent exponential factor like those in (III-10) and (III-11).

PLEASE NOTE:

Computer print-out on pages
191-244 has very small type.
Filmed as received.

UNIVERSITY MICROFILMS.


```

PERTANY IV OF RELEASE 740          Y418          DATE = 7632          19/03/76

0030          01 00 I=1,100
0031          I=1,100
0032          20-XX
0033          01 01 J=1,100
0034          I(1)=I+20
C ////////////////////////////////////////////////////
C CALCULATE ENERGY AFTER SETTING GEOMETRY AS A FUNCTION OF SWORD LENGTH OF
C REACTING C-H BOND.
0041          CALL PLAGE(2(1))
0042          CALL DIST
0043          CALL ANGLE
0044          CALL FCT6
0045          E=PE+12.725200
C ////////////////////////////////////////////////////
C TEST FOR MINIMUM ENERGY (REACTION COORDINATE POSITION) ALONG THE H-H INCRE
C MENTATION SCAN.
0046          1/// H(1)=1) 20,21,21
0047          21 I=1
0048          GO TO 22
0049          20 I=ABS(I/3.0+00-60.0001)
0050          H(1)=1) 70,70,71
0051          71 I=61
0052          70 CONTINUE
0053          P(L,N)=E
0054          K=K+1
0055          H(1)=I*MAX) 400,400,401
C ////////////////////////////////////////
C STORE GEOMETRY OF MAXIMUM ENERGY CONFIGURATION.
0056          401 I*AX=EE
0057          DO 402 I=1,6
0058          XM=AX(IK)=X(IK)
0059          YM=AX(IK)=Y(IK)
0060          ZM=AX(IK)=Z(IK)
0061          402 AMAX(IK)=AM(IK)*180.000/PI
0062          DO 403 I=1,15
0063          403 RM=AX(IK)=R(IK)
0064          400 CONTINUE
0065          GO TO 50
C ////////////////////////////////////////
C INCREMENT H-H DISTANCE.
0066          22 Z6=Z6+3.00-4
0067          51 CONTINUE
C ////////////////////////////////////////
C INCREMENT C-H DISTANCE
0068          50 Z(1)=Z(1)-3.00-4
0069          DO 60 I=1,12
0070          M=5*(I-1)+1
0071          WRITE(6,102) PPP,(P(M,N),N=1,100)
0072          PPP=PPP-0.20
0073          102 FORMAT(1X,F5.2,'X,100A1)
0074          103 FORMAT(8X,100A1)
0075          01 01 J=1,4
0076          M=5*(I-1)+J+1
0077          61 WRITE(6,103) (P(M,N),N=1,100)
0078          60 CONTINUE
0079          PPP=0.0
0080          WRITE(6,102) PPP,(P(61,N),N=1,100)
0081          WRITE(6,105)

```

FORTRAN IV 61 RELEASE 2.0

MAIN

DATE = 76302

10/03/48

```

0082      175  FORMAT(40X,10HREACTION COORDINATE)
0083      777  CONTINUE
0084      WRITE(6,101)
0085      WRITE(6,404)
0086      404  FORMAT(20X,30HEENERGY AND GEOMETRY OF THE SADDLE-POINT//
1 10X,6HATOM 1,15X,6HATOM 2,15X,6HATOM 3,15X,6HATOM 4,15X,6HATOM 5,
2 15X,6HATOM 6//)
0087      WRITE(6,405) XMAX,YMAX,ZMAX
0088      405  FORMAT(1X,1HX,2X,6(1PD21.14)/1X,1HY,2X,6(1PD21.14)/1X,1HZ,2X,6(1PD
121.14)//)
0089      DO 406 I=1,15
0090      406  WRITE(6,407) I,KMAX(I)
0091      407  FORMAT(15X,1HR,12,1H=,1X,1PD22.15)
0092      WRITE(6,408) AMAX
0093      408  FORMAT(//20X,6HANGLES//10X,3HT1=,3PD15.6,2X,3HT2=,3PD15.6,2X,
1 3HT3=,3PD15.6,2X,3HT4=,3PD15.6,2X,3HT5=,3PD15.6,2X,3HT6=,3PD15.6,
2 //)
0094      TMAX=(TMAX-0.4000)*23.060500
0095      WRITE(6,409) TMAX
0096      409  FORMAT(10X,20HBARRIER HEIGHT IN KCAL/MOLE=,2PD25.15)
0097      GO TO 500
0098      END

```

FORTRAN IV G LEVEL 21

POT6

DATE = 76044

14/04/741

```

0001      SUBROUTINE POT6
C *****
C      SEE REFERENCE: L. M. RAFF, J. CHEM. PHYS., VOL. 50, 2220(1974)
C      SUBROUTINE TO CALCULATE THE CH4-H SURFACE
C      REQUIRES SUBROUTINES DIST, ANGLE, AND TRI
C      ALSO COMPUTES DE/DR FOR ALL R AND STORES RESULTS IN ARRAY DER
C *****
0002      IMPLICIT REAL*8 (A-H,O-Z)
0003      DIMENSION FR(4), DFR(4)
0004      DIMENSION X(6), Y(6), Z(6), R(15), DER(15), AG(6), R2(15), D1(3), D2(3),
1 ALPH(3), RF(3), BETA(3), CC(3), AA(3), SIG(3), RSTR(3), ACS(6), DK(6),
2 Y1(6), Y2(6), ASS(6), F(4), DF(4), RX(6), PX(6), PY(6), PZ(6), DX(6),
3 DY(6), DZ(6), DPX(6), DPY(6), DPZ(6), GF(15,3)
0005      DIMENSION APARM(5)
0006      COMMON X, Y, Z, R, DEP, AG, R2, D1, ALPH, RE, D3, BETA, CC, AA, SIG, PSTP, TAU,
1 RV, DIJ, CP, EE, ACS, ASS, RX, XI1, VI, V2, V3, V4, RMAX,
2 PSS, VR, PEF, HH, PX, PY, PZ, WH, WC, WBR, WW, DT, DX, DY, DZ, DPX, DPY, DPZ, T, GF,
3 TEMP, RRT, START, APARM, PI, T3PI, FL6PI, S6PI,
4 I1, J1, K1, L1, NV1, NV2, NV3, NV4, J1, NI, KEF
0007      EXP(X)=DEXP(X)
0008      SQRT(X)=DSQRT(X)
0009      COS(X)=DCOS(X)
0010      SIN(X)=DSIN(X)
0011      ARCOS(X)=DARCOS(X)
0012      ARSIN(X)=DARSIN(X)
C ////////////////////////////////////////////////////
C COMPUTE THE INTERPARTICLE DISTANCES R
C CALL DIST
C *****
C CHECK FOR THE FIFTH ATOM--I.E.--CH4--(H)
C BY DEFINITION THE FIFTH H ATOM IS THE ONE WHOSE C-H DISTANCE IS MAXIMUM
C ////////////////////////////////////////////////////
0013      RHMAX=R(1)
0014      KMAX=1
0015      IF(R(2).LT.RHMAX) GO TO 1100
0016      RHMAX=R(2)
0017      KMAX=2
0018      1100 IF(R(3).LT.RHMAX) GO TO 1101
0019      RHMAX=R(3)
0020      KMAX=3
0021      1101 IF(R(4).LT.RHMAX) GO TO 1102
0022      RHMAX=R(4)
0023      KMAX=4
0024      1102 IF(R(5).LT.RHMAX) GO TO 1103
0025      RHMAX=R(5)
0026      KMAX=5
0027      1103 CONTINUE
C CALL SWITCH(KMAX,1)
C *****
C COMPUTE THE HCH ANGLES AND STORE RESULTS IN ARRAY AG
C CALL ANGLE
C *****
0028      DO 50 I=1,15
0029      50 DER(I)=0.000
C COMPUTE THE FOUR TRIATOMIC TERMS
0030      CALL TRI(P(1),R(5),R(6),DER(1),DER(5),DER(6),1,3,2,EE)
0031      CALL TRI(R(2),R(5),R(7),DER(2),DER(7),DER(7),1,3,2,E)
0032      EE=EE+E

```

FORTRAN IV G LEVEL 21

POT6

DATE = 76044

14/04/41

```

0033      DFR(5)=DEF(5)+DR2
0034      CALL TRI(R(3),R(5),R(8),DFR(3),DR2,DEF(8),1,3,2,E)
0035      EF=EE+F
0036      DFR(5)=DFR(5)+DR2
0037      CALL TRI(R(4),R(5),P(0),DER(4),DR2,DER(0),1,3,2,F)
0038      EE=EE+E
0039      DER(5)=DER(5)+DR2
C*****
C COMPUTE FORCE CONSTANTS
C COMPUTE ATTENUATION TERMS
0040      XA=R(1)-RE(1)
0041      XB=R(2)-RE(1)
0042      XC=R(3)-RE(1)
0043      XD=R(4)-RE(1)
0044      XA2=XA*XA
0045      XB2=XB*XB
0046      XC2=XC*XC
0047      XD2=XD*XD
0048      XXA=R(6)-RE(2)
0049      XXB=R(7)-RE(2)
0050      XXC=R(8)-RE(2)
0051      XXD=R(9)-RE(2)
0052      EXA11=EXP(-APARM(2)*R2(6))
0053      EXA12=EXP(-APARM(2)*R2(7))
0054      EXA13=EXP(-APARM(2)*R2(8))
0055      EXA14=EXP(-APARM(2)*R2(9))
0056      EXA21=EXP(-APARM(5)*XXA*XXA)
0057      EXA22=EXP(-APARM(5)*XXB*XXB)
0058      EXA23=EXP(-APARM(5)*XXC*XXC)
0059      EXA24=EXP(-APARM(5)*XXD*XXD)
0060      A11=1.0D0-EXA11
0061      A12=1.0D0-EXA12
0062      A13=1.0D0-EXA13
0063      A14=1.0D0-EXA14
0064      A21=APARM(3)+APARM(4)*EXA21
0065      A22=APARM(3)+APARM(4)*EXA22
0066      A23=APARM(3)+APARM(4)*EXA23
0067      A24=APARM(3)+APARM(4)*EXA24
0068      EXF1=EXP(-A21*XA2)
0069      EXF2=EXP(-A22*XB2)
0070      EXF3=EXP(-A23*XC2)
0071      EXF4=EXP(-A24*XD2)
0072      F(1)=A11*EXF1
0073      F(2)=A12*EXF2
0074      F(3)=A13*EXF3
0075      F(4)=A14*EXF4
C DK'S ARE THE FORCE CONSTANTS
0076      DK(1)=APARM(1)*F(1)*F(2)
0077      DK(2)=APARM(1)*F(1)*F(3)
0078      DK(3)=APARM(1)*F(1)*F(4)
0079      DK(4)=APARM(1)*F(2)*F(3)
0080      DK(5)=APARM(1)*F(2)*F(4)
0081      DK(6)=APARM(1)*F(3)*F(4)
C*****
C COMPUTE THE EQUILIBRIUM ANGLES
C FIND THE LARGEST C-H DISTANCE
0082      RGR=R(1)
0083      KLM=1

```

```

FORTRAN IV G LEVEL 21          P016          DATE = 76044          14/04/41

0084          IF(R(2).LT.RGR) GO TO 800
0085          RGR=R(2)
0086          KLM=2
0087          800  IF(R(3).LT.RGR) GO TO 801
0088          RGR=R(3)
0089          KLM=3
0090          801  IF(R(4).LT.RGR) GO TO 802
0091          KLM=4
0092          RGR=R(4)
0093          802  RCH=5JRT(R2(KLM)+R2(5)-2.000*R(KLM)*R(5)*COS(TAU))
0094          IF(R(KLM+5).GT.RCH) GO TO 4000
0095          DIJF=DIJ
0096          CPF=CP
0097          DAA=0.000
0098          GO TO 4001
0099          4000 IF(R(5).GT.DIJ) GO TO 4002
0100          CPF=0.33975700/(R(5)-RE(1))
0101          DIJF=R(5)
0102          DAA=-CPF/(R(5)-RE(1))
0103          DAA=-DAA*(RGR-RE(1))
0104          GO TO 4001
0105          4002 CPF=CP
0106          DAA=0.000
0107          DIJF=DIJ
0108          4001 IF(RGR.GT.DIJF) GO TO 803
0109          IF(RGR.LT.PE(1)) GO TO 804
C COMPUTE EQUILIBRIUM FRONTSIDE ANGLE
0110          ASF=TAU-CPF*(RGR-RE(1))
C COMPUTE BACKSIDE EQUILIBRIUM ANGLE
0111          XYZ=SIN(ASF)
0112          ASB=ARCCOS(1.000-1.500*XYZ*XYZ)
C COMPUTE DERIVATIVES OF EQUILIBRIUM ANGLE WITH RESPECT TO RGR
0113          DASB=-CPF
0114          DASJ=-3.000*CPF*XYZ*COS(ASF)/SIN(ASB)
0115          GO TO 805
0116          803 ASF=PI/2.000
0117          ASB=T3PI
0118          DASB=0.000
0119          DASJ=0.000
0120          GO TO 805
0121          804 ASF=TAU
0122          ASB=TAU
0123          DASB=0.000
0124          DASJ=0.000
C*****
C COMPUTE CONTRIBUTION TO THE TOTAL ENERGY FROM THE ANGLE TERMS
0125          805 GO TO (806,807,808,809),KLM
0126          806 SUM=0.000
0127          IF1=1
0128          IF2=2
0129          IF3=3
0130          IF4=4
0131          IF5=5
0132          IF6=6
0133          DO 810 I=1,3
0134          C=AG(I)-ASF
0135          Y1(I)=0
0136          Y2(I)=C*0

```


FORTRAN IV G LEVEL 21

PDT6

DATE = 76044

14/04/41

```

0137      810  SUM=SUM+DK(I)*Y2(I)
0138          DO 330 I=4,6
0139          Y1(I)=AG(I)-ASB
0140          Y2(I)=Y1(I)*Y1(I)
0141      830  SUM=SUM+DK(I)*Y2(I)
0142          EE=EE+0.5D0*SUM
C#####
0143          IF(KEE.EQ.-1)RETURN
C#####
0144          GO TO 820
0145      807  SUM=0.0D0
0146          IF1=1
0147          IF2=4
0148          IF3=5
0149          IB1=2
0150          IB2=3
0151          IB3=6
0152          O=AG(1)-ASF
0153          Y1(1)=O
0154          Y2(1)=O*O
0155          SUM=SUM+DK(1)*Y2(1)
0156          DO 811 I=4,5
0157          O=AG(I)-ASF
0158          Y1(I)=O
0159          Y2(I)=O*O
0160      811  SUM=SUM+DK(I)*Y2(I)
0161          DO 831 I=2,3
0162          Y1(I)=AG(I)-ASB
0163          Y2(I)=Y1(I)*Y1(I)
0164      831  SUM=SUM+DK(I)*Y2(I)
0165          Y1(6)=AG(6)-ASB
0166          Y2(6)=Y1(6)*Y1(6)
0167          SUM=SUM+DK(6)*Y2(6)
0168          EE=EE+0.5D0*SUM
C#####
0169          IF(KEE.EQ.-1)RETURN
C#####
0170          GO TO 820
0171      808  SUM=0.0D0
0172          IF1=2
0173          IF2=4
0174          IF3=6
0175          IB1=1
0176          IB2=3
0177          IB3=4
0178          DO 812 I=2,6,2
0179          Y1(I)=AG(I)-ASF
0180          Y2(I)=Y1(I)*Y1(I)
0181      812  SUM=SUM+DK(I)*Y2(I)
0182          DO 832 I=1,5,2
0183          Y1(I)=AG(I)-ASB
0184          Y2(I)=Y1(I)*Y1(I)
0185      832  SUM=SUM+DK(I)*Y2(I)
0186          EE=EE+0.5D0*SUM
C#####
0187          IF(KEE.EQ.-1)RETURN
C#####
0188          GO TO 820

```

FORTRAN IV G LEVEL 21

POT6

DATE = 76044

14/04/41

```

0189      809 SUM=0.000
0190      IF1=3
0191      IF2=5
0192      IF3=6
0193      IB1=1
0194      IB2=2
0195      IB3=4
0196      Y1(3)=AG(3)-ASF
0197      Y2(3)=Y1(3)*Y1(3)
0198      SUM=DK(3)*Y2(3)
0199      DO 813 I=5,6
0200      Y1(I)=AG(I)-ASF
0201      Y2(I)=Y1(I)*Y1(I)
0202      813 SUM=SUM+DK(I)*Y2(I)
0203      DO 833 I=1,2
0204      Y1(I)=AG(I)-ASB
0205      Y2(I)=Y1(I)*Y1(I)
0206      833 SUM=SUM+DK(I)*Y2(I)
0207      Y1(4)=AG(4)-ASB
0208      Y2(4)=Y1(4)*Y1(4)
0209      SUM=SUM+DK(4)*Y2(4)
0210      EF=EE+0.5DO*SUM
C *****
0211      IF(KEE.EQ.-1)RETURN
C *****
C *****
C COMPUTE DERIVATIVES OF THE ANGLE ATTENUATION TERMS WITH RESPECT TO R6,R7,K8,
C AND R9
0212      820 DFR(1)=2.000*APARM(2)*R(6)*EXA11*EXF1+A11*EXF1*XA2*2.000*APARM(4)*
1 APARM(5)*XXA*EXA21
0213      DFR(2)=2.000*APARM(2)*R(7)*EXA12*EXF2+A12*EXF2*XB2*2.000*APARM(4)*
1 APARM(5)*XXB*EXA22
0214      DFR(3)=2.000*APARM(2)*R(8)*EXA13*EXF3+A13*EXF3*XC2*2.000*APARM(4)*
1 APARM(5)*XXC*EXA23
0215      DFR(4)=2.000*APARM(2)*R(9)*EXA14*EXF4+A14*EXF4*XD2*2.000*APARM(4)*
1 APARM(5)*XXD*EXA24
C COMPUTE DERIVATIVES OF ATTENUATION TERMS WITH RESPECT TO R1,R2,R3, AND R4
0216      DF(1)=-2.000*A21*XA*F(1)
0217      DF(2)=-2.000*A22*XB*F(2)
0218      DF(3)=-2.000*A23*XC*F(3)
0219      DF(4)=-2.000*A24*XD*F(4)
C *****
C ADD IN CONTRIBUTION TO DER FROM DK/DR ANGLE TERMS AND D(THE TA)/DR TERMS
C FIRST THREE ANGLE TERMS
0220      DO 900 I=1,3
0221      STP=0.500*DK(I)*Y2(I)
0222      W=DK(I)*Y1(I)
0223      DER(I)=DER(I)+STP*DF(I)/F(I)+W*(-1.000/(R(I+1)*ASS(I))+ACS(I)/
1 (R(I)*ASS(I)))
0224      DER(I+1)=DER(I+1)+STP*DF(I+1)/F(I+1)+W*(-1.000/(R(I)*ASS(I))+
1 ACS(I)/(ASS(I)*R(I+1)))
0225      DER(6)=DER(6)+STP*DFR(I)/F(I)
0226      DER(I+6)=DER(I+6)+STP*DFR(I+1)/F(I+1)
0227      900 DER(I+9)=DER(I+9)+W*R(I+9)/(R(I)*R(I+1)*ASS(I))
C *****
C FOURTH AND FIFTH ANGLE TERMS
0228      DO 901 I=4,5
0229      STP=0.500*DK(I)*Y2(I)

```

FCRTRAN IV G LEVEL 21

PRTF

DATE = 76044

14/04/41

```

0230      W=DK(I)*Y1(I)
0231      DER(2)=DF(2)+STP*DF(1)/F(2)+W*(-1.000/(ASS(I)*R(I-1))+
1 ACS(I)/(ASS(I)*R(2)))
0232      DER(7)=DF(7)+STP*DF(2)/F(2)
0233      DER(I-1)=DER(I-1)+STP*DF(I-1)/F(I-1)+W*(-1.000/(ASS(I)*R(2))+
1 ACS(I)/(ASS(I)*R(I-1)))
0234      DER(I+4)=DER(I+4)+STP*DF(I-1)/F(I-1)
0235      901 DER(I+9)=DER(I+9)+W*R(I+9)/(R(2)*R(I-1)*ASS(I))
C CONTRIBUTION FROM SIXTH ANGLE TERM
0236      STP=0.510*DK(6)*Y2(6)
0237      W=DK(6)*Y1(6)
0238      DER(3)=DER(3)+STP*DF(3)/F(3)+W*(-1.000/(ASS(6)*R(4))+
1 ACS(6)/(ASS(6)*R(3)))
0239      DER(8)=DER(8)+STP*DF(3)/F(3)
0240      DER(4)=DER(4)+STP*DF(4)/F(4)+W*(-1.000/(ASS(6)*R(2))+
1 ACS(6)/(ASS(6)*R(4)))
0241      DER(9)=DER(9)+STP*DF(4)/F(4)
0242      DER(15)=DER(15)+W*R(15)/(ASS(6)*R(3)*R(4))
C *****
C CONTRIBUTION FROM EQ. ANGLE VARIATION TO D(ANGLE)/DR *****
0243      DER(KLM)=DER(KLM)-(DK(IF1)*Y1(IF1)+DK(IF2)*Y1(IF2)+DK(IF3)*Y1(IF3)
1 )*DASE -(DK(IB1)*Y1(IB1)+DK(IB2)*Y1(IB2)+
2 DK(IB3)*Y1(IB3))*DASE
0244      DER(5)=DER(5)-(DK(IF1)*Y1(IF1)+DK(IF2)*Y1(IF2)+DK(IF3)*Y1(IF3))*
1 DAA -(DK(IB1)*Y1(IB1)+DK(IB2)*Y1(IB2)+DK(IB3)*Y1(IB3))
2 *2.000*SIN(ASF)*C13(ASF)*DAA/SIN(ASB)
C *****
C CALL SWITCH (KMAX,2)
0245      RETURN
0246      END

```

FORTRAN IV G LEVEL 21

TRI

DATE = 76044

14/04/41

```

0001      SUBROUTINE TRI(RR1,RR2,RR3,DR1,DR2,DR3,I,J,K,F)
C*****
C      SEE REFERENCE: L. M. RAFF, J. CHEM. PHYS., VOL. 60, 2220(1974)
C      ROUTINE TO CALCULATE THREE-BODY ENRGY FOR ABC SYSTEM
C      RR1,RR2,RR3 ARE THE THREE INTERPARTICLE DISTANCES
C      DR1,DR2,DR3 ARE THE THREE DERIVATIVES WITH RESPECT TO RR1,RR2, AND RR3
C      I,J, AND K GIVE THE ARRAY NUMBER FOR THE APPROPRIATE POTENTIAL PARAMETERS
C      F IS THE FINAL THREE-BODY ENERGY
C*****
0002      IMPLICIT REAL*8 (A-H,O-Z)
0003      DIMENSION APARM(5)
0004      DIMENSION X(6),Y(6),Z(6),R(15),DER(15),AG(6),P2(15),D1(3),D2(3),
1 ALPH(3),RE(3),BETA(3),CC(3),AA(3),SIG(3),RSTR(3),ACS(6),DK(6),
2 Y1(6),Y2(6),ASS(6),F(4),GF(4),RX(6),PX(6),PY(6),PZ(6),DX(6),
3 DY(6),DZ(6),DPX(6),DPY(6),DPZ(6),DF(15,3)
0005      COMMON X,Y,Z,R,DER,AG,P2,D1,ALPH,RE,D2,BETA,CC,AA,SIG,RSTR,TAU,
1 PV,DIJ,CP,EE,ACS,ASS,PX,XII, V1,V2,V3,V4,BMAX,
2 RSS,VP,PEK,H,PX,PY,PZ,WH,WC,WBR,W,DT,DX,DY,DZ,DPX,DPY,DPZ,T,DF,
3 TEMP,RFT,START,APARM,PI,T3PI,ELSP1,S6PI,
4 I11,JJJ,KKK,LLL,NV1,NV2,NV3,NV4,JJ,NI,KCF
0006      SQRT(X)=DSQRT(X)
0007      EXP(X)=DEXP(X)
0008      A=RR1-RE(I)
0009      B=RR2-RE(J)
0010      C=RR3-RE(K)
0011      A1= EXP(-ALPH(I)*A)
0012      B1= EXP(-ALPH(J)*B)
0013      C1= EXP(-ALPH(K)*C)
0014      A2=A1*A1
0015      B2=B1*B1
0016      C2=C1*C1
0017      E1AB=D1(I)*(A2-2.000*A1)
0018      F1AC=D1(J)*(B2-2.000*B1)
0019      E1BC=D1(K)*(C2-2.000*C1)
0020      DF1AB=2.000*ALPH(I)*D1(I)*(A1-A2)
0021      DF1AC=2.000*ALPH(J)*D1(J)*(B1-B2)
0022      DF1BC=2.000*ALPH(K)*D1(K)*(C1-C2)
0023      IF (RR1-RSTR(I))1,2,2
0024      1 AA1= EXP(-BETA(I)*A)
0025      AA2=AA1*AA1
0026      E3AB=D3(I)*(AA2+2.000*AA1)
0027      DE3AB=-2.000*BETA(I)*D3(I)*(AA1+AA2)
0028      GO TO 3
0029      2 AA1= EXP(-SIG(I)*RR1)
0030      F3AB=CC(I)*(CP1+AA(I))*AA1
0031      DF3AB=CC(I)*AA1*(1.000-SIG(I)*RR1-SIG(I)*AA(I))
0032      3 IF (RR2-RSTR(J))4,5,5
0033      4 BB1= EXP(-BETA(J)*B)
0034      BB2=BB1*BB1
0035      E3AC=D2(J)*(BB2+2.000*BB1)
0036      DE3AC=-2.000*BETA(J)*D2(J)*(BB1+BB2)
0037      GO TO 6
0038      5 BB1= EXP(-SIG(J)*RR2)
0039      F3AC=CC(J)*(RR2+AA(J))*BB1
0040      DE3AC=CC(J)*BB1*(1.000-SIG(J)*RR2-SIG(J)*AA(J))
0041      6 IF (RR3-RSTR(K)) 7,8,8
0042      7 CC1= EXP(-BETA(K)*C)
0043      CC2=CC1*CC1

```

FORTRAN IV C L VFL 21

TRI

DATE = 76044.

14/04/61

```

0044      E3BC=D3(K)*(CC2+2.000*CC1)
0045      DF3BC=-2.000*BFTA(K)*D3(K)*(CC1+CC2)
0046      GU TD 9
0047      8      CC1=EXP(-SIG(K)*RR3)
0048      E3BC=CC(K)*(RR3+AA(K))*CC1
0049      DE3BC=CC(K)*CC1*(1.000-SIG(K)*RR3-SIG(K)*AA(K))
0050      9      QAB=(E1AB+E3AB)/2.000
0051      QAC=(E1AC+E3AC)/2.000
0052      QBC=(E1BC+E3BC)/2.000
0053      ALAB=(E1AB-E3AB)/2.000
0054      ALAC=(E1AC-E3AC)/2.000
0055      ALBC=(E1BC-E3BC)/2.000
0056      XX=ALAB-ALBC
0057      YY=ALBC-ALAC
0058      ZZ=ALAC-ALAB
0059      U=(XX*XX+YY*YY+ZZ*ZZ)/2.000
0060      U=SQRT(U)
0061      E=QAB+QBC+QAC-U
0062      BR=4.000*U
0063      DR1=(DE1AB+DE3AB)/2.000-(2.000*ALAB-ALBC-ALAC)*(DE1AB-DE3AB)/BR
0064      DR2=(DE1AC+DE3AC)/2.000-(2.000*ALAC-ALAB-ALBC)*(DE1AC-DE3AC)/BR
0065      DR3=(DE1BC+DE3BC)/2.000-(2.000*ALBC-ALAC-ALAB)*(DE1BC-DE3BC)/BR
0066      RETURN
0067      END

```

FORTRAN IV G LEVEL 2*

PLACE

DATE = 76044

14/04/41

```

0001      SUBROUTINE PLACE(R1)
C*****
C      SEE REFERENCE: L. M. PAFF, J. CHEM. PHYS., VOL. 60, 2220(1974)
C      ROUTINE TO PLACE H2, H3, AND H4 IN EQUILIBRIUM POSITIONS FOR A GIVEN
C      H1 DISTANCE EQUAL TO R1
C*****
0002      IMPLICIT REAL*8 (A-H,O-Z)
0003      DIMENSION APARM(5)
0004      DIMENSION X(6),Y(6),Z(6),R(15),DEF(15),AG(6),R2(15),D1(3),D2(3),
1 ALPH(3),RE(3),BETA(3),CC(3),AA(3),SIG(3),RSTR(3),ACS(6),DK(6),
2 Y1(6),Y2(6),ASS(6),F(4),GF(4),RX(6),PX(6),PY(6),PZ(6),DX(6),
3 DY(6),DZ(6),DPX(6),DPY(6),DPZ(6),DF(15,3)
0005      COMMON X,Y,Z,R,DEF,AG,R2,C1,ALPH,RE,D3,BETA,CC,AA,SIG,RSTR,TAU,
1 RV,DIJ,CP,EE,ACS,ASS,RX,XII, V1,V2,V3,V4,BMAX,
2 RSS,VP,PEP,H,PX,PY,PZ,WH,WC,WBR,W,DT,DX,DY,DZ,DPX,DPY,DPZ,T,DF,
3 TEMP,PPT,START,APARM,PI,T3PI,EL6PI,S6PI,
4 III,JJJ,KKK,LLL,NV1,NV2,NV3,NV4,JJ,NI,KFE
0006      SIN(X)=DSIN(X)
0007      ARCOS(X)=DARCOS(X)
0008      COS(X)=DCOS(X)
0009      SQR(X)=DSQRT(X)
C//////
C      SFT ANGLE OUT OF THE XY PLANE DESCRIBED BY THE C-H BONDS IN THE CH3 GROUP.
C      BASED ON THE R1 DISTANCE FED TO THIS ROUTINE.
0010      IF(R1.LT.DIJ)GO TO 9
0011      R TS=PI/2.000
0012      GO TO 10
0013      9 IF(R1.LT.PF(1))GO TO 11
0014      TS=TAU-CP*(R1-RE(1))
0015      10 CONTINUE
0016      GO TO 12
0017      11 TS=TAU
0018      12 CONTINUE
C//////
C      CALCULATE ALL CARTESIAN COORDINATE ATOM POSITIONS EXCEPT Z(1) AND Z(6)
C      WHICH ARE SFT IN THE MAIN PROGRAM.
0019      S=SIN(TS)
0020      C=COS(TS)
0021      X(1)=0.000
0022      Y(1)=0.000
0023      X(2)=0.000
0024      Y(2)=RE(1)*S
0025      Z(2)=RE(1)*C
0026      X(3)=RE(1)*S*COS(EL6PI)
0027      Y(3)=RE(1)*S*SIN(EL6PI)
0028      Z(3)=RE(1)*C
0029      X(4)=RE(1)*S*COS(S6PI)
0030      Y(4)=RE(1)*S*SIN(S6PI)
0031      Z(4)=RE(1)*C
0032      X(5)=0.000
0033      Y(5)=0.000
0034      Z(5)=0.000
0035      X(6)=0.000
0036      Y(6)=0.000
0037      RETURN
0038      END

```

FORTRAN IV G LEVEL 21 DIST DATE = 76044 14/04/74

```

0001      SUBROUTINE DIST
C *****
C      SEE REFERENCE: L. M. PAFF, J. CHEM. PHYS., VOL. 60, 2220(1974)
C      ROUTINE TO COMPUTE THE INTERPARTICLE DISTANCES FROM THE CARTESIAN
C      COORDINATES OF THE ATOMS
C *****
0002      IMPLICIT REAL*8 (A-H,O-Z)
0003      DIMENSION APARM(5)
0004      DIMENSION X(6),Y(6),Z(6),R(15),DER(15),AG(6),R2(15),D1(3),D2(3),
1      ALPH(3),RE(3),BETA(3),CC(3),AA(3),SIG(3),RSTR(3),ACS(6),DK(6),
2      Y1(6),Y2(6),ASS(6),F(4),GF(4),RX(6),PX(6),PY(6),PZ(6),DX(6),
3      DY(6),DZ(6),DPX(6),DPY(6),DPZ(6),DF(15,3)
0005      COMMON X,Y,Z,R,DER,AG,R2,D1,ALPH,RE,D3,BETA,CC,AA,SIG,FSTR,TAU,
1      RV,DIJ,CP,EE,ACS,ASS,RX,XII, V1,V2,V3,V4,BMAX,
2      RSS,VP,PF,H,PX,PY,PZ,WH,WC,WBR,W,DT,DX,DY,DZ,DPX,DPY,DPZ,T,DF,
3      TEMP,R,T,START,APARM,PI,T3PI,EL6PI,S6PI,
4      IIT,JJJ,KKK,LLL,NV1,NV2,NV3,NV4,JJ,NI,KEE
0006      SQRT(X)=DSQRT(X)
0007      DO 1 I=1,4
0008      DF(I,1)=X(I)-X(5)
0009      DF(I,2)=Y(I)-Y(5)
0010      DF(I,3)=Z(I)-Z(5)
0011      R2(I)=DF(I,1)*DF(I,1)+DF(I,2)*DF(I,2)+DF(I,3)*DF(I,3)
0012      1 R(I)= SQRT(R2(I))
0013      DF(5,1)=X(5)-X(6)
0014      DF(5,2)=Y(5)-Y(6)
0015      DF(5,3)=Z(5)-Z(6)
0016      R2(5)=DF(5,1)*DF(5,1)+DF(5,2)*DF(5,2)+DF(5,3)*DF(5,3)
0017      R(5)= SQRT(R2(5))
0018      DO 2 I=1,4
0019      J=I+5
0020      DF(J,1)=X(I)-X(6)
0021      DF(J,2)=Y(I)-Y(6)
0022      DF(J,3)=Z(I)-Z(6)
0023      R2(J)=DF(J,1)*DF(J,1)+DF(J,2)*DF(J,2)+DF(J,3)*DF(J,3)
0024      2 R(J)= SQRT(R2(J))
0025      DO 3 I=1,3
0026      J=I+1
0027      K=I+9
0028      DF(K,1)=X(I)-X(J)
0029      DF(K,2)=Y(I)-Y(J)
0030      DF(K,3)=Z(I)-Z(J)
0031      R2(K)=DF(K,1)*DF(K,1)+DF(K,2)*DF(K,2)+DF(K,3)*DF(K,3)
0032      3 R(K)= SQRT(R2(K))
0033      DO 4 I=1,2
0034      J=I+2
0035      K=I+12
0036      DF(K,1)=X(I)-X(J)
0037      DF(K,2)=Y(I)-Y(J)
0038      DF(K,3)=Z(I)-Z(J)
0039      R2(K)=DF(K,1)*DF(K,1)+DF(K,2)*DF(K,2)+DF(K,3)*DF(K,3)
0040      4 R(K)= SQRT(R2(K))
0041      DF(15,1)=X(3)-X(4)
0042      DF(15,2)=Y(3)-Y(4)
0043      DF(15,3)=Z(3)-Z(4)
0044      R2(15)=DF(15,1)*DF(15,1)+DF(15,2)*DF(15,2)+DF(15,3)*DF(15,3)
0045      R(15)= SQRT(R2(15))
0046      RETURN
0047      END

```

FORTRAN IV G LEVEL 21

ANGLE

DATE = 76044

14/04/71

```

0001      SUBROUTINE ANGLE
C *****
C      SEE REFERENCE: L. M. RAFF, J. CHEM. PHYS., VOL. 67, 2220(1974)
C ROUTINE TO COMPUTE CH4 ANGLES FROM THE INTERPARTICLE DISTANCES
C *****
0002      IMPLICIT REAL*8 (A-H,O-Z)
0003      DIMENSION APARAM(5)
0004      DIMENSION X(6), Y(6), Z(6), R(15), DER(15), AG(6), R2(15), D1(3), D2(3),
1 ALPH(3), PE(3), BETA(2), CC(3), AA(3), SIG(3), PSTR(3), ACS(6), DK(6),
2 Y1(6), Y2(6), ASS(6), F(4), GF(4), RX(6), PX(6), PY(6), PZ(6), DX(6),
3 DY(6), DZ(6), DPX(6), DPY(6), DPZ(6), DF(15,3)
0005      COMMON X, Y, Z, R, DER, AG, R2, D1, ALPH, PE, D3, BETA, CC, AA, SIG, PSTR, TAU,
1 RV, DI, CP, EE, ACS, ASS, RX, XII, V1, V2, V3, V4, BMAX,
2 RSS, VB, PER, H, PX, PY, PZ, WH, WC, WBR, W, DT, DX, DY, DZ, DPX, DPY, DPZ, T, CF,
3 TEMP, KRT, START, APARAM, PI, T3PI, EL6PI, S6PI,
4 III, JJJ, KKK, LLL, NV1, NV2, NV3, NV4, JJ, NI, KEE
0006      SQRT(X)=DSQRT(X)
0007      ARCCOS(X)=DARCCOS(X)
0008      DO 2 I=1,3
0009      X=(R2(I)+R2(I+1)-R2(I+9))/(2.000*R(1)*R(I+1))
0010      ACS(I)=X
0011      ASS(I)=SQRT(1.000-X*X)
0012      2 AG(I)= ARCCOS(X)
0013      DO 3 I=1,2
0014      X=(R2(2)+R2(I+2)-R2(I+12))/(2.000*R(2)*R(I+2))
0015      ACS(I+3)=X
0016      ASS(I+3)=SQRT(1.000-X*X)
0017      3 AG(I+3)= ARCCOS(X)
0018      X=(R2(3)+R2(4)-R2(15))/(2.000*R(3)*R(4))
0019      ACS(6)=X
0020      ASS(6)=SQRT(1.000-X*X)
0021      AG(6)= ARCCOS(X)
0022      RETURN
0023      END

```



```

FORTRAN IV G LEVEL 21          READ          DATE = 76044          14/04/41

0001          SUBROUTINE READ
C          REFERENCE: L. M. RAFF, J. CHEM. PHYS., VOL. 60, 2220(1974)
C ROUTINE TO READ IN INITIAL POTENTIAL SURFACE PARAMETERS
C ROUTINE ALSO READS IN INITIAL DYNAMIC VARIABLES
0002          IMPLICIT REAL*8 (A-H,C-Z)
0003          DIMENSION X(6),Y(6),Z(6),R(15),DEP(15),AG(6),R2(15),D1(3),D3(3),
1          ALPH(3),RE(3),BETA(3),CC(3),AA(3),SIG(3),RSTR(3),ACS(6),DK(6),
2          Y1(6),Y2(6),ASS(6),F(4),GF(4),RX(6),PX(6),PY(6),PZ(6),DX(6),
3          DY(6),DZ(6),DPX(6),DPY(6),DPZ(6),DF(15,3)
0004          DIMENSION APARM(5)
0005          COMMON X,Y,Z,R,DER,AG,R2,D1,ALPH,RE,D3,BETA,CC,AA,SIG,RSTR,TAU,
1          RV,DIJ,CP,EE,ACS,ASS,RX,XII,          V1,V2,V3,V4,BMAX,
2          RSS,VR,PPR,H,PX,PY,PZ,WH,WC,WBR,W,DT,DX,DY,DZ,DPX,DPY,DPZ,T,DF,
3          TEMP,RT,START,APARM,P1,T3PI,EL6PI,S6PI,
4          I11,J11,K11,LLL,NV1,NV2,NV3,NV4,J11,NI,KFE
0006          READ(5,100) D1,D3,ALPH,RE,BETA,CC,AA,SIG,RSTR
0007          100 FORMAT(3D15.8)
0008          READ(5,101) TAU,RV
0009          READ(5,101) DIJ,CP
0010          101 FORMAT(2D15.8)
0011          102 FORMAT('H1')
0012          WRITE(6,102)
0013          WRITE(6,103)
0014          103 FORMAT(3X,'SURFACE PARAMETERS',///)
0015          WRITE(6,104)
0016          104 FORMAT(19X,'C-H',23X,'H-X',23X,'C-X',/,33X,'SINGLET-STATE PARAMETERS',///)
1RS',//)
0017          WRITE(6,105) D1,ALPH,RE
0018          105 FORMAT(5X,2HD1,3X,3(1PD20.8),/,3X,4HALPH,3X,3(1PD20.8),/,
1          5X,2HRE,3X,3(1PD20.8),//)
0019          WRITE(6,106)
0020          106 FORMAT(33X,'TRIPLET-STATE PARAMETERS',///)
0021          WRITE(6,107) D3,BETA,CC,AA,SIG,RSTR
0022          107 FORMAT(5X,2HD3,3X,3(1PD20.8),/,3X,4HBETA,3X,3(1PD20.8),/,
1          6X,4HC,3X,3(1PD20.8),/,6X,4HA,3X,3(1PD20.8),/,
2          4X,4HSIG,3X,3(1PD20.8),/,3X,4HRSTR,3X,3(1PD20.8),///)
0023          WRITE(6,108) TAU,RV
0024          108 FORMAT(25X,28HEQUILIBRIUM ANGLE PARAMETERS,/,15X,4HTAU=,1PD20.12,
1          5X,3HEV=,1PD20.12,///)
0025          WRITE(6,109) DIJ,CP
0026          109 FORMAT(25X,28HEQUILIBRIUM ANGLE PARAMETERS,/,15X,
1          8HUPPER LIMIT PARAMETER-FRONTSIDE ANGLE=,1PD20.12,/,15X,
2          6HSLCPF PARAMETER-FRONTSIDE ANGLE=,1PD20.12,/)
C READ IN INITIAL RANDOM NUMBER--7 DECIMAL DIGITS.0
0027          READ(5,101) RX(1)
C READ CH4 FUNDAMENTAL FREQUENCIES
0028          READ(5,110) V1,V2,V3,V4
0029          110 FORMAT(4D15.8)
C READ IN MASSES
0030          READ(5,110) WH,WC,WBR
C READ IN BMAX AND RSS
0031          READ(5,101) BMAX,RSS
C READ IN INITIAL VIBRATIONAL QUANTUM NUMBERS
0032          READ(5,111) NV1,NV2,NV3,NV4
0033          111 FORMAT(4I12)
C READ INTEGRATION STEP SIZE
0034          READ(5,101) DT
C READ INITIAL RELATIVE VELOCITY

```

```

FORTRAN IV G LEVEL 2)          READ          DATE = 76044          14/04/41

0035          READ(5,101) VR
C READ TEMPERATURE FOR ROTATIONAL AVERAGING
0036          READ(5,101) TEMP
0037          WRITE(6,112) PX(1)
0038          112 FORMAT(15X,22HINITIAL RANDOM NUMBER=,1PD20.12,/)
0039          WRITE(6,113) V1,V2,V3,V4
0040          113 FORMAT(15X,'METHANE FUNDAMENTAL FREQUENCIES (IN EV.):',/,20X,3HV1=,
1 ,D20.10,5X,3HV2=,D20.10,5X,3HV3=,D20.10,5X,3HV4=,D20.10,/)
0041          WRITE(6,114) WH,WC,WBP
0042          114 FORMAT(15X,6HMASSFS,5X,2HH=,1PD20.10,5X,2HC=,2PD20.10,5X,2HX=,1PD2
10.10,/)
0043          WRITE(6,115) BMAX,RSS
0044          115 FORMAT(15X,25HMAXIMUM IMPACT PARAMETER=,1PD20.8,5X,4HRS=,1PD20.8,/)
1 /)
0045          WRITE(6,116) NV1,NV2,NV3,NV4
0046          116 FORMAT(15X,32HINITIAL VIBRATION STATES OF CH4:,5X,4HNV1=,I3,5X,
1 4HNV2=,I3,5X,4HNV3=,I3,5X,4HNV4=,I3,/)
0047          WRITE(6,117) VR,DT,TEMP
0048          117 FORMAT(15X,18HRELATIVE VELOCITY=,1PD20.8,5X,'INTEGRATION STEP SIZE=
1 =',1PD20.9,/,15X,'ROTATIONAL TEMPERATURE=,1PD20.8,/)
C READ CONTROL PARAMETERS
0049          READ(5,111) III,JJJ,KKK,LLL
0050          READ(5,101) RPT,START
C READ IN ANGULAR PARAMETERS
0051          READ(5,120) APARM
0052          120 FORMAT(5D15.8)
0053          WRITE(6,121)(I,APARM(I),I=1,5)
0054          121 FORMAT(15X,'ANGULAR ATTENUATION PARAMETERS:',/,10X,
1 3(5X,'APARM(',I2,')=',1PD18.10),/,/,10X,2(5X,'APARM(',I2,')=',1PD18
*,10),/)
0055          WRITE(6,122) RRT,START
0056          122 FORMAT(15X,'DISTANCE PARAMETERS',/,20X,'FINAL TEST DISTANCE=',
1 1PD20.10,5X,'TWO-BODY DISTANCE=',1PD20.10,/)
0057          WRITE(6,102)
0058          RETURN
0059          END

```

FORTRAN IV G LEVEL 21

TETRAH

DATE = 76044

14/04/71

```

0001      SUBROUTINE TETRAH(TAU,PI)
C        A DOUBLE PRECISION VALUE FOR PI MUST BE SUPPLIED
C        THIS ROUTINE CALCULATES THE TETRAHEDRAL ANGLE TO DOUBLE PRECISION ACCURACY.
C#####
C        X=HEIGHT OF EQUILATERAL TRIANGLE FACE OF REGULAR TETRAHEDRON (EDGE=1).
C        THETA=INTERNAL ANGLE BETWEEN FACES.
C        PHI=INTERNAL ANGLE BETWEEN FACE AND AN EDGE OF TETRAHEDRON.
C        H=HEIGHT OF PYRAMID (REGULAR TETRAHEDRON).
C        Y=LENGTH BETWEEN ANY CORNER AND CENTER OF ANY FACE.
C        GAMMA=ANGLR BETWEEN LINE H AND CORRESPONDING EDGE.
C        TAU=TETRAHEDRAL ANGLE.
C#####
0002      IMPLICIT REAL*8(A-H, O-Z)
0003      X=DSIN(PI/3.000)
0004      C=(2.000*(X*X)-1.000)/(2.000*(X*X))
0005      THETA = DARCOS(C)
0006      PHI=(PI-THETA)/2.000
0007      Y=0.500/X
0008      D=(Y*Y)+1.000-(2.000*Y*DCOS(PHI))
0009      H=DSQRT(D)
0010      F=((H*H)+1.000-(Y*Y))/(2.000*H)
0011      GAMMA=DARCOS(F)
0012      TAU=PI-(2.000*GAMMA)
0013      TAUD=(TAU/PI)*130.000
0014      WRITE(6,1)TAU,TAUD
0015      1 FORMAT(/,1X,'TETRAHEDRAL ANGLE =',1PD24.16,' RADIANS OR ',
13PD24.14,' DEGREES',/)
0016      RETURN
0017      END

```



```

FCRTRAN IV 0 LEVEL 21          MAIN          DATE = 76148          11/58/59

C READ IN CONFIGURATION GEOMETRY
C *****
0027 IF(IRC)4,3,3
C *****
C READ IN INITIAL INTERATOMIC DISTANCES
C USING "4D20.13" FORMAT.
C *****
0028 5 READ(5,771)(R(I),I=1,15)
0029 771 FORMAT(4D20.13)
0030 UR1=R(1)
0031 WRITE(6,772)(I,R(I),I=1,15)
0032 772 FORMAT(/,5X,'INITIAL INTERATOMIC DISTANCES',/,15(7X,'R',I2,'=',1P
      *D20.10,/))
0033 GO TO 5
C *****
C READ IN CARTESIAN COORD. OF THE ATOMS IN ORDER OF THEIR ATOM NUMBER
C ONE ATOM PER CARD USING "3D20.13" FORMAT.
C *****
0034 4 READ(5,773)(X(I),Y(I),Z(I),I=1,6)
0035 773 FORMAT(3D20.13)
0036 WRITE(6,774)(I,X(I),Y(I),Z(I),I=1,6)
0037 774 FORMAT(/,1X,'ATOM',9X,'X',19X,'Y',19X,'Z',/,6(14,2X,3D20.12,/))
C CALCULATE INTERATOMIC DISTANCES IF CARTESIAN COORDINATES WERE READ IN.
C CALL DIST
C UR1=R(1)
0038 UR1=R(1)
0039 WRITE(6,772)(I,R(I),I=1,15)
0040 5 CONTINUE
0041 WRITE(6,775)
0042 775 FORMAT('1')
0043 C ///////////////////////////////////////////////////
C CALCULATE DOUBLE PRECISION PI AND FRACTIONS OF PI.
0044 PI=2.000*0ARSIN(1.000)
0045 T3PI=(2.000*PI)/3.000
0046 EL6PI=(11.000*PI)/6.000
0047 S6PI=(17.000*PI)/6.000
C ///////////////////////////////////////////////////
C CALCULATE DOUBLE PRECISION TETRAHEDRAL ANGLE NECESSARY FOR GEOMETRY CALCULA
C TIONS.
0048 CALL TETRAH(TAU,PI)
0049 IF(IRC)7,6,6
C ///////////////////////////////////////////////////
C IF INTERATOMIC DISTANCES WERE READ IN, CALCULATE THE CH3 CARTESIAN COORDIN
C -ATE ATOM POSITIONS BASED ON H1 ATOM ABSTRACTION DISTANCE R(1).
0050 6 CALL PLACE(UR1)
0051 Z(1)=UR1
0052 Z(6)=R(5)
C ///////////////////////////////////////////////////
C CALCULATE INTERATOMIC DISTANCES FROM CARTESIAN COORDINATES.
0053 CALL DIST
0054 7 CONTINUE
0055 DO 8 I=1,15
0056 8 RK(I)=R(I)
C ///////////////////////////////////////////////////
C CALCULATE HCH ANGLES BASED ON INTERATOMIC DISTANCES.
0057 CALL ANGLE
0058 DO 9 I=1,6
0059 XK(I)=X(I)
0060 YK(I)=Y(I)

```

```

FORTRAN IV LEVEL 21          MAIN          DATE = 76148          11/58/59

0061          ZK(I)=Z(I)
0062          9 AGK(I)=AG(I)
0063          WRITE(6,775)PI
0064          776 FORMAT(//,1X,'PI=',1PD24.15)
0065          WRITE(6,776)(I,R(I),I=1,15)
0066          776 FORMAT(//,6X,'INTERATOMIC DISTANCES',//,15(7X,'R',12,'=',1PD20.12,/)
              1))
0067          WRITE(6,777)(I,AG(I),I=1,6)
0068          777 FORMAT(5X,'HCH ANGLES THETA',//,1X,6('T',11,'=',1PD17.10,1X)/)
C ///////////////////////////////////////////////////
C CALCULATE EQUILIBRIUM GEOMETRY ENERGY.
0069          CALL PUT6
C ///////////////////////////////////////////////////
C CALCULATE FORCE CONSTANT CONVERSION FACTORS
C FACTOR TO CONVERT EV / (BOHR RADIUS)**2 TO MDYNE/ANGSTROM
0070          FACT=0.16021000/(0.52916700*0.52916700)
C FACTOR TO CONVERT EV TERMS TO MDYNE-ANGSTROM (ANGLE TERMS)
0071          TFACT=0.16021000
C FACTOR TO CONVERT EV / (RADIAN*BOHR RADIUS) TO MDYNE/RADIAN
C (ANGLE-STRETCH CROSS TERMS)
0072          CFACT=0.16021000/0.52916700
0073          WRITE(6,774)(I,XK(I),YK(I),ZK(I),I=1,6)
0074          WRITE(6,775)
0075          I=1
0076          EEE=EEL*18.323200
C *****
C E = CALCULATED ENERGY MATRIX CAPABLE OF STORING 49 INCREMENTAL ENERGIES
C NEEDED FOR CALCULATING EACH INTERNAL COORDINATE FORCE CONSTANT IN THE
C 13X13 MATRIX
C D = FIRST DERIVATIVE MATRIX BY SEVEN POINT METHOD
C DD = SECOND DERIVATIVE MATRIX BY SEVEN POINT METHOD
C DD3 = SECOND DERIVATIVE MATRIX BY 3 POINT METHOD
C XK, YK, ZK, XKC, YKC, AND ZKC = CARTESIAN COORDINATE CONSTANTS FOR RESETTIN
C G ATUM POSITIONS TO THE ORIGINAL OR AN INTERMEDIATE CONFIGURATION
C RK, AGK, AND AGKC = INTERATOMIC DISTANCE AND HCH ANGLE CONSTANTS FOR RESETT
C ING INCREMENTED COORDINATES
C A, B, AND C = COEFFICIENTS OF THE SEVEN POINT DIFFERENTIATION METHOD
C EQUATION
C *****
0077          DO 10 I=1,15
0078          DO 10 IC=1,15
0079          DD(I,IC)=0.000
0080          DD3(I,IC)=0.000
0081          DO 10 IN=1,7
0082          D(I,IC,IN)=0.000
0083          DO 10 INC=1,7
0084          KE=IN+INC
0085          IF(KE.EQ.8)GO TO 12
0086          E(I,IC,IN,INC)=0.000
0087          GO TO 10
0088          12 E(I,IC,IN,INC)=EEE
0089          10 CONTINUE
C START INCREMENTING FOR ENERGY SETS
0090          A=0.7500
0091          B=-0.1500
0092          C=0.1500/9.000
0093          KEY=1
0094          KO=1

```

FCRTRAN IV G LEVEL 21

MAIN

DATE = 76148

11/56/59

```

C095          DAX=0.000
C096          DAY=0.000
C097          DG 21 I=1,15
C ///////////////////////////////////////////////////
C          NO INTERNAL COORDINATES CORRESPOND TO PUT6 COORDINATES 5, 7, 8, AND 9.
C098          IF(I.EQ.5.OR.I.EQ.9)GO TO 21
C ///////////////////////////////////////////////////
C          INTERNAL COORDINATE LINEAR BENDS ARE KEYED BY LABELS FOR PUT6 COORDINATES
C          7 & 8.
C099          IF(I.EQ.7.OR.I.EQ.8)KEY=I-6
C100          DO 20 IC=1,15
C101          IF(IC.EQ.5.OR.IC.EQ.9)GO TO 20
C102          IF(IC.EQ.7.OR.IC.EQ.8)KU=IC-6
C103          DO 19 IN=1,7
C104          IF(I.EQ.IC)GO TO 80
C105          BH=RINK*(IN-4)
C106          GO TO 81
C107          80 IF(IN.GT.1.AND.IN.LT.7)GO TO 19
C108          GO TO 641
C109          81 CONTINUE
C110          K(I)=RK(I)+BH
C111          IF(I.GE.10)AG(I-9)=AGK(I-9)+BH
C112          IF(I.EQ.7.OR.I.EQ.8)GO TO 60
C113          GO TO 64
C114          60 CONTINUE
C115          GO TO (61,62),KEY
C116          61 ALPHAX=PI+BH
C          DAX=PI-ALPHAX
C117          JAX=-1.000*BH
C118          WRITE(6,785)DAX,DAY
C119          GO TO 63
C120          62 ALPHAY=PI+BH
C          DAY=PI-ALPHAY
C121          JAY=-1.000*BH
C122          WRITE(6,785)DAX,DAY
C123          63 CALL ALBEND(DAX,DAY)
C124          WRITE(6,784)KEY
C125          785 FORMAT(1X,'DAX=',1PD20.12,10X,'DAY=',1PD20.12)
C126          784 FORMAT(1X,'KEY=',I3)
C127          64 CONTINUE
C ///////////////////////////////////////////////////
C          SET PUT6 COORDINATES 5,7,8, & 9 TO CORRESPOND TO THE INTERNAL COORDINATE INC
C          REMENT FOR THE I TH COORDINATE.
C128          IF(I.EQ.1)CALL Q1(DAX,DAY)
C129          IF(I.EQ.6)CALL J6(DAX,DAY)
C130          IF(I.GT.1.AND.I.LT.5)CALL QRESET(I,RK,XK,YK,ZK,AGK)
C131          IF(I.GT.9)CALL JANSET(I,RK,XK,YK,ZK,AGK)
C132          641 CONTINUE
C133          DO 16 KK=1,6
C134          XK(KK)=X(KK)
C135          YK(KK)=Y(KK)
C136          ZK(KK)=Z(KK)
C137          16 AGK(KK)=AG(KK)
C138          DO 161 KK=1,15
C139          161 RK(KK)=R(KK)
C140          DO 18 INC=1,7
C141          IF(I.EQ.IC)GO TO 85
C142          CH=RINK*(INC-4)

```

```

PCRTAN IV G LEVEL 21          MAIN          DATE = 76140          11/58/59

0143      GO TO 86
0144      85 IF((IN+INC).EQ.8)GO TO 18
0145      CH=RINK*(IN+INC-8)
0146      86 CONTINUE
0147      R(IC)=RK(IC)+CH
0148      IF(IC.GE.10)AG(IC-9)=AGK(IC-9)+CH
C        CROSS IC TERMS
0149      IF(IC.EQ.7.OR.IC.EQ.8)GO TO 65
0150      GO TO 69
0151      65 CONTINUE
0152      GO TO (66,67),KJ
0153      66 ALPHAX=P1+CH
C        DAX=P1-ALPHAX
0154      DAX=-1.000*CH
0155      WRITE(6,785)DAX,DAY
0156      GO TO 68
0157      67 ALPHAY=P1+CH
C        DAY=P1-ALPHAY
0158      DAY=-1.000*CH
0159      WRITE(6,785)DAX,DAY
0160      68 CALL ALBEND(DAX,DAY)
0161      WRITE(6,786)KU
0162      786 FORMAT(1X,'KU=',I3)
0163      69 CONTINUE
C ///////////////////////////////////////////////////////////////////
C      SET POT6 COORDINATES 5,7,8, & 9 TO CORRESPOND TO THE INTERNAL COORDINATE INC
C      REMENT FOR THE IC TH COORDINATE.
0164      IF(IC.EQ.1)CALL Q1(DAX,DAY)
0165      IF(IC.EQ.6)CALL Q6(DAX,DAY)
0166      IF(IC.GT.1.AND.IC.LT.5)CALL QRESET(IC,RKC,XKC,YKC,ZKC,AGKC)
0167      IF(IC.GT.9)CALL QANSET(IC,RKC,XKC,YKC,ZKC,AGKC)
0168      357 CONTINUE
C ///////////////////////////////////////////////////////////////////
C      CALCULATE AND STORE INCREMENTED INTERNAL COORDINATE POT6 ENERGY
0169      CALL PCT6
0170      E(1,IC,IN,INC)=EE+18.3232D0
0171      DO 17 KK=1,6
0172      X(KK)=XK(KK)
0173      Y(KK)=YK(KK)
0174      Z(KK)=ZK(KK)
0175      17 AG(KK)=AGKC(KK)
0176      CALL DIST
0177      18 CONTINUE
C ///////////////////////////////////////////////////////////////////
C      RESET ALL PARAMETERS TO ORIGINAL CONFIGURATION
0178      DO 131 KK=1,6
0179      X(KK)=XK(KK)
0180      Y(KK)=YK(KK)
0181      131 Z(KK)=ZK(KK)
0182      CALL DIST
0183      CALL ANGLE
0184      DAX=0.000
0185      DAY=0.000
0186      19 CONTINUE
0187      IF(1.NE.1C)GO TO 851
C      STORE DUPLICATE ENERGY VALUES FOR DIAGONAL MATRIX ELEMENT CALCULATION.
0188      DO 95 IN=1,7
0189      DO 95 INC=1,7

```


FORTRAN IV G LEVEL 21

QRESET

DATE = 76044

14/06/51

```

0091      RP3=R(3)*DCOS(AG(2)-(PI/2.000))
0092      CTP6=((RP3*RP3)+(RKP4*RKP4)-(RP15*RP15))/(2.000*RP3*RKP4)
0093      TP6=DARCCS(CTP6)
0094      DTP6=(T3PI-TP6)/2.000
0095      SG4=(PI/6.000)+DTP6
0096      X(4)=-RP4*DCOS(SG4)
0097      Y(4)=-RP4*DSIN(SG4)
0098      46 CONTINUE
0099      Z(4)=-R(4)*DSIN(P4)
0100      GO TO 80
C
ROUTINE FOR THETA4 INCREMENT RESET
0101      50 P2=AG(1)-(PI/2.000)
0102      P3=AG(2)-(PI/2.000)
0103      RP2=R(2)*DCOS(P2)
0104      RP3=R(3)*DCOS(P3)
0105      R13=(R(2)*R(2))+R(3)*R(3)-(2.000*R(2)*R(3)*DCOS(AG(4)))
0106      P(13)=DSQRT(R13)
0107      IF(Z(2).NE.Z(3))GO TO 51
0108      RP13=R(13)
0109      GO TO 52
0110      51 S13=DABS(Z(3)-Z(2))/R(13)
0111      RP13=R(13)*DCOS(DARSIN(S13))
0112      52 CONTINUE
0113      CTP4=((RP2*RP2)+(RP3*RP3)-(RP13*RP13))/(2.000*RP2*RP3)
0114      TP4=DARCCS(CTP4)
0115      DTP4=(T3PI-TP4)/2.000
0116      IF(X(2).EQ.2.000)GO TO 54
0117      53 S2=X(2)/RP2
0118      AX2=DARSIN(S2)
0119      TAX2=AX2+DTP4
0120      GO TO 55
0121      54 CONTINUE
0122      TAX2=DTP4
0123      55 CONTINUE
0124      X(2)=RP2*DSIN(TAX2)
0125      Y(2)=RP2*DCOS(TAX2)
0126      IF(XK(3).NE.X(3).OR.YK(3).NE.Y(3))GO TO 57
C
THETA6 OR R3 MUST BE CROSSED WITH THETA4 IF TRANSFER TO ST. 57 OCCURS.
C
THIS MEANS THAT TAX2=DTP4 ONLY IF NO TRANSFER OCCURS.
0127      56 TAX3=(PI/6.000)-DTP4
0128      X(3)=RP3*DCOS(TAX3)
0129      Y(3)=-RP3*DSIN(TAX3)
0130      GO TO 59
0131      57 IF(AGK(6).NE.AG(6))GO TO 58
0132      IF(RK(3).NE.R(3))GO TO 56
0133      IF(AGK(2).NE.AG(2))GO TO 56
0134      GO TO 99
0135      58 RP15=RK(15)
0136      RP4=R(4)*DCOS(AG(3)-(PI/2.000))
0137      CTP6=((RP3*RP3)+(RP4*RP4)-(RP15*RP15))/(2.000*RP3*RP4)
0138      TP6=DARCCS(CTP6)
0139      DTP6=(T3PI-TP6)/2.000
0140      SG3=(PI/6.000)+DTP6-DTP4
0141      X(3)=RP3*DCOS(SG3)
0142      Y(3)=-RP3*DSIN(SG3)
0143      59 CONTINUE
0144      Z(2)=-R(2)*DSIN(P2)
0145      Z(3)=-R(3)*DSIN(P3)

```


FORTRAN IV G LEVEL 21

ORSET

DATE = 75044

14/06/51

```

0146      GO TO 80
C      ROUTINE FOR THETA5 INCREMENT RESET (SHOULD RESEMBLE THETA4 RESET)
0147 60 P2=AG(1)-(PI/2.000)
0148    P4=AG(2)-(PI/2.000)
0149    RP2=R(2)*DCOS(P2)
0150    RP4=R(4)*DCOS(P4)
0151    R14=((R(2)*R(2))+R(4)*R(4))-(2.000*R(2)*R(4)*DCOS(AG(5)))
0152    R(14)=DSQRT(R14)
0153    IF(Z(2).NE.Z(4))GO TO 61
0154    RP14=R(14)
0155    GO TO 62
0156 61 S14=DABS(Z(4)-Z(2))/R(14)
0157    RP14=R(14)*DCOS(DARSIN(S14))
0158 62 CONTINUE
0159    CTP5=((RP2*RP2)+(RP4*RP4)-(RP14*RP14))/(2.000*RP2*RP4)
0160    TP5=DARCCOS(CTP5)
0161    DTP5=(T3PI-TP5)/2.000
0162    IF(X(2).EQ.0.000)GO TO 64
0163 63 S2=X(2)/RP2
0164    AX2=DARSIN(S2)
0165    TAX2=AX2-DTP5
0166    GO TO 65
0167 64 TAX2=-DTP5
0168 65 CONTINUE
0169    X(2)=RP2*DSIN(TAX2)
0170    Y(2)=RP2*DCOS(TAX2)
0171    IF(XK(4).NE.X(4).OR.YK(4).NE.Y(4))GO TO 67
0172 66 TAX4=(PI/6.000)-DTP5
0173    X(4)=-RP4*DCOS(TAX4)
0174    Y(4)=-RP4*DSIN(TAX4)
0175    GO TO 69
0176 67 IF(AGK(6).NE.AG(6))GO TO 68
0177    IF(RK(4).NE.R(4))GO TO 66
0178    IF(AGK(3).NE.AG(3))GO TO 66
0179    GO TO 99
0180 68 RP15=RK(15)
0181    RP3=R(3)*DCOS(AG(2)-(PI/2.000))
0182    CTP6=((RP3*RP3)+(RP4*RP4)-(RP15*RP15))/(2.000*RP3*RP4)
0183    TP6=DARCCOS(CTP6)
0184    DTP6=(T3PI-TP6)/2.000
0185    SG4=(PI/6.000)+DTP6-DTP5
0186    X(4)=-RP4*DCOS(SG4)
0187    Y(4)=-RP4*DSIN(SG4)
0188 69 CONTINUE
0189    Z(2)=-R(2)*DSIN(P2)
0190    Z(4)=-R(4)*DSIN(P4)
0191    GO TO 80
C      ROUTINE FOR THETA6 INCREMENT RESET
0192 70 P3=AG(2)-(PI/2.000)
0193    P4=AG(3)-(PI/2.000)
0194    RP3=R(3)*DCOS(P3)
0195    RP4=R(4)*DCOS(P4)
0196    R15=((R(3)*R(3))+R(4)*R(4))-(2.000*R(3)*R(4)*DCOS(AG(6)))
0197    R(15)=DSQRT(R15)
0198    IF(Z(3).NE.Z(4))GO TO 71
0199    RP15=R(15)
0200    GO TO 72
0201 71 S15=DABS(Z(4)-Z(3))/R(15)

```

FORTRAN IV G LEVEL 21

QRESET

DATE = 76044

14/06/51

```

0202      RP15=P(15)*DCOS(DARSIN(S15))
0203      72 CONTINUE
0204      CTP6=((RP3*RP2)+(RP4*RP4)-(RP15*RP15))/(2.000*RP3*RP4)
0205      TP6=DARCCS(CTP6)
0206      DTP6=(T3PI-TP6)/2.000
0207      IF(XK(2).NE.X(3).OR.YK(3).NE.Y(3))GO TO 75
0208      IF(XK(4).NE.X(4).OR.YK(4).NE.Y(4))GO TO 77
0209      73 TX34=(PI/6.000)+DTP6
0210      X(3)=RP3*DCOS(TX34)
0211      Y(3)=-RP3*DSIN(TX34)
0212      X(4)=-RP4*DCOS(TX34)
0213      Y(4)=-RP4*DSIN(TX34)
0214      GO TO 79
0215      75 IF(AG(4).NE.AG(4))GO TO 76
0216      IF(RK(3).NE.R(3))GO TO 73
0217      GO TO 99
0218      76 RP13=RK(13)
0219      P2=AG(1)-(PI/2.000)
0220      RP2=R(2)*DCOS(P2)
0221      CTP4=((RP2*RP2)+(RP3*RP3)-(RP13*RP13))/(2.000*RP2*RP3)
0222      TP4=DARCCS(CTP4)
0223      DTP4=(T3PI-TP4)/2.000
0224      TX4=(PI/6.000)-DTP4+DTP6
0225      X(3)=RP3*DCOS(TX4)
0226      Y(3)=-RP3*DSIN(TX4)
0227      TX6=(PI/6.000)+DTP6
0228      X(4)=-RP4*DCOS(TX6)
0229      Y(4)=-RP4*DSIN(TX6)
0230      GO TO 79
0231      77 IF(AG(5).NE.AG(5))GO TO 78
0232      IF(RK(4).NE.R(4))GO TO 73
0233      GO TO 99
0234      78 RP14=RK(14)
0235      P2=AG(1)-(PI/2.000)
0236      RP2=R(2)*DCOS(P2)
0237      CTP5=((RP2*RP2)+(RP4*RP4)-(RP14*RP14))/(2.000*RP2*RP4)
0238      TP5=DARCCS(CTP5)
0239      DTP5=(T3PI-TP5)/2.000
0240      TX5=(PI/6.000)-DTP5+DTP6
0241      X(4)=-RP4*DCOS(TX5)
0242      Y(4)=-RP4*DSIN(TX5)
0243      TX6=(PI/6.000)+DTP6
0244      X(3)=RP3*DCOS(TX6)
0245      Y(3)=-RP3*DSIN(TX6)
0246      79 CONTINUE
0247      Z(3)=-R(3)*DSIN(P3)
0248      Z(4)=-R(4)*DSIN(P4)
0249      80 CONTINUE
0250      CALL DIST
0251      RETURN
0252      99 WRITE(6,'00')I
0253      100 FORMAT(1X,'SUBROUTINE QRESET INDICATES NO RESET POSSIBLE FOR I=',I3,/)
0254      13./)
0254      RETURN
0255      END

```

FORTRAN IV G LEVEL 21

MAIN

DATE = 75044

22/42/70

```

C *****
C                               EXGEN ROUTINE
C   INTERNAL COORDINATE TO CARTESIAN COORDINATE FORCE CONSTANT CONVERSION
C *****
0001   IMPLICIT REAL*8 (A-H,O-Z)
0002   DIMENSION F(18,18),R(13,18),NF(3),NC(3),DAT(3),WKAR(400)
          1,NRO(9),NCO(9),NFO(9),Z(9),FO(9)
          2,KFR(4),KFC(4),DATNF(4),D(18,18),DD(18,18),A(18,18)
0003   REAL*8 SUMB,SUMA,DF(18,18),FX(18,18)
C ////////////////////////////////////////////////////////////////////
C   THIS PROGRAM READS IN SINGLE PRECISION F AND B-MATRIXES AND MULTIPLIES
C   THEM TOGETHER SUCH THAT FX = F * B
C   FX(18X18) = B*(18X13) F(13X13) B(13X18)
C   THE FX MATRIX GENERATED IS A CARTESIAN COORDINATE REPRESENTATION OF THE
C   INTERNAL COORDINATE FORCE CONSTANT MATRIX F.
C   THE B MATRIX USED IS OBTAINED FROM THE G-MATRIX FORMULATION PART OF THE
C   SCHACHTSCHNEIDER PROGRAM FOR THE CALCULATION OF NORMAL MODE FREQUENCIES.
C   THE FX MATRIX IS PUNCHED ON CARDS READY TO BE READ INTO THE SCHACHTSCHNEIDE
C   R NORMAL MODE FREQUENCY CALCULATION PROGRAM.
C ////////////////////////////////////////////////////////////////////
0004   1 READ(5,12)NF,NATOM,NZ,NFZ,NFX
0005   12 FORMAT(8I3)
C ////////////////////////////////////////////////////////////////////
C   NF = SIZE OF SQUARE F-MATRIX
C   NATOM = # OF ATOMS
C   NZ = # OF Z-MATRIX ENTRIES
C   NFZ = # OF FORCE CONSTANTS USED IN F-MATRIX SET-UP
C ////////////////////////////////////////////////////////////////////
0006   IF(NATOM+NF)2,1,2
0007   2 IF(NF+10)1111,1111,3
0008   3 NA=3*NATOM
0009   DO 9 I=1,NF
0010   DO 8 J=1,NA
0011   D(I,J)=0.000
0012   DD(I,J)=0.000
0013   7 F(I,J)=0.000
0014   8 B(I,J)=0.000
0015   9 READ(5,10)(NR(I),NC(I),DAT(I),I=1,3)
0016   10 FORMAT(2I3,E18.9,2I3,F18.9,2I3,F18.9)
0017   DO 20 I=1,3
0018   IF(5+NR(I))21,22,20
0019   20 B(NR(I),NC(I))=DAT(I)
0020   GO TO 9
0021   21 WRITE(6,11)
0022   11 FORMAT(//,1X,'ERROR IN B MATRIX CARD FOLLOWS',/)
0023   WRITE(6,12)(NR(I),NC(I),DAT(I),I=1,3)
0024   22 WRITE(6,16)
0025   16 FORMAT('1','BMATRIX')
0026   DO 23 I=1,NF
0027   23 WRITE(6,14)I,(B(I,J),J=1,NA)
0028   14 FORMAT(//,1X,'ROW # ',I3,/,8(1P16.7))
0029   READ(5,13)(NRO(I),NCO(I),NFO(I),Z(I),I=1,NZ)
0030   WRITE(6,13)(NRO(I),NCO(I),NFO(I),Z(I),I=1,NZ)
0031   READ(5,15)(FO(I),I=1,NFZ)
0032   WRITE(6,15)(FO(I),I=1,NFZ)
0033   13 FORMAT(4(3I3,F9.6))
0034   15 FORMAT(6F12.8)
0035   DO 30 I=1,NZ

```

FORTRAN IV G LEVEL 21

MAIN

DATE = 75344

22/42/22

```

0036      F(NRD(I),NCD(I))=Z(I)*F0(NF(I))
0037      30 F(NCD(I),NPD(I))=F(NRD(I),NCD(I))
0038      WRITE(6,17)
0039      17 FORMAT('1','F-MATRIX')
0040      DO 24 I=1,NF
0041      24 WRITE(6,14)I,(F(I,J),J=1,NF)
0042      DO 26 I=1,NA
0043      DO 26 K=1,NF
0044      SUMA=0.000
0045      DO 25 J=1,NF
0046      25 SUMA=SUMA+B(J,I)*F(J,K)
0047      26 BF(I,K)=SUMA
0048      DO 28 I=1,NA
0049      DO 28 K=1,NA
0050      SUMB=0.000
0051      DO 27 J=1,NF
0052      27 SUMB=SUMB+BF(I,J)*B(J,K)
0053      28 FX(I,K)=SUMB
0054      WRITE(6,18)
0055      18 FORMAT('1','CARTESIAN COORDINATE FX-MATRIX')
0056      DO 29 I=1,NA
0057      29 WRITE(6,14)I,(FX(I,J),J=1,NA)
0058      WRITE(7,19)((I,J,FX(I,J),J=1,NA),I=1,NA)
0059      I=-2
0060      WRITE(7,19)I
0061      19 FORMAT(4(2I3,1PD14.7))
0062      GO TO 1
0063      1111 CALL EXIT
0064      END

```

FORTRAN IV G LEVEL 21

MAIN

DATE = 76149

21/49/59

```

C *****
C CARTESIAN COORDINATE FORCE CONSTANT ROUTINE
C *****
0001 IMPLICIT REAL*8 (A-H,O-Z)
0002 REAL*8 DUB(3,6,3,6),BC(4),BC3(4)
0003 REAL*8 ECC(7,3,6,7,3,6),D(7,3,6,3,6),DD(3,6,3,6),XK(6),YK(6),ZK(6),XKC(6),
    *YKC(6),ZKC(6)
0004 DIMENSION X(6),Y(6),Z(6),R(15),DER(15),AG(6),R2(15),D1(3),D3(3),
    1 ALPH(3),RL(3),BETA(3),CC(3),AA(3),SIG(3),RSTR(3),ACS(6),DK(6),
    2 Y1(6),Y2(6),ASS(6),F(4),GF(4),RX(6),PX(6),PY(6),PZ(6),DX(6),
    3 UY(6),DZ(6),DPX(6),DPY(6),DPZ(6),DF(15,3)
    4,X(20),YY(20),CO(11),XYZ(3),KC(3,6),KCR(4),KCC(4)
0005 DIMENSION APARM(5)
0006 COMMON X,Y,Z,R,DER,AG,R2,D1,ALPH,RE,D3,BETA,CC,AA,SIG,RSTR,TAU,
    1 RV,DIJ,CP,EE,ACS,ASS,RX,XII, V1,V2,V3,V4,BMAX,
    2 RSS,VR,PER,H,PX,PY,PZ,WH,WG,WBR,w,UT,DX,DY,DZ,UPX,DPY,DPZ,T,DF,
    3 TEMP,RKT,STAKT,APARM,PI,T3PI,EL6PI,S6PI,
    4 I11,JJJ,KKK,LLL,NV1,NV2,NV3,NV4,JJ,NI,KEE
0007 DATA XYZ/'X(','Y(','Z('
C ////////////////////////////////////////////////////////////////////
C THIS PROGRAM CALCULATES THE CARTESIAN COORDINATE FORCE CONSTANTS
C (THE SECOND DERIVATIVE OF A POTENTIAL ENERGY SURFACE NAMED "POT6" WITH
C RESPECT TO THE CARTESIAN COORDINATE COORDINATES OF THE CH5 SYSTEM) USING
C NUMERICAL PARTIAL DIFFERENTIATION TECHNIQUES.
C ////////////////////////////////////////////////////////////////////
C *****
C ECC = CALCULATED ENERGY MATRIX, CAPABLE OF STORING 49 INCREMENTAL ENERGIES
C NEEDED FOR CALCULATION OF EACH FORCE CONSTANT IN THE 18X18 MATRIX.
C D = FIRST DERIVATIVE MATRIX
C DD = SECOND DERIVATIVE MATRIX BY SEVEN POINT METHOD
C DD3 = SECOND DERIVATIVE MATRIX BY 3 POINT METHOD
C XK, YK, AND ZK = GEOMETRY COORDINATE CONSTANTS FOR RESETTING GEOMETRY
C AFTER INCREMENTATION.
C XKC, YKC, AND ZKC = COORDINATE FOR RESETTING GEOMETRY TO A PREVIOUSLY
C INCREMENTED GEOMETRY.
C ////////////////////////////////////////////////////////////////////
0008 A=0.7500
0009 B=-0.1500
0010 C=0.1500/9.000
0011 KEE=-1
C ////////////////////////////////////////////////////////////////////
0012 READ IN POT6 DATA
0013 CALL READ
0014 PI=2.000*0.437337358
0015 EL6PI=(11.000*PI)/6.000
0016 S6PI=(7.000*PI)/6.000
C ////////////////////////////////////////////////////////////////////
C CALCULATE DOUBLE PRECISION TETRAHEDRAL ANGLE NEEDED FOR GEOMETRY CALCULA-
C TIONS.
0017 CALL TETRAH(TAU,PI)
C ZERO OUT MATRICES
0018 DO I KA=1,6
0019 XK(KA)=0.000
0020 YK(KA)=0.000
0021 ZK(KA)=0.000

```

FORTRAN IV LEVEL 21

MAIN

DATE = 76149

21/49/59

```

0022      XK(KA)=0.000
0023      YK(KA)=0.000
0024      ZK(KA)=0.000
0025      DO 1 KX=1,3
0026      DO 1 IX=1,3
0027      DO 1 IC=1,6
0028      DO(KX,KA,IX,IC)=0.000
0029      DO3(KX,KA,IX,IC)=0.000
0030      DO 1 IJ=1,7
0031      U(IJ,KX,KA,IX,IC)=0.000
0032      DO 1 IJC=1,7
0033      FCC(IJ,KX,KA,IJC,IX,IC)=0.000
0034      1 CONTINUE
C ////////////////////////////////////////////////////////////////////
C
C   THE INTEGER "IRC" TELLS THE PROGRAM WHETHER IT IS TO READ IN THE
C   INTERATOMIC DISTANCES (IF IRC IS GREATER THAN OR EQUAL ZERO)
C   OR IF THE PROGRAM IS TO READ IN THE CARTESIAN COORDINATES OF THE ATOMS (IF
C   IRC IS LESS THAN ZERO).
C   "RINK" IS THE INCREMENT SIZE.
C ////////////////////////////////////////////////////////////////////
0035      READ(5,770)IRC,RINK
0036      770 FORMAT(I2,010.3)
0037      IF(IRC)3,2,2
0038      2 READ(5,771)(R(I),I=1,15)
0039      771 FORMAT(4D20.13)
0040      OR1=R(1)
0041      WRITE(6,772)(I,R(I),I=1,15)
0042      772 FORMAT(//,5X,'INTERATOMIC DISTANCES',/,15(7X,'R',12,'=',1PD20.10,/)
*)
0043      GO TO 4
0044      3 READ(5,773)(X(I),Y(I),Z(I),I=1,6)
0045      773 FORMAT(3D20.13)
0046      WRITE(6,774)(I,X(I),Y(I),Z(I),I=1,6)
0047      774 FORMAT(1X,'ATOM',9X,'X',19X,'Y',19X,'Z',/,6(14,2X,3D20.12,/,//)
CALL DIST
0048      OR1=R(1)
0049      WRITE(6,772)(I,R(I),I=1,15)
0050      4 CONTINUE
0051      WRITE(6,775)
0052      775 FORMAT('1')
0053      IF(IRC)6,5,5
0054      5 CALL PLACE(OR1)
0055      Z(1)=OR1
0056      Z(6)=R(5)
0057      CALL DIST
0058      WRITE(6,772)(I,R(I),I=1,15)
0059      6 CONTINUE
0060      CALL ANGLE
0061      WRITE(6,777)(I,AG(I),I=1,6)
0062      777 FORMAT(5X,'HIGH ANGLES THETA',/,1X,6('T',11,'=',1PD17.10,1X)/)
DO 7 I=1,6
0063      XK(I)=X(I)
0064      YK(I)=Y(I)
0065      ZK(I)=Z(I)
0066      7 CONTINUE
0067      WRITE(6,774)(I,XK(I),YK(I),ZK(I),I=1,6)
0068
0069

```


FORTRAN IV G LEVEL 21

MAIN

DATE = 70149

21/49/59

```

C ///////////////////////////////////////////////////
C   CALCULATE THE POTENTIAL ENERGY CORRESPONDING TO THE MOLECULAR GEOMETRY.
0111   CALL PCTG
0112   ECC(IJ,KX,KI,IJC,IX,IC)=EE+18.3232DU
0113   DO 309 IA=1,6
0114   X(IA)=XKC(IA)
0115   Y(IA)=YKC(IA)
0116   Z(IA)=ZKC(IA)
0117   309 CONTINUE
0118   30 CONTINUE
0119   DO 310 IA=1,6
0120   X(IA)=XK(IA)
0121   Y(IA)=YK(IA)
0122   Z(IA)=ZK(IA)
0123   310 CONTINUE
0124   31 CONTINUE
0125   IF(IX.NE.KX.OR.IC.NE.KI)GO TO 71
C   STORE DUPLICATED ENERGY VALUES FOR DIAGONAL ELEMENT FORCE CONSTANT CALCULATION.
0126   DO 70 IJ=1,7
0127   DO 70 IJC=1,7
0128   KEC=IJ+IJC
0129   IF(IJ.EQ.1.OR.IJ.EQ.7)GO TO 70
0130   GO TO (52,52,53,54,55,56,57,58,59,60,61,62,63,64),KEC
0131   52 ECC(IJ,KX,KI,IJC,IX,IC)=ECC(1,KX,KI,1,IX,IC)
0132   GO TO 70
0133   53 ECC(IJ,KX,KI,IJC,IX,IC)=ECC(1,KX,KI,2,IX,IC)
0134   GO TO 70
0135   54 ECC(IJ,KX,KI,IJC,IX,IC)=ECC(1,KX,KI,3,IX,IC)
0136   GO TO 70
0137   55 ECC(IJ,KX,KI,IJC,IX,IC)=ECC(1,KX,KI,4,IX,IC)
0138   GO TO 70
0139   56 ECC(IJ,KX,KI,IJC,IX,IC)=ECC(1,KX,KI,5,IX,IC)
0140   GO TO 70
0141   57 ECC(IJ,KX,KI,IJC,IX,IC)=ECC(1,KX,KI,6,IX,IC)
0142   GO TO 70
0143   58 ECC(IJ,KX,KI,IJC,IX,IC)=ECC(1,KX,KI,7,IX,IC)
0144   GO TO 70
0145   59 ECC(IJ,KX,KI,IJC,IX,IC)=ECC(7,KX,KI,2,IX,IC)
0146   GO TO 70
0147   60 ECC(IJ,KX,KI,IJC,IX,IC)=ECC(7,KX,KI,3,IX,IC)
0148   GO TO 70
0149   61 ECC(IJ,KX,KI,IJC,IX,IC)=ECC(7,KX,KI,4,IX,IC)
0150   GO TO 70
0151   62 ECC(IJ,KX,KI,IJC,IX,IC)=ECC(7,KX,KI,5,IX,IC)
0152   GO TO 70
0153   63 ECC(IJ,KX,KI,IJC,IX,IC)=ECC(7,KX,KI,6,IX,IC)
0154   GO TO 70
0155   64 ECC(IJ,KX,KI,IJC,IX,IC)=ECC(7,KX,KI,7,IX,IC)
0156   70 CONTINUE
0157   71 CONTINUE
C ///////////////////////////////////////////////////
C   CALCULATE SEVEN POINT FIRST DERIVATIVES
0158   DO 75 IJ=1,7
0159   DEA=ECC(IJ,KX,KI,5,IX,IC)-ECC(IJ,KX,KI,3,IX,IC)
0160   DEB=ECC(IJ,KX,KI,6,IX,IC)-ECC(IJ,KX,KI,2,IX,IC)
0161   DEC=ECC(IJ,KX,KI,7,IX,IC)-ECC(IJ,KX,KI,1,IX,IC)
0162   D(IJ,KX,KI,IX,IC)=(A*DEA+B*DEB+C*DEC)/RINK

```



```

FCRTRAN IV G LEVEL 21      MAIN      DATE = 76149      21/49/59

0163      75 CONTINUE
C ///////////////////////////////////////////////////
C      CALCULATE SEVEN POINT SECOND DERIVATIVES
0164      DDEA=D(5,KX,KI,IX,IC)-D(3,KX,KI,IX,IC)
0165      DDEB=D(6,KX,KI,IX,IC)-D(2,KX,KI,IX,IC)
0166      DDEC=D(7,KX,KI,IX,IC)-D(1,KX,KI,IX,IC)
0167      DD(KX,KI,IX,IC)=((A*DDEA+B*DDEB+C*DDEC)/RINK)*FACT
0168      WRITE(6,780)XYZ(KX),KI,XYZ(IX),IC,RINK
0169      700 FORMAT('1',IX,'THE ENERGY SETS AND FIRST DERIVATIVES USED TO CALCU
LATE THE SECOND DERIVATIVE WITH RESPECT TO:',//,IX,A2,I2,') AND ',A2,I2
2A2,I2,') USING AN INCREMENT OF RINK =',1PD22.13,///)

C170      DU 76 IJ=1,7
C171      IXD=IJ-4
C172      WRITE(6,791)
0173      791 FORMAT(18X,'1*RINK',24X,'2*RINK',24X,'3*RINK')
0174      WRITE(6,792)(ECC(IJ,KX,KI,IA,IX,IC),IA=5,7)
C175      792 FORMAT(2X,'E+',2X,3(1PD30.15))
0176      WRITE(6,793)ECC(IJ,KX,KI,3,IX,IC),ECC(IJ,KX,KI,2,IX,IC),ECC(IJ,KX,KI
IKI,1,IX,IC)
0177      793 FORMAT(2X,'E-',2X,3(1PD30.15))
0178      WRITE(6,794)XYZ(IX),IC,XYZ(KX),KI,IXD,D(IJ,KX,KI,IX,IC)
0179      794 FORMAT(6X,'DV/D(',A2,I2,')') AT ('',A2,I2,')',I2,'*RINK)='',1PD25.15,
1/)

0180      76 CONTINUE
C181      WRITE(6,795)XYZ(KX),KI,XYZ(IX),IC,DD(KX,KI,IX,IC)
0182      795 FORMAT(2X,'DDV/D(',A2,I2,')D(',A2,I2,')='',1PD25.15,///)
C ///////////////////////////////////////////////////
C      CALCULATE 3 POINT SECOND DERIVATIVES
0183      EXY=ECC(4,KX,KI,4,IX,IC)
0184      EPP=ECC(5,KX,KI,5,IX,IC)
0185      EMM=ECC(3,KX,KI,3,IX,IC)
0186      EPM=ECC(5,KX,KI,3,IX,IC)
0187      EMP=ECC(3,KX,KI,5,IX,IC)
0188      DHS=RINK*RINK
0189      EDD=(EPP+EMM-(2.000*EXY))/DHS
0190      EED=(EPM+EMP-(2.000*EXY))/DHS
0191      DD3(KX,KI,IX,IC)=(EDD-EED)/4.000
0192      DD3(KX,KI,IX,IC)=DD3(KX,KI,IX,IC)*FACT
0193      WRITE(6,797)
0194      797 FORMAT(//,5X,'SECOND DERIVATIVE BY 3 POINT METHOD',/)
0195      WRITE(6,795)XYZ(KX),KI,XYZ(IX),IC,DD3(KX,KI,IX,IC)
0196      IF(KX.EQ.IX.AND.KI.EQ.IC)GO TO 540
0197      GO TO 551
0198      540 CONTINUE
C ///////////////////////////////////////////////////
C      SET-UP AND CALCULATE DIAGONAL FORCE CONSTANT MATRIX ELEMENTS BY POLYNOMIAL
LEAST SQUARES FIT METHOD.
C199      DO 550 IK=1,7
0200      DU 550 IY=1,7
0201      IF(IK.GT.1.AND.IY.LI.7)GO TO 550
0202      KS=IK+IY-1
0203      KFC=KS-7
0204      XX(KS)=KFC*RINK
0205      YY(KS)=ECC(IY,KX,KI,IK,IX,IC)
0206      550 CONTINUE
0207      CALL LESQ(2,13,XX,YY,C0)
0208      WRITE(6,560)
0209      560 FORMAT(2X,'SECOND DERIVATIVE OF THE POLYNOMIAL LEAST SQUARES EQUATION FOLL

```

FURKAN IV G LEVEL 21

MAIN

DATE = 70149

21/49/59

```

          IION FOLLOWS',/)
0210      DDP=0.000
0211      DDP=2.000*CO(3)*FACT
0212      WRITE(6,775)XYZ(KX),KI,XYZ(IX),IC,DDP
0213      551 CONTINUE
0214      300 CONTINUE
0215      311 CONTINUE
0216      KCX=0
0217      DO 42 I=1,6
0218      DO 42 KX=1,3
0219      KCX=KX+1
0220      KC(KX,I)=KCX
0221      42 CONTINUE
0222      WRITE(6,775)
0223      WRITE(6,768)
0224      760 FORMAT(1X,'CARTESIAN COORDINATE FORCE CONSTANT MATRIX BY 3 POINT M
          IETHOD:')
          KCT=0
0225      DO 439 I=1,4
0226      KCR(I)=0
0227      KCC(I)=0
0228      439 BC(I)=0.000
0229      KR=0
0230      DO 445 KI=1,6
0231      DO 445 KX=1,3
0232      KR=KR+1
0233      WRITE(6,761)KR
0234      WRITE(6,760)(DD3(KX,KI,IX,I),IX=1,3),I=1,6)
0235      KCT=0
0236      C //////////////////////////////////////
0237      C CNSTRUCT AND PUNCH CARTESIAN COORDINATE FORCE CONSTANT MATRIX BY 7 POINT
0238      C METHOD.
0239      DO 444 I=1,6
0240      DO 444 IX=1,3
0241      IF(DABS(DD3(KX,KI,IX,I)).LE.0.1D-9)GO TO 441
0242      KCT=KCT+1
0243      KCR(KCT)=KC(KX,KI)
0244      KCC(KCT)=KC(IX,I)
0245      BC(KCT)=DD3(KX,KI,IX,I)
0246      IF(KCT.EQ.4)GO TO 440
0247      441 IF(I.EQ.6.AND.IX.EQ.3)GO TO 440
0248      GO TO 444
0249      440 CONTINUE
0250      WRITE(7,763)(KCR(KCX),KCC(KCX),BC(KCX),KCX=1,4)
0251      WRITE(6,763)(KCR(KCX),KCC(KCX),BC(KCX),KCX=1,4)
0252      KCT=0
0253      DO 442 IZ=1,4
0254      KCR(IZ)=0
0255      KCC(IZ)=0
0256      BC(IZ)=0.000
0257      442 CONTINUE
0258      444 CONTINUE
0259      445 CONTINUE
0260      WRITE(6,775)
0261      WRITE(6,762)
0262      762 FORMAT(1X,'CARTESIAN COORDINATE FORCE CONSTANT MATRIX BY 7 POINT M
          IETHOD:')
          NEND=-2
0261      NEND=-2

```


FORTRAN IV G LEVEL 21

MAIN

DATE = 76149

21/49/59

```

0312      DO 47 IX=1,3
0313      IF(KC(IX,IC).LT.4.DR.KC(IX,IC).GT.15)GO TO 93
0314      IF(DABS(DD(KX,KI,IX,IC)).LT.1.0E-10)DD(KX,KI,IX,IC)=0.000
0315      IF(DD(KX,KI,IX,IC).EQ.0.000)GO TO 47
0316      KCT=KCT+1
0317      KCR(KCT)=KC(KX,KI)-3
0318      KCC(KCT)=KC(IX,IC)-3
0319      BC(KCT)=DD(KX,KI,IX,IC)
0320      IF(IX.EQ.3.AND.IC.EQ.6)GO TO 49
0321      GO TO 50
0322  49 IF(KX.EQ.3.AND.KI.EQ.6)GO TO 51
0323  50 CONTINUE
0324      IF(KCT.NE.4)GO TO 47
0325      GO TO 51
0326  93 IF(KCT.GT.0)GO TO 51
0327      GO TO 47
0328  51 CONTINUE
0329      WRITE(6,763)(KCR(I),KCC(I),BC(I),I=1,4)
0330      WRITE(7,763)(KCR(I),KCC(I),BC(I),I=1,4)
0331      DO 46 I=1,4
0332      KCR(I)=0
0333      KCC(I)=0
0334      BC(I)=0.000
0335  46 CONTINUE
0336      KCT=0
0337  47 CONTINUE
0338  48 CONTINUE
0339      WRITE(6,765)NEND
0340      WRITE(7,765)NEND
0341      WRITE(6,767)
0342      WRITE(7,767)
0343  767 FORMAT(2X,'CARTESIAN COORDINATE FORCE CONSTANT SET FOR CH3. BY 3 PT.
      IF. METHOD')
0344      DO 85 I=1,4
0345      KCR(I)=0
0346      KCC(I)=0
0347      BC(I)=0.000
0348  85 CONTINUE
0349      KCT=0
0350      DO 88 KI=1,6
0351      DO 88 KX=1,3
0352      IF(KC(KX,KI).LT.4.DR.KC(KX,KI).GT.15)GO TO 88
0353      DO 87 IC=1,6
0354      DO 87 IX=1,3
0355      IF(KC(IX,IC).LT.4.DR.KC(IX,IC).GT.15)GO TO 92
0356      IF(DABS(DD3(KX,KI,IX,IC)).LT.1.0E-10)DD3(KX,KI,IX,IC)=0.000
0357      IF(DD3(KX,KI,IX,IC).EQ.0.000)GO TO 87
0358      KCT=KCT+1
0359      KCR(KCT)=KC(KX,KI)-3
0360      KCC(KCT)=KC(IX,IC)-3
0361      BC(KCT)=DD3(KX,KI,IX,IC)
0362      IF(IX.EQ.3.AND.IC.EQ.6)GO TO 89
0363      GO TO 90
0364  89 IF(KX.EQ.3.AND.KI.EQ.6)GO TO 91
0365  90 CONTINUE
0366      IF(KCT.NE.4)GO TO 87
0367      GO TO 91
0368  92 IF(KCT.GT.0)GO TO 91

```

FCRIRAN IV U LEVEL 21

MAIN

DATE = 76149

21/49/59

```
0369      GO TO 87
0370      91 CONTINUE
0371      WRITE(6,763)(KCK(I),KCC(I),BC(I),I=1,4)
0372      WRITE(7,763)(KCK(I),KCC(I),BC(I),I=1,4)
0373      DO 86 I=1,4
0374      KCK(I)=0
0375      KCC(I)=0
0376      BC(I)=0.000
0377      86 CONTINUE
0378      KLT=0
0379      87 CONTINUE
0380      88 CONTINUE
0381      WRITE(6,765)NENU
0382      WRITE(7,765)NENU
0383      1111 STOP
0384      LND
```


PORTFAN IV G1 RELEASE 2.0

MAIN

DATE = 76302

10/04/47

```

0012          92 CONTINUE
0013          97 READ(5,6)(RECORD(I),I=1,40)
0014          6  FORMAT(20A4)
0015          ROTC=C.000
0016          ASSM=0.000
0017          IF(NRGT.EQ.0)GO TO 102
0018          READ(5,11)ROTC,ASSM
0019          11  FORMAT(F12.6,48X,F12.6)
0020          102 IF(NOTEM)103,103,000
0021          800 IF(KIND-1)802,802,103
0022          802 IF(NUMB-1)804,804,103
C          READ TEMPERATURES AT WHICH KIES ARE TO BE CALCULATED
C          ONLY IF KIND=1 AND NUMB=1 *****
0023          804 READ(5,10)(TEMS(I),I=1,NCTEM)
0024          103 CONTINUE
C ////////////////////////////////////////////////////////////////////
C          READ CALCULATED FREQUENCIES FOR A GIVEN MOLECULAR ISOTOPIC CONFIGURATION.
0025          DO 300 I=1,NQ
0026          300 DV(I)=0.000
0027          READ(5,10)(DV(I),I=1,NQ)
0028          10  FORMAT(6F12.6)
C ////////////////////////////////////////////////////////////////////
C          READ ATOMIC WEIGHTS BY ATCM NUMBER.
0029          324 READ(5,10)(WT(I),I=1,NGAT)
C          READ MOMENTS OF INERTIA INTO TMOM(I).
C          TMASS = MOLECULAR WEIGHT OF ISOTOPIC CONFIGURATION.
0030          READ(5,7)(TMOM(I),I=1,3),TMASS
0031          7  FORMAT(4E18.9)
0032          IF(NOTEM)280,280,806
0033          806 CALL THERMU
0034          280 CONTINUE
0035          GO TO 90
0036          END

```



```

FLRTRAN IV G LLVEL 21          THERMO          DATE = 76247          23/04/44

0016      928 TMOM(I)=1.000
0017      930 CONTINUE                      32I 3660
0018      TMAF=1.000
C ////////////////////////////////////////////////////
C      MUI ALLOWS FOR MORE THAN ONE REACTANT TO BE INCLUDED IN ALL TERMS.
C      IF MUI > 0 THEN THE DATA SET IS ASSUMED TO BE A PART OF THE PREVIOUS ONE.
0019      IF (MUI.GT.0) TMAF=TMASFA(KIND,NUMB)
C ////////////////////////////////////////////////////
C      CALCULATE MMI ELEMENT.
0020      948 TMASFA(KIND,NUMB)=(TMCM(1)*TMOM(2)*TMOM(3))*0.500*TMASS**1.500*TM32I 367
      IAF
0021      IF (MUI) 951,950,951
0022      950 UGTL(KIND,NUMB)=0.000
0023      951 CONTINUE
0024      952 DO 960 I=1,NMUI                      32I 369
0025      950 UGTL(KIND,NUMB)=UGTL(KIND,NUMB)+1.500*ALOG(WT(I))          32I 370
0026      960 CONTINUE                      32I 371
0027      IF (MUI) 965,964,965
0028      964 OGFR(KIND,NUMB)=0.000          32I 372
0029      965 CONTINUE
0030      968 DO 980 I=1,NG                      32I 373
0031      972 IF (C.100-DV(I)) 976,980,980          32I 374
0032      976 OGFR(KIND,NUMB)=OGFR(KIND,NUMB)+ALOG(DV(I))          32I 375
0033      980 CONTINUE                      32I 376
0034      IF (MUI) 987,984,987
0035      984 SUMNU(KIND,NUMB)=0.000          32I 377
0036      986 SSUMNU(KIND,NUMB)=0.000          32I 378
0037      988 ONUIM(KIND,NUMB)=0.000
0038      987 CONTINUE
0039      988 DO 999 I=1,NG
0040      992 IF (0.1-DV(I)) 994,996,996          32I 380
0041      994 SUMNU(KIND,NUMB)=SUMNU(KIND,NUMB)+DV(I)/2.000
0042      996 GO TO 998
0043      998 IF (-1.0-DV(I)) 998,998,997
0044      997 ONUIM(KIND,NUMB)=-DV(I)
0045      998 DVT=DV(I)**2
0046      999 SSUMNU(KIND,NUMB)=SSUMNU(KIND,NUMB)+SIGN(DVT,DV(I))
0047      IF (NCO(I).EQ.1) GO TO 904
0048      1200 WRITE(6,1400) NPROB,KIND,NUMB,(RECORD(I),I=1,20)
0049      1400 FORMAT(38H1 THERMODYNAMIC QUANTITIES PROBLEM NO.18,15H MOLECULE K32I 385
      IIND,I3,7H NUMBER,I3,/,12X,20A4)
0050      1204 WRITE(6,1404)(TMOM(I),I=1,3),TMASS          32I 387
0051      1404 FORMAT(6H1 IA= F12.6,6H IB= F12.6,6H IC= F12.6,8H MASS= F12.6) 32I 388
0052      1208 WRITE(6,1408) TMASFA(KIND,NUMB)          32I 389
0053      1408 FORMAT(27H0 ((1A*1B*1C)**1/2)*M**3/2=E18.9)          32I 390
0054      1212 WRITE(6,1412)(DV(I),I=1,NQ)          32I 391
0055      1214 WRITE(6,1414) SUMNU(KIND,NUMB),SSUMNU(KIND,NUMB)          32I 392
0056      1412 FORMAT(21H0 FREQUENCIES IN CM-1/(7F16.6))          32I 393
0057      1414 FORMAT(11H0 SUM NU/2=E18.9,17HCM-1 SUM NU**2=E18.9,4HCM-2) 32I 394
0058      904 DO 1550 L=1,NUTEM
0059      IF (MUI) 909,908,909
0060      908 BEXC(KIND,NUMB,L)=1.000
0061      909 CONTINUE
0062      910 SUMU=0.000
C ////////////////////////////////////////////////////
C      CALCULATE U FACTORS
0063      912 DO 944 I=1,NQ                      32I 398
0064      913 YOU(I)=1.438800*DV(I)/TEMS(L)

```

```

FCRTRAN IV G LEVEL 21          THERMO          DATE = 76247          23/04/44

0065      916 IF(0.1-DV(I))920,924,924          321 400
C ///////////////////////////////////////////////////
C CALCULATE EXC ELEMENT
0066      920 BEXC(KIND,NUMB,L)=BEXC(KIND,NUMB,L)*(1.000-EXP(-YOU(I)))          321 401
0067      924 CONTINUE          321 402
0068      936 IF(0.1-DV(I))940,944,944          321 403
0069      940 SUMU=SUMU+YOU(I)/2.000
0070      944 CONTINUE          321 405
0071      IF(NCO(1).EQ.1)GO TO 1550
0072      1216 WRITE(6,1416)TEMS(L)          321 406
0073      1416 FORMAT(15H0 TEMPERATURE=F12.6)          321 407
0074      1217 WRITE(6,1417)(YOU(I),I=1,NG)          321 408
0075      1417 FORMAT(24H0 THE VALUES OF U FOLLOW/(10F12.6))          321 409
0076      1220 WRITE(6,1420)BEXC(KIND,NUMB,L),SUMU          321 410
0077      1550 CONTINUE
0078      1420 FORMAT(19H EXCITATION FACTOR=F12.8,10H 1/2SUM U=F14.6)          321 411
C ///////////////////////////////////////////////////
C CALCULATE ISOTOPIIC RATIOS.
0079      1000 IF(KIND-2)1084,1004,1084          321 412
0080      1004 RMASFA(NUMB)=TMASFA(2,NUMB)/TMASFA(1,NUMB)          321 413
0081      1020 DOGTL=OGTL(1,NUMB)-CGTL(2,NUMB)          321 414
0082      1024 TRFA=RMASFA(NUMB)*EXP(DOGTL)          321 415
0083      1028 DUGFR(NUMB)=DUGFR(2,NUMB)-DUGFR(1,NUMB)          321 416
0084      1032 PRUDFA=EXP(DUGFR(NUMB))          321 417
0085      1035 TRKULE=PRUDFA/TRFA          321 418
0086      1036 DSUMNU(NUMB)=SUMNU(1,NUMB)-SUMNU(2,NUMB)          321 419
0087      DSUMNU(NUMB)=SSUMNU(1,NUMB)-SSUMNU(2,NUMB)
0088      IF(NCO(1).EQ.1)GO TO 1037
0089      1226 WRITE(6,1426)NUMB,NOPROB,NUMB,MOPROB(1,NUMB)          321 420
0090      1428 FORMAT(56H1 THERMODYNAMIC QUANTITIES FOR MOLECULE OF KIND 2 NUMBER321 421
          113,12H PROBLEM NO.18/42H WITH RESPECT TO MOLECULE OF KIND 1 NUMBER321 422
          213,12H PROBLEM NO.18)          321 423
0091      1232 WRITE(6,1432)TRRULE          321 424
0092      1432 FORMAT(81H0 RATIO PRODUCT NU2/PRODUCT NU1 TO MASS FACTOR=1.0 (TELL321 425
          TER=REDLICH) OR=NULL/NU2L=E18.9)          321 426
0093      1037 DO 1551 L=1,NUMB
0094      1038 RBEXC(L,NUMB)=BEXC(1,NUMB,L)/BEXC(2,NUMB,L)          321 428
0095      DSUMU=1.438800*(SUMNU(1,NUMB)-SUMNU(2,NUMB))/TEMS(L)
0096      1039 EXSUMU=EXP(DSUMU)          321 430
0097      1040 QRAT=RMASFA(NUMB)*RBEXC(L,NUMB)*EXSUMU          321 431
0098      1044 EFFR=PRUDFA*RBEXC(L,NUMB)*EXSUMU          321 432
0099      IF(NCO(1).EQ.1)GO TO 1551
0100      1236 WRITE(6,1436)TEMS(L)          321 433
0101      1436 FORMAT(15H0 TEMPERATURE=F12.6)          321 434
0102      1240 WRITE(6,1440)RMASFA(NUMB),RBEXC(L,NUMB),EXSUMU,DSUMU,Q          321 435
          1KAT          321 436
0103      1440 FORMAT(66H Q2/Q1=MASS FACTOR (2/1)*EXCITATION FACTOR (1/2)*ZERO-PO321 437
          1INT (1-2)=E18.9,1H*E 18.9/50X,1H*E18.9,10H (OR EXP E18.9,2H)=E18.9321 438
          2)          321 439
0104      1244 WRITE(6,1444)EFFR          321 440
0105      1551 CONTINUE
0106      1444 FORMAT(10H0 S2/S1 F=E18.9)          321 441
0107      1046 IF(N2UMB)1084,1084,1052          321 442
0108      1052 RRMAS=RMASFA(N2UMB)/RMASFA(NUMB)          321 443
0109      1056 KPROD=EXP(DUGFR(N2UMB)-DUGFR(NUMB))          321 444
0110      1058 RATIO=RRMAS/RPROD
0111      WRITE(6,1600)
0112      1600 FORMAT('1',' ABSOLUTE RATE THEORY EQUATIONS FOLLOW ',//)

```

```

FCRTRAN IV G LEVEL 21          THERMO          DATE = 76247          23/04/44

0113          IF(NC0(1).EQ.1)GO TO 1060
0114          1252 WRITE(6,1452)MOPROB(2,N2UMB),MOPROB(2,NUMB)          32I 446
0115          1452 FORMAT(81H0 RATIOS OF RATIOS OF THERMODYNAMIC QUANTITIES. IN THE N32I 447
          NUMERATOR 2 IS PROBLEM NO.18/36H IN THE DENCMINATOR 2 IS PRGBLEM NO32I 448
          2.18,1H.)          32I 449
C116          1256 WRITE(6,1456)RATIO          32I 450
0117          1456 FORMAT(19H0 Q RATIO/F RATIO= E18.9)          32I 451
C ///////////////////////////////////////////////////
C CALCULATE FINAL RATIO TERMS FOR MMI, EXC, & ZPE.
C118          1060 DO 1552 L=1,NOTEM
C119          1064 RRBEXC=RBEXC(L,N2UMB)/RBEXC(L,NUMB)          32I 453
C CALCULATE ZPE TERM
C ///////////////////////////////////////////////////
C120          1063 RRSUMU=EXP(1.438800*(DSUMNU(N2UMB)-DSUMNU(NUMB))/TEMS(L))          32I 454
0121          1072 QRAT(L)=RRMAS*RRBEXC*RRSUMU          32I 455
0122          1076 KEFFK(L)=RPROD*RRBEXC*RRSUMU
C ///////////////////////////////////////////////////
C CALCULATE TUNNELLING FACTORS
0123          WTUN(L)=1.000
0124          BTUN(L)=1.000
0125          BEXTUN(L)=1.000
0126          IF(CNUIM(2,NUMB))1080,1080,1078
0127          1078 WTUN(L)=(1.000+(1.000/24.000)*(1.438800*ONUIM(1,NIUMB)/TEMS(L))**2
          1)/(1.000+(1.000/24.000)*(1.438800*ONUIM(2,NUMB)/TEMS(L))**2)
C128          BTUN(L)=(CNUIM(1,NIUMB)*SIN(1.438800*ONUIM(2,NUMB))/(2.000*TEMS(L32I 4557
          1)))/(ONUIM(2,NUMB)*SIN(1.438800*ONUIM(1,NIUMB)/(2.000*TEMS(L))
          2)
C129          UTUN1=1.438800*ONUIM(1,NIUMB)/TEMS(L)
C130          UTUN2=1.438800*ONUIM(2,NUMB)/TEMS(L)
C131          BETUN1=1.000+(UTUN1*UTUN1/24.000)+(7.000*(UTUN1**4)/5760.000)
C132          BETUN2=1.000+(UTUN2*UTUN2/24.000)+(7.000*(UTUN2**4)/5760.000)
C133          BEXTUN(L)=BETUN1/BETUN2
0134          1080 WRQRAT(L)=RQRAT(L)*WTUN(L)
C135          BRQRAT(L)=RQRAT(L)*BTUN(L)
0136          BXQRAT(L)=RQRAT(L)*BEXTUN(L)
0137          1260 WRITE(6,1436)TEMS(L)          32I 457
0138          1264 WRITE(6,1464)RRMAS,RRBEXC,RRSUMU,RQRAT(L)          32I 458
0139          1464 FORMAT(51H0 Q RATIO=MASS FACTOR*EXCITATION FACTOR*ZERO-POINT=E18.932I 459
          1,1H*E18.9/50X,1H*E18.9,1H=E18.9)          32I 460
C140          1268 WRITE(6,1468)RPROD,RRBEXC,RRSUMU,REFFR(L)          32I 461
0141          1552 CONTINUE
0142          1468 FORMAT(54H0 F RATIO=PRDUCT FACTOR*EXCITATION FACTOR*ZERO-POINT=E132I 462
          18.9,1H*E18.9/50X,1H*E18.9,1H=E18.9)          32I 463
0143          1270 WRITE(6,1470)MOPROB(2,N2UMB),MOPROB(2,NUMB)          32I 463
C144          1470 FORMAT(60H1 RATIOS OF RATIOS OF Q'S. IN THE NUMERATOR 2 IS PROBLEM32I 463
          1 NO.18/36H IN THE DENOMINATOR 2 IS PROBLEM NO.18,1H./1H0,5X11HTEMP32I 463
          2ERATURE6X,7H0 RATIO7X,13HWIGNER TUNNEL,3X,14HTUNNEL Q RATIO,3X,11H32I 463
          3BELL TUNNEL,3X,14HTUNNEL Q RATIO,3X,*BTUN EXPAN.',2X,*TUNNEL Q RAT32I 463
          410',/)          32I 463
C ///////////////////////////////////////////////////
0145          ZL=0
0146          SX=0.000
0147          SX2=0.000
C148          DO 1510 I=1,4
0149          SY(I)=0.000
C150          1510 SXY(I)=0.000
0151          DO 1272 L=1,NOTEM          32I EJLO
0152          XL(L)=1.000/TEMS(L)

```



```

FCRTRAN IV G LEVEL 21                THERMO                DATE = 76247                23/04/44

0201      C   CALCULATE LINEAR LEAST SQUARES FIT TO K1/K2 VERSUS 1/T.
          C   CALL LESQ(1,L,XL,YL,CDEF)
          C   //////////////////////////////////////
          C   CALCULATE QUADRATIC LEAST SQUARES FIT TO K1/K2 VERSUS 1/T OR K1/K2 VERSUS
          C   1/(T**2)
0202      C   CALL LESQ(2,L,XL,YL,CDEF)
          C   ROTATIONAL AND ANHARMONIC CORRECTION TO Q RATIO (I.E. REACTANT ZPE
          C   CORRECTION).
0203      3300 IF (ROTC.EQ.0.000)GO TC 2221
0204          DU 3301 L=1,NUTEM
0205          RQR=RQRAT(L)*EXP(ROTC/TEMS(L))
0206          YL(L)=ALOG(ABS(RQR))
0207      3301 CONTINUE
0208          WRITE(6,3302)
0209      3302 FORMAT('1',1X,'LESQ FIT TO REACTANT ZPE CORRECTION',/)
0210          WRITE(6,3202)
0211          WRITE(6,3305)ROTC
0212      3305 FORMAT(1,1X,'ZPE CORRECTION FACTOR ROTC =',F12.6,/)
0213          CALL LESQ(1,L,XL,YL,CDEF)
0214          CALL LESQ(2,L,XL,YL,CDEF)
0215      2221 IF (ASSM.EQ.0.000)GO TO 1084
0216          DU 3501 L=1,NUTEM
0217          RAR=RQRAT(L)*EXP(ASSM/TEMS(L))
0218          YL(L)=ALOG(ABS(RAR))
0219      3501 CONTINUE
0220          WRITE(6,3502)ASSM
0221      3502 FORMAT('1',1X,'LESQ FIT TO REACTANT ZPE CORRECTION',//,1X,'REACTANT
          *T CORRECTION FACTOR ASSM =',F12.6,/)
          WRITE(6,3202)
0222      3202 FORMAT(1X,'THE COLUMNS LABELED X = 1/T , Y = LN( KIE ) AND EXP(Y) = KIE',/
          *= KIE',/)
0224          CALL LESQ(1,L,XL,YL,CDEF)
0225          CALL LESQ(2,L,XL,YL,CDEF)
0226      1084 RETURN
0227          END

```

```

321 464
321 465

```

FORTRAN IV G LEVEL Z1

LESQ

DATE = 76247

23/04/44

```

0001      SUBROUTINE LESQ(M,NUMBER,X,Y,C)
0002      IMPLICIT REAL*8 (A-H,C-Z)
0003      DIMENSION X(40),Y(40),A(11,11),B(11),C(11),P(40)
C ////////////////////////////////////////////////////////////////////
C      LEAST SQUARES PROGRAM
C      X AND Y VALUES MUST BE PAIRED CORRECTLY.
C      NUMBER = ACTUAL # X,Y DATA PAIRS
C      M=DEGREE OF THE POLY.,MAX.=10
C      N=NO. OF EQUATIONS (=M+1)
C      X,Y=ARRAYS FOR THE DATA PAIRS
C      A= ARRAY FOR SUMS, WHICH BECOME COEFF. IN THE SIMULTANEOUS EQTNS.
C      B=ARRAY FOR THE CONSTANT TERMS IN THE SIMULTANEOUS EQTNS.
C      C=ARRAY FOR THE UNKNOWN, WHICH BECOME THE COEFF. IN THE POLY.
C      P=ARRAY FOR THE POWERS OF THE X(I) FROM 1 TO 2*M.
C ////////////////////////////////////////////////////////////////////
C      SDY = STANDARD DEVIATION IN Y
C      SDLY = STANDARD DEVIATION IN THE EXP(Y)
C      SDA = STANDARD DEVIATION IN THE PREEXPONENTIAL FACTOR A1/A2.
C      SDDL = STANDARD DEVIATION IN THE ACTIVATION ENERGY DIFFERENCES
C ////////////////////////////////////////////////////////////////////
C      CALCULATE SUMS OF X POWERS
C      MX2=M*2
C      DO 23 I=1,MX2
C      P(I)=0.0D0
C      DO 23 J=1,NUMBER
C      P(I)=P(I)+X(J)**I
C      SUBSTITUTE INTO MATRIX A(11,11)
C      N=M+1
C      DO 24 I=1,N
C      DO 24 J=1,N
C      K=1+J-2
C      IF(K)26,26,25
C      25 A(I,J)=P(K)
C      GO TO 24
C      26 A(I,1)=NUMBER
C      24 CONTINUE
C      SUM UP Y VALUES
C      B(1)=0.0D0
C      DO 21 J=1,NUMBER
C      B(1)=B(1)+Y(J)
C      DO 22 I=2,N
C      B(I)=0.0D0
C      DO 22 J=1,NUMBER
C      B(I)=B(I)+Y(J)*X(J)**(I-1)
C      NM1=N-1
C      DO 300 K=1,NM1
C      KPL=K+1
C      L=K
C      DO 400 I=KPL,N
C      ATEMP=DABS(A(I,K))-DABS(A(L,K))
C      IF(ATEMP)400,400,401
C      401 L=I
C      400 CONTINUE
C      IF(L-K)500,500,405
C      405 DO 410 J=K,N
C      TEMP=A(K,J)
C      A(K,J)=A(L,J)

```

FCRTRAN IV G LEVEL 21

LESQ

DATE = 16247

23/04/44

```

0038      410 A(L,J)=TEMP
0039          TEMP=B(K)
0040          B(K)=B(L)
0041          B(L)=TEMP
0042      500 DO 300 I=KPI,N
0043          FACTOR=A(I,K)/A(K,K)
0044          A(I,K)=0.000
0045          DO 301 J=KPI,N
0046      301 A(I,J)=A(I,J)-FACTOR*A(K,J)
0047      300 B(I)=B(I)-FACTOR*B(K)
0048          C(N)=B(N)/A(N,N)
0049          I=NM1
0050      710 IPI=I+1
0051          SUM=0.000
0052          DO 700 J=IPI,N
0053      700 SUM=SUM+A(I,J)*C(J)
0054          C(I)=(B(I)-SUM)/A(I,I)
0055          I=I-1
0056          IF(I)800,800,710
0057      800 WRITE(6,791)
0058      791 FORMAT(1X,'LEAST SQUARES POLYNOMIAL COEFFICIENTS OF THE FORM C1 +
          1C2*X + C3*X**2 + ...')
          WRITE(6,901)(I,C(I),I=1,N)
0059      901 FORMAT(5(2X,2HC(,13,2H)=,D17.10))
0060          WRITE(6,902)
0061      902 FORMAT(//,11X,'X',15X,'X**2',16X,'Y',15X,'YCALC',13X,'DEVY',13X,'E
          *XP(Y)',12X,'DEVEXP',/)
0063          DEYSQ=0.000
0064          DYSQ=0.000
0065          SUMSQX=0.000
0066          SUMX=0.000
0067          DO 900 NC=1,NUMBER
0068          YICALC=0.000
0069          DO 889 I=1,N
0070      889 YICALC=YICALC+(C(I)*X(NC)**(I-1))
0071          DEVY=Y(NC)-YICALC
0072          DYSQ=DYSQ+(DEVY*DEVY)
0073          XSQ=X(NC)*X(NC)
0074          EXPY=DEXP(Y(NC))
0075          DEXPY=DEXP(YICALC)
0076          DEYSQ=DEYSQ+(DEXPY*DEXPY)
0077          WRITE(6,904)X(NC),XSQ,Y(NC),YICALC,DEVY,EXPY,DEXPY
0078      904 FORMAT(2X,7(D18.10))
0079          SUMSQX=SUMSQX+XSQ
0080          SUMX=SUMX+X(NC)
0081      900 CONTINUE
0082          IF(NUMBER.LT.3)RETURN
0083          SUMXSQ=SUMX*SUMX
0084          DNM=(NUMBER*SUMSQX)-SUMXSQ
          C CALCULATE STANDARD DEVIATIONS
0085          SDY=DSQRT(DYSQ/(NUMBER-2))
0086          SDEY=DSQRT(DEYSQ/(NUMBER-2))
0087          WRITE(6,903)SDY,SDEY
0088      903 FORMAT(//,'STD. DEV. IN Y =',D18.10,20X,'STD. DEV. IN EXP(Y) =',D18.10)
          *18.10,///)
0089          SDB=SDY*DSQRT(SUMSQX/DNM)
0090          SDA=DEXP(C(1)+SDB)-DEXP(C(1))
0091          SDDE=SDY*DSQRT(NUMBER/DNM)*1.987200

```

```
FORTRAN IV C LEVEL 21          LESQ          DATE = 76247          23/04/44

0092          WRITE(6,910)SDA,SDDE
0093          910 FORMAT(/,1X,'SDA=',1PD18.10,20X,'SDDE=',1PD18.10)
0094          WRITE(6,905)SUMSQX,SUMXSQ,DNM
0095          905 FORMAT(/,1X,'SUM(X**2)=' ,D18.10,5X,'(SUMX)**2 =' ,D18.10,5X,'N*SUM(
          *X**2)-(SUMX)**2 =' ,D18.10,/)
0096          RETURN
0097          END
```


VITA ²

Terry Don Marriott

Candidate for the Degree of

Doctor of Philosophy

Thesis: KINETIC ISOTOPE EFFECTS IN THE $\text{CH}_4 + \text{H}^{\ddagger}\text{CH}_3 + \text{H}_2$ SYSTEM.
PREDICTIONS OF THE LMR SIX-BODY POTENTIAL-ENERGY REACTION
HYPERSURFACE

Major Field: Chemistry

Biographical:

Personal Data: Born in Watonga, Oklahoma, on November 7, 1943,
the son of Mr. and Mrs. D. L. Marriott, Watonga, Oklahoma.

Education: Graduated from Watonga High School, Watonga, Oklahoma,
in May, 1962; received Bachelor of Science degree from
Oklahoma State University, Stillwater, Oklahoma in May, 1969,
with a major in Chemistry; completed requirements for the
Doctor of Philosophy degree at Oklahoma State University,
December, 1976.

Professional Experience: Summer Trainee, Kerr McGee Research
Center, Oklahoma City, Oklahoma, 1969; Graduate Teaching
Assistant, Oklahoma State University, 1969-75; Oklahoma State
University Graduate College Summer Research Awardee, 1971;
Oklahoma State University Chemistry Department Special Summer
Appointment, 1975; ERDA Research Associate, spring 1976.

Membership in Honorary and Professional Societies: Member of Phi
Lambda Upsilon, Honorary Chemical Society.